

University of Alberta

**Substrate Transformations Promoted by Adjacent Group 8 and 9
Metals**

by

Rahul G. Samant

A thesis submitted to the Faculty of Graduate Studies and Research
in partial fulfillment of the requirements for the degree of

Doctor of Philosophy

Department of Chemistry

©Rahul Samant
Fall 2009
Edmonton, Alberta

Permission is hereby granted to the University of Alberta Libraries to reproduce single copies of this thesis and to lend or sell such copies for private, scholarly or scientific research purposes only. Where the thesis is converted to, or otherwise made available in digital form, the University of Alberta will advise potential users of the thesis of these terms.

The author reserves all other publication and other rights in association with the copyright in the thesis and, except as herein before provided, neither the thesis nor any substantial portion thereof may be printed or otherwise reproduced in any material form whatsoever without the author's prior written permission.

Examining Committee

Martin Cowie, Department of Chemistry, University of Alberta

Steven H. Bergens, Department of Chemistry, University of Alberta

Roderick E. Wasylshen, Department of Chemistry, University of Alberta

Jillian M. Buriak, Department of Chemistry, University of Alberta

Phillip Y. K. Choi, Department of Chemical and Materials Engineering, University of Alberta

David J. H. Emslie, Department of Chemistry, McMaster University

Abstract

The use of transition metal catalysts – either homogenous (discrete well-defined metal complexes) or heterogeneous (more poorly-defined metal surfaces) – plays an important role in the transformations of small substrates into larger, value-added compounds. Although heterogeneous catalysts have the greater industrial applicability, there has been enormous interest in homogenous transition metal systems for effecting selective transformations of small substrate molecules. The bulk of these homogenous systems are mononuclear. Perhaps surprisingly, very little research has focused on systems with adjacent metal centres. Binuclear systems possess adjacent metals that may interact and possibly lead to transformations not observed in monometallic systems. It is the opportunity for adjacent metal involvement in substrate activation that is the focus of this dissertation. The goal of this research is to gain an increased understanding of metal-metal cooperativity and adjacent metal involvement in substrate transformations; how can adjacent metal involvement lead to substrate activations not seen in monometallic counterparts, and what role does each metal play in these interactions, particularly when the two metals are different?

Throughout this dissertation examples of transformations unique to systems with at least two metals are presented and examined with a particular focus on the *roles* of the two metals and any associated binding modes in these transformations. In addition, by comparing the RhOs, RhRu and IrRu systems, the influence of metal substitution is also examined. For example, diazoalkane activation and C-C bond formation promoted by the Rh-based systems is investigated, the roles of adjacent metals of the IrRu system in

the conversion of methylene groups to oxygenates is examined, and the unusual geminal C-H bond activation olefinic substrates is explored.

Overall, the work presented within this thesis adds to the growing understanding of adjacent metal cooperatively, leading us towards a more rational approach to the design of homogenous homo- and heterobimetallic catalysts, heterogeneous catalysts, and nanoparticle catalysts for selective substrate transformations.

Acknowledgements

There are a number of people without whose support this thesis would not have been possible. Firstly, I would like to thank Martin Cowie for his patience, encouragement and mentorship. When I first met Marty I asked him “what will I learn if I join your group?” to which he simply replied “problem solving.” There was certainly a problem or two during the course of my PhD studies. Marty is an incredible teacher because he is an incredible communicator, he has an uncanny ability to dissect a topic and present it in a manner that is easy understand, he truly is an educator in every sense of the word. Although I will most likely never attain the mastery of communication that Marty possesses, he has, by way of torturous practice talks and painful revisions, taught me how to effectively communicate as well (and my ChemDraws aren’t half bad now either).

I would also like to thank past Cowie group members whom I have had the pleasure of working with. James ‘Wiggy’ Wigginton, Steve Trepanier and Jim Dennett, who were post-docs when I first joined the group, along with fellow graduate students Amala Choksi, Bryan Rowsell and Jason Anderson, had the patience to teach me the synthetic skills that made the research in this thesis possible. I’d like to thank Kyle Wells, who joined the group shortly after myself, for always keeping things ‘interesting’ (to say the least). Thanks go to Mathias Berenstiel for intellectual discussions. Lindsay Hounjet, Matt Zamora, Tiffany Ulmer, Mike Slaney and Hosnay Mobarok all joined the group during my tenure and I’d like to thank them for all their stimulating gatherings about the chalk board and for help in preparing this thesis. Thank you all for making the Cowie group what it is.

There are countless people who make the University of Alberta Department of Chemistry such a wonderful place to do research and I’d like to thank all of them. In particular I’d like to thank Bob McDonald and Mike Ferguson of the X-ray crystallography lab, not only for their work on the crystal structures reported in this thesis, but also for listening to my rants over coffee or (occasional) beer. I would also like to give my deepest gratitude to the staff of the NMR spectroscopy laboratory, particularly Mark Miskolzie and Glen Bigam.

Without their assistance and vast knowledge of NMR spectroscopy much of this thesis would not have been possible.

I'd like to thank the all the great people I've had the pleasure of meeting during grad school and who have been a significant part of my life during this time. In no particular order, Rob Polakowski, Ania Liakos, Gavin Searle, Nicola Webster, Colin Hessel, Glen Shoemaker, Sarah Pelletier, Robin Clugston, Owen Lightbody, Igor Sinelnikov, Christina Tatarniuk, Marie-Josée Dumont, Cathy and Kwadwo Kyeremanteng, Paul Tiede, Vickie Russell, Travis and Suzanne Sjovold, Lisa Carosi, Eric Pelletier, Lesley Baldwin, Matt Ross, Wendy Topic, Kris Harris, De-ann Rollings, Eric Henderson, Tai Telesco, Vince Ziffle, Michelle Forgeron, Eli Stoffman, Sheri Macleod, Matt Willans, Kirk Fiendel, Bryan Demko, Dave and Fonda Norman, Liz Ferguson, and Liz Dennett. I hope I haven't forgotten anyone. Many thanks to all of you for your various distractions, from trips to the mountains to hike and ski, to trips to the bar for a pint or two or three.

Last, but by no means least, I'd like to thank my family. I'd like to acknowledge my father, Ganesh, who always encouraged me to accept only the best of myself, no compromise. It is truly unfortunate that he will not see this come to its conclusion. I'd like to thank my mother, Judy, for her constant love and support; you have dedicated your life to your sons and we are eternally grateful. To Bill, thank you for teaching me the value of hard work and discipline; these valuable lessons gave me the tools to succeed. I'd like to thank Luke and Kim and my niece, Marlee for all the encouragement over the years. Thank you to my extended family, Popi, Jaloo, Neville, Manik, Suresh, Mayuresh and Choti for showing me the strength of the family bond. To Erin Mackenzie, we have shared this entire experience together and I couldn't have done it without your love and support; you are the best. I'd like to take this opportunity to congratulate you on your achievement as well!

I hope that I have not forgotten anyone, and if I have, my deepest apologies. One last time, I'd like to thank all of you for your being a part of this thesis, and my life, over the course of these studies. I am forever indebted to each and every one of you.

Table of Contents

1. Chapter 1: Introductions	1
1.1 Two metals are better than one	1
1.2 Transformations of Interest	10
1.2.1 Reactions of Bridging Methylene Groups/Generation of Substituted Bridging Alkylidenes	10
1.2.2 Migratory Insertion	13
1.2.3 Olefin Activation	16
1.3 References	19
2. Chapter 2: Coordination and Activation of Diazoalkanes in the Presence of Rh/Ru and Rh/Os Metal Combinations	25
2.1 Introduction	25
2.2 Experimental Section	27
2.2.1 General Comments	27
2.2.2 Preparation of Compounds	32
2.3 Results and Compounds Characterization	39
2.3.1 Treatment of Methylene Bridged Complexes with Diazomethane	39
2.3.2 Diazoalkane Complexes	42
2.4 Discussion	50
2.4.1 Methylene and Alkylidene Coupling	50
2.4.2 Diazoalkane and Related Complexes	51
2.4.3 Comparison of N_2CH_2 and N_2CRR'	53

2.5	Conclusions	55
2.6	References	56
3.	Chapter 3: Unsymmetrically Bridged Acyl Groups as Intermediates in the Transformation of Bridging Methylene to Bridging Acyl Groups: Ligand Migrations and Migratory Insertions in Mixed Metal IrRu Complexes	62
3.1	Introduction	62
3.2	Experimental	64
3.2.1	General Comments	64
3.2.2	Preparation of Comounds	69
3.3	Results and Discussion	77
3.3.1	Methyl Complexes	77
3.3.2	Acetyl Bridged Complexes	89
3.3.4	Reactions with H ₂	96
3.4	Conclusions	101
3.5	References	103
4.	Chapter 4: Geminal C-H Activation of α-Olefins Promoted by IrRu Systems: Mechanistic Insights	109
4.1	Introduction	109
4.2	Experimental	112
4.2.1	General Comments	112
4.2.2	Preparation of Compounds	116
4.3	Results and Discussion	126

4.3.1	Olefin Activation	126
4.3.2	Cumulene Activation	131
4.3.3	Mechanistic Studies	136
4.3.4	Reactions of the Vinylidene Bridge	152
4.4	Conclusions	155
4.5	References	157
5.	Chapter 5: Conclusions	163
5.1	Concluding Remarks	164
5.2	References	173
6.	Appendix I: Selected NMR Spectra	175
AI.1	Chapter 3	175
AI.2	Chapter 4	
7.	Appendix II: Drying Agents for Solvents	183
8.	Appendix III: Co-author Contributions	184

Table of Figures

Chapter 1

- Figure 1.1 The prominent mechanistic proposals for chain propagation in the FT process 4

Chapter 2

- Figure 2.1 Perspective view of the $[\text{RhOs}(\text{CO})_3(\mu\text{:}\eta^1\text{:}\eta^1\text{-}\underline{\text{N}}=\underline{\text{N}}\text{C}(\underline{\text{C}}\text{OH})\text{CO}_2\text{Et})\{\text{dppm}\}_2]^+$ complex cation of compound **27** 44

Chapter 3

- Figure 3.1 Perspective view of the complex cation of $[\text{IrRu}(\text{CH}_3)(\text{CO})_5(\text{dppm})_2]^{2+}$ (**36**) 83
- Figure 3.2 Perspective view of the complex cation of $[\text{IrRu}(\text{CO})_4(\mu\text{-C}(\text{CH}_3)\text{O})(\text{dppm})_2][\text{BF}_4]_2$ (**39-BF₄**) 91
- Figure 3.3 Perspective view of the complex cation of $[\text{IrRu}(\text{CO})_3(\mu\text{-C}(\text{CH}_3)\text{O})(\text{dppm})_2][\text{BF}_4]_2$ (**40**) 93
- Figure 3.4 Perspective view of the complex cation of $[\text{IrRu}(\text{OSO}_2\text{CF}_3)(\text{CO})_2(\mu\text{-C}(\text{CH}_3)\text{O})(\text{dppm})_2][\text{CF}_3\text{SO}_3]$ (**42**) 96

Chapter 4

- Figure 4.1 Perspective view of the $[\text{IrRu}(\text{CO})_3(\mu\text{-CO})(\mu\text{-C}=\text{CH}_2)(\text{dppm})_2]^+$ complex cation of compound **47** 128

Figure 4.2	Perspective view of the [IrRu(CO) ₃ (μ-CO) (μ-C=CHCH ₃)(dppm) ₂] ⁺ cation of compound 48	130
Figure 4.3	Proton labeling scheme for the 3-methyl-1,3- butadienylidene fragment of compound 50	134
Figure 4.4	Selected region of the ¹ H NMR spectrum of compound 53	143
Figure 4.5	Isotope distribution patterns (m/z=1201) for the product mixture in the reaction of compound 6 with 1,1-d ₂ ethylene	149

Appendix I

Figure AI.1	EXSY spectroscopy spectrum of compound 38 at -60 °C	175
Figure AI.2	T ₁ measurement of compound 44	176
Figure AI.3	³¹ P{ ¹ H} spectra from the variable- temperature NMR studies of the reaction of 6 with ethylene	177
Figure AI.4	³¹ P{ ¹ H} NMR spectra the reaction mixture of 6 and acetylene after 16h at 0 °C	178
Figure AI.5	Selected regions of the ¹ H{selective ³¹ P} NMR spectra of compound 54	179
Figure AI.6	³¹ P{ ¹ H} NMR spectra of a mixture of compounds 6 , 55 and 56 taken at -80 °C	180
Figure AI.7	Selected regions of the ¹ H NMR spectra of a mixture of 6 , 55 and 56 showing the agostic proton resonance of 55 (δ -2.5) and the hydride resonance of 56 (δ -10.0)	181

Table of Tables

Chapter 2

Table 2.1	Spectroscopic Data for Compounds Prepared.	29
Table 2.2	Crystallographic Experimental Details for Compound 27 .	38
Table 2.3	Selected Distances and Angles for Compound 27 .	44

Chapter 3

Table 3.1	Spectroscopic Data for Compounds Prepared.	66
Table 3.2	Crystallographic Data for Compounds 36 , 39 , 40 and 42 .	74
Table 3.3.	Selected Distances and Angles for Compound 36 .	84
Table 3.4	Selected Distances and Angles for Compound 39-BF₄ .	91
Table 3.5	Selected Distances and Angles for Compound 40 .	93
Table 3.6	Selected Distances and Angles for Compound 42 .	96

Chapter 4

Table 4.1	Spectroscopic Data for Compounds Prepared.	113
Table 4.2	Crystallographic Experimental Details for Compound 47 .	123
Table 4.3	Crystallographic Experimental Details for Compound 48 .	125
Table 4.4	Selected Distances and Angles for Compound 47 .	128
Table 4.5	Selected Distances and Angles for Compound 48 .	130

Table of Schemes

Chapter 1

Scheme 1.1	Fluoride abstraction from IV-F .	8
Scheme 1.2	Synthesis of $[\text{MM}'(\text{CO})_4(\text{dppm})_2][\text{OTf}]$.	9
Scheme 1.3	Methylene group coupling promoted by a RhOs system.	11
Scheme 1.4	Proposed mechanism of methylene group coupling.	11
Scheme 1.5	Reactions of 5 and 6 with N_2CH_2 .	12
Scheme 1.6	Migratory insertion reactions of RhOs and RhRu systems.	15
Scheme 1.7	Geminal C-H activation of butadiene by compound 21 .	18

Chapter 2

Scheme 2.1	Reactions of compounds 24 and 25 with substituted diazoalkanes.	40
Scheme 2.2	Reactions of compounds 1 and 5 with substituted diazoalkanes.	43
Scheme 2.3	Formation of compounds 27 and 28 by Keto-enol tautomerization.	52
Scheme 2.4	Coupling of a methylene bridge with a diazoalkane-generated alkylidene unit.	55

Chapter 3

Scheme 3.1	Conversion of a bridging-methylene to a terminal-methyl group.	78
Scheme 3.2	Protonation of 33 to give 35 .	85
Scheme 3.3	Migratory insertion of compound 36 to give the acyl-bridged	

	compound 36 and thermolysis reactions of 36 .	90
Scheme 3.4	Heterolytic cleavage of H ₂ by 40 or 41 to give 43 .	97
Scheme 3.5	Homolytic cleavage of H ₂ by compound 42 .	99
Chapter 4		
Scheme 4.1	Olefin C-H bond cleavage at monometallic Ir centres.	110
Scheme 4.2	Reaction of compound 6 with olefins and alkynes.	126
Scheme 4.3	Reaction of compound 6 with allene and methylallene.	132
Scheme 4.4	Reaction of compound 6 with 1,1-dimethylallene.	132
Scheme 4.5	Reaction of IV-C with 1,1-dimethylallene.	135
Scheme 4.6	Low-temperature reactions of 6 with ethylene and acetylene.	136
Scheme 4.7	Low-temperature reactions of 6 with propene and propyne.	141
Scheme 4.8	The geminal and vincinal mechanistic proposals.	145
Scheme 4.9	Formation of isotopomers by reaction of 6 with 1,1-d ₂ ethylene.	146
Scheme 4.10	Proposed mechanism of double C-H activation of allene and methyle allene by 6 .	149
Scheme 4.11	Proposed mechanism of double C-H activation of 1,1-dimethylallene by 6 .	152
Scheme 4.12	Reaction of compound 52 with diazomethane and DEDM.	153

Table of Charts

Chapter 1

Chart 1.1	6
Chart 1.2	9
Chart 1.3	19

Chapter 2

Chart 2.1	25
Chart 2.2	41
Chart 2.3	47

Chapter 3

Chart 3.1	63
Chart 3.2	94

Chapter 4

Chart 4.1	111
Chart 4.2	140

List of Abbreviations

mL	milliliter
μg	microlitre
mg	milligram
μg	microgram
OTf	triflate
dppm	bis-(diphenylphosphino)methane
depn	bis-(diethylphoshino)methane
Et ₂ O	diethyl ether
THF	tetrahydrofuran
DEDM	diethyl diazomalonate
EDA	ethyl diazoacetate
TMSDM	trimethylsilyl diazomethane
MS	mass spec
EA	elemental analysis
IR	infrared
NMR	nuclear magnetic resonance
Ph	phenyl
Me	methyl
Et	ethyl

Chapter 1: Introduction

1.1 Two Metals are Better Than One

The selective transformation of small molecules into larger more complex target molecules is one of the central themes in chemical research, and must involve the breaking of existing bonds and the formation of new ones. Of the numerous strategies that have been developed to achieve selective bond cleavage and formation, perhaps none has had more success in turning inexpensive and readily available chemicals into value-added products, particularly at the industrial scale, than the use of transition metals (TM) as catalysts for the targeted transformations. Countless TM catalysts have been developed for a wide range of transformations, including for example, olefin metathesis,¹⁻¹¹ methanol carbonylation for the production of acetic acid,¹²⁻¹⁵ the conversion of inexpensive monomers into valuable polymers having a wide range of physical properties,^{1,6,11,16-19} and the production of fuels, oils and waxes from syn gas (CO and H₂) in the Fisher-Tropsch (FT) process.²⁰⁻²⁵ Although a number of industrial processes such as the first two examples above utilize well-defined homogenous catalysts, the vast majority employ heterogeneous catalysts due to their low-cost and ease of separation from the final product.

In heterogeneous, metal-based catalyst systems the catalyst is either a metal surface or a metal adsorbed onto a solid support, over which the substrate (either a liquid or gas) is passed (usually at elevated temperatures and pressures).²⁶ Although heterogeneous catalysts have many successful applications, the harsh conditions often required combined with the diversity of active sites on the catalyst surface result in a low specificity, leading to undesired byproducts that must be separated from the target product. From a mechanistic perspective the poorly defined nature of most heterogeneous systems means that very little is understood about the steps involved in substrate transformations on a catalyst

surface,^{27,28} making catalyst design more of an empirical approach than one of rational design.

Muetterties articulated the connection between metal complexes and metal surfaces stating that “Surface chemistry is coordination chemistry. If the molecule or molecules in question are organic, then the surface chemistry is organometallic chemistry.”²⁹ This connection between surface chemistry and organometallic chemistry provides a strategy for mechanistic investigations of heterogeneously catalyzed processes: the use of well-defined homogenous complexes as models for heterogeneous systems. These model systems can be more easily studied using traditional and well-established spectroscopic methods, such as NMR, and the detailed information so obtained can then be used to infer what might be happening on the surface of heterogeneous analogues.

Mononuclear complexes, containing only one metal centre, are the most easily manipulated and understood, but are poor models for heterogeneous systems as they lack adjacent metal sites that are present in these latter systems. Clusters are a more representative model for metal surfaces;²⁹ the larger the cluster, the more closely it can mimic surface behavior. Unfortunately, clusters suffer from a variety of technical problems, ranging from their low solubility to the complexity of their characterization and study. A binuclear system, with two adjacent metal centres, is much easier to investigate and characterize than large clusters yet still possesses the minimum two adjacent metals required to mimic the involvement of adjacent metals in surface reactivity. Furthermore, on a metal surface bridged binding modes of substrates often spanning two metal centres are commonly observed suggesting that a pair of metals, able to mimic this binding, can offer insights into any associated reactivity modes.³⁰ Of course we must recognize that such a model is a gross oversimplification of surface reactivity, but nevertheless binuclear models can provide an improved understanding of how adjacent metals interact with and transform substrate molecules.

An area of particular interest to us is the **FT** process mentioned earlier. The **FT** process converts syn gas, usually generated from either coal or natural gas, into a variety of hydrocarbon products as shown in equation 1. In 1923,



during their work at the Kaiser Wilhelm Institute for Coal Research Franz Fischer and Hans Tropsch first reported the production of liquid hydrocarbons from syn gas using either iron or cobalt heterogeneous catalysts.³¹ Initial production of liquid petrochemicals derived from **FT** technology began in 1936 and was used on a large scale by Germany for the production of diesel fuel during WWII. After WWII interest in **FT** technology continued particularly in Germany and South Africa, which have large coal reserves, and in 1950 the South African government created the South African Coal Oil and Gas Corporation, now Sasol, which subsequently became the largest user of **FT** technology worldwide. Elsewhere, there has been much less interest in **FT** technology due to the availability of cheaper ‘conventional’ oil reserves in the Middle East as well as other regions of the globe, making **FT**-derived hydrocarbons economically less viable. However, increasing oil prices due to depleting conventional deposits and the increasing energy needs of emerging economies like China and India, along with North America’s demand for energy independence, has led many to believe that **FT** technology will play an important economic role in the future, making better use of the vast underutilized coal and natural gas deposits.

With the resurgent interest in **FT** technology, interest in the mechanistic details has also been rekindled. A number of proposals have been presented for carbon-carbon chain growth in **FT** chemistry,^{21,24,31-33} however the most accepted proposals have come from Fischer and Tropsch,³¹ Dry,²¹ Brady and Pettit^{32,33} and Maitlis²⁴ (see Figure 1.1). Although each proposal differs, one theme that they all have in common is the importance of the bridging methylene unit in the coupling process. Without going into details, the major differences in the four proposals

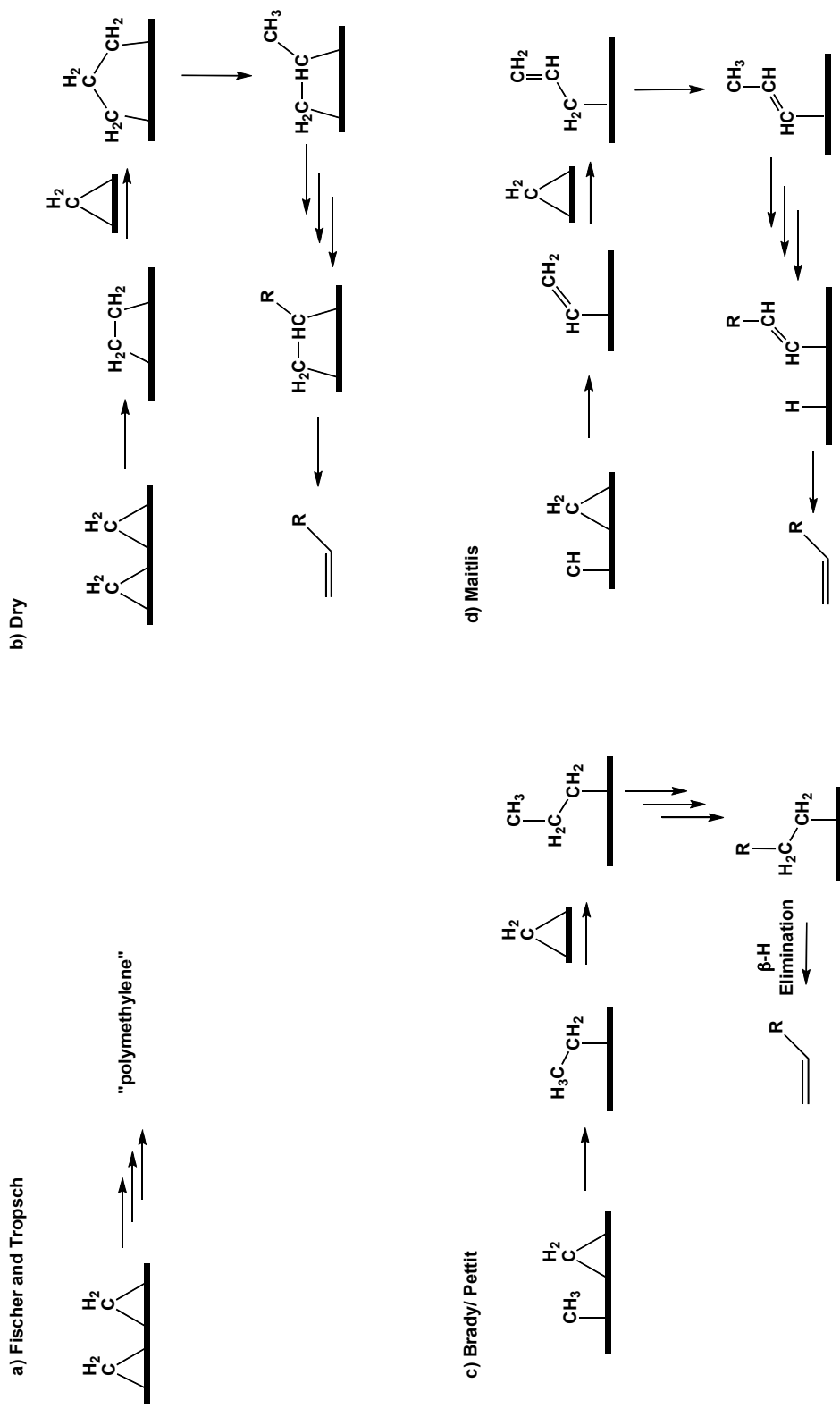


Figure 1: The four prominent proposals for carbon-carbon chain growth in the FT process by a) Fischer and Tropsch, b) Dry, c) Brady and Pettit and d) Maitlis

relates to the hydrocarbyl group(s) with which the methylene fragment couples in the carbon-carbon chain growth. In the Fischer-Tropsch proposal,³¹ sequential coupling of methylene groups was proposed, yielding polymethylene. The Dry proposal is closely related except the chain-growth step in this proposal involves the coupling of a C₂-bridging (a surface-bound olefin) unit with a methylene unit to yield a C₃-bridging fragment which rearranges to give another C₂-bridging fragment. In the Brady and Pettit proposal chain propagation is mediated by alkyl-group migration to surface-bound methylene groups.^{32,33} Finally, in the Maitlis proposal initiation occurs by coupling of a methylene with a methyne group to give a surface bound vinyl (alkenyl) group and chain growth occurs by alkenyl group migration to surface-bound methylenes.^{22-24,34} The reader is referred to the original papers (*vide supra*) for additional data, and in particular the papers by Maitlis deal with the mechanistic details most thoroughly.

Although heterogeneous catalysts have the greater industrial applicability, there has been enormous interest in homogenous transition metal systems for effecting selective transformations of small substrate molecules. One of the main attractions to homogeneous systems over heterogeneous ones is their tunability, whereby subtle changes in the steric and electronic properties of the ligand architecture can have profound influences on the system's reactivity. Perhaps one of the greatest successes of ligand design has been in asymmetric catalysis wherein the introduction of chirality in the ligand architecture can influence the chirality of the resulting product(s), providing a synthetic route to optically pure targets.³⁵⁻³⁸

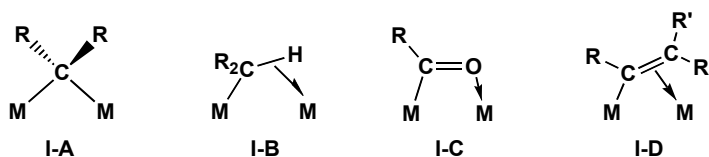
The bulk of these homogenous systems are mononuclear. Perhaps surprisingly, very little research has focused on systems with adjacent metal centres. Such multimetal systems (clusters) could, in principle, exhibit some of the advantages of both heterogeneous and homogeneous systems, having several metal centres for substrate activation, while being readily modified, through ligand modification, and studied. As mentioned earlier, the simplest multi-nuclear systems are those that contain only two metal centres. These binuclear systems, while being much easier to manipulate and characterize, still possess adjacent metals that may interact and possibly lead to transformations not observed in monometallic systems. This metal-metal cooperativity may manifest itself in a number of ways, for example, the migration of an ancillary ligand

from one metal to the other can open a vacant coordination site for substrate attack, or the activation of a substrate that is bound at one metal centre by the adjacent metal.³⁹ In addition, adjacent metals have the potential to act as electron reservoirs as well as allow for metal-metal bond formation for stabilizing otherwise electronically unsaturated complexes.³⁹ Moreover, this ability (to behave as electron reservoirs) facilitates transformations that involve redox reactions.³⁹ Some examples of adjacent metal cooperativity are discussed later.

In addition to influencing reactivity through ligand design, binuclear systems offer the possibility of further tailoring the selectivity of the system by combining *different* metals. What reactivity will arise when two different metals, each with their own reactivity profiles, work together? It is this question that has drawn us to heterobimetallic systems of the group 8 (Ru, Os) and 9 (Rh, Ir) metals, both of which have a rich history in a number of industrial processes.⁴⁰ In attempting to understand the roles of the different metals in mixed-metal systems, we maintain that it is necessary to compare the different reactivities of different metal combinations. Previous studies in our group have focused on both the RhOs and RhRu systems, and a portion of the study presented in this thesis is a continuation of some of this work. However, the majority of the work presented in this thesis focuses on the much less explored IrRu system and seeks to examine both its similarities and differences with the RhOs and RhRu combinations.

One of the most important features of a binuclear system is the possibility for a substrate to bridge both metal centres, a binding mode unavailable to their mononuclear counterparts. Chart 1.1 shows some hydrocarbyl bridging fragments that play important

Chart 1.1



roles throughout the work presented within this dissertation: the bridging alkylidene unit (**I-A**) (Chapter 2), the unsymmetrically bridging alkyl group (μ -agostic alkyl) (**I-B**)

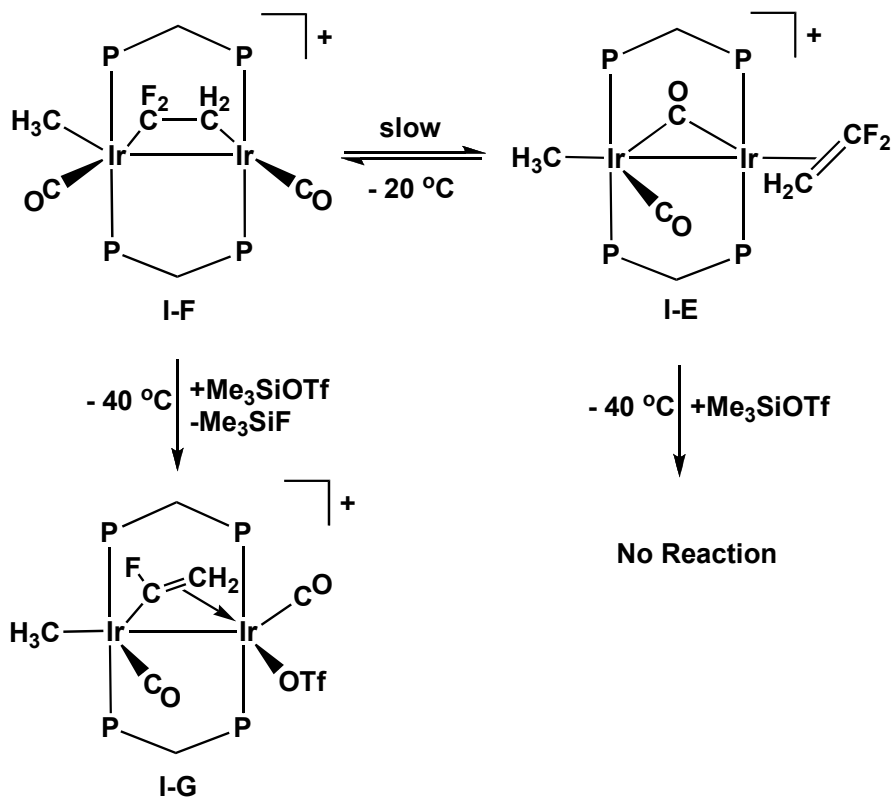
(Chapter 3), the bridging acyl group (**I-C**) (Chapter 3) and the σ - π $\eta^1:\eta^2$ -bridging vinyl (**I-D**) (Chapter 4). It is expected that the reactivity for a particular fragment bridging two metal centres should differ from that observed when bound to only one. For example, it is believed that carbon monoxide activation in processes such as the **FT** process is mediated through the bridging mode by coordination of both the carbon and the oxygen atoms to different metal centres.⁴¹ Supporting this notion is the observation of a number of well-characterized multinuclear systems in which coordination of a CO ligand bridging two metals in an $\eta^1:\eta^1$ fashion results in a significant weakening of the CO bond, observed by either reduction of the CO stretching frequency in the IR spectra (to 1780-1330 cm^{-1}),⁴²⁻⁴⁷ or the elongation of the CO bond from 1.13 Å in free CO to as high as 1.30 Å.⁴⁷

An excellent example of binuclear activation leading to enhanced catalytic activity was presented by Stanley and coworkers;⁴⁹ they demonstrated that the dirhodium system, $[\text{Rh}_2((\text{Et}_2\text{PCH}_2\text{CH}_2)(\text{Ph})\text{PCH}_2\text{P}(\text{Ph})(\text{CH}_2\text{CH}_2\text{PEt}_2))(\text{nbid})_2][\text{BF}_4]_2$ (nbid = norbornadiene) is an excellent hydroformylation catalyst and is 40% faster than the commercially employed Rh/ PPh_3 catalyst. In order to establish that the enhanced activity of this binuclear system was a result of metal-metal cooperativity, Stanley *et al* compared its activity to that of four analogous mononuclear Rh systems using the ligands $\text{Et}_2\text{PCH}_2\text{CH}_2\text{PEt}_2$, $\text{Et}_2\text{PCH}_2\text{CH}_2\text{P}(\text{Me})\text{Ph}$, $\text{Et}_2\text{PCH}_2\text{CH}_2\text{PPh}_2$, $\text{Ph}_2\text{PCH}_2\text{CH}_2\text{PPh}_2$, all of which proved to be poor hydroformylation catalysts, converting less than 2% of the alkenes to aldehydes after 3 h. Furthermore, to establish that the two metals were not behaving as two isolated metal centres, but were working in concert during substrate activation, they prepared the related dirhodium complexes using ligand systems that increased the metal-metal separation, thereby minimizing metal-metal interactions. Once again they found that these systems were poor catalysts for hydroformylation.

In another example, reported by our group, a bridging binding mode was found to be essential in the cleavage of a C-F bond of 1,1-difluoroethylene (as well as other fluoroolefins) in the diiridium complex $[\text{Ir}_2(\text{CH}_3)(\text{CO})_2(\text{C}_2\text{H}_2\text{F}_2)(\text{dppm})_2][\text{OTf}]$, shown in Scheme 1.1.⁵⁰ The 1,1-difluoroethylene adduct exists as two isomers, one in which the olefin binds terminally to one Ir centre (**I-E**) and another in which the olefin is bridging both metals (**I-F**). The 1,1-difluoroethylene ligand in **I-E** is found to be unreactive

towards Me_3SiOTf , whereas its isomer, **I-F**, containing the $\mu\text{-}\eta^1\text{:}\eta^1\text{-olefin}$ adduct, reacts readily with Me_3SiOTf at temperatures as low as $-40\text{ }^\circ\text{C}$ to give the fluorovinyl species **I-G** through the cleavage of a C-F bond.

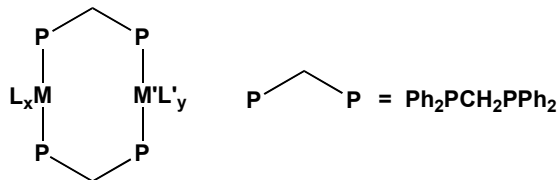
Scheme 1.1



One particular challenge associated with the use of binuclear complexes to effect substrate transformations is ensuring that the integrity of the complex is maintained (keeping the metals in close proximity) during the transformations being studied. This can be achieved through the use of a ligand system that bridges the two metal centres creating a robust framework.^{25,50} We have chosen to use the bis(diphenylphosphino)-methane (dppm) ligand system in which the two metals are bridged by the diphosphine, as shown in Chart 1.2. This ligand system binds effectively to low-valent, late TM's and prefers the bridging mode, yet is flexible enough to provide substrate access while still

maintaining an intermetallic distance suitable for metal-metal cooperativity. In addition to the stability of the diphosphine system, the 100% abundant, NMR active ^{31}P nucleus is

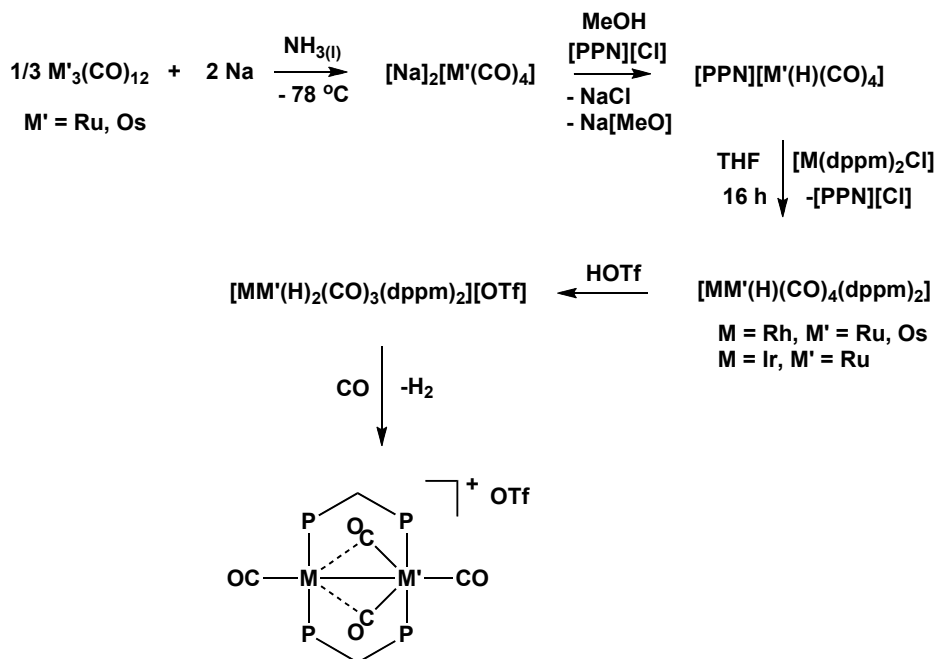
Chart 1.2



an important spectroscopic tool, assisting in the observation and characterization of labile, transient species.

Earlier, it was mentioned that we have become interested in mixed-metal systems of the group 8 and 9 metals. Scheme 1.2 below shows the $[\text{MM}'(\text{CO})_4(\text{dppm})_2][\text{OTf}]$ ($\text{M} = \text{Rh}, \text{Ir}; \text{M}' = \text{Ru}, \text{Os}$)⁵¹⁻⁵⁴ system, the archetypical system of study, and describes the

Scheme 1.2



synthetic route to preparing RhRu, RhOs, and IrRu compounds of this type. Reduction of the $\text{M}'_3(\text{CO})_{12}$ cluster gives the hyper-reduced mononuclear complex $[\text{Na}]_2[\text{M}'(\text{CO})_4]$ ⁵⁵⁻⁵⁷

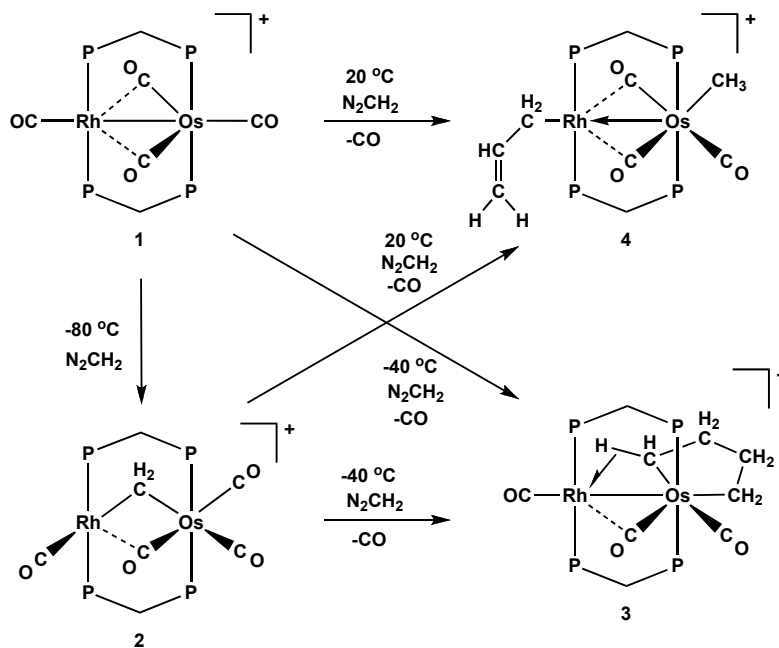
and protonation by methanol accompanied by cation exchange yields the metal hydride salt $[\text{PPN}][\text{M}'(\text{H})(\text{CO})_4]$ (PPN = bis(triphenylphosphoranylidene)ammonium).⁵¹ Reaction of this carbonylate with the bis-dppm complex $[\text{M}(\text{dppm})_2][\text{Cl}]$ ($\text{M} = \text{Rh},^{58} \text{Ir}^{53}$) yields the neutral binuclear hydride, $[\text{MM}'(\text{H})(\text{CO})_3(\text{dppm})_2]$. Subsequent protonation (with triflic acid (HOTf) in this case) yields the cationic dihydride $[\text{MM}'(\text{H})_2(\text{CO})_3(\text{dppm})_2][\text{OTf}]$.⁵¹⁻
⁵⁴ Finally, reaction with CO results in the elimination of H_2 and the addition of one CO ligand to give the tetracarbonyl species $[\text{MM}'(\text{CO})_4(\text{dppm})_2][\text{OTf}]$, the precursors in much of the chemistry studied in the Cowie group. As mentioned earlier, the majority of the work presented with this dissertation focuses on the reactivity of the IrRu metal combination, with the exception of Chapter 2, which focuses on the RhOs and RhRu systems.

1.2 Transformations of Interest

1.2.1 Reactions of Bridging Methylene Groups/Generation of Substituted Bridging Alkylidenes

As noted earlier, a number of mechanistic proposals have been postulated for the formation of hydrocarbons from syn gas in the FT process, outlining the importance of surface-bound methylene units in carbon-carbon chain growth. Previously in our group, a series of methylene-bridged complexes were prepared in order to investigate the coupling of methylene units. In the case of the RhOs metal combination, up to four diazomethane-generated methylene units can be incorporated and coupled to selectively yield different products, depending on reaction conditions, as outlined in Scheme 1.3. Addition of diazomethane at $-78\text{ }^\circ\text{C}$ to the tetracarbonyl compound, $[\text{RhOs}(\text{CO})_4(\text{dppm})_2][\text{OTf}]$ (**1**), results in the incorporation of one methylene unit, giving the methylene-bridged species $[\text{RhOs}(\text{CO})_4(\mu\text{-CH}_2)(\text{dppm})_2][\text{OTf}]$ (**2**). Treatment of either **1** or **2** with an excess of diazomethane at approximately $-40\text{ }^\circ\text{C}$ results in the coupling of four methylene units to yield the osmacyclic compound, $[\text{RhOs}(\text{C}_4\text{H}_8)(\text{CO})_3(\text{dppm})_2][\text{OTf}]$ (**3**). Reaction of **1** or **2** with diazomethane at ambient

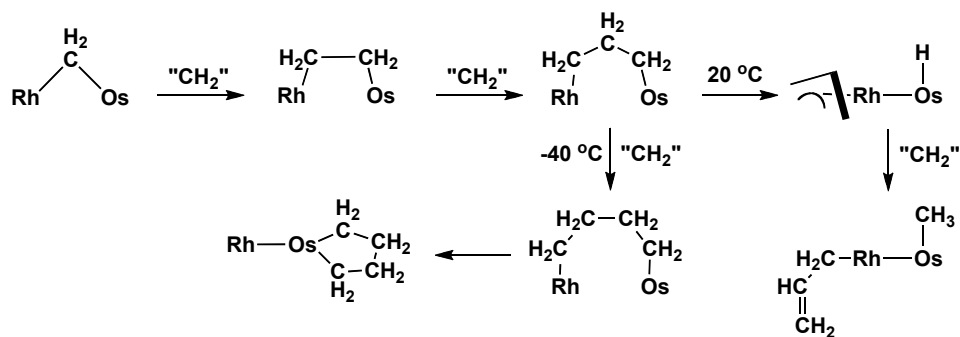
Scheme 1.3



temperature gives a third product, $[\text{RhOs}(\text{C}_3\text{H}_5)(\text{CH}_3)(\text{CO})_3(\text{dppm})_2][\text{OTf}]$ (4), which, like compound 3, has formed by the incorporation of four diazomethane-generated methylene units. Interestingly, warming 3 does not result in the formation of 4. Furthermore, addition of H_2 to compounds 2-4 resulted in the formation of methane (from compounds 2 and 4),^{59,60} propene (from compound 4)⁵⁹ or butane (from compound 3),⁵⁹ modeling the formation of a range of linear hydrocarbons in the FT process.

Based on a series of ^{13}C and ^2H labeling experiments, the mechanism shown in Scheme 1.4 was proposed. This proposal involves the sequential coupling of methylene

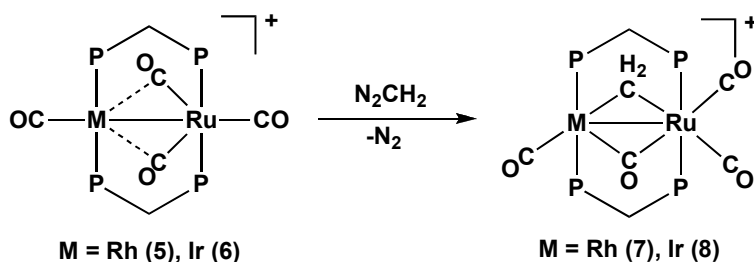
Scheme 1.4



units to give C₂- and C₃-bridged intermediates. At -40 °C coupling of a fourth methylene unit gives a C₄-bridged intermediate, followed by rearrangement to yield compound **3**, whereas at higher temperatures, β-H elimination followed by the incorporation of an additional methylene unit to give compound **4** becomes competitive and dominates at 20 °C. In both cases this proposal is consistent with that of Dry, presented in Figure 1.1.²¹

Surprisingly, neither the RhRu nor IrRu system has proven effective at promoting carbon-carbon chain growth.^{52,54} Reaction of the tetracarbonyl species [MRu(CO)₄(dppm)₂][OTf] (M = Rh (**5**), Ir (**6**)) with diazomethane (N₂CH₂) over a range of temperatures gives only the methylene-bridged species [MRu(CO)₄(μ-CH₂)(dppm)₂][OTf] (M = Rh (**7**), Ir (**8**)) (see Scheme 1.5). Unlike the RhOs system, no further methylene-group incorporation is observed at ambient and lower temperatures.

Scheme 1.5



It was proposed that the key difference between the RhOs system, which promotes carbon-carbon chain growth, and the RhRu and IrRu systems, which do not, is the nature of the carbonyl in the bridging position of the methylene complexes **2**, **7**, and **8**, respectively. Although this carbonyl bridges in all three systems, its interaction with the group 9 metal is weakest in the RhOs system. The resulting lability of this carbonyl in compound **2** means that it is more readily displaced by the weak nucleophile diazomethane. This insipient unsaturation allows for the incorporation of additional methylene units.

In order to learn more about the putative C₂-, C₃- and C₄-bridged intermediates in the above methylene coupling transformation a number of studies were initiated to investigate their reactivity with respect to the carbon-carbon chain growth in the RhOs system. Moreover we wished to solidify our proposal regarding the importance of

hydrocarbyl-bridged species in this chemistry.^{61,62} However, since all of our previous work had addressed the reactivity of unsubstituted methylene units, we sought to investigate the influence of substituted alkylidenes. Two strategies were envisioned: first, the reaction of substituted diazoalkanes (N_2CRR') with the methylene-bridged compounds **2** and **7** in attempts to generate C_2 - (or higher) bridged species; and second, the generation of bridging alkylidene species, $[RhM'(CO)_4(\mu-CRR')(dppm)_2][OTf]$, via the reaction of the carbonyl species **1** and **5** with substituted diazoalkanes, and the investigation of the subsequent chemistry of these species. This work is presented in Chapter 2.

1.2.2 Migratory insertion

Carbonyl insertion involving metal alkyls,^{63,64} is a fundamental organometallic reaction and is one of the most important metal-mediated transformations at the industrial scale, playing a prominent role in a number of processes such as CO and ethylene copolymerization,⁶⁵⁻⁷⁰ methanol carbonylation,¹²⁻¹⁵ hydroformylation (the most widely used TM-mediated transformation at the industrial level),⁷¹⁻⁷³ and the formation of oxygenates in the **FT** process.^{74,75} The last example is heterogeneously catalyzed and poorly understood, whereas the former three are catalyzed by homogenous, monometallic, systems involving the late transition metals, and their mechanistic details are generally well understood. However, there has been increasing interest in bimetallic systems for the mediation of CO migratory insertion reactions,^{14,48,76} seeking to determine if the presence of an adjacent metal centre can influence the reactivity. For example, in the case presented earlier, Stanley and coworkers suggested that the adjacent Rh centres play a key role in the hydrogenolysis step in the hydroformylation of olefins.⁴⁸

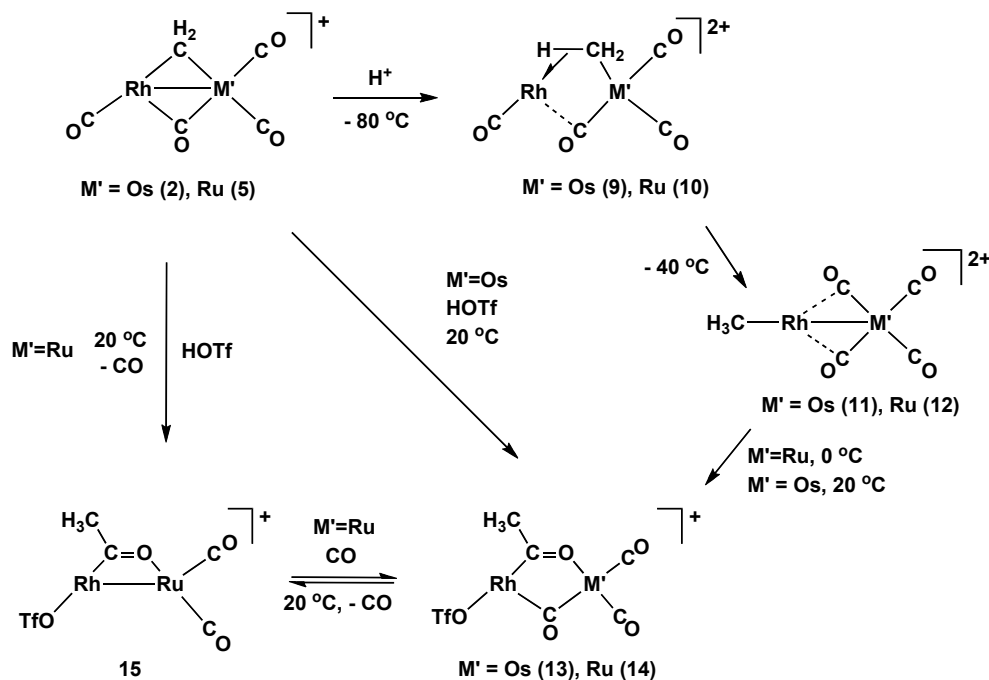
There has been significant interest in CO migratory insertion reactions promoted by heterobimetallic complexes as well,⁷³ with the hope that metal-metal cooperativity will give rise to an increase in the CO migratory insertion rate, generally the rate-limiting step in transformations involving CO insertion. For example, Komiya and coworkers reported an 80-fold increase in CO migratory insertion rates of a bimetallic PdCo system over an analogous monometallic Pd complex (unfortunately no comparison to an

analogous monometallic Co complexes was made).⁷⁶⁻⁷⁸ In a series of DFT studies they outlined the roles of the two metals in which alkyl group migration from Pd to Co occurred first, followed by CO migratory insertion at Co, and finally, migration of the acyl group back to the Pd centre to give the observed product. This illustrates a key feature of heterobimetallic metal-metal cooperativity, the involvement of each metal's specific properties to enhance the overall reactivity. In this example, migration of the alkyl group to the more labile Co metal results in more facile migratory insertion,⁶³ while the stronger Pd-C bond in the final product stabilizes the product. Together this serves to give a marked enhancement of the overall process over monometallic Pd (kinetic enhancement) or Co (thermodynamic enhancement) complexes.

It is clearly of interest to gain a better understanding of the roles of the adjacent metals in these bimetallic systems, and in the case of heterobimetallic systems, to determine at which metal each step occurs. Moreover, an improved understanding of processes occurring in bimetallic complexes may give us clues to the involvement of the different metals on bimetallic surfaces during related processes. For example, it was mentioned above that CO migratory insertion may be involved in the formation of oxygenates in the **FT** process and surprisingly, this is still very poorly understood. We aim to gain a more complete picture of oxygenate formation in **FT** chemistry using bimetallic systems. In two related studies of the RhOs and RhRu combinations the roles of the different metals were investigated through the individual steps of the transformation, from bridging methylene to bridging acyl groups, much as might occur on a metal surface in the formation of oxygenates in the **FT** reaction.

To a first approximation, the reactivity of both systems is the same, as shown in Scheme 1.6 below. Protonation of **2** or **5** at $-80\text{ }^{\circ}\text{C}$ generates the bridged, agostic methyl compounds, $[\text{RhM}'(\text{CO})_4(\mu\text{-CH}_3)(\text{dppm})_2][\text{OTf}]_2$ ($\text{M}' = \text{Os}$ (**9**), Ru (**10**)) in which the methyl groups are unsymmetrically bridging the two metal centres, like in **I-B** of Chart 1.1. Warming to $-40\text{ }^{\circ}\text{C}$ results in the migration of the methyl group from the group 8 metal to Rh, where it is terminally bound, to give the intermediates $[\text{RhM}'(\text{CO})_4(\text{CH}_3)(\text{dppm})_2][\text{OTf}]_2$ ($\text{M}' = \text{Os}$ (**11**), Ru (**12**)), and further warming results

Scheme 1.6



* dppm groups omitted for clarity

in migratory insertion to give the acetyl-bridged complexes $[\text{RhM}'(\text{CO})_3(\text{OTf})(\mu\text{-C}(\text{CH}_3)\text{O})(\text{dppm})_2][\text{OTf}]$ ($\text{M}' = \text{Os}$ (**13**), Ru (**14**)). However, the migratory insertion process is more facile for the RhRu combination, occurring at only $0\text{ }^\circ\text{C}$, compared to RhOs which requires ambient temperature. Moreover spontaneous, reversible loss of one CO ligand is observed only for the RhRu combination to give the dicarbonyl species $[\text{RhRu}(\text{CO})_3(\text{OTf})(\mu\text{-C}(\text{O})\text{CH}_3)(\text{dppm})_2][\text{OTf}]$ (**15**).

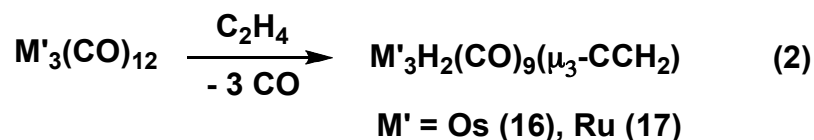
An important observation comes from these two parallel studies; in both systems the migratory insertion process is occurring at Rh and although not intimately involved in this step, the group 8 metal influences the lability of the transformation - the RhRu system displays more facile migratory insertion. Presumably the increased lability of Ru over Os results in more facile migration of a carbonyl from the group 8 metal to the Rh centre at which migratory insertion occurs.⁶³

Clearly it was of interest to investigate the IrRu system in this transformation to compare and contrast its reactivity with that of both the RhOs and RhRu metal

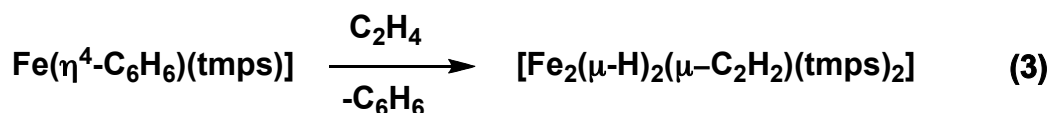
combinations. With Ir, an obvious question is how the stronger Ir–C bond will influence the reactivity. Will migratory insertion still occur at the group 9 metal, or will it instead occur at the more labile Ru? Moreover, the CATIVA[®] process utilizes an IrRu system for the carbonylation of methanol, a process for which migratory insertion is known to be pivotal. Although it has been established that the role of Ru in this process is iodide removal from the iridium iodo precursor, making migratory insertion more facile (the rate-limiting step in Ir-mediated migratory insertion), the potential that this pair of metals may be capable of more extensive metal-metal cooperativity is appealing. The study presented in Chapter 3 focuses on the steps in the conversion of a bridging methylene unit into a bridging acetyl group and aims to understand the differences that arise from metal substitution.

1.2.3 Olefin Activation

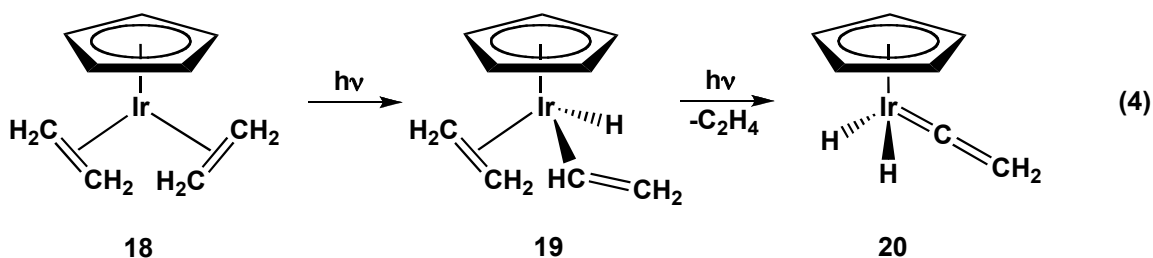
The cleavage of the strong C-H bond is an important step in the transformations of small organic substrates into larger more complex molecules.⁷⁹⁻⁸² Numerous systems have been developed, both heterogeneous and homogenous ones, that are capable of the cleavage, or “activation”, of the C-H bond.^{30,81-86} However, very few systems have been reported that are capable of activating multiple C-H bonds on the same carbon atom, i.e. geminal C-H activation. In most cases, these reports involve the activation of geminal C-H bonds of ancillary ligands, or substrates that have strong binding affinities through the presence of heteroatoms.^{82,85-96} In both cases, precoordination places the carbon atom bearing the C-H bonds in a position that is favourable for multiple C-H bond cleavage steps. There have been very few reports of geminal C-H activation of hydrocarbon substrates, such as α -olefins, that do not contain heteroatoms. Only five systems have been reported that can effect such a transformation.⁹⁷⁻¹⁰² The first report by Deeming and Underhill in 1972, involved the reaction shown in equation 2 in which treatment of the $M'_3(CO)_{12}$ ($M' = Os,$ ⁹⁷ Ru ⁹⁹) clusters in refluxing octane with an ethylene rich atmosphere yields the $\mu_3:\eta^1:\eta^1:\eta^2$ -vinylidene complexes, $[M'_3H_2(CCH_2)(CO)_9]$ ($M' = Os$ (**16**), Ru (**17**)).



Ten years later Green and coworkers would report that the mononuclear Fe complex $[Fe(\eta^4-C_6H_6)(tmps)]$ ($tmps = (Me)Si(CH_2PMe_2)_3$) reacts with ethylene to give the diiron vinylidene-bridged dihydride complex $[Fe_2(\mu-H)_2(\mu-C_2H_2)(tmps)_2]$,¹⁰¹ in which the vinylidene bridge has been formed by the cleavage of two geminal C-H bonds of the ethylene substrate (see equation 3 below).



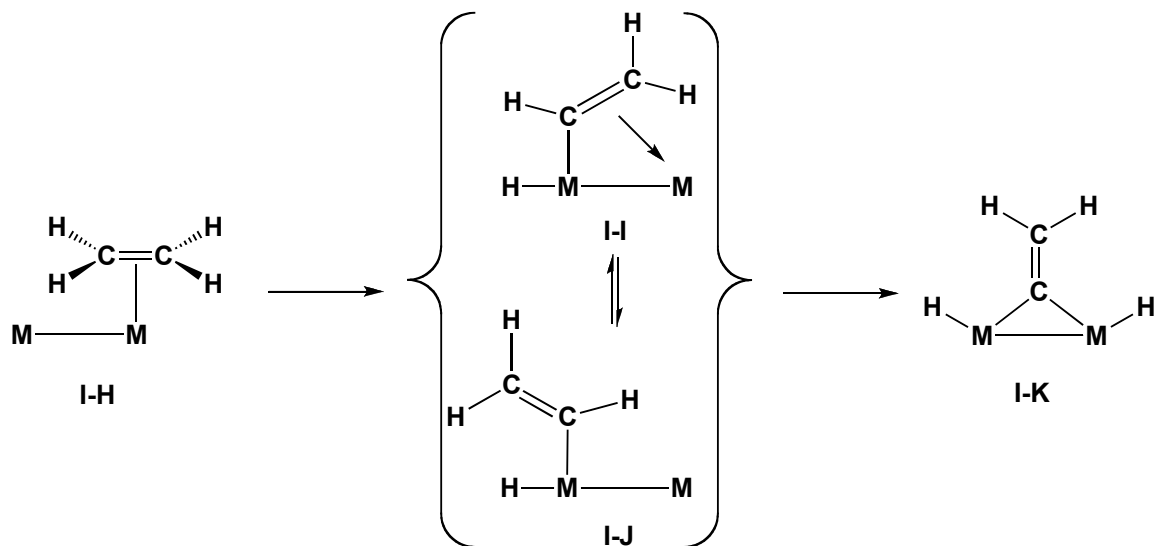
More recently, Perutz and coworkers observed a third example; they reported that the “piano-stool” complex, $[CpIr(C_2H_4)_2]$ (**18**), isolated in an Ar matrix, could undergo the photochemically-induced, stepwise activation of one and two geminal C-H bonds of an ethylene ligand to give the respective compounds, $[CpIr(H)(C_2H_4)(C_2H_3)]$ (**19**) and $[CpIr(H)_2(C_2H_2)]$ (**20**) (equation 3).¹⁰²



In the most recently published example of geminal C-H activation, our group reported that the diiridium complex, $[Ir_2(CH_3)(CO)_2(dppm)_2][OTf]$ (**21**) (Scheme 1.7), promotes the cleavage of two geminal C-H bonds in butadiene under ambient conditions to give the bridging vinylvinylidene complex, $[Ir_2(H)_2(CH_3)(CO)_2(\mu-C=C(H)-C(H)=CH_2)(dppm)_2][OTf]$ (**22**).¹⁰³ Low-temperature NMR spectroscopy experiments revealed initial binding of the butadiene occurs *via* an $\eta^2:\eta^2$ binding mode to give the

undergo subsequent activation by the adjacent metal to yield the bridging vinylidene group (I-K).

Chart 1.3



No evidence of such geminal C-H activation had been reported for mixed-metal complexes, so it was of interest to establish whether an IrRu system, related to the above Ir₂ systems, was capable of such reactivity. If so, we sought to determine the roles of the adjacent metals in the multiple activations. Neither the RhOs (**4**) nor RhRu (**3**) systems have been observed to react with terminal olefins in this manner. Our results on geminal activation by the IrRu system are presented in Chapter 4.

1.3References

1. Bielawski, C. W.; Grubbs, R. H. *Prog. Polym. Sci.* **2007**, *32*, 1.
2. Grubbs, R. H. *Angew. Chem. Int. Ed.* **2006**, *45*, 3760.
3. Grubbs, R. H. *Tetrahedron* **2004**, *60*, 7117.
4. Grubbs, R. H.; Miller, S. J.; Fu, G. C. *Acc. Chem. Res.* **1995**, *28*, 446.
5. Hoveyda, A. H.; Zhugralin, A. R. *Nature* **2007**, *450*, 243.
6. Novak, B. M.; Risse, W.; Grubbs, R. H. *Adv. Polym. Sci.* **1992**, *102*, 47.
7. Schrock, R. R. *Angew. Chem. Int. Ed.* **2006**, *45*, 3748.
8. Schrock, R. R.; Czekelius, C. *Adv. Syn. Cat.* **2007**, *349*, 55.

9. Schrock, R. R.; Hoveyda, A. H. *Angew. Chem. Int. Ed.* **2003**, *42*, 4592.
10. Tsang, W. C. P.; Hultsch, K. C.; Alexander, J. B.; Bonitatebus, P. J.; Schrock, R. R.; Hoveyda, A. H. *J. Am. Chem. Soc.* **2003**, *125*, 2652.
11. Vougioukalakis, G. C.; Grubbs, R. H. *J. Am. Chem. Soc.* **2008**, *130*, 2234.
12. Howard, M. J.; Jones, M. D.; Roberta, M. S.; Taylor, S. A. *Catal. Today* **1993**, *18*, 325.
13. Yoneda, N.; Kusano, S.; Yasui, M.; Pujado, P.; Wilcher, S. *Appl. Catal.* **2001**, *221*, 253.
14. Haynes, A.; Maitlis, P. M.; Morris, G. E.; Sunley, G. J.; Adams, H.; Badger, P. W.; Bowers, C. M.; Cook, D. B.; Elliot, P. I. P.; Ghaffer, T.; Green, H.; Griffin, T. R.; Payne, M.; Pearson, J. M.; Taylor, M. J.; Vichers, P. W.; Watt, R. J. *J. Am. Chem. Soc.* **2004**, *126*, 2847.
15. Haynes, A.; Mann, B. E.; Morris, G. E.; Maitlis, P. M. *J. Am. Chem. Soc.* **1993**, *115*, 4093.
16. Domski, G. J.; Rose, J. M.; Coates, G. W.; Bolig, A. D.; Brookhart, M. *Prog. Polym. Sci.* **2007**, *32*, 30.
17. Li, H. B.; Marks, T. J. *Proc. Nat. Acad. Sci. U.S.A.* **2006**, *103*, 15295.
18. Matsugi, T.; Fujita, T. *Chem. Soc. Rev.* **2008**, *37*, 1264.
19. Terao, H.; Nagai, N.; Fujita, T. *J. Synth. Org. Chem Jpn.* **2008**, *66*, 444.
20. Dry, M. E. *J. Chem. Technol. Biotechnol.* **2002**, *77*, 43.
21. Dry, M. E. *ACS Symp. Ser.* **1987**, *328*, 18.
22. Maitlis, P. M. *J. Organomet. Chem.* **1995**, *500*, 239.
23. Maitlis, P. M.; Long, H. C.; Quyoum, R.; Turner, M. L.; Wang, Z. Q. *Chem. Commun.* **1996**, 1.
24. Maitlis, P. M.; Ma, F.; Martinez, J.; Byers, P. K.; Saez, I.; Sunley, G. J. *Adv. Chem. Ser.* **1992**, 565.
25. Cowie, M. *Can. J. Chem.* **2005**, *83*, 1043.
26. Bond, G. C. *Heterogenous Catalysis*; Claredon: Oxford, 1987.
27. Niemantsverdriet, J. W.; Moulijn, J. A.; van Leeuwen, P. W.; Santen, R. A. In *Catalysis*; Elsevier: Netherlands, 1993.
28. Campbell, I. M. *Catalysis on Surfaces*; Chapman and Hall: New York, 1988.

29. Muetterties, E. L. *Pure Appl. Chem.* **1982**, *54*, 83.
30. Fiedler, D.; Leung, D. H.; Bergman, R. G.; Raymond, K. N. *Acc. Chem. Res.* **2005**, *38*, 349.
31. Fischer, F.; Tropsch, H. *Brennst. Chem.* **1923**, *4*, 276.
32. Brady, R. C.; Pettit, R. *J. Am. Chem. Soc.* **1980**, *102*, 6181.
33. Brady, R. C.; Pettit, R. *J. Am. Chem. Soc.* **1981**, *103*, 1287.
34. Maitlis, P. M. *J. Mol. Catal. A: Chem.* **2003**, *204*, 55.
35. Sharpless, K. B. *Angew. Chem. Int. Ed.* **2002**, *41*, 2024.
36. Knowles, W. S. *Angew. Chem. Int. Ed.* **2002**, *41*, 1998.
37. Noyori, R. *Adv. Synth. Catal.* **2003**, *345*, 15.
38. Trost, B. M. *Proc. Nat. Acad. Sci. U.S.A.* **2004**, *101*, 5348.
50. see for example Ritleng, V.; Chetcuti, M. J. *Chem. Rev.* **2007**, *107*, 797 and references contained therein.
40. Elschenbroich, C. *Organometallics*; Third ed.; Wiley-VCH: Weinheim, Germany, 2006.
41. Herrmann, W. A. *Angew. Chem. Int. Ed.* **1982**, *21*, 117.
42. Hamilton, D. M. J.; Williams, W. S.; Stucky, G. D. *J. Am. Chem. Soc.* **1981**, *103*, 4255.
43. Ulmer, S. W.; Skarstad, P. M.; Burlitch, J. M.; Hughes, R. E. *J. Am. Chem. Soc.* **1973**, *95*, 4469.
44. Burlitch, J. M.; Petersen, R. B. *J. Organomet. Chem.* **1970**, *24*, C65.
45. Gainsford, G. J.; Schrieke, R. R.; Smith, J. D. *J. Chem. Soc. Chem. Commun.* **1972**, 650.
46. Schrieke, R. R.; Smith, J. D. *J. Organomet. Chem.* **1971**, *31*, C46.
47. Tilley, T. D.; Andersen, R. A. *J. Chem. Soc. Chem. Commun.* **1981**, 985.
48. Herrmann, W. A.; Biersack, H.; Zeigler, M. L.; Weidenhammer, K.; Siegel, R.; Rehder, D. *J. Am. Chem. Soc.* **1981**, *103*, 1692.
49. Broussard, M. E.; Juma, B.; Train, S. G.; Peng, W. J.; Laneman, S. A.; Stanley, G. G. *Science* **1993**, *260*, 1784.
50. Anderson, D. J.; McDonald, R.; Cowie, M. *Angew. Chem. Int. Ed.* **2007**, *46*, 3741.

51. Antonelli, D. M.; Cowie, M. *Organometallics* **1990**, *9*, 1818.
52. Dell'Anna, M. M.; Trepanier, S. J.; McDonald, R.; Cowie, M. *Organometallics* **2001**, *20*, 88.
53. Hilts, R. W.; Franchuk, R. A.; Cowie, M. *Organometallics* **1991**, *10*, 1297.
54. Rowsell, B. D.; Trepanier, S. J.; Lam, R.; McDonald, R.; Cowie, M. *Organometallics* **2002**, *21*, 3228.
55. Walker, M. W.; Ford, P. C. *J. Organomet. Chem.* **1981**, *214*, C43.
56. Geog, R. D.; Knox, S. A. R.; Stone, F. A. G. *J. Chem. Soc. Dalton Trans.* **1973**, 972.
57. Collman, J. P.; Murphy, D. W.; Fleisher, E. B.; Swift, D. *Inorg. Chem.* **1974**, *13*, 1.
58. James, B. R.; Mahajan, D. *Can. J. Chem.* **1979**, 180.
59. Trepanier, S. J.; Dennett, J. N. L.; Sterenberg, B. T.; McDonald, R.; Cowie, M. *J. Am. Chem. Soc.* **2004**, *126*, 8046.
60. Samant, R. G.; Cowie, M. *Unpublished Work*; University of Alberta: Edmonton AB, Canada 2005.
61. Wigginton, J. R.; Chokshi, A.; Graham, T. W.; McDonald, R.; Ferguson, M. J.; Cowie, M. *Organometallics* **2005**, *24*, 6398.
62. Chokshi, A.; Rowsell, B. D.; Trepanier, S. T.; Ferguson, M. J.; Cowie, M. *Organometallics* **2004**, *23*, 4759.
63. Collman, J. P.; Hegedus, L. S.; Norton, J. R.; Finke, R. G. *Principles and Applications of Organotransition Metal Chemistry*; University Science Books: Mill Valley, CA, 1987.
64. Niu, S.; Hall, M. B. *Chem. Rev.* **2000**, *100*, 353.
65. Sen, A. *Acc. Chem. Res.* **1993**, *26*, 303.
66. Drent, E.; Budzelaar, P. H. M. *Chem. Rev.* **1996**, *96*, 663.
67. Bianchini, C.; Meli, A.; Oberhauser, W. *J. Chem. Soc. Dalton Trans.* **2003**, 2627.
68. Cavinato, G.; Vavasar, A.; Anadio, E.; Toniolo, L. *J. Mol. Catal. A: Chem.* **2007**, *278*, 251.
69. Rampersad, M. V.; Zuidema, E.; Ernsting, J. M.; van Leeuwen, P. W.; Darensbourg, M. Y. *Organometallics* **2007**, *26*, 783.

70. Muñoz-Moreno, B. K.; Claver, C.; Ruij, A.; Bianchini, C.; Meli, A.; Oberhauser, W. *J. Chem. Soc. Dalton Trans.* **2008**, 274.
71. Pruet, R. L. *Adv. Organomet. Chem.* **1979**, 17, 1.
72. Pruet, R. L. *Chem. Educ.* **1986**, 63, 196.
73. Trzeciak, A. M.; Zjolkowski, J. J. *Coord. Chem. Rev* **1999**, 190-192, 883.
74. Rowsell, B. D.; McDonald, R.; Cowie, M. *Organometallics* **2004**, 23, 3873.
75. Trepanier, S. T.; McDonald, R.; Cowie, M. *Organometallics* **2003**, 22, 2638.
76. Komiya, S.; Yasuda, T.; Hirano, M.; Fukuoka, M. *J. Mol. Catal. A: Chem.* **2000**, 159, 63.
77. Fukuska, A.; Fukugawa, S.; Hirano, M.; Koga, N.; Komiya, S. *Organometallics* **2001**, 20, 2065.
78. Fukuska, A.; Fukugawa, S.; Hirano, M.; Komiya, S. *Chem. Lett.* **1997**, 377.
79. Lewis, J. C.; Bergman, R. G.; Ellman, J. A. *Acc. Chem. Res.* **2008**, 41, 1013.
80. Dyker, G. *Handbook of C-H Transformations*; Wiley-VCH: Weinheim, 2005.
81. Labinger, J. A.; Bercaw, J. E. *Nature* **2002**, 417, 507.
82. Slugovc, C.; Padilla-Martinez, I.; Sirol, S.; Carmona, E. *Coord. Chem. Rev.* **2001**, 213, 129.
83. Bergman, R. G. *Adv. Chem. Ser.* **1992**, 211.
84. Crabtree, R. H. *J. Chem. Soc. Dalton Trans.* **2001**, 2437.
85. Gusev, D. G.; Lough, A. J. *Organometallics* **2002**, 21, 2601.
86. Hong, S. H.; Chlenov, A.; Day, M. W.; Grubbs, R. H. *Angew. Chem. Int. Ed.* **2007**, 46, 5148.
87. Kee, T. P.; Gibson, V. C.; Clegg, W. *J. Organomet. Chem.* **1987**, 325, C14.
88. Gutierrez-Puebla, E.; Monge, A.; Nicasio, M. C.; Perez, P. J.; Poveda, M. L.; Carmona, E. *Chem. Eur. J.* **1998**, 4, 2225.
89. Slugovc, C.; Mereiter, K.; Trofimenko, S.; Carmona, E. *Angew. Chem. Int. Ed.* **2000**, 39, 2158.
90. Slugovc, C.; Mereiter, K.; Trofimenko, S.; Carmona, E. *Helv. Chim. Acta.* **2001**, 84, 2868.
91. Lee, D.-G.; Chen, J.; Fuller, J. W.; Crabtree, R. H. *Chem. Commun.* **2001**, 213.
92. Kakiuchi, F.; Chatani, N. *Adv Synth. Catal.* **2003**, 345, 1077.

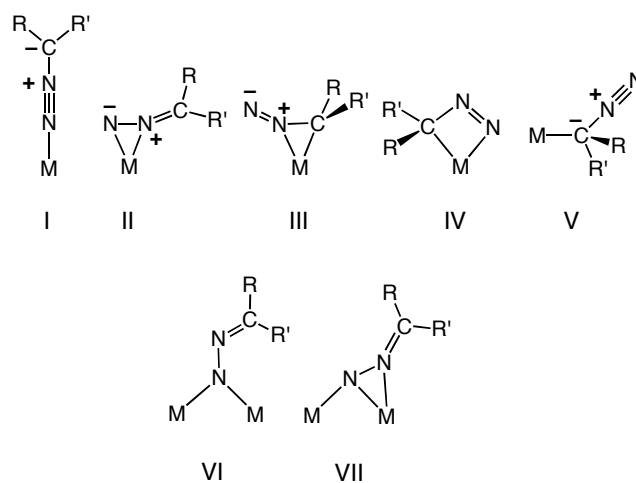
93. Crabtree, R. H. *J. Organomet. Chem.* **2004**, 689, 4083.
94. Clot, E.; Chen, J.; Lee, D.-G.; Sung, S. Y.; Appelhans, L. N.; Faller, J. W.; Crabtree, R. H.; Eisenstien, O. *J. Am. Chem. Soc.* **2004**, 126, 8795.
95. Grotjahn, D. B.; Hoerter, J. M.; Hubbard, J. L. *J. Am. Chem. Soc.* **2004**, 126, 8866.
96. Rankin, M. A.; MacLean, D. F.; Schatte, G.; McDonald, R.; Stradiotto, M. *J. Am. Chem. Soc.* **2007**, 129, 15855.
97. Deeming, A. J.; Underhill, M. *J. Organomet. Chem.* **1972**, 42, C60.
98. Deeming, A. J.; Hasso, S.; Underhill, M. *J. Chem. Soc., Chem. Commun.* **1974**, 807.
99. Deeming, A. J.; Underhill, M. *J. Chem. Soc., Chem. Commun.* **1973**, 277.
100. Deeming, A. J.; Underhill, M. *J. Chem. Soc., Dalton Trans.* **1974**, 1415.
- 101 (a) Boncella, J. M.; Green, M. L. H.; O'Hare, D. *J. Chem. Soc., Chem. Commun.* **1986**, 618. (b) Boncella, J. M.; Green, M. L. H. *J. Organomet. Chem.* **1987**, 325, 217.
102. Bell, T. W.; Haddleton, D. M.; McCamley, A.; Partridge, M. G.; Perutz, R. N.; Willner, H. *J. Am. Chem. Soc.* **1990**, 112, 9212.
103. Ristic-Petrovic, D.; Torkelson, J. R.; Hilts, R. W.; McDonald, R.; Cowie, M. *Organometallics* **2000**, 19, 4432.
104. Slaney, M.; Cowie, M. *Unpublished Work*; University of Alberta: Edmonton AB, Canada 2008.

Chapter 2: Coordination and Activation of Diazoalkanes in the Presence of Rh/Ru and Rh/Os Metal Combinationsⁱ

2.1 Introduction

Diazoalkanes are important reagents in both cyclopropanation reactions¹⁻⁵ and for the generation of metallacarbene complexes.^{2,5-7} In addition to their role as carbene sources, the coordination chemistry of diazoalkanes is equally rich,^{5,6,8,9} displaying a variety of coordination modes as shown in Chart 1.⁶ When

Chart 2.1



bound to a single metal center two coordination modes have commonly been observed, involving either η^1 , end-on coordination (type **I**),¹⁰⁻³² which can assume a number of valence-bond formulations and associated geometries, or the η^2 -NN side-on coordination (type **II**).^{20,33-39} In addition, three other coordination modes can also be envisioned although they have yet to be observed: an η^2 -NC side-on coordination (type **III**), a four-member “MCNN” metallacycle (type **IV**), and a

ⁱ The work presented in this chapter has been previously reported. See Samant, R. G.; Graham, T.W.; Rowsell, B. D.; McDonald, R; Cowie, M. *Organometallics* **2008**, 27, 3070.

η^1 -C-bound coordination (type **V**). In binuclear complexes containing two metal centers, diazoalkane coordination at either one of the metals, as illustrated above in structures **I** – **V**, can again occur, however, additional modes are also possible in which the diazoalkane bridges the pair of metals. Two bridging modes have been observed – one in which the diazoalkane ligand bridges both metals through the terminal nitrogen (type **VI**)⁴⁰⁻⁴³ and a related mode in which the diazoalkane again bridges *via* the terminal nitrogen while also binding in an η^2 -fashion to one metal *via* the pair of nitrogen atoms (type **VII**).⁴⁴⁻⁵⁴

Our primary interest in diazoalkanes has stemmed from their utility as synthons for the generation of alkylidene-bridged bimetallic compounds, and in the subsequent carbon-carbon bond formation involving these alkylidene units.⁵⁵⁻⁶⁵ In a previous study, and also briefly discussed in Chapter 1, we reported facile methylene-group incorporation and coupling by reaction of $[\text{RhOs}(\text{CO})_4(\text{dppm})_2][\text{X}]$ (**1**) ($\text{X} = \text{CF}_3\text{SO}_3; \text{BF}_4$) with diazomethane to give either $[\text{RhOs}(\text{CO})_4(\mu\text{-CH}_2)(\text{dppm})_2][\text{X}]$ (**2**), $[\text{RhOs}(\text{C}_4\text{H}_8)(\text{CO})_3(\text{dppm})_2][\text{X}]$ (**3**) or $[\text{RhOs}(\text{C}_3\text{H}_5)(\text{CH}_3)(\text{CO})_3(\text{dppm})_2][\text{X}]$ (**4**), depending on reaction temperature.^{56, 63} On the basis of labeling studies we proposed a reaction sequence in which the coupling of methylene groups occurred *via* C_2H_4 - and C_3H_6 -bridged intermediates. Surprisingly, the analogous Rh/Ru species (**5**) did not promote the coupling of methylene groups, but instead incorporated only a single methylene group to give $[\text{RhRu}(\text{CO})_4(\mu\text{-CH}_2)(\text{dppm})_2][\text{X}]$ (**7**).⁵⁸ In order to gain a better understanding of the above methylene-coupling sequence, we set out to generate stable C_2 - and C_3 -bridged analogues of the putative C_2H_4 - and C_3H_6 -bridged intermediates noted above, incorporating substituents into the hydrocarbyl fragments. Two strategies were adopted, involving either the reaction of substituted diazoalkanes with the methylene-bridged Rh/Os species **2** and the related tricarbonyl, $[\text{RhOs}(\text{CO})_3(\mu\text{-CH}_2)(\text{dppm})_2][\text{OTf}]$ (**24**), in attempts to generate substituted C_2 or higher fragments, or through the generation of the alkylidene-bridged products, $[\text{RhOs}(\text{CO})_n(\mu\text{-CRR}')(\text{dppm})_2][\text{X}]$, the chemistry of which, with regards to C-C bond formation, could subsequently be pursued. In addition, we also investigated the related chemistry of the Rh/Ru metal

combination, in hopes of learning more about the subtle reactivity differences that can arise from different metal combinations. This chemistry is described herein.

2.2 Experimental Section

2.2.1 General Comments:

All solvents were dried (using appropriate drying agents), distilled before use and stored under nitrogen. Reactions were performed under an argon atmosphere using standard Schlenk techniques. Triosmium dodecacarbonyl was purchased from Colonial Metals Inc., while rhodium trichloride hydrate and triruthenium dodecacarbonyl were purchased from Strem Chemicals. Diazomethane was generated from Diazald[®], N₂¹³CH₂ was generated from suitably labelled Diazald[®] and diazoethane was generated from 1-ethyl-3-nitro-1-nitrosoguanidine (ENNG), all of which were obtained from Aldrich, as were ethyl diazoacetate (EDA) and trimethylsilyl diazomethane (TMSDM; 2M, Et₂O solution). The compounds [RhOs(CO)₄(dppm)₂][CF₃SO₃] (**1**),⁶⁶ [RhRu(CO)₄(dppm)₂][CF₃SO₃] (**5**),⁵⁸ [RhOs(CO)₄(μ-CH₂)(dppm)₂][CF₃SO₃] (**2**),⁵⁶ [RhRu(CO)₄(μ-CH₂)(dppm)₂][CF₃SO₃] (**7**),⁵⁸ [RhOs(CO)₃(μ-CH₂)(dppm)₂][CF₃SO₃] (**24**),⁵⁶ and [RhRu(CO)₃(μ-CH₂)(dppm)₂][CF₃SO₃] (**25**)⁵⁸ were prepared by literature procedures. Diethyl diazomalonate (DEDM) was prepared by a standard route.⁶⁷

The ¹H NMR, and ³¹P{¹H} NMR spectra were recorded on a Varian Inova 400 spectrometer operating at 399.8 MHz and 161.8 MHz, respectively. ¹³C{¹H} NMR and all variable- temperature NMR spectra were recorded on a Varian Unity spectrometer operating at 100.6 MHz for ¹³C, 161.9 MHz for ³¹P and 399.8 MHz for ¹H. Infrared spectra were recorded in CH₂Cl₂ solution on a Nicolet Avatar 370 DTGS spectrometer unless otherwise noted. Elemental analyses were performed by the microanalytical services within the department. Mass Spectrometry measurements were performed by the electro-spray ionization technique on a Micromass ZabSpec TOF spectrometer in the mass spectrometry

facility of the department. Spectroscopic data for all new compounds are given in Table 2.1. Photolysis experiments were conducted in NMR tubes that were irradiated using a Hanovia 450 Watt high pressure mercury lamp placed six inches from the reaction vessel, all of which was enclosed in a photolysis chamber.

Table 2.1. Spectroscopic Data for the Compounds Prepared

Compound	IR (cm ⁻¹) ^a	NMR ^{c, d}	
		$\delta(^3\text{P}\{\text{H}\})^e$	$\delta(\text{H})^f$
[RhOs(CO) ₃ (η^2 -CH ₂ =CHCO ₂ Et)(dppm) ₂]-[CF ₃ SO ₃] (26).	2047 (m), 1981 (m), 1942 (m), 1683 (m), $\nu(\text{C}=\text{C})$ 1558 (w)	25.3 (dm, 2P, ¹ J _{RhP} = 113 Hz), -4.1 (dm, 1P, ² J _{PP} = 259 Hz), -10.5 (dm, 1P, ² J _{PP} = 259 Hz)	$\delta(^{13}\text{C}\{\text{H}\})^f$ CH ₂ CHCO ₂ Et: CH ₂ : 3.80 (s) OsCO: 182.8 (t, ² J _{CP} = 8.0 Hz), 185.5 (t, ² J _{CP} = 7.1 Hz); RhCO: 182.5 (dt, ¹ J _{RhC} = 77.6, ² J _{CP} = 16.8)
[RhOs(CO) ₃ (μ - η^1 : η^1 -N ₂ C(CO ₂ Et)COH)(dppm) ₂]-[CF ₃ SO ₃] (27) ^b	3058 (m), 2020 (s), 1970 (s, br), 1633 (s), ^f	0.3 (m, 2P), 28.1 (dm, 2P, ¹ J _{RhP} = 147 Hz)	dppm: CH ₂ : 4.47 (br, m, 1H), 4.27 (br, m, 1H), 4.10 (br, m, 1H), 3.12 (br, m, 1H) CH ₂ CHCO ₂ Et: CH ₂ : 1.08 (br, m, 1H, ³ J _{HH} = 8 Hz, ¹ J _{HC} = 144 Hz), 1.72 (br, m, 1H, ³ J _{HH} = 8 Hz, ¹ J _{HC} = 157 Hz); CH: 2.77 (br, m, 1H, br,s, 1H, ³ J _{HH} = 8 Hz); CH ₂ : 4.23 (qq, 2H, ³ J _{HH} = 7 Hz); CH ₃ : 1.32 (t, 3H, ³ J _{HH} = 7 Hz)
[RhRu(CO) ₃ (μ - η^1 : η^1 -N ₂ C(CO ₂ Et)COH)(dppm) ₂]-[CF ₃ SO ₃] (28)	3054 (s), 2026 (m), 1969 (m), 1997 (m), 1691 (m), ^f	37.0 (m, 2P), 28.2 (dm, 2P)	OsCO: 177.9 (t, ² J _{CP} = 8.5 Hz), 179.6 (t, ² J _{CP} = 13.9 Hz); RhCO: 195.5 (dt, ¹ J _{RhC} = 63.2 Hz, ² J _{CP} = 15.6 Hz) dppm: CH ₂ : 17.9 (m) CO ₂ Et: CH ₂ : 61.2 (s); CH ₃ : 14.7 (s) COH: 231.6 (t, ² J _{CP} = 8.3 Hz) RuCO: 194.3 (t, ² J _{CP} = xx Hz), 197.8 (t, ² J _{CP} = 10.7 Hz); RhCO: 196.8 (dt, ¹ J _{RhC} = 64.7 Hz, ² J _{CP} = 15 Hz) COH: 244.1 (t, ² J _{CP} =)

Table 2.1. (continued) Spectroscopic Data for the Compounds Prepared

Compound	IR (cm ⁻¹) ^a	NMR ^{c, d}	
		$\delta(^3\text{P}\{\text{H}\})^c$	$\delta(^1\text{H})^e$ $\delta(^{13}\text{C}\{\text{H}\})^f$
[RhOs(CO) ₃ (μ-η ¹ :η ¹ -N ₂ C-(CO ₂ Et) ₂)(dppm) ₂]-[CF ₃ SO ₃] (29)	2027 (m), 1992 (s), 1963 (m), 1699 (m) ^f , 1690 (m) ^f ,	11.1 (m, 2P), 26.4 (dm, ¹ J _{RhP} = 151 Hz)	dppm: CH ₂ : 3.16 (m, 2H), 3.13 (m, 2H) CO ₂ Et: CH ₂ : 4.37 (q, 2H, ³ J _{HH} = 7 Hz), 1.86 (q, 2H, ³ J _{HH} = 7 Hz); CH ₃ : 1.41 (t, 3H, ³ J _{HH} = 7 Hz), 0.62, 3H, ² J _{HH} = 7 Hz)
[RhRu(CO) ₃ (μ-η ¹ :η ¹ -N ₂ C-(CO ₂ Et) ₂)(dppm) ₂]-[CF ₃ SO ₃] (30)	2036 (m), 1996 (s), 1969 (m), 1725 (w) ^f , 1641 (m) ^f ,	37 (m, 2P), 28.3 (dm, 2P, ¹ J _{RhP} = 148 Hz)	dppm: CH ₂ : 3.24 (m, 2H), 3.08 (m, 2H) CO ₂ Et: CH ₂ : 4.35 (q, 2H, ³ J _{HH} = 7 Hz), 1.91 (q, 2H, ³ J _{HH} = 7 Hz); CH ₃ : 1.40 (t, 3H, ³ J _{HH} = 7 Hz), 0.62 (t, 3H, ³ J _{HH} = 7 Hz)
[RhOs(CO) ₂] ⁻ (PMc ₃)(μ-η ¹ :η ¹ -N ₂ C(CO ₂ CH ₂ CH ₃) ₂ -(dppm) ₂][CF ₃ SO ₃] (31)	2092 (m), 2003 (m), 1752 (m), 1686 (m, br) ^f	-18.5(dt, 1P, ¹ J _{RhP} = 129 Hz, ² J _{Pp} = 42 Hz), 12.1 (m, 2P), 28.4 (dm, 2P, ¹ J _{RhP} = 162 Hz)	OsCO: 172.0 (t, ² J _{CP} = 7.6 Hz), 180.0 (t, ² J _{PC} = 6.0 Hz); RhCO: 195.5 (dt, ¹ J _{RhC} = 63.2 Hz, ² J _{CP} = 15.6 Hz) dppm: CH ₂ , 20.3 (m) CO ₂ Et: CH ₃ : 13.3 (s), 15.2 (s); CH ₂ : 60.0(s), 61.2 (s) N ₂ C: 125.9 (br,s); CO: 165.8 (s), 153.0
			RuCO: 197.0 (bs), 195.6(bs); RhCO: 195.4 (bd, ¹ J _{RhP} = 63.7 Hz) dppm: CH ₂ : 13.5 (m) CO ₂ Et: CH ₂ : 61.0(s), 59.8 (s); CH ₃ : 15.4 (s), 13.5 (s); C(O)O: 165.7 (s), 155.3 (s)
			OsCO: 171.0 (t, ² J _{CP} = 8 Hz), 181.0 (t, ² J _{CP} = 6.5 Hz)

Table 2.1. (continued) Spectroscopic Data for the Compounds Prepared

Compound	IR (cm ⁻¹) ^a	NMR ^{c,d}	
		$\delta(^3\text{P}\{\text{H}\})^e$	$\delta(^1\text{H})^e$ $\delta(^{13}\text{C}\{\text{H}\})^f$
[RhOs(CO) ₃ (η^1 -N ₂ CH-Si(CH ₃) ₃)(dppm) ₂]-[CF ₃ SO ₃] (32)	2059 (s), 1977 (m), 1804 (m)	1.0(m, 2P), 26.0 (dm, 2P), ¹ J _{RHP} = 115 Hz	RhCO: 181.2 (dm, 1C), ¹ J _{RhC} = 80.3 Hz OsCO: 194.6 (m, 2C), ¹ J _{Hc} = 3.3 Hz

^a IR abbreviations: s = strong, m = medium, br = broad. Dichloromethane solution; in units of cm⁻¹. ^b IR obtained by IR microscope. ^c NMR abbreviations: s = singlet, d = doublet, t = triplet, m = multiplet, br = broad, bs = broad singlet, bd = broad doublet. NMR data at 27 °C in CD₂Cl₂ unless otherwise indicated. ^d ³¹P chemical shifts referenced to external 85% H₃PO₄. ^e ¹H and ¹³C chemical shifts referenced to TMS. Chemical shifts for the phenyl carbons not given. ^f $\nu(\text{CO})$ for CO₂Et fragment.

2.2.2 Preparation of Compounds:

(a) [RhOs(CO)₃(η^2 -CH₂=C(H)CO₂CH₂CH₃)(dppm)₂][CF₃SO₃] (26). *Method (i):* A solution of compound **24** (19.2 mg, 0.015 mmol), dissolved in 0.7 mL of CD₂Cl₂ in an NMR tube and cooled to -78 °C, was treated with 1.7 μ L (0.016 mmol) of N₂C(H)CO₂Et *via* a gas-tight syringe. The NMR tube was then transferred to the NMR probe which had been precooled to -80 °C, and the reaction monitored by NMR spectroscopy while warming in 10 °C intervals. No change was observed below -20 °C. Holding the sample at -20 °C for 1.7 h resulted in the formation of the product (**37**) in a 3:2 ratio with unreacted compound **24**. After 1.7 h decomposition of **26** into numerous unidentified products began to occur. *Method (ii):* To a stirring deep red solution of compound **24** (30 mg, 0.023 mmol) in 1.5 mL of CH₂Cl₂ at 20 °C, was added 2.4 μ L of N₂C(H)CO₂Et (0.023 mmol). The solution instantly turned light brown and was left to stir for 5 min, then cooled to -80 °C to prevent rapid decomposition of the product. A beige solid was precipitated by the slow addition of 20 mL of pentane (precooled to -80 °C), the solvent was decanted by canula, the solid rinsed twice with 5 mL of Et₂O and finally dried *in vacuo* (yield 50% as determined by integration of the ³¹P NMR spectra relative to residual bis(triphenylphosphoranylidene) ammonium chloride; we were unable to separate compound **26** from the numerous unidentified decomposition products. HRMS *m/z* Calcd for C₆₀H₅₂O₅P₄RhOs (M⁺ - CF₃SO₃): 1247.1426. Found: 1247.1437.

(b) Reaction of compound 2 with diazoalkanes at ambient temperature. [RhOs(CO)₄(μ -CH₂)(dppm)₂][CF₃SO₃] (**2**) (10 mg, 0.008 mmol) was placed in an NMR tube and dissolved in 0.7 mL of CD₂Cl₂ at ambient temperature to produce a yellow solution. To this was added one equiv of diazoalkane either neat (EDA and DEDM), or as a 2 M ethereal solution (TMSDM). After 60 h the ³¹P and ¹H NMR spectra were recorded. In all cases the products detected were unreacted starting material (ca. 80%), compound **1** (ca. <10%), unidentified decomposition products (ca. 10%) and the corresponding olefin (H₂C=CRR'; R = H, R' = CO₂Et, SiMe₃; R = R' = CO₂Et).

(c) Reaction of compound 7 with diazoalkanes at ambient temperature. The reaction of 10 mg of [RhRu(CO)₄(μ -CH₂)(dppm)₂][CF₃SO₃] (**7**) (0.008 mmol) with either EDA, DEDM or TMSDM was carried out exactly as described in part (b). After 60 h ³¹P and ¹H NMR

spectroscopy revealed the products to be starting material (ca. 70%), compound **5** (ca. 10%), uncharacterized decomposition products (ca. 20%) and the corresponding olefin, as observed in part (b).

(d) Reaction of compound 24 with diazoalkanes at ambient temperature. One equiv of either EDA, DEDM or TMSDM was added to 15 mg (0.011 mmol) of $[\text{RhOs}(\text{CO})_3(\mu\text{-CH}_2)(\text{dppm})_2][\text{CF}_3\text{SO}_3]$ (**24**) in 0.7 mL of CD_2Cl_2 in an NMR tube at 22 °C. After one min the solution became lighter in color and after 20 min the complete disappearance of **24** and quantitative generation of the substituted olefin accompanied by compound **1** (ca. 10%) and numerous decomposition products (ca. 90%) was confirmed by ^{31}P and ^1H NMR spectroscopy.

(e) Reaction of compound 25 with diazoalkanes at ambient temperature. $[\text{RhRu}(\text{CO})_3(\mu\text{-CH}_2)(\text{dppm})_2][\text{CF}_3\text{SO}_3]$ (**25**) (15 mg, 0.012 mmol) was dissolved in 0.7 mL of CD_2Cl_2 in an NMR tube at 22 °C. The resulting yellow solution was treated with one equiv of each of the above diazoalkanes causing the solution to lighten in color within seconds. After 20 min ^{31}P and ^1H NMR spectroscopy indicated the presence of compound **5** (ca. 10%), the corresponding substituted olefin, and numerous uncharacterized decomposition products (ca. 90%).

(f) Reactions (d) and (e) at low temperature. Procedures (d) and (e) were repeated, but in this instance the solutions were cooled to -78 °C prior to the addition of the diazoalkane. After treatment with the diazoalkane at -78 °C, the sample was inserted into an NMR probe precooled to -80 °C. The reaction was monitored by NMR while warming in 10 °C intervals. In all cases, formation of a short-lived species spectroscopically similar to **26** (ca. 10% by integration) was observed at -20 °C along with numerous unidentified decomposition products. At temperature above -20 °C, only decomposition products were observed.

(g) $[\text{RhOs}(\text{CO})_3(\mu\text{-}\eta^1\text{:}\eta^1\text{-N}_2\text{C}(\text{CO}_2\text{CH}_2\text{CH}_3)\text{COH})(\text{dppm})_2][\text{CF}_3\text{SO}_3]$ (27**).** To a yellow solution of **1** (45 mg, 0.034 mmol) in 5 mL of CH_2Cl_2 at ambient temperature was added 40 μL of ethyl diazoacetate (EDA) as a 1 M ethereal solution. This mixture was allowed to stir for 24 h during which time no color change was noted. However, the ^{31}P NMR spectrum indicated the complete conversion to the product (**27**). Slow addition of 20 mL of Et_2O afforded a yellow powder which, after decanting the clear supernatant, was rinsed with two 5 mL washings of Et_2O before being dried under a stream of argon followed by drying *in vacuo* (yield 88%). HRMS: m/z Calcd for $\text{C}_{58}\text{H}_{50}\text{O}_6\text{N}_2\text{P}_4\text{RhOs}$ ($\text{M}^+ - \text{CF}_3\text{SO}_3$): 1289.1280. Found: 1289.1289.

(h) [RhRu(CO)₃(μ-η¹:η¹-N₂C(CO₂CH₂CH₃)COH)(dppm)₂][CF₃SO₃] (28). To a stirring yellow solution of 25 mg (0.020 mmol) of **5** in 15 mL of CH₂Cl₂ at ambient temperature, was added 55 μL (0.053 mmol) of N₂CH(CO₂Et). Over the course of 1 h the yellow solution turned bright orange, at which point it was concentrated to 2 mL followed by the slow addition of Et₂O to afford an orange powder. After removal of the clear supernatant, the product was recrystallized from CH₂Cl₂/Et₂O (1 mL/10 mL) yielding bright orange microcrystals which were isolated by filtration and dried *in vacuo* (yield 75%). Anal. Calcd for C_{62.1}H_{55.2}Cl_{0.2}F₃N₂O₁₁P₄RhRuS: C, 52.33; H 3.73; N, 2.07; Cl, 0.52. Found: C, 52.16; H, 3.74; N, 1.98; Cl, 0.54. The presence of 0.1 equiv of CH₂Cl₂ was confirmed by ¹H NMR spectroscopy in THF-d₈. HRMS *m/z* Calcd for C₅₈H₅₀O₆N₂P₄RhRu (M⁺ – CF₃SO₃): 1199.0718. Found: 1199.0718.

(i) [RhOs(CO)₃(μ-η¹:η¹-N₂C(CO₂CH₂CH₃)₂)(dppm)₂][CF₃SO₃] (29). Compound **1** (53 mg, 0.040 mmol) was dissolved in 5 mL of CH₂Cl₂ at ambient temperature yielding a yellow solution. To this solution was added 0.05 mL (0.24 mmol) of N₂C(CO₂CH₂CH₃)₂ causing the solution to darken slightly. The solution was allowed to stir for 24 h at which time the solution was dark orange and only the product, compound **29** was observed by ³¹P NMR spectroscopy. The solvent volume was reduced to 2 mL and a bright yellow powder was precipitated by the addition of 20 mL of Et₂O. After removing the clear supernatant, the yellow product was rinsed twice with 5 mL of Et₂O and the product dried under an argon stream and then *in vacuo* (yield 85%). Anal. Calcd for C_{61.1}H_{54.2}N₂O₁₀F₃SP₄Cl_{0.2}RhOs: C, 49.19; H, 3.66; N 1.89. Found: C, 48.70; H, 4.02; N, 1.73. The presence of 0.1 equiv of CH₂Cl₂ was confirmed by ¹H NMR spectroscopy in THF-d₈. HRMS *m/z* Calcd for C₆₀H₅₄O₇N₂P₄RhOs (M⁺ – CF₃SO₃): 1333.1542. Found: 1333.1526.

(j) [RhRu(CO)₃(μ-η¹:η¹-N₂C(CO₂CH₂CH₃)₂)(dppm)₂][CF₃SO₃] (30). 36 mg (0.028 mmol) of **5** was dissolved in 20 mL of CH₂Cl₂ at ambient temperature followed by the addition of 24 μL of N₂C(CO₂Et)₂ (0.14 mmol). The resulting yellow solution darkened slightly within 15 min. After 2 h, only compound **30** remained as confirmed by ³¹P NMR spectroscopy of the deep red solution from which a salmon-red product was precipitated by the slow addition of 30 mL of Et₂O. After removing the solvent, the precipitate was rinsed with two 5 mL portions of Et₂O and dried under a stream of argon then *in vacuo* (yield 82%). Anal. Calcd for

$C_{61}H_{54}F_3N_2O_{10}SP_4RhRu$: C, 52.63; H, 3.91; N, 2.01. Found: C, 52.26; H, 3.93; N, 1.91. HRMS m/z Calcd for $C_{60}H_{54}O_7N_2P_4RhRu$ ($M^+ - CF_3SO_3$): 1243.0980. Found: 1243.0980.

(k) $[RhOs(CO)_2(PMe_3)(\mu-\eta^1:\eta^1-N_2C(CO_2CH_2CH_3)_2)(dppm)_2][CF_3SO_3]$ (31). In an NMR tube at ambient temperature, 10 mg of compound **29** (0.0068 mmol) was dissolved in 0.7 mL of CD_2Cl_2 to which was added 7 μ L of a 1M solution of PMe_3 (in toluene) (0.007mmol). After 2.5 d quantitative conversion to the product (**31**) was confirmed by ^{31}P NMR spectroscopy. The solution was left to stand for a period of 2 weeks, over which time no further transformations were observed by ^{31}P NMR spectroscopy. Anal. Calcd for $C_{63}H_{63}F_3N_2O_{10}P_5RhOsS$: C, 48.97; H 4.11; N, 1.81; S, 2.08. Found: C, 49.18; H, 4.53; N, 1.74; S, 2.97.

(l) $[RhOs(CO)_3(\eta^1-N_2C(H)Si(CH_3)_3)(dppm)_2][CF_3SO_3]$ (32). *Method (i)*: A yellow solution of compound **1** (55 mg, 0.042 mmol) in 5 mL of CH_2Cl_2 at ambient temperature was treated with 0.30 mL of a 2 M solution of $N_2C(H)Si(CH_3)_3$ in Et_2O . After 16 h ^{31}P NMR spectroscopy revealed 25 % conversion to compound **32** and after 4 d compound **32** was the only product observed. The solvent was removed *in vacuo* and the crude brown residue was redissolved in CH_2Cl_2 and a brown powder was obtained by the slow addition of 10 mL of Et_2O . The solid was rinsed several times with Et_2O before being dried *in vacuo* (yield 72%). *Method (ii)*: If the same procedure noted in method (i) was repeated, except a slow stream of Ar was also passed over the solution, the reaction proceeded to completion in 16 h. Anal. Calcd for $C_{58}H_{54}N_2F_3O_6P_4SSiRhOs$: C, 49.43; H, 3.86; N, 1.99; S, 2.28 Found: C, 49.59; H, 4.03; N, 1.23; S, 2.42. MS m/z = 1147. The elemental analysis was performed within one hour of isolation of the solid sample to minimize decomposition.

(m) Photolysis experiments. Compounds **27**, **28**, **29**, and **30** (ca. 15 mg) were each dissolved in 0.7 mL of CD_2Cl_2 in separate NMR tubes. The samples were irradiated in the photolysis chamber described above for 16 h and monitored by ^{31}P NMR spectroscopy. No changes were observed.

(n) Thermolysis experiments. *Method (i)*: Compounds **27**, **28**, **29**, and **30** (ca. 25 mg) were each dissolved in 2 mL of freshly distilled THF. The solutions were left to reflux and the reactions observed by $^{31}P\{^1H\}$ NMR spectroscopy. No new species were noted after 16 h. *Method (ii)*: The reaction described in method (i) was repeated using freshly distilled toluene instead of THF. Again, no new species were observed.

(o) Attempted reaction of 5 with N₂C(H)Si(CH₃)₃. *Method (i):* Compound **5** (99.5 mg, 0.081 mmol) was dissolved in 10 mL of CH₂Cl₂. To this solution was added 50 μL of 2M N₂C(H)Si(CH₃)₃ in Et₂O (0.100 mmol). No reaction was detected by ³¹P{¹H} NMR spectroscopy after a period of 24 h. *Method (ii):* To a solution of compound **2** (72 mg, 0.058 mmol) in 10 mL of CH₂Cl₂ was added 0.30 mL of N₂C(H)Si(CH₃)₃ (2M in Et₂O; 0.60 mmol) and left to stir for 24 h under a slow flow of Ar. After 24 h only a brown residue remained which consisted of unidentified decomposition products as determined by ³¹P{¹H} NMR spectroscopy. *Method (iii):* To a yellow solution of compound **5** (45 mg, 0.036 mmol) and 125 μL of N₂C(H)Si(CH₃)₃ (2M in Et₂O) in 5 mL of CH₂Cl₂ was added 3.01 mg of Me₃NO (0.04 mmol) at which point the solution instantly darkened to a reddish brown. The solution was left to stir for 5 min and addition of 40 mL of Et₂O followed by 20 mL of pentane afforded a deep yellow powder. After removal of the clear supernatant, the yellow powder was rinsed with two 10 mL portions of Et₂O and dried *in vacuo*. ³¹P and ¹H NMR spectroscopy revealed the presence of numerous uncharacterized decomposition products.

(p) Attempted reaction of 1 with N₂C(H)CH₃. *Method (i):* Compound **1** (50 mg, 0.038 mmol) was dissolved in 5 mL of CH₂Cl₂ and the solution was cooled to -78 °C. Diazoethane, generated from ENNG (100 mg, 0.95 mmol) was passed through the solution and the mixture was stirred for 2.5 h. The solution was allowed to warm to room temperature and an aliquot of 0.5 mL was removed. ³¹P{¹H} NMR spectroscopy on this sample detected only **1**. *Method (ii):* 50 mg (0.038 mmol) of compound **1** was dissolved in 2 mL of CH₂Cl₂. Diazoethane, generated from ENNG (50 mg, 0.31 mmol), was slowly passed through the solution over the course of 1 h. No reaction was detected by ³¹P{¹H} NMR spectroscopy after 3 d. *Method (iii):* 57 mg of compound **1** (0.043 mmol) was dissolved in 4 mL of CH₂Cl₂ and diazoethane (generated from ENNG (50 mg, 0.31 mmol)) was passed through the solution for 30 min then cooled to -15 °C. 0.7 μL of a 3mg/mL Me₃NO in CH₂Cl₂ solution was added and the solution darkened immediately. The solution was allowed to stir for 1h over which time only compound **1** (50%) accompanied by numerous decomposition products was observed by ³¹P NMR spectroscopy. *Method (iv):* In an NMR tube, 25 mg (0.020 mmol) of compound **1** was dissolved in 0.7 mL of CD₂Cl₂ and cooled to -78 °C. Diazoethane (generated from ENNG (50 mg, 0.31 mmol)) was passed through the solution and the mixture inserted into the NMR probe that had been precooled to -80 °C. The reaction was monitored by NMR techniques while warming in 10 °C

intervals. No reaction was observed over the temperature range tested ($-80\text{ }^{\circ}\text{C}$ to $27\text{ }^{\circ}\text{C}$) by ^{31}P NMR spectroscopy. However, ^1H NMR spectroscopy revealed the presence of *trans*- and *cis*-butene.

(q) Attempted reaction of 5 with $\text{N}_2\text{C(H)CH}_3$. *Method (i)*: Compound **2** (50 mg, 0.041 mmol) was dissolved in 5 mL of CH_2Cl_2 and the solution was cooled to $-78\text{ }^{\circ}\text{C}$. Diazoethane, generated from ENNG (100 mg, 0.95 mmol), was passed through the solution and the mixture was stirred for 2.5 h. The solution was allowed to warm to room temperature and an aliquot of 0.5 mL was removed. $^{31}\text{P}\{^1\text{H}\}$ NMR spectroscopy on this sample detected only compound **5**. After 24 h, ^{31}P NMR spectroscopy still detected only starting materials. *Method (ii)*: If the above reaction was carried out at ambient temperatures, ^{31}P NMR spectroscopy detected only starting material after 24 h.

(r) Decomposition of Diazoethane. *Method (i)*: Diazoethane, generated from ENNG (50 mg, 0.041 mmol), was passed through 0.7 mL of CD_2Cl_2 in an NMR tube for several min. ^1H NMR spectroscopy of the clear solution revealed only the presence of *trans*- and *cis*-butene. *Method (ii)*: In an NMR tube, 0.7 mL of CD_2Cl_2 was cooled to $-78\text{ }^{\circ}\text{C}$. Diazoethane, generated from ENNG (50 mg, 0.041 mmol), was passed through the CD_2Cl_2 for several minutes. The sample was placed into the NMR probe which had been precooled to $-80\text{ }^{\circ}\text{C}$. ^1H NMR spectroscopy revealed the presence of only *trans*- and *cis*-butene. *Method (iii)*: Methods (i) and (ii) were repeated using THF-d_4 . Again, only *trans*- and *cis*-butene were detected by NMR.

(s) X-ray Data Collection. X-ray data collection and structure solution and refinement was performed by Dr. Bob McDonald of the X-ray crystallography laboratory in the Department of Chemistry at the University of Alberta. Yellow-orange crystals of $[\text{RhOs}(\text{CO})_3(\mu\text{-}\eta^1, \eta^1\text{-N}=\text{NC}(\text{COH})\text{CO}_2\text{Et})(\text{dppm})_2][\text{CF}_3\text{SO}_3]\cdot\text{C}_2\text{H}_4\text{Cl}_2$ (**27**) were obtained by slow evaporation of a 1,2-dichloroethane solution of the compound. Data were collected at $-80\text{ }^{\circ}\text{C}$ on a Bruker PLATFORM/SMART 1000 CCD diffractometer⁶⁸ using $\text{Mo K}\alpha$ radiation. Unit cell parameters were obtained from a least-squares refinement of the setting angles of 5554 reflections from the data collection. The space group was determined to be $P1$ (No. 2). The data were corrected for absorption through use of Gaussian integration (involving face-indexing of the crystal). See Table 2.2 for a summary of crystal data and X-ray data collection information.

Structure Solution and Refinement. The structure of **27** was solved using the Patterson location of heavy atoms and structure expansion routines as implemented in the *DIRDIF-96*⁶⁹

Table 2.2. Crystallographic Experimental Details for Compound **27**.

A. Crystal Data	
formula	$C_{61}H_{54}Cl_2F_3N_2O_9OsP_4RhS$
formula weight	1536.01
crystal dimensions (mm)	$0.63 \times 0.37 \times 0.28$
crystal system	triclinic
space group	$P\bar{1}$ (No. 2)
unit cell parameters ^a	
a (Å)	11.3899 (7)
b (Å)	15.0631 (9)
c (Å)	18.4369 (11)
α (deg)	87.7008 (12)
β (deg)	76.4194 (11)
γ (deg)	88.4252 (11)
V (Å ³)	3071.7 (3)
Z	2
ρ_{calcd} (g cm ⁻³)	1.661
μ (mm ⁻¹)	2.627
B. Data Collection and Refinement Conditions	
diffractometer	Bruker PLATFORM/SMART 1000 CCD ⁶⁸
radiation (λ [Å])	graphite-monochromated Mo K α (0.71073)
temperature (°C)	-80
scan type	ω scans (0.2°) (20 s exposures)
data collection 2θ limit (deg)	52.76
total data collected	17696 ($-14 \leq h \leq 14, -17 \leq k \leq 18, -23 \leq l \leq 23$)
independent reflections	12323 ($R_{\text{int}} = 0.0162$)
number of observed reflections (NO)	11411 [$F_o^2 \geq 2\alpha(F_o^2)$]
structure solution method	Patterson search/structure expansion (<i>DIRDIF-99</i> ⁶⁹)
refinement method	full-matrix least-squares on F^2 (<i>SHELXL-97</i> ^b)
absorption correction method	Gaussian integration (face-indexed)
range of transmission factors	0.5205–0.2696
data/restraints/parameters	12323 [$F_o^2 \geq -3\alpha(F_o^2)$] / 0 / 761
goodness-of-fit (S) ^c	1.038 [$F_o^2 \geq -3\alpha(F_o^2)$]
final R indices ^d	
R_1 [$F_o^2 \geq 2\alpha(F_o^2)$]	0.0281
wR_2 [$F_o^2 \geq -3\alpha(F_o^2)$]	0.0765
largest difference peak and hole	1.749 and -1.048 e Å ⁻³

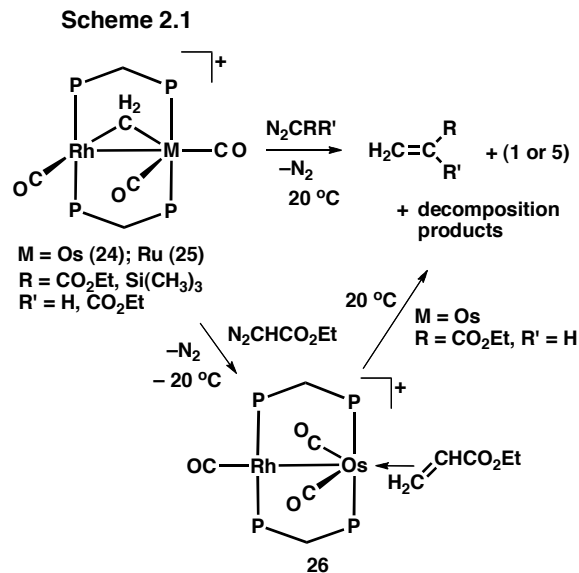
^aObtained from least-squares refinement of 5554 centered reflections. ^bObtained from least-squares refinement of 5554 centered reflections. ^c $S = [\sum w(F_o^2 - F_c^2)^2 / (n - p)]^{1/2}$ (n = number of data; p = number of parameters varied; $w = [\sigma^2(F_o^2) + (0.0454P)^2 + 3.7359P]^{-1}$ where $P = [\text{Max}(F_o^2, 0) + 2F_c^2]/3$). ^d $R_1 = \sum ||F_o| - |F_c|| / \sum |F_o|$; $wR_2 = [\sum w(F_o^2 - F_c^2)^2 / \sum w(F_o^4)]^{1/2}$.

program system. Refinement was completed using the program *SHELXL-93*. Hydrogen atoms were assigned positions based on the geometries of their attached carbon atoms and were given thermal parameters 20% greater than those of the attached carbons, with the exception of hydrogen H(40), which was located and freely refined. The final model for **27** was refined to values of $R_1(F) = 0.0281$ (for 11411 data with $F_o^2 \geq 2\sigma(F_o^2)$) and $wR_2(F^2) = 0.0765$ (for all 12323 independent data)

2.3 Results and Compound Characterization

2.3.1 Treatment of Methylene-Bridged Complexes with Diazoalkanes.

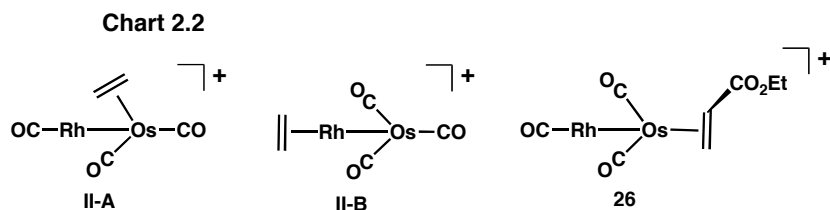
Reaction of the methylene-bridged tetracarbonyl species $[\text{RhM}(\text{CO})_4(\mu\text{-CH}_2)(\text{dppm})_2][\text{CF}_3\text{SO}_3]$ (M = Os (**2**), Ru (**7**)) with either ethyl diazoacetate (EDA), trimethylsilyldiazomethane (TMSDM) or diethyldiazomalonate (DEDM) results in the generation of the respective free olefins over the period of several days, as verified by comparison of their NMR spectra to those reported in the literature ($\text{H}_2\text{C}=\text{CRR}'$; R = H, R' = CO_2Et , SiMe_3 ; R = R' = CO_2Et).⁷⁰ The formation of these olefins corresponds to expected coupling of the diazoalkane-generated alkylidene unit and the methylene group. In all cases, the phosphorus-containing compounds remaining were identified by $^{31}\text{P}\{^1\text{H}\}$ NMR spectroscopy as unreacted compounds **2** or **7**, the respective byproducts **1** or **5**, and numerous uncharacterized decomposition products all in varying proportions depending on the diazoalkane. In contrast, the tricarbonyl analogues $[\text{RhM}(\text{CO})_3(\mu\text{-CH}_2)(\text{dppm})_2][\text{CF}_3\text{SO}_3]$ (M = Os (**24**), Ru (**25**)), react instantly with these diazoalkanes at ambient temperature, resulting in the rapid evolution of the free olefin, together with the respective compounds **1** or **5**, again accompanied by numerous uncharacterized decomposition products as determined by ^{31}P NMR spectroscopy. This reactivity is summarized in Scheme 2.1. We assume that formation of the tetracarbonyl species **1** and **5**, from the tricarbonyl precursors **24** and **25**, respectively, results from carbonyl scavenging from the decomposition products.



Quenching the reaction involving compound **25** and EDA by cooling the sample to -20 °C allows the isolation of a new species, $[\text{RhOs}(\eta^2\text{-H}_2\text{C=CHCO}_2\text{Et})(\text{CO})_3(\text{dppm})_2][\text{CF}_3\text{SO}_3]$ (**26**), (also shown in Scheme 2.1). In the $^{31}\text{P}\{^1\text{H}\}$ NMR spectrum, compound **26** gives rise to three complex multiplets at δ 25.3, -4.1 , and -10.5 in a 2:1:1 intensity ratio. The two high-field signals appear as the C and D portion of an ABCDX spin system ($X = ^{103}\text{Rh}$) and clearly correspond to the inequivalent phosphorus nuclei at the Os-bound ends of the dppm ligands, on the basis of the higher-field chemical shifts⁶⁶ and the absence of Rh coupling. The strong coupling between the pair of signals corresponding to the ^{31}P nuclei bound to Os ($^2J_{\text{PcPd}} = 259$ Hz) indicates a mutually *trans* phosphine arrangement at this metal. The low-field resonance of double intensity corresponds to the two accidentally degenerate A and B resonances for the Rh-bound ends of the dppm ligand, and appears as an approximate doublet of multiplets with strong coupling to Rh (approximately 113 Hz).

In the $^{13}\text{C}\{^1\text{H}\}$ NMR spectrum of **26** three carbonyl resonances appear: two triplets at δ 182.8 and 185.5, displaying no Rh coupling, correspond to two terminally bound carbonyls on Os, and a doublet of triplets at δ 182.5, showing strong Rh coupling ($^1J_{\text{RhC}} = 77.6$ Hz), corresponds to the carbonyl that is terminally bound to Rh. If $^{13}\text{CH}_2$ -enriched compound **24** is used in the above reaction an additional $^{13}\text{C}\{^1\text{H}\}$ resonance at δ 3.80 in the $^{13}\text{C}\{^1\text{H}\}$ NMR spectrum, corresponding to the CH_2 end of the coordinated olefin, is observed which shows no coupling to any of the ^{31}P nuclei or to Rh. The ^1H NMR spectrum of **26** shows two resonances at

δ 1.08 and 1.72, both of which display coupling of approximately 8 Hz to an additional proton resonance at δ 2.77. These three protons correspond to the three olefinic protons of the coordinated olefin. Although one might expect different *cis/trans* coupling constants for the olefinic protons, rehybridization of the olefin upon coordination presumably results in equivalent coupling involving the pseudo-*cis* and pseudo-*trans* protons. In the $^{13}\text{CH}_2$ -enriched sample of compound **26** the two high-field protons display coupling to the ^{13}C nucleus of 144 Hz and 157 Hz coupling, respectively, indicating that they correspond to this CH_2 group. These one-bond C-H coupling constants lie between those typical for an olefin (ca. 160 Hz) and an that of an alkane (ca. 130 Hz),⁷¹ reflecting some degree of rehybridization, as noted above. The dppm methylene protons appear as four separate broad multiplets at δ 4.47, 4.27, 4.10 and 3.12, indicating a lack of front-back and top-bottom symmetry, rendering each proton chemically unique. This suggests that olefin rotation is slow on the NMR timescale. Finally, the ethyl fragment of the ethyl acrylate ligand resonates at δ 1.32 (CH_3) and δ 4.23 (CH_2) similar to that of free ethyl acrylate.⁷⁰ We have ruled out an olefin-bridged structure for compound **26** since in such an arrangement the olefin could be considered a 1,2-dimetallated ethane unit, with essentially complete rehybridization of the olefinic carbons to sp^3 . This is inconsistent with the large C-H coupling constants noted above. In addition, the absence of spin-spin coupling involving either end of the olefin and the Rh nucleus establishes that the ethyl acrylate ligand is bound solely to Os. Compound **26** can be compared to two related mono-ethylene adducts, $[\text{RhOs}(\text{C}_2\text{H}_4)(\text{CO})_3(\text{dppm})_2][\text{BF}_4]$ (**II-A**) and $[\text{RhOs}(\text{CO})_3(\text{C}_2\text{H}_4)(\text{dppm})_2][\text{BF}_4]$ (**II-B**), shown in Chart 2.2^{56b} (dppm ligands omitted). A structure like **II-B** can be immediately ruled out, since as



established above, the olefin is bound to Os while one carbonyl is on Rh. In addition, the spectral data do not fit structure **II-A**. It has been established that terminal carbonyls that lie adjacent to another metal, and therefore having weak interactions with this adjacent metal, usually resonate downfield of those that lie remote from the adjacent metal;⁷² this is clearly seen

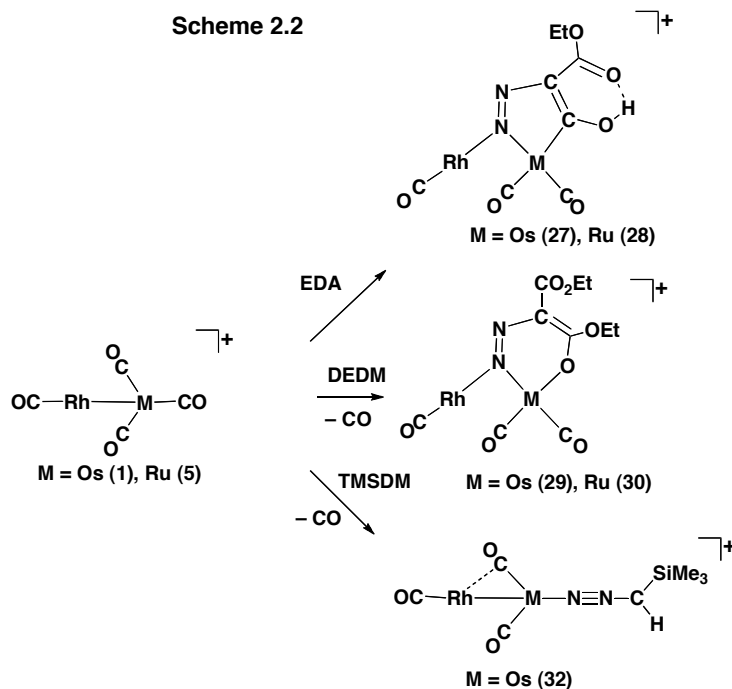
in compound **II-A** in which the chemical shift of the two Os-bound carbonyls differ by 10 ppm. In contrast, the pair of Os-bound carbonyls in **26** are very similar, having a chemical-shift difference of only 2.7 ppm. Furthermore, the relatively low-field shift for the Os-bound carbonyls suggests that they are adjacent to the Rh center, possibly interacting weakly with this second metal (generally, terminal carbonyls on 3rd row metals appear significantly upfield from those of the 2nd row analogues). On the basis of the above NMR data, the structure shown in Scheme 2.1 and Chart 2.2 is proposed in which an ethyl acrylate ligand is bound to Os in an η^2 fashion opposite the metal-metal bond with both Os-bound carbonyls adjacent to the metal-metal bond. The IR spectrum of **26** shows a stretch for the CO₂Et group at 1683 cm⁻¹ and three terminally bound carbonyl ligands (2047 cm⁻¹, 1981 cm⁻¹, and 1942 cm⁻¹). In addition, a weak band at 1558 cm⁻¹ can be assigned to the olefinic C-C stretch shifted significantly from that of free ethyl acrylate (1638 cm⁻¹).⁷⁰

Compound **26** is labile, decomposing in solution above -20 °C into free ethyl acrylate, compound **1**, and numerous unidentified phosphorus-containing products. Attempts to displace the ethyl acrylate ligand in **26** by ethylene, under an ethylene atmosphere, gave no evidence of an ethylene adduct over the temperature range from 22 to -80 °C. Again, only decomposition of **26** resulted over time or upon warming. Although we have not been able to isolate analogous olefin adducts in the reactions of **24** with the other substituted diazoalkanes we have observed such species in small quantities (<10% by integration of all phosphorus-containing species) in the ³¹P{¹H} NMR spectra at -20 °C, having very similar ³¹P{¹H} NMR spectral parameters to those of **26**. We assume that the greater lability of these intermediates results from destabilizing repulsions involving the additional ester substituent in the case of the DEDM reaction or the larger trimethylsilyl substituent in the case of TMSDM. In the case of the Rh/Ru complex **25**, no olefin adduct analogous to **26** was observed in any of the diazoalkane reactions although the same olefins were ultimately obtained.

2.3.2 Diazoalkane Complexes.

In attempts to generate alkylidene-bridged complexes analogous to compounds **2** and **7** *via* N₂ loss from the parent diazoalkane, the reactions of **1** and **5** with a number of substituted diazoalkanes were attempted. Treatment of both compounds **1** and **5** with EDA yields the

unusual products, $[\text{RhM}(\text{CO})_3(\mu\text{-}\eta^1\text{:}\eta^1\text{-N=NC}(\text{CO}_2\text{Et})\text{COH})(\text{dppm})_2][\text{CF}_3\text{SO}_3]$, ($\text{M} = \text{Os}$ (**27**), Ru (**28**)), diagrammed in Scheme 2.2 (dppm ligands omitted). High resolution mass



spectrometry for both products verifies that dinitrogen loss has not occurred from the diazoalkane molecule, and this is confirmed by the X-ray structure of **27** shown in Figure 2.1. The X-ray study also demonstrates that although N_2 loss has not occurred, the diazoalkane molecule has transformed into a new diazoalkane-like moiety *via* coupling with a carbonyl ligand, accompanied by hydrogen migration from the diazoalkane carbon to the carbonyl oxygen to give and metalla-enol functionality. Migratory insertions, involving carbonyl ligands, are very common⁷³ and have been observed with diazoalkane-generated⁷⁴ or metal-bound⁷⁵ alkylidene groups, and with imido groups that have resulted from N–N bond cleavage in diazoalkanes.⁷⁶ However, we are unaware of any report involving condensation of a carbonyl ligand with an intact diazoalkane group. The new diazo-containing group in **27** binds in a bridging arrangement bound to both metals through the terminal nitrogen (not unlike bonding type **VI** shown in Chart 2.1) while chelating to Os *via* the enol carbon to give a five-membered Os–N–N–C–C metallacycle. Within this metallacycle, the bond lengths and angles, given in Table 2.3, are consistent with the valence-bond formulation shown in Scheme 2. Therefore, the N(1)-

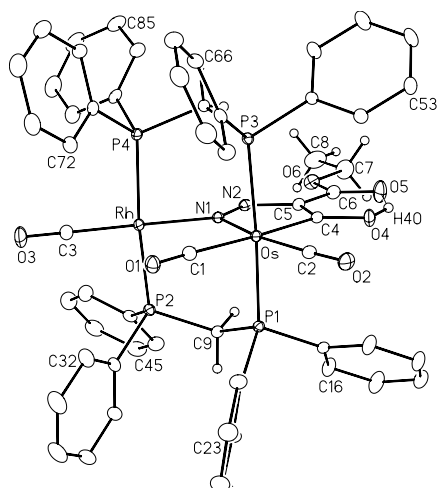


Figure 2.1: Perspective view of the $[RhOs(CO)_3\{\mu:\eta^1,\eta^1-N=NC(OH)CO_2Et\}(dppm)_2]^+$ complex cation of compound 27, showing the atom labelling scheme. Non-hydrogen atoms are represented by Gaussian ellipsoids at the 20% probability level. Hydrogen atoms are shown with arbitrarily small thermal parameters except for phenyl hydrogens, which are not shown.

Table 2.3: Selected Distances and Angles for Compound 27.

<i>Distances (Å)</i>					
Atom 1	Atom 2	Distance	Atom 1	Atom 2	Distance
Os	Rh	3.3206(3)	O(4)	H(40)	0.87(6)
Os	N(1)	2.088(2)	O(5)	C(6)	1.227(5)
Os	C(1)	1.976(3)	O(5)	H(40)	1.85(6) [†]
Os	C(2)	1.904(3)	O(6)	C(6)	1.326(4)
Os	C(4)	2.055(3)	O(6)	C(7)	1.464(5)
Rh	N(1)	2.023(3)	N(1)	N(2)	1.270(4)
Rh	C(3)	1.842(4)	N(2)	C(5)	1.402(4)
O(1)	C(1)	1.139(4)	C(4)	C(5)	1.391(4)
O(2)	C(2)	1.145(4)	C(5)	C(6)	1.455(5)
O(3)	C(3)	1.143(5)	C(7)	C(8)	1.473(7)
O(4)	C(4)	1.328(4)			

<i>Angles (deg)</i>							
Atom 1	Atom 2	Atom 3	Angle	Atom 1	Atom 2	Atom 3	Angle
N(1)	Os	C(1)	98.9(1)	Os	C(1)	O(1)	173.3(3)
N(1)	Os	C(2)	166.8(1)	Os	C(2)	O(2)	174.3(3)
N(1)	Os	C(4)	75.6(1)	Rh	C(3)	O(3)	178.9(4)
C(1)	Os	C(2)	94.2(1)	Os	C(4)	O(4)	125.0(2)
C(1)	Os	C(4)	174.5(1)	Os	C(4)	C(5)	114.1(2)
C(2)	Os	C(4)	91.3(1)	O(4)	C(4)	C(5)	120.9(3)
N(1)	Rh	C(3)	176.5(1)	N(2)	C(5)	C(4)	117.1(3)
C(4)	O(4)	H(40)	114(4)	N(2)	C(5)	C(6)	121.3(3)
C(6)	O(6)	C(7)	115.9(3)	C(4)	C(5)	C(6)	121.6(3)
Os	N(1)	Rh	107.8(1)	O(5)	C(6)	O(6)	122.3(3)
Os	N(1)	N(2)	119.9(2)	O(5)	C(6)	C(5)	121.8(3)
Rh	N(1)	N(2)	132.3(2)	O(6)	C(6)	C(5)	115.9(3)
N(1)	N(2)	C(5)	113.3(3)	O(6)	C(7)	C(8)	108.0(4)

[†] Non-bonded distance

N(2) distance (1.270(4) Å) is that of a typical N=N double bond, while the N(2)-C(5) distance (1.402(4) Å) is as expected for a single bond between sp² hybridized N and C atoms.⁷⁷ The newly formed C(4)-C(5) bond (1.391(4) Å) is typical of an enolic double bond,⁷⁷ while the C(5)-C(6) and C(4)-O(4) distances (1.455(5), 1.328(4) Å, respectively) are consistent with single bonds within such groups. Within the N₂-containing metallacycle, the angles are all somewhat smaller (range 113.3(3)° - 119.9(2)°) than the idealized value for sp² hybridization, reflecting a degree of strain within this group, as a result of the acute N(1)-Os-C(4) bite angle (75.6(1)°). The diazo-containing fragment bridges in an unsymmetrical manner in which the Os-N(1) distance is significantly shorter than Rh-N(1) (2.088(2) vs. 2.223(3) Å). The reasons for this asymmetry are not clear, although the restrictions resulting from the 5-membered Os metallacycle may play a role.

The X-ray study has also allowed the unambiguous location and successful refinement of the enol hydrogen, placing it within obvious bonding distance of the enol oxygen (O(4)-H(40) = 0.87(6)Å), but also in a position to be hydrogen-bonded to the carbonyl oxygen of the CO₂Et group (O(5)-H(40) = 1.85(6) Å), with this separation being significantly less than the sum of the van der Waals radii of 2.6 Å. The presence of hydrogen bonding is further substantiated by the planar arrangement of the six-membered ring that results (see Figure 2.1), involving the enol and carbonyl functionalities; a repulsive interaction between H(40) and O(5) would lead to rotation of the OH group out of the enol plane.

The diazo-containing ligand in compounds **27** and **28** functions as a dianionic 6 e⁻ donor, to the Rh(I)/M(II) (M = Os, Ru) centres. In keeping with these oxidation-state formulations, the coordination geometry at Rh is square planar, while that of Os is octahedral. This formulation differs from that shown in the compounds displaying structure **VI** (Chart 2.1) owing to the additional enolate functionality, which donates an additional pair of electrons.

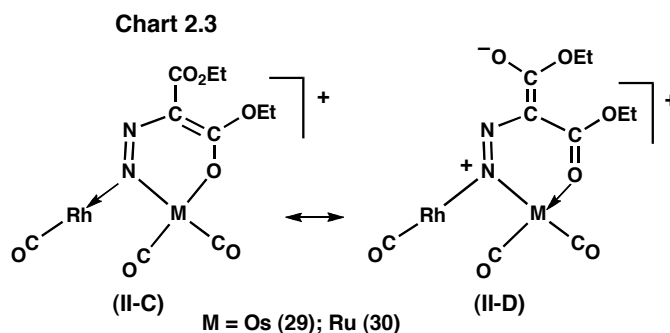
The transformation of compounds **1** and **5** into the products **27** and **28**, respectively, is irreversible most likely a result of the condensation and hydrogen migration steps. Moreover addition of CO to either of the products gives no further reaction. For compounds **27** and **28** the spectral parameters are closely comparable (see Table 2.1), so compound **28** is assumed to have the same structure as that established for **27**. In the ¹H NMR spectrum of **27** the dppm methylene and the ethyl group resonances are as expected, while the hydroxyl proton appears as a singlet at δ 11.04, as is characteristic of a hydrogen-bonded hydroxyl proton.⁷¹ ¹³C{¹H} NMR

data show only three terminal carbonyl resonances; two triplets at δ 177.9 and 179.6 correspond to the Os-bound groups, while a doublet of triplets at δ 195.5, with 63.2 Hz coupling to the Rh nucleus, corresponds to the Rh-bound CO (surprisingly, in this case the Os-bound carbonyl that is adjacent to Rh cannot be differentiated from the one which occupies the remote position). The enol carbon is observed as a triplet at δ 231.6 ($^2J_{CP} = 8.3$ Hz) with coupling to the pair of Os-bound ^{31}P nuclei. A solution IR of a sample of **27** shows two terminal carbonyl stretches (2020 cm^{-1} (s), 1970 cm^{-1} (s, br)), a stretch at 1633 cm^{-1} , attributed to the CO_2Et group and a stretch at 3058 cm^{-1} which is assigned to the OH functionality.

The corresponding reactions of compounds **1** and **5** with DEDM yield the respective diazoalkane-bridged complexes $[\text{RhM}(\text{CO})_3(\mu\text{-}\eta^1\text{:}\eta^1\text{-N=NC}(\text{CO}_2\text{Et})_2)(\text{dppm})_2][\text{CF}_3\text{SO}_3]$ ($\text{M} = \text{Os}$ (**29**), Ru (**30**)) (Scheme 2), in which the DEDM ligand is again proposed to bridge *via* the terminal nitrogen. Although binding of DEDM is accompanied by the loss of one carbonyl, the reactions cannot be reversed by addition of CO. The presence of an N_2 moiety within these complexes is verified by HRMS and elemental analysis, while the loss of a carbonyl is seen in the $^{13}\text{C}\{^1\text{H}\}$ NMR spectra of ^{13}CO -enriched samples, in which only three equal intensity resonances are observed. For compound **30**, the pair of Ru-bound carbonyls appear at δ 197.0 and 195.6, whereas the one bound to Rh appears at δ 195.4, with typical coupling (63.7 Hz) to Rh. All resonances display typical patterns consistent with coupling to the adjacent pair of ^{31}P nuclei. The ester carbonyls on the DEDM ligand appear at δ 165.7 and 155.3, demonstrating the inequivalence of these two ester groups. This inequivalence is also evident in the ethyl group resonances in the ^1H NMR spectrum with one group appearing at δ 1.40 (CH_3) and 4.35 (CH_2), while the other appears at δ 0.62 (CH_3) and 1.91 (CH_2). The NMR spectral parameters for the Os analogue very much mirror those given above, except that the Os-bound carbonyls appear upfield to those bound to Ru, as is typically observed in these cases.

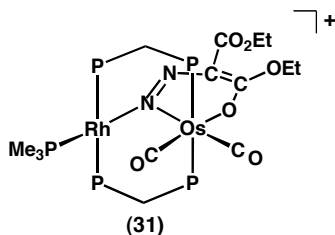
On the basis of the significant inequivalence of the pair of ester groups in each complex and the presence of only two Ru- or Os-bound carbonyls, as was observed in compounds **27** and **28**, we propose that coordination of one of the ester groups to Ru or Os occurs, as diagrammed for one valence-bond representation in Scheme 2.2. Similar binding of DEDM, *via* both nitrogen and an ester carbonyl, has been proposed.³⁶ The valence-bond representation shown in Scheme 2.2 for compounds **29** and **30** would be expected to give rise to two very different ester carbonyl stretches in the IR spectrum – one at a value close to that of free DEDM and another

(corresponding to the coordinated ester) at a significantly lower frequency. In the case of the Ru species (**30**) these stretches are observed at 1725 and 1641 cm^{-1} , in support of the formulation given. This lowering of the ester carbonyl stretches has also been observed by Eisenberg *et al.*⁷⁸ However, for the Os analogue (**29**) the ester stretches both appear at the intermediate values, 1699 and 1690 cm^{-1} , suggesting a structure in which there is significant delocalization over the pair of ester groups. Two limiting valence-bond formulations for the coordinated DEDM ligand in compounds **29** and **30** are shown in Chart 2.3 (dppm groups omitted). Structure **II-C**



corresponds to the bonding extreme proposed in the Rh/Ru species (**30**) while the structure proposed for the Rh/Os species (**29**) is presumably a hybrid of **II-C** and **II-D**. In either case, the ligand functions as a dianionic 6 e^- donor to the Rh(I)/M(II) centers (M = Os, Ru), with the square planar and octahedral geometries about the respective metals. Unfortunately, attempts to obtain X-Ray quality crystals of **29** and **30** in different solvents and by exchanging the triflate anion for BF_4^- and BPh_4^- were unsuccessful.

Addition of PMe_3 to compound **29** in attempts to displace the Os-bound ester group, instead gives the product, $[\text{RhOs}(\text{CO})_2(\text{PMe}_3)(\mu\text{-}\eta^1\text{:}\eta^1\text{-N}_2\text{C}(\text{CO}_2\text{Et})_2)(\text{dppm})_2][\text{CF}_3\text{SO}_3]$ (**31**), the structure of which is diagrammed below, *via* substitution of a carbonyl. The ^{31}P NMR spectrum



of this product exhibits three multiplets of 2:2:1 intensity ratio at δ 28.4, δ 12.1 and δ -18.5. The low-field signal, being the AA' portion of an AA'BB'CX spin system, corresponds to the Rh-bound phosphorus nuclei of the dppm ligand, clearly evident by its strong coupling to the Rh nucleus ($^1J_{\text{RhP}} = 162$ Hz) and additional coupling to the other phosphines of the dppm bridge as well as to the PMe_3 ligand, whereas the signal at δ 12.1 (the BB' portion) corresponds to the Os-bound phosphines of the dppm ligand on the basis of its higher-field chemical shift and absence of Rh coupling. Finally, a doublet of triplets at δ -18.5 is assigned to the PMe_3 ligand and shows strong coupling to both the Rh-bound phosphines of the dppm ligands ($^2J_{\text{PP}} = 42$ Hz) and the Rh nucleus ($^1J_{\text{RhP}} = 129$ Hz) to which it is bound. This clearly establishes that coordination of PMe_3 to Rh and not to Os has occurred. A solution of compound **31** was monitored over a period of two weeks by ^{31}P NMR spectroscopy and no further transformations were observed. Again, attempts to obtain X-Ray quality crystals of **31** failed. Interestingly, the IR spectrum of **31** shows ester stretches at 1752 and 1686 cm^{-1} , more in line with structure **II-C** and with that of the Rh/Ru species **30**.

Treatment of compound **1** with $\text{N}_2\text{CHSiMe}_3$ (TMSDM) also leads to a carbonyl-substitution product $[\text{RhOs}(\text{CO})_3(\text{N}_2\text{CHSi}(\text{CH}_3)_3)(\text{dppm})_2][\text{CF}_3\text{SO}_3]$ (**32**), again containing the intact diazoalkane group, as confirmed by elemental analysis. In addition, the mass spectrometry fragmentation pattern observed strongly suggests a product in which the intact diazoalkane group is present, showing peaks associated with the loss of both the CHSiMe_3 and $\text{N}_2\text{CHSiMe}_3$ fragments. The formation of compound **32** is accompanied by the formation of numerous unknown silane products, presumably from the decomposition of TMSDM. Furthermore, this product is unstable, even in the solid state, decomposing over several hours into an oily residue composed of a complex mix of unknown products, limiting our characterization of **32**.

In the $^{13}\text{C}\{^1\text{H}\}$ NMR spectrum two carbonyl resonances are observed in a 2:1 intensity ratio. The latter appears as a doublet of multiplets at δ 181.2 with coupling to the pair of Rh-bound ^{31}P nuclei and to ^{103}Rh ($^1J_{\text{RhC}} = 80.3$ Hz), establishing that it is terminally bound to this metal, while the other resonance, at δ 194.6, appears as a doublet of multiplets of double intensity and displays coupling to the Os-bound phosphines, as well as weak coupling to the ^{103}Rh nucleus of 3.3 Hz. The lower-field resonance for the Os-bound carbonyls is consistent with these groups being bound primarily to Os but having a weak semi-bridging interaction with

Rh,^{66,72} a formulation that is supported by the small Rh-C coupling observed. However, the IR spectrum, which shows two terminal ($\nu(\text{CO}) = 2059, 1977 \text{ cm}^{-1}$) and one bridging CO stretch (1804 cm^{-1}), suggests a slightly different interpretation in which one Os-bound carbonyl is terminally bound while the other is semi-bridging, as diagrammed earlier in Scheme 2.2 (a classical bridging carbonyl is ruled out on the basis that the averaged $^1J_{\text{RhC}}$ would be higher than the 3.3 Hz observed). Facile exchange of these carbonyls between the terminal and semi-bridging positions is rapid on the NMR time scale and probably involves the movement of only a few tenths of an angstrom. As a consequence, only the average signal is seen in the $^{13}\text{C}\{^1\text{H}\}$ NMR spectrum, even at -80°C , whereas the faster time-scale of the IR experiment allows both the bridging and terminal stretches to be observed. Similar dynamics have been reported previously in related species.^{56b,79}

The four dppm methylene protons are equivalent on the NMR timescale, appearing as a single multiplet at $\delta 4.03$, even at -80°C , indicating the same average chemical environment on each side of the RhOsP_4 plane. This suggests that the diazoalkane is bound in a linear or close-to-linear manner in the site opposite the Rh-Os bond; any other site would result in the loss of symmetry about the RhOsP_4 plane resulting in the chemical inequivalence of the two pairs of dppm methylene protons. In addition, occupation of any other site on the Os center by the TMSDM ligand would not allow the facile carbonyl exchange noted above. Linearly-bound diazoalkane ligands are well documented.^{10,12} The structure proposed is similar to those reported previously, for the symmetric isomer of the mono-ethylene and bis-ethylene compounds $[\text{RhOs}(\text{CO})_3(\eta^2\text{-C}_2\text{H}_4)(\text{dppm})_2][\text{BF}_4]$ and $[\text{RhOs}(\text{CO})_2(\eta^2\text{-C}_2\text{H}_4)_2(\text{dppm})_2][\text{BF}_4]$, respectively, which have similar symmetries with respect to the pair of Os-bound carbonyls. Consistent with the proposal of similar structures, the spectral parameters for these ethylene complexes are closely comparable to those of **32**.^{56b} In particular, the Os-bound carbonyls for these two ethylene adducts appear at $\delta 198.0$ ($^1J_{\text{RhC}} = 6 \text{ Hz}$) and 195.5 ($^1J_{\text{RhC}} = 6 \text{ Hz}$), respectively in the $^{13}\text{C}\{^1\text{H}\}$ NMR spectra, very close to the low-field resonances of **32**.

Attempts to generate the Rh/Ru analogue of **32**, namely $[\text{RhRu}(\text{CO})_3(\text{N}_2\text{CHSiMe}_3)(\text{dppm})_2][\text{CF}_3\text{SO}_3]$, failed giving either no reaction or uncharacterized decomposition products, depending on the reaction conditions.

Having the series of metal-bound diazoalkanes in which these ligands were either bridging the pairs of metals (compounds **27-30**) or terminally bound to one (compound **32**), we

were interested in determining whether these coordination modes activated these ligands towards N₂ loss. However, photolysis or subjecting compounds **27** – **30** to reflux in a number of solvents, even for extended periods, did not induce N₂ loss, leaving the complexes unchanged. Compound **32** decomposed to unidentified products under these conditions, as described earlier.

2.4 Discussion

2.4.1 Methylene and Alkylidene Coupling.

Although the reaction of [RhOs(CO)₄(μ-CH₂)(dppm)₂][X] (**2**) with diazomethane is facile at temperatures above –50 °C yielding C₃ or C₄ fragments coordinated to the metals,^{56,63} the analogous reactions of **2** with the substituted diazoalkanes, N₂CRR' (R = H, R' = CO₂Et, SiMe₃; R = R' = CO₂Et) are extremely slow even at ambient temperature. Furthermore, in these latter reactions no metal-bound hydrocarbyl fragments are observed and after several days only the olefins that correspond to coupling of the bridging methylene group and the diazoalkane-generated alkylidene fragment, together with compound **1** and decomposition products are observed. Carrying out the reactions at low temperature only serves to slow the reactions further, without allowing the observation of reaction intermediates. The Rh/Ru analogue (**7**) reacts similarly. However, the same reactions using the tricarbonyl complexes [RhM(CO)₃(μ-CH₂)(dppm)₂][X] (M = Os (**24**), Ru (**25**)) are almost immediate at ambient temperature, again yielding the free olefins and (where identified) the same metal-containing products.

If the reaction involving **24** and EDA (N₂CHCO₂Et) is carried out at –20 °C, an olefin-containing species, [RhOs(CO)₃(η²-H₂C=C(H)CO₂Et)(dppm)₂][X] (**26**), is observed as diagrammed in Scheme 2.1. This product has resulted from coupling of the methylene and alkylidene fragments at the adjacent metals. This olefin complex does not have a targeted olefin-bridged structure; instead this group appears to be terminally bound to Os. Furthermore, unlike the ethylene analogue prepared by the reaction of **24** with diazomethane, which is stable upon warming to ambient temperature,^{56b} compound **26** readily undergoes loss of ethyl acrylate at temperatures above –20°C. We assume that the greater lability of **26** compared to its ethylene

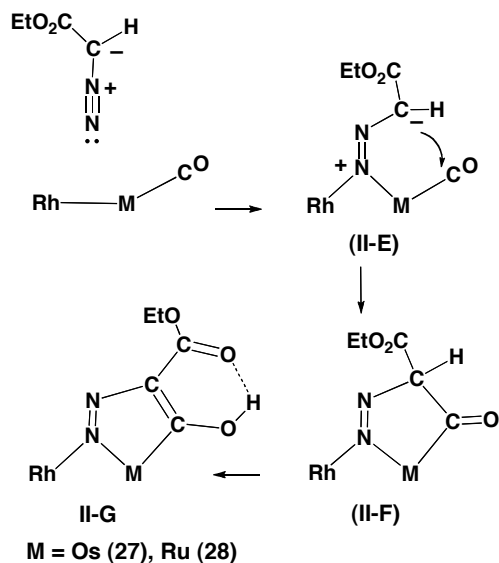
analogue results from unfavorable steric interactions involving the dppm phenyl groups and the bulky CO₂Et group.

The olefin adducts, analogous to **26**, involving the larger SiMe₃ substituents (from TMSDM) and the two CO₂Et substituents (from DEDM) are even less stable than **7**, appearing in only small quantities relative to decomposition products at temperatures below –20 °C. In the case of the Rh/Ru analogues, no olefin adduct is observed down to –80 °C, even for ethyl acrylate, presumably owing to the weaker olefin binding to Ru compared to Os.⁸⁰

2.4.2 Diazoalkane and Related Complexes.

Attempts to generate substituted alkylidene-bridged analogues of compounds **2** and **7**, by the reactions of **1** and **5**, respectively, with a series of diazoalkanes also did not yield the targeted products. Instead an interesting series of complexes has been generated in which the “NNC” moiety of the diazoalkane precursors has remained intact. Of the three different diazoalkanes investigated the most surprising result involves EDA in which coordination in the bridging site is accompanied by condensation of the diazoalkane carbon and an adjacent carbonyl group with subsequent hydrogen transfer from this diazoalkane to the carbonyl oxygen yielding an enolate moiety. Formation of a metallacyclic-enol product from a metal-carbonyl precursor suggests the involvement of a keto-enol tautomerization⁸¹ step. This proposal is outlined in Scheme 2.3 (ancillary ligands omitted), in which reaction of ethyl diazoacetate with the “RhM(CO)₄” fragment is proposed to first yield the diazoalkane-bridged intermediate (**II-E**), similar to other diazoalkane-bridged complexes.⁴⁰⁻⁴³ Nucleophilic attack of the diazoalkane carbon at the carbonyl ligand would yield the metallacycloketone (**II-F**) which could then tautomerize to the metallacyclic enol (**II-G**). This enol product is presumably stabilized by conjugation between the olefinic double bond and both the diazo and the ester carbonyl functionalities and also by the hydrogen bond between the enol and ester carbonyl group. Reactions of the very analogous homobinuclear complexes [Rh₂(CO)₂(μ-H)₂(dppm)₂] and [Ru₂(CO)₄(μ-CO)(dppm)₂] with EDA did not yield metallacyclic products like **27** and **28**, but instead gave simple diazoalkane-bridged products, depicted by bonding type **VI** of Chart 2.1.^{43,78} Although, as noted earlier, condensations involving diazoalkanes and carbonyl ligands have not been observed on a metal

Scheme 2.3



template, the transformations reported for **27** and **28** are reminiscent of the coupling reactions involving ethyl diazoacetate and aldehydes, using a variety of catalysts.⁸²

In an attempt to observe and characterize a species that would model either the diazoalkane bridged species **II-E** or the metallacyclic ketone species **II-F**, we undertook the reactions of **1** and **5**, with diethyl diazomalonate (DEDM), which lacks a hydrogen substituent on the diazoalkane carbon, ruling out the possibility of keto-enol tautomerism. This strategy has succeeded in generating a diazoalkane-bridged product, with both the Rh/Os and the Rh/Ru systems. However, in both of these cases one of the ester carbonyl groups also displaces a carbonyl ligand, and binds to the group 8 metal as a dianionic, 6 e⁻ donor diazoalkane ligand. The failure of DEDM to yield a metallacyclic ketone similar to structure **II-F** (Scheme 2.3), that would result from coupling of the bridging diazoalkane ligand and an adjacent carbonyl ligand may result from the increased steric crowding in the disubstituted diazoalkane (DEDM) ligand, which inhibits approach of the diazoalkane carbon to the carbonyl ligand. The entropy increase that results from the carbonyl displacement in generating compounds **29** and **30** also cannot be overlooked as a driving force for the observed transformation.

The singly-substituted TMSDM group having hydrogen and trimethylsilyl substituents on the diazoalkane carbon, has no carbonyl oxygen with which to chelate to the group 8 metal, ruling out products analogous to compounds **29** and **30**. However it has the potential to yield a

condensation product such as **II-E** and in principle can also undergo a tautomerization step yielding a metallacyclic enol similar to **II-G**. In this case however, the absence of an ester carbonyl group means that such an enol product would have neither the stabilization of the hydrogen bond nor the stabilization resulting from conjugation involving the olefin and carbonyl functionalities that exist in **27** and **28**. In this case however, no product containing a bridging diazoalkane group is observed. Instead the unstable product (**32**) contains a terminally bound diazoalkane ligand as shown in Scheme 2.2.

In order to minimize the steric bulk of the diazoalkane we also investigated reactions involving diazoethane ($\text{N}_2\text{C}(\text{H})\text{CH}_3$) and compounds **1** and **5**. Surprisingly, no reaction involving this diazoalkane and these compounds was observed between $-80\text{ }^\circ\text{C}$ and ambient temperature. We certainly observed the formation of both *cis*- and *trans*-butene, under the conditions investigated, however, these olefins were also obtained under the same conditions in the absence of compounds **1** and **5**, so their formation was not metal-mediated.

2.4.3 Comparisons of N_2CH_2 and $\text{N}_2\text{CRR}'$.

The reactions of the mixed-metal complexes described above with substituted diazoalkanes and with diazomethane differ significantly. In the reactions involving the methylene-bridged Rh/Os complexes **2** and **7**, all diazoalkanes (including N_2CH_2) initially behave similarly, resulting in coupling of the bridging methylene group with the alkylidene fragment of the diazoalkane. However, whereas diazomethane reacted with **2** to give multiple methylene-couplings, the substituted diazoalkanes yield olefins arising from coupling of an alkylidene fragment with the metal-bound methylene group. We suggest that this may be a consequence of steric factors which labilize the substituted olefins, first forcing them out of the bridging site, where methylene coupling is proposed to occur in this system,^{56b,63} and subsequently leading to olefin loss, whereas with the prototypical diazomethane these steric interactions are greatly reduced and so the C_2 -bridged intermediate is more stable, allowing for additional methylene incorporation.

Whereas the methylene-bridged Rh/Ru complex (**4**)⁵⁸ had behaved very differently than its Rh/Os analogue⁵⁶ in failing to react further with diazomethane, this complex did react with the substituted diazoalkanes yielding olefins, paralleling the chemistry observed with Rh/Os. In

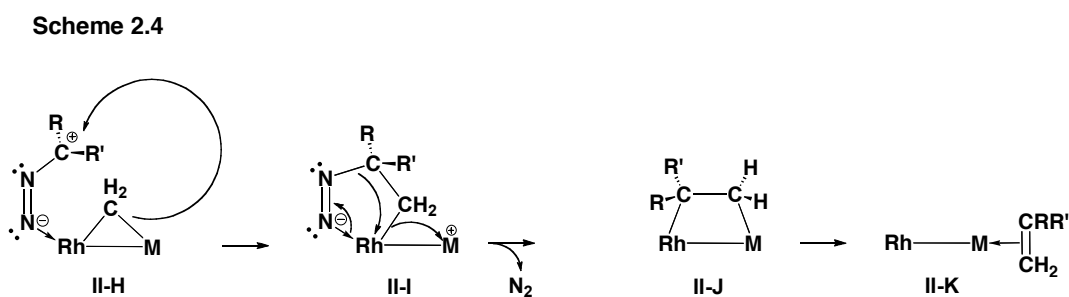
both cases, the methylene-bridged tricarbonyls were much more reactive than the tetracarbonyl analogues.

In the reactions of diazoalkanes with the tetracarbonyl complexes $[\text{RhM}(\text{CO})_4(\text{dppm})_2][\text{X}]$ ($\text{M} = \text{Os}$ (**1**), Ru (**5**)), the differences between the prototype (N_2CH_2) and the substituted diazoalkanes studied is even more pronounced. With diazomethane, no species was ever observed containing the intact N_2CH_2 ligand; instead N_2 extrusion was extremely facile (occurring even at -80°C) generating methylene groups and other hydrocarbyl ligands formed from methylene-group condensations. In contrast, the substituted diazoalkanes (with the exception of diazoethane, which failed to react) formed only diazoalkane complexes or related species and could not be induced to undergo N_2 loss when heated or photolyzed. Milstein, Martin and coworkers have argued convincingly that "...an important requirement for the carbene formation is the viability of an $\eta^1\text{-C}$ coordinated diazo complex", and have shown that the viability of this key intermediate is largely determined by steric factors;¹³ the greater the steric demand of the diazoalkane substituents, the less favorable will be this pivotal intermediate. In support of these ideas, our only observation of carbene formation is with unsubstituted diazomethane. Coordination of the diazoalkane or related moiety through the terminal nitrogen, in a bridging (compounds **27-30**) or terminal $\eta^1\text{-N}$ mode (compound **32**) does not lead to carbene formation, even under forcing conditions. Although it may not be surprising that complexes **27-30** exhibit this stability as they are bound through the bridging nitrogen while chelating to the group 8 metal, either through an enolate carbon (compounds **27** and **28**) or through a carboxylate oxygen (compounds **29** and **30**), the stability of **32** with respect to thermolysis, photolysis and CO substitution is surprising.

Finally, it seems puzzling in reaction of **1** and **5** with diazoalkanes results in coordination of the intact diazoalkane ligand and *no alkylidene formation is observed*, yet alkylidene formation clearly occurs at some stage in reactions involving the more crowded methylene-bridged complexes **2**, **7**, **24** and **25**, since the corresponding olefins ($\text{CH}_2=\text{CRR}'$) are obtained, through coupling of the methylene fragment with the diazoalkane-generated alkylidene fragment. It appears unlikely that in these reactions the requisite $\eta^1\text{-C}$ coordinated diazoalkane complex can be accessed to allow alkylidene formation for subsequent coupling with the bridging methylene group, since such reactivity was not observed for the less crowded complexes **1** and **5**. For this reason, we propose that coupling of the intact diazoalkane ligand and the methylene

group may occur prior to N₂ extrusion, instead of the opposite pathway although we have no evidence of diazoalkane coordination prior to olefin formation.

We propose the sequence shown in Scheme 2.4 in which initial binding of the diazoalkane occurs at Rh through the terminal nitrogen to give a species like **II-H**. Subsequent coupling of the diazoalkane and the bridging methylene group leads to the five membered Rhodocyclic species, **II-I** shown in Scheme 2.4. N₂ extrusion and rearrangement of the new olefin fragment yields the C₂-bridged species **II-J**, which rapidly rearranges once more to give the olefin adduct **II-K**, compound **26** in the case of the reaction of **2** with EDA.



2.5 Conclusions

Although our efforts to generate substituted C₁- and C₂-bridged species through the use of substituted diazoalkanes were not successful, we were able to characterize an interesting, unstable ethyl acrylate complex, resulting in the coupling of an ethyl diazoacetate-generated alkylidene and the metal-bridging methylene group. It appears that our failure to generate the targeted species is largely a result of steric influences of the diazoalkane substituents; generation of the η¹-C coordinated diazoalkanes as prerequisites to the targeted bridging alkylidene species appears to be inhibited by the bulk of the diazoalkane substituents, and the olefin-bridged targets appear to be unstable, again for steric reasons. However, in our unsuccessful attempts to generate alkylidene-bridged products we were able to generate three interesting and rather different complexes that involve incorporation of the intact "NNC" part of diazoalkane molecules, adding further to the interesting coordination chemistry of these species. Unlike our previous studies involving diazomethane, for which the Rh/Ru and Rh/Os metal combinations

displayed very different reactivities, both metal combinations reacted quite analogously with the substituted diazoalkanes studied.

2.6 References

1. Blaser, H. U.; Schmidt, E. *Asymmetric Catalysis on the Industrial Scale: Challenges, Approaches and Solutions*; Wiley-VCH Verlag GmbH & Co. KGaA: Weinheim, 2004.
2. Doyle, M. P. *Chem. Rev.* **1986**, *86*, 919.
3. Padwa, A.; Weingarten, M. D. *Chem. Rev.* **1996**, *96*, 223.
4. Davies, H. M. L.; Panaro, S. A. *Tetrahedron* **2000**, *56*, 4871.
5. Mizobe, Y.; Ishii, Y.; Hidai, M. *Coord. Chem. Rev.* **1995**, *139*, 281.
6. Dartiguenave, M.; Menu, M., Joelle; Deydier, E.; Dartiguenave, Y.; Siebald, H. *Coord. Chem. Rev.* **1998**, *178-180*, 623.
7. Herrmann, W. A. *Angew. Chem. Int. Ed.* **1978**, *17*, 800.
8. Sutton, D. *Chem. Rev.* **1993**, *93*, 995.
9. Hidai, M.; Mizobe, Y. *Chem. Rev.* **1995**, *95*, 1115.
10. Menu, M. J.; Crocco, G.; Dartinguenave, M.; Dartinguenave, Y.; Bertrand, G. *J. Chem. Soc., Chem. Commun.* **1988**, 1598.
11. Harada, Y.; Mizobe, Y.; Hidai, M. *J. Organomet. Chem.* **1999**, *574*, 24.
12. Werner, H.; Mahr, N.; Wolf, J.; Fries, A.; Laubender, M.; Bleuel, E.; Garde, R.; Lahuerta, P. *Organometallics* **2003**, *22*, 3566.
13. Cohen, R.; Rybtchinski, B.; Gandelman, M.; Rozenberg, H.; Martin, J. M. L.; Milstein, D. *J. Am. Chem. Soc.* **2003**, *125*, 6532.
14. Harada, Y.; Mizobe, Y.; Ishii, Y.; Hidai, M. *Bull. Chem. Soc. Jpn.* **1998**, *71*, 2701.

15. Hidai, M.; Mizobe, Y.; Sato, M.; Kodama, T.; Uchida, Y. *J. Am. Chem. Soc.* **1978**, *100*, 5740.
16. Ishii, Y.; Miyagi, H.; Jitsukuni, S.; Seino, H.; Harkness, B. S.; Hidai, M. *J. Am. Chem. Soc.* **1992**, *114*, 9890.
17. Oshita, H.; Mizobe, Y.; Hidai, M. *J. Organomet. Chem.* **1993**, *461*, 43.
18. Hillhouse, G. L.; Haymore, B. L. *J. Am. Chem. Soc.* **1982**, *104*, 1537.
19. Cowie, M.; Loeb, S. J.; McKeer, I. R. *Organometallics* **1986**, *5*, 854.
20. Straub, B. F.; Rominger, F.; Hofmann, P. *Inorg. Chem. Commun.* **2000**, *3*, 214.
21. Kool, L. B.; Rausch, M. D.; Alt, H. G.; Herberhold, M.; Hill, A. F.; Thewalt, U.; Wolf, B. *J. Chem. Soc. Chem. Commun.* **1986**, 408.
22. Schramm, K. D.; Ibers, J. A. *J. Am. Chem. Soc.* **1978**, *100*, 2932.
23. Schramm, K. D.; Ibers, J. A. *Inorg. Chem.* **1980**, *19*, 2435.
24. Schramm, K. D.; Ibers, J. A. *Inorg. Chem.* **1980**, *19*, 1231.
25. Brandt, L.; Wolf, J.; Werner, H. *J. Organomet. Chem.* **1993**, *444*, 235.
26. Wolf, J.; Brandt, L.; Fries, A.; Werner, H. *Angew. Chem. Int. Ed.* **1990**, *29*, 510.
27. Head, R. A.; Hitchcock, P. B. *J. Chem. Soc., Dalton Trans.* **1980**, 1150.
28. Colquhoun, H. M.; King, T. J. *J. Chem. Soc. Chem. Commun.* **1980**, 879.
29. Colquhoun, H. M.; Williams, D. J. *J. Chem. Soc., Dalton Trans.* **1984**, 1675.
30. Smegal, J. A.; Meier, I. K.; Schwartz, J. *J. Am. Chem. Soc.* **1986**, *108*, 1322.
31. Curtis, M. D.; Messerle, L. *Organometallics* **1987**, *6*, 1713.
32. Messerle, L.; Curtis, M. D. *J. Am. Chem. Soc.* **1982**, *104*, 889.
33. Polse, J. L.; Kaplan, A. W.; Andersen, R. A.; Bergman, R. G. *J. Am. Chem. Soc.* **1998**, *120*, 6316.

34. Nakamura, A.; Yoshida, T.; Cowie, M.; Otsuka, S.; Ibers, J. A. *J. Am. Chem. Soc.* **1977**, *99*, 2108.
35. Polse, J. L.; Kaplan, A. W.; Andersen, R. A.; Bergman, R. G. *J. Am. Chem. Soc.* **1998**, *120*, 6316.
36. Gambarotta, S.; Floriani, C.; Chiesi-Villa, A.; Guastini, C. *J. Am. Chem. Soc.* **1982**, *104*, 1918.
37. Otsuka, S.; Nakamura, A.; Koyama, T.; Tatsuno, Y. *J. Chem. Soc. Chem. Commun.* **1972**, 1105.
38. Nakamura, A.; Aotake, M.; Otsuka, S. *J. Am. Chem. Soc.* **1974**, *96*, 3456.
39. Schramm, K. D.; Ibers, J. A. *Inorg. Chem.* **1980**, *19*, 2441.
40. Messerle, L.; Curtis, M. D. *J. Am. Chem. Soc.* **1980**, *102*, 7749.
41. Eisenberg, R.; Woodcock, C. *Organometallics* **1995**, *4*, 4.
42. Minhas, R. K.; Edema, J. J. H.; Gambarotta, S.; Meetsma, A. *J. Am. Chem. Soc.* **1993**, *115*, 6710.
43. Gao, Y.; Jennings, M. C.; Puddephatt, R. J.; Jenkins, H. A. *Organometallics* **2001**, *20*, 3500.
44. Bell, L. K.; Herrmann, W. A.; Kriechbaum, G. W.; Pfisterer, H.; Ziegler, M. L. *J. Organomet. Chem.* **1982**, *240*, 381.
45. Herrmann, W. A.; Bell, L. K. *J. Organomet. Chem.* **1982**, *239*, C4.
46. Herrmann, W. A.; Kriechbaum, G. W.; Ziegler, M.; Pfisterer, H. *Angew. Chem. Int. Ed.* **1982**, *21*, 707.
47. Herrmann, W. A. *J. Organomet. Chem.* **1983**, *250*, 319.
48. Herrmann, W. A.; Menjon, B.; Herdtweck, E. *Organometallics* **1991**, *10*, 2134.
49. Herrmann, W. A.; Bell, L. K.; Ziegler, M. L.; Pfisterer, H.; Pahl, C. *J. Organomet. Chem.* **1983**, *247*, 39.

50. Curtis, M. D.; Messerle, L.; D'Errico, J. J.; Butler, W. M.; Hay, M. S. *Organometallics* **1986**, *5*, 2283.
51. Gambarotta, S.; Floriani, C.; Chiesi-Villa, A.; Guastini, C. *J. Am. Chem. Soc.* **1983**, *105*, 7295.
52. Arvanitis, G. M.; Schwartz, J.; Van Engen, D. *Organometallics* **1986**, *5*, 2157.
53. Arvanitis, G. M.; Smegal, J.; Meier, I.; Wong, A. C. C.; Schwartz, J.; Van Engen, D. *Organometallics* **1989**, *8*, 2717.
54. D'Errico, J. J.; Messerle, L.; Curtis, M. D. *Inorg. Chem.* **1983**, *22*, 849.
55. McKeer, I.R.; Sherlock, S.J.; Cowie, M. *J. Organomet. Chem.* **1988**, *352*, 205.
56. (a) Trepanier, S. J.; Sterenberg, B. T.; McDonald, R.; Cowie, M. *J. Am. Chem. Soc.* **1999**, *121*, 2613. (b) Trepanier, S. J.; Dennett, J. N. L.; Sterenberg, B. T.; McDonald, R.; Cowie, M. *J. Am. Chem. Soc.* **2004**, *126*, 8046.
57. Dell'Anna, M. M.; Trepanier, S. J.; McDonald, R.; Cowie, M. *Organometallics* **2001**, *20*, 88.
58. Rowsell, B. D.; Trepanier, S. J.; Lam, R.; McDonald, R.; Cowie, M. *Organometallics* **2002**, *21*, 3228.
59. Trepanier, S.J.; McDonald, R.; Cowie, M. *Organometallics* **2003**, *232*, 2638.
60. Rowsell, B.D.; McDonald, R.; Ferguson, M.J.; Cowie, M. *Organometallics* **2003**, *22*, 2944.
61. Rowsell, B.D.; McDonald, R.; Cowie, M. *Organometallics* **2004**, *23*, 3873.
62. Chokshi, A.; Rowsell, B.D.; Trepanier, S.J.; Ferguson, M.J.; Cowie, M. *Organometallics* **2004**, *23*, 4759.
63. Cowie, M. *Can. J. Chem.* **2005**, *83*, 1043.
64. Wigginton, J.R.; Trepanier, S.J.; McDonald, R.; Ferguson, M.J.; Cowie, M. *Organometallics* **2005**, *24*, 6194.

65. Wigginton, J.R.; Chokshi, A.; Graham, T.W.; McDonald, R.; Ferguson, M.J.; Cowie, M. *Organometallics* **2005**, *24*, 6398.
66. Hilts, R. W.; Franchuk, R. A.; Cowie, M. *Organometallics* **1991**, *10*, 304.
67. Searle, N. E. *Org. Synth.* **1956**, *36*, 25.
68. Programs for diffractometer operation, data collection, data reduction, and absorption correction were those supplied by Bruker.
69. Beurskens, P. T.; Beurskens, G.; Bosman, W. P.; de Gelder, R.; Garcia Granda, S.; Gould, R. O.; Israel, R.; Smits, J. M. M. (1996). The DIRDIF-96 program system. Crystallography Laboratory, University of Nijmegen, The Netherlands.
70. http://www.aist.go.jp/RIODB/SDBS/cgi-bin/cre_index.cgi.
71. Silverstein, R. M.; Webster, F. X. *Spectroscopic Identification of Organic Compounds*; John Wiley and Sons, Inc.: New York, 1998.
72. George, D. S. A.; McDonald, R.; Cowie, M. *Organometallics* **1998**, *17*, 2553.
73. (a) Collman, J. P.; Hegedus, L. S.; Norton, J. S.; Finke, R.G., *Principles and Applications of Organotransition Metal Chemistry*, University Science Books, Mill Valley, CA, 1987; Chapter 12. (b) Niu, S.; Hall, M.B.; *Chem. Rev.* **2000**, *100*, 353.
74. Herrmann, W. A.; Plank, J.; Ziegler, M. L.; Weidenhammer, K. *J. Am. Chem. Soc.*, **1979**, *101*, 3133.
75. Proulx, G.; Bergman, R.G. *Science*, **1993**, *259*, 661.
76. Li, B.; Tan, X.; Xu, S.; Song, H.; Wang, B. *J. Organomet. Chem.* **2008**, *693*, 667.
77. Allen, F. H.; Kennard, O.; Watson, D. G.; Brammer, L.; Orpen, A. G.; Taylor, R. *J. Chem. Soc. Perkin Trans. II* **1987**, S1.
78. Woodcock, C.; Eisenberg, R. *Organometallics* **1985**, *4*, 4.
79. Ristic-Petrovic, D.; Anderson, D.J.; Torkelson, J.R.; Ferguson, M.J.; McDonald, R.; Cowie, M. *Organometallics* **2005**, *24*, 3711.

80. (a) Li, J.; Schreckenbach, G.; Ziegler, T. *Inorg. Chem.* **1995**, *34*, 3245. (b) Burke, M.R.; Takats, J.; Grevels, F.-W.; Reuvers, J.G.A. *J. Am. Chem. Soc.* **1983**, *105*, 4092.
81. Clayden, J.; Greeves, N.; Warren, S.; Wothers, P. *Organic Chemistry*; Oxford University Press: Oxford, 2001.
82. (a) Evans, D. A.; Truesdale, L. K.; Grimm, K. G. *J. Org. Chem.* **1976**, *41*, 3335. (b) Yao, W.; Wang, J. *J. Org. Chem.* **2003**, *5*, 1527. (c) Xiao, F.; Liu, Y.; Wang, J. *Tet. Lett.* **2007**, *48*, 1147. (d) Kantam, M. L.; Balasurbrahmanyam, V.; Kumar, K. B. S.; Venkanna, G. T.; Figueras, F. *Adv. Synth. Catal.* **2007**, *349*, 1887.

Chapter 3: Unsymmetrically Bridged Methyl Groups as Intermediates in the Transformation of Bridging Methylene to Bridging Acetyl Groups: Ligand Migrations and Migratory Insertions in Mixed Ir/Ru Complexesⁱ

3.1 Introduction

Migratory insertion involving metal-bound alkyl and carbonyl groups^{1,2} is a pivotal step in a range of important processes including olefin hydroformylation,³⁻⁵ methanol carbonylation,⁶⁻⁹ and the copolymerization of carbon monoxide and alkenes,^{10,11} and may also play a role in the formation of oxygen-containing products in the Fischer-Tropsch (FT) reaction.¹²⁻¹⁷ In several of these processes^{3-9,12-17} metals of the Co triad play a prominent role. Whereas the FT process is heterogeneously catalyzed, and is not yet well understood, the first three processes noted above are homogeneous, have been extensively studied, and are consequently reasonably well understood. Nevertheless, migratory insertion and the influences of the metals and the ancillary ligands on this transformation continue to be of interest.^{18,19}

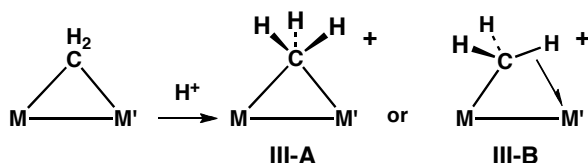
A recent development in the above carbonyl-insertion processes has been the interest in the cooperative involvement of adjacent metals in both homobinuclear^{20,21} and heterobinuclear^{5, 22-29} systems. In such systems it is clearly of interest to determine the roles of the adjacent metals in the different steps leading to product formation, and in the case of the mixed-metal systems, it is of additional interest to determine at which metal each step occurs. In one particularly interesting study, Komiya and coworkers reported the enhancement of

ⁱ The work presented in this chapter has been accepted for publication elsewhere: Samant, R. G.; Trepanier, S. J.; Wigginton, J. R.; Xu, L.; Berenstiel, M.; McDonald, M.; Ferguson, M. J.; Cowie, M. *Organometallics*, **2009**, in press.

migratory insertion at Pd by an adjacent Co center, and on the basis of DFT calculations a mechanism was proposed in which the roles of the different metals were outlined.²⁹

In related studies, involving the Rh/Ru³⁰ and Rh/Os^{31,32} combinations of metals, we have investigated the roles of the different metals in the individual steps leading from bridging methylene groups to bridging acyl groups, using low temperature multinuclear NMR techniques to study intermediates in the transformation. One of the key steps in this conversion is the formation of a bridging methyl ligand by protonation of the bridging methylene group (see Chart 3.1). The two most common binding modes for bridging methyl groups are

Chart 3.1



the symmetrically bridged geometry (**III-A**),³³⁻⁴⁵ containing a three-centered M-C-M interaction, and the unsymmetrically bridged geometry (**III-B**)^{30-32,46-52} in which the methyl group is σ -bound to one metal while engaging in a three-centered M-H-C agostic interaction with the other. For late-transition metal complexes the unsymmetric mode **III-B** is by far the more common with only a few examples reported of species of type **III-A**.⁴¹⁻⁴⁵

In this chapter our previous studies on the Rh/Ru³⁰ and Rh/Os^{31,32} systems are extended to include the Ir/Ru metal combination. We are attempting to obtain a more complete understanding of the roles of different metals in organometallic transformations through studies involving a range of metal combinations, in order to compare the effects of changing from one metal to another.

In addition to complementing our previous work, the Ir/Ru system is particularly relevant to migratory insertion in methanol carbonylation since the

CATIVA™ process⁵³ utilizes a mixed Ir/Ru catalyst system. Although mechanistic studies have established that the role of Ru in this system is limited to iodide abstraction from Ir, at which all fundamental steps in the process (oxidative addition, migratory insertion and reductive elimination) appear to occur,⁹ the possibility that adjacent Ir and Ru centers could play greater roles in this and related processes is intriguing.

3.2 Experimental

3.2.1 General Comments. All solvents were dried (using appropriate drying agents), distilled before use, and stored under nitrogen. Reactions were performed under an argon atmosphere using standard Schlenk techniques. HBF₄•Me₂O, CF₃SO₃H, and PMe₃ (1M in toluene) were purchased from Aldrich. Carbon-13-enriched CO (99.4% enrichment) was purchased from Cambridge Isotopes Laboratories, while hydrogen gas was purchased from Praxair. [IrRu(CO)₄(μ-CH₂)(dppm)₂][X] (X= CF₃SO₃, BF₄) (**8**) and [IrRu(PMe₃)(CO)₃(μ-CH₂)(dppm)₂][X] (X= CF₃SO₃, BF₄) (**33**) were prepared as previously reported.⁵⁶ The triflate salt of **8** was prepared by an analogous route using triflic acid instead of tetrafluoroboric acid in the protonation step, and the triflate salt of **33** was prepared by reaction of **8**-CF₃SO₃ with PMe₃. NMR spectra were recorded on a Bruker AM-400 spectrometer operating at 400.1 MHz for ¹H, 161.9 MHz for ³¹P, and 100.6 MHz for ¹³C nuclei, or a Varian spectrometer operating at 399.9, 161.8 and 100.6 MHz for the respective nuclei. Infrared spectra were obtained on a Nicolet Magna 750 FTIR Spectrometer with a NIC-Plan IR Microscope. Spectroscopic data for all new compounds are presented in Table 1. The elemental analyses were performed by the micro-analytical service within the department. Electrospray mass spectra were run on a Micromass ZabSpec instrument. In all cases the distribution of isotope peaks for the appropriate parent ion matched very closely that calculated for the formulation given.

In all the complexes in which there is no coordinating anion the complex cations involving both the BF₄⁻ and CF₃SO₃⁻ salts have identical spectral

properties and are therefore interchangeable. Spectroscopic data for all new compounds prepared is given in Table 3.1.

Table 3.1: Spectroscopic Data for Compounds Prepared

Compound	IR (cm ⁻¹) ^a	NMR ^{b,c}	
		$\delta(^1\text{H})^d$	$\delta(^{13}\text{C}\{\text{H}\})^d$
[IrRu(CO) ₄ (μ-CH ₃)- (dppm) ₂][CF ₃ SO ₃] ₂ (34) ^e	N/A	P(Ru): 25.8 (m, 2P) P(Ir): -13.7 (m, 2P) μ-CH ₂ H: -10.88 (br, 1H); (¹ J _{CH} = 65 Hz) ^h μ-CH ₂ H: 3.79 (m, br, 2H); (¹ J _{CH} = 146 Hz) ^h dppm: 4.14 (m, br, 2H), 5.06 (m, br, 2H).	CO(Ir): 170.0 (br, 1C); 161.2 (br, 1C) CO(Ru): 195.6 (br, 1C); 186.0 (br, 1C) CH ₃ : 18.7 (m, br)
[IrRu(CH ₃)(CO) ₄ - (dppm) ₂][CF ₃ SO ₃] ₂ (35) ^f	N/A	P(Ru): 19.8 (m, 2P) P(Ir): 18.3 (m, 2p) CH ₃ : 2.10 (t, 3H, ³ J _{P(Ir)H} = 9Hz); (¹ J _{CH} = 135 Hz) ^h dppm: 3.79 (m, 4H)	CH ₃ : 39.8 (s, br, 1C) μ-CO: 215.8 (m, 2C) CO(Ru): 187.0 (t, 2C, ² J _{PC} = 9 Hz)
[IrRu(CO) ₅ (CH ₃)- (dppm) ₂][CF ₃ SO ₃] ₂ (36)	2071(m), 2037(s), 2009(m)	P(Ru): 20.9 (m, 2P) P(Ir): -19.5 (m, 2P) CH ₃ 1.11 (t, br, 3H, ³ J _{P(Ir)H} = 5Hz); (¹ J _{CH} = 140 Hz) ^h dppm: 4.58 (m, 4H)	CO(Ru): 202.0 (t, 2C, ² J _{P(Ru)C} : 12 Hz); 185.7 (t, 1C, ² J _{P(Ru)C} = 9 Hz) CO(Ir): 181.6 (t, 2C, ² J _{P(Ir)C} = 11 Hz) CH ₃ : -18.5 (br, t, ² J _{PC} = 3.2 Hz)
[IrRu(CH ₃)(OSO ₂ CF ₃)- (CO) ₃ (dppm) ₂]- [CF ₃ SO ₃] ₂ (37)	2039 (s), 1980 (s), 1784 (m)	P(Ru): 18.0 (m, 2P) P(Ir): 19.8 (m, 2P) CH ₃ : 1.58 (t, 3H, ³ J _{P(Ir)H} = 8 Hz); (¹ J _{CH} = 133 Hz) ^h dppm: 3.42 (m, 2H); 3.08 (m, 2H)	CO(Ru): 222.5 (dt, 1C ² J _{P(Ru)C} = 11 Hz); 212.4 (m, 1C); 188.4 (m, 1C) CH ₃ : 33.6 (t, ² J _{PC} = 8 Hz)
[IrRu(CO) ₃ (PMe ₃)(μ- η ¹ :η ² -CH ₃)(dppm) ₂]- [CF ₃ SO ₃] ₂ (38) ^g	2041 (m) 2004 (s)	P(Ru): 18.2, (m, 2H) P(Ir): -17.1 (m, 2H) PMe ₃ (Ru): -45.7 (m) μ-CH ₂ H: -9.09 (br, 1H, ² J _{HH} = 13Hz); (¹ J _{CH} = 72 Hz) ^h μ-CH ₂ H: 2.93 (br, 2H, ² J _{HH} = 13 Hz); (¹ J _{CH} = 140 Hz) ^h PMe ₃ : 1.10 (d, 9H, ² J _{PH} = 11 Hz) dppm: 4.13 (m, 2H); 3.87 (m, 2H)	CO(Ru): 203.5 (dt, 1C, ² J _{P(Ru)C} = 10 Hz, ² J _{P(Me₃)C} = 6 Hz); 184.6 (dt, 1C, ² J _{P(Ru)C} = 15 Hz, ² J _{P(Me₃)C} = 18 Hz) CO(Ir): 177.4 (t, 1C, ² J _{P(Ir)C} = 14 Hz) CH ₃ : (-60 °C) 12.8 (td, ¹ J _{CH} = 140 Hz, ¹ J _{CH} = 72 Hz); (-20 °C) 12.9 (q, ¹ J _{CH} = 117 Hz); (27 °C) 13.0 (q, ¹ J _{CH} = 133 Hz).

Table 3.1: (continued) Spectroscopic Data for Compounds Prepared

Compound	IR (cm ⁻¹) ^a	NMR ^{b,c}		
		$\delta(^3\text{P}\{^1\text{H}\})^c$	$\delta(^1\text{H})^d$	$\delta(^{13}\text{C}\{^1\text{H}\})^d$
[IrRu(CO) ₄ (μ-C(CH ₃)O)(dppm) ₂]-[CF ₃ SO ₃] ₂ (39)	2108(s), 2075(s), 2052(s), 1990(s)	P(Ru): 16.4(m) P(Ir): -17.9(m)	dppm: 4.51 (m, 2H); 4.37 (m, 2H)	CH ₃ CO: 251.2 (m, 1C) CO(Ru): 204.6 (m, 1C); 187.5 (m, 1C) CO(Ir): 172.4 (m, 1C); 157.7 (m, 1C) CH ₃ CO: 287.0 (m, 1C) CO(Ru): 206.0 (m, 1C); 179.8 (t, 1C, ² J _{P(Ru)C} = 12 Hz) CO(Ir): 189.0 (m, 1C)
[IrRu(CO) ₃ (μ-C(CH ₃)O)(dppm) ₂]-[BF ₄] ₂ (40)	2017(m), 2002(s), 1961(s)	P(Ru): 19.2(m) P(Ir): 12.5(m)	CH ₃ : 2.02 (br, 3H) dppm: 4.27 (m, 2H); 3.16 (m, 2H)	CH ₃ CO: 231.4 (s, br, 1C) CO(Ru): 205.6 (m, 1C, ² J _{P(Ru)C} = 11 Hz); 186.7 (m, 1C, ² J _{P(Ru)C} = 15 Hz) CO(Ir): 168.6 (s, br, 1C)
[IrRu(OSO ₂ CF ₃)(CO) ₃ -(μ-C(CH ₃)O)(dppm) ₂]-[CF ₃ SO ₃] (41)	2045(s), 2012(s), 1961(s)	P(Ru): 19.9(m) P(Ir): -14.6(m)	CH ₃ : 2.46 (s, 3H) dppm: 4.10 (m, 2H); 3.45 (m, 2H)	CH ₃ CO: 231.4 (t, 1C, ² J _{P(Ir)C} = 4 Hz) CO(Ru): 205.6 (t, 1C, ² J _{P(Ru)C} = 11 Hz); 186.7 (m, 1C, ² J _{P(Ru)C} = 15 Hz) CO(Ir): 168.6 (s, br, 1C)
[IrRu(OSO ₂ CF ₃)(CO) ₂ -(μ-C(CH ₃)O)(dppm) ₂]-[CF ₃ SO ₃] (42)	2041(s), 1988(s)	P(Ru): 18.0(m) P(Ir): 15.1(m)	CH ₃ : 1.57 (s, 3H) dppm: 3.73 (m, 2H); 2.45 (m, 2H)	CH ₃ CO: 231.4 (t, 1C, ² J _{P(Ir)C} = 4 Hz) CO(Ru): 205.6 (t, 1C, ² J _{P(Ru)C} = 11 Hz); 186.7 (m, 1C, ² J _{P(Ru)C} = 15 Hz)

Table 3.1: (continued) Spectroscopic Data for Compounds Prepared

		NMR ^{b,c}	
Compound	IR (cm ⁻¹) ^a	$\delta(^1\text{H})^c$	$\delta(^{13}\text{C}\{^1\text{H}\})^d$
[IrRu(H)(CO) ₃ (μ-C(CH ₃)O)(dppm) ₂]-[CF ₃ SO ₃] (43)	2070(m), 2010(s), 1966(s)	CH ₃ : 1.22 (br, 3H) dppm: 3.95 (m, 4H) H: -10.35 (t, 1H, ³ J _{P(Tr)H} = 12 Hz)	CH ₃ CO: 260.2 (dm, 1C, ² J _{CC} = 30 Hz) CO(Ru): 212.0 (t, 1C, ² J _{P(Ru)C} = 10 Hz); 188.0 (t, 1C, ² J _{P(Ru)C} = 12 Hz) CO(Tr): 183.4 (dm, 1C, ² J _{CC} = 30 Hz)
[IrRu(CO) ₂ (H ₂)(μ-C(CH ₃)O)(dppm) ₂]-[CF ₃ SO ₃] ₂ (44) ^e	N/A	CH ₃ : 1.52 (s, 3H) dppm: 3.67 (m, 2H); 2.37 (m, 2H) H ₂ : -0.03 (br, 2H)	CH ₃ CO: 211.8 (m, 1C) CO(Ru): 203.1 (m, 1C, ² J _{P(Ru)C} = 13 Hz); 202.5 (t, 1C, ² J _{P(Ru)C} = 11 Hz)
[IrRu(H) ₂ (OS) ₂ CF ₃ -(CO) ₂ (μ-C(CH ₃)O)-(dppm) ₂][CF ₃ SO ₃] (45)	2040(s) 1992(s)	CH ₃ : 0.94 (s, 3H) dppm: 6.18 (m, 2H); 4.88 (m, 2H) H: -12.28 (m, 1H, ² J _{P(Tr)H} = 12 Hz; ³ J _{HH} = 5 Hz) H: -9.95 (m, 1H, ² J _{P(Ru)H} = 3 Hz; ³ J _{HH} = 5 Hz, ⁴ J _{HH(dppm)} = 3 Hz)	CH ₃ CO: 235.6 (t, 1C, ² J _{CP(Tr)} = 5 Hz) CO(Ru): 192.8 (tm, 1C, ² J _{P(Ru)C} = 14 Hz); 191.8 (m, 1C) (t, 1C, ² J _{P(Ru)C} = 8.8 Hz);
[IrRu(H) ₂ (CO) ₃ (μ-C(CH ₃)O)(dppm) ₂][CF ₃ SO ₃] ₂ (46)	2015(s) 2022(s) 1963(s)	CH ₃ : 2.27 (s, 3H) dppm: 4.86 (m, 2H); 4.14 (m, 2H) H: -13.42 (br, 1H); -12.40 (br, 1H)	CO(Ru): 194.2 (t, 1C, ² J _{P(Ru)C} = 10.6 Hz); 190.2 (CO(Tr): 167.3 (td, 1C, ² J _{P(Tr)C} = 10.5 Hz), ² J _{CC} = 4.4 Hz); C(O)CH ₃ : 262.0 (m, 1C, ² J _{CC} = 4.4 Hz).

^aIR abbreviations: S = strong, m = medium, br = broad. Dichloromethane solution: in units of cm⁻¹. ^bNMR abbreviations: s = singlet, d = doublet, t = triplet, m = multiplet, br = broad, bs = broad singlet, bd = broad doublet. NMR data at 27 °C in CD₂Cl₂ unless otherwise indicated. ^c¹H chemical shifts referenced to external 85% H₃PO₄. ^d¹³C chemical shifts referenced to TMS. Chemical shifts for the phenyl protons are not given; these labeled dppm are for the methylene groups. ^eNMR data in CD₂Cl₂ at -90 °C. ^fNMR data in CD₂Cl₂ at -60 °C. ^g¹³CH₃-enriched sample

3.2.2 Preparation of Compounds.

(a) [IrRu(CO)₄(μ-CH₃)(dppm)₂][CF₃SO₃]₂ (34). Triflic acid (0.7 μL, 0.0075 mmol) was added to a CD₂Cl₂ solution (0.5 mL) of [IrRu(CO)₄(μ-CH₂)(dppm)₂][CF₃SO₃] (**8**) (10 mg, 0.008 mmol) in an NMR tube, cooled to -90 °C using a diethylether/liquid nitrogen bath and monitored with a thermometer. The solution remained yellow; nevertheless, NMR spectra at -90 °C clearly showed the quantitative conversion to a new species (**34**). Compound **34** was unstable, transforming to other species at temperatures above -90 °C and was therefore characterized by multinuclear NMR techniques at this temperature.

(b) [IrRu(CH₃)(CO)₄(dppm)₂][CF₃SO₃]₂ (35). *Method (i):* An NMR sample of compound **34** at -90 °C was warmed to -80 °C over a 30 min period. Although the solution remained yellow, the ¹H and ³¹P NMR spectra indicated the quantitative formation of a new compound (**35**). Again, this product was unstable, transforming to compounds **36** and **37** as the temperature was raised and was therefore characterized by multinuclear NMR techniques at -80 °C. *Method (ii):* Triflic acid as an ethereal solution (1.5 μL in 5 mL, 0.15 mmol) was added to a yellow solution of **8** (20mg, 0.016 mmol) in 4 mL of CH₂Cl₂ at -78 °C.

(c) Mixture of [IrRu(CH₃)(CO)₅(dppm)₂][CF₃SO₃]₂ (36) and [IrRu(CH₃)(CF₃SO₃)(CO)₃(dppm)₂][CF₃SO₃] (37). An NMR sample of compound **35** at -78 °C was gradually warmed to 25 °C. The ¹H and ³¹P NMR spectra indicated the presence of compounds **35**, **36** and **37** in a 1:1:1 mixture. Compound **37** did not persist in solution over a 24 h period, decomposing into several unidentified products, so its characterization was based on NMR studies of fresh reaction solutions.

(d) [IrRu(CH₃)(CO)₅(dppm)₂][CF₃SO₃]₂ (36). Carbon monoxide was passed through a solution of compound **35** (40 mg, 0.027 mmol) in CH₂Cl₂ (5 mL) at -78 °C for one min, resulting in the change of the solution color to a paler shade of yellow. The solution was stirred for 30 min as it was allowed to warm to ambient temperature. Diethyl ether (20 mL) was then added to precipitate a yellow solid. This precipitate was then washed with three 5 mL portions of ether and dried *in*

vacuo (yield 86%). Anal. Calcd for $C_{57}H_{47}O_8F_3SP_4IrRu$: C: 45.97, H: 3.13. Found: C: 45.54, H: 3.25. HRMS: m/z Calcd for $C_{56}H_{46}O_5P_4IrRu$ ($M^+ - H^+ - 2CF_3SO_3^-$): 1217.0968. Found: 1217.0960. NMR spectra of the redissolved solid showed compound **36** as the only detectable product.

(e) [IrRu(PMe₃)(CO)₃(μ-CH₃)(dppm)₂][CF₃SO₃]₂ (38). A slight excess of triflic acid (1.4 μL, 0.016 mmol) was added to a CD₂Cl₂ solution (0.7 mL) of [IrRu(PMe₃)(CO)₃(μ-CH₂)(dppm)₂][CF₃SO₃] (**33**) (20 mg, 0.014 mmol) in an NMR tube. NMR spectroscopy showed quantitative conversion to a new species (**38**). Precipitation with diethyl ether afforded a yellow solid which was rinsed with three 5 mL portions of ether before being dried *in vacuo*. Anal. Calcd for $C_{59}H_{56}F_6O_9P_5S_2IrRu$: C 46.09, H: 3.67. Found: C: 46.37, H: 3.57. HRMS: m/z Calcd for $C_{57}H_{55}O_3P_5IrRu$ ($M^+ - H^+ - 2CF_3SO_3^-$): 1237.1507. Found: 1237.1511.

(f) [IrRu(CO)₄(μ-C(CH₃)O)(dppm)₂][CF₃SO₃]₂ (39). A solution of compound **36** (40 mg, 0.026 mmol) in 10 mL of CH₂Cl₂ was stirred for two days, followed by concentration of the solution to 5 mL under an argon stream. Diethyl ether (20 mL) was added to precipitate a yellow solid, which was collected, washed with three 5 mL portions of ether and dried *in vacuo* (yield 91%). Spectral characterization of this product showed it to be the only species present. HRMS: m/z Calcd for $C_{55}H_{47}O_4P_4IrRu$ ($M^{2+} - CO - 2CF_3SO_3^-$): 595.0543. Found: 595.0543.

(g) [IrRu(CO)₃(μ-C(CH₃)O)(dppm)₂][BF₄]₂ (40). Compound **39-BF₄** (280 mg, 0.200 mmol) was prepared as described for the preparation of **39-CF₃SO₃**, except using HBF₄•OEt₂ to protonate the BF₄⁻ salt of **1**. A suspension of **39-BF₄** in CH₂Cl₂ (30 mL) was refluxed for 5 h under an Ar atmosphere. The resulting suspension was filtered and the red-orange solid was washed with 30 mL of CH₂Cl₂ and 30 mL of pentane and then dried *in vacuo* (yield 70%). Anal. Calcd for $C_{55}H_{47}B_2F_8O_4P_4IrRu$: C: 48.48, H: 3.45. Found: C: 47.96, H: 3.52. MS: m/z 595 ($M^+ - 2BF_4^-$).

(h) [IrRu(OSO₂CF₃)(CO)₃(μ-C(CH₃)O)(dppm)₂][CF₃SO₃] (41). A solution of 100 mg (0.067 mmol) of compound **39**, as the triflate salt, in 6 mL of CH₂Cl₂ was refluxed for 2 h with a continuous slow stream of argon. The color of the solution

changed from yellow to orange. After allowing the solution to cool, diethyl ether (20 mL) and pentane (20 mL) were added to precipitate a pale orange solid, which was washed with three 5 mL portions of ether and dried *in vacuo* (yield 90%). Anal. Calcd for C₅₇H₄₇F₆O₁₀P₄S₂IrRu: C: 46.03, H: 3.19. Found: C: 45.64, H: 3.17. MS: *m/z* 595 (M²⁺ – 2CF₃SO₃[–]).

(i) [IrRu(OSO₂CF₃)(CO)₂(μ-C(CH₃)O)(dppm)₂][CF₃SO₃] (42). A slurry of 100 mg (0.067 mmol) of compound **39**, as the triflate salt, in 30 mL of THF was refluxed for 6 h while purging with argon. The color of the solution changed from yellow to red-orange and a red precipitate formed. After cooling to ambient temperature, diethyl ether (20 mL) was added to fully precipitate the pale red solid. This solid was washed with three 5 mL portions of ether and dried *in vacuo* (yield 88%). Anal. Calcd for C₅₆H₄₇F₆O₉P₄S₂IrRu: C, 46.09; H, 3.25. Found: C, 45.68; H, 3.28. MS: *m/z* 581 (M²⁺ – 2CF₃SO₃[–]).

(j) [IrRu(H)(CO)₃(μ-C(CH₃)O)(dppm)₂][BF₄] (43). *Method (i):* Compound **40** (100 mg, 0.073 mmol) was suspended in 10 mL of CH₂Cl₂ and H₂ was passed through the mixture for 30 min at a rate of approximately 0.05 mL/sec, turning the solution from orange to clear yellow. Ether (50 mL) was added to the solution affording a yellow precipitate which was subsequently washed with pentane (2 x 15 mL) and dried *in vacuo* (yield 100%). Anal. Calcd for C₅₅H₄₈BF₄O₄P₄IrRu: C, 51.74; H, 3.76. Found: C, 51.19; H, 3.79. MS: *m/z* 1191 (M⁺ – BF₄[–]). The triflate salt of compound **43** was prepared by an analogous procedure, but starting from compound **41** rather than **40**. *Method (ii):* Compound **43-CF₃SO₃** was also prepared through addition of super-hydride (LiBEt₃H) (1M in THF) (2 μL, 0.015 mmol) to a THF solution (10 mL) of **41** (20 mg, 0.015 mmol) at ambient temperature. After 10 min diethyl ether (30 mL) was slowly added to precipitate a pale yellow solid. ³¹P NMR spectroscopy showed quantitative conversion to **43**.

(k) [IrRu(H₂)(CO)₂(μ-C(CH₃)O)(dppm)₂][CF₃SO₃]₂ (44). A CD₂Cl₂/CD₃NO solution (0.65 mL/0.05 mL) of compound **42** (10 mg, 0.007 mmol) was cooled to –90 °C and then saturated with H₂. Approximately 50% of compound **42** was converted to **44**, along with numerous other decomposition products. Compound **44** was characterized by NMR spectroscopy at –90 °C since it converted back to

42 at higher temperatures and formed compound **45** above $-60\text{ }^{\circ}\text{C}$. Removal of H_2 by vacuum or an Ar stream at $-90\text{ }^{\circ}\text{C}$ also resulted in the conversion of **44** into **42**.

(l) [IrRu(H)₂(OSO₂CF₃)(CO)₂(μ -C(CH₃)O)(dppm)₂][CF₃SO₃] (45). Compound **42** (20 mg, 0.014 mmol) was dissolved in 10 mL of CH_2Cl_2 at ambient temperature and H_2 was passed through the yellow solution for 5 min at a rate of 0.05 ml/s. The solution was stirred for a further 30 min, after which diethyl ether (20 mL) and pentane (20 mL) were added to precipitate a pale yellow solid. The solid was washed with three 5 mL aliquots of ether and dried *in vacuo* (yield 90%). Anal. Calcd for: $\text{C}_{56}\text{H}_{55}\text{O}_9\text{F}_6\text{P}_4\text{S}_2\text{IrRu}$: C: 45.77, H: 3.78. Found: C: 46.05, H: 4.26.

(m) [IrRu(H)₂(CO)₃(μ -C(CH₃)O)(dppm)₂][CF₃SO₃]₂ (46). Carbon monoxide was passed through a solution of **45** (20 mg, 0.014 mmol) in 2 mL of CH_2Cl_2 at a rate of 0.1 mL/sec for 2 min. ^{31}P NMR confirmed complete conversion of **45** to **46**. The solution volume was reduced to 50% *in vacuo* and the addition of 5 mL of ether afforded a yellow powder, which was rinsed three times with 1 mL portions of ether before being dried *in vacuo* (yield 85%). HRMS: m/z Calcd 596.0627 ($\text{M}^{2+}-2(\text{CF}_3\text{SO}_3)$), found 596.0635.

(n) Reaction of 43 with CO. Carbon monoxide was passed through a solution of **43** (15 mg, 0.010 mmol) in 0.7 mL of CD_2Cl_2 at a rate of 0.1 mL/sec for 2 min. ^{31}P NMR of the sample revealed the formation of previously known species $[\text{IrRu}(\text{CO})_4(\text{dppm})_2][\text{CF}_3\text{SO}_3]$ accompanied by numerous unknown decomposition products (approximately 50% of all phosphorus-containing products based on integration of the $^{31}\text{P}\{^1\text{H}\}$ NMR spectra), whereas ^1H NMR of the sample showed approximately 0.2 equiv of acetaldehyde.

(o) X-ray Data Collection and Structure Solution. Dr. Bob McDonald and Dr. Michael Ferguson of the X-ray crystallography laboratory in the Department of Chemistry at the University of Alberta carried out all X-ray studies. (a) Pale yellow crystals of $[\text{IrRu}(\text{CH}_3)(\text{CO})_5(\text{dppm})_2][\text{CF}_3\text{SO}_3]_2 \cdot 3\text{CH}_2\text{Cl}_2$ (**36**) were obtained *via* slow diffusion of diethyl ether into a dichloromethane solution of the compound. Data were collected on a Bruker PLATFORM/SMART 1000 CCD

diffractometer⁵⁷ using Mo K α radiation at -80 °C. Unit cell parameters were obtained from a least-squares refinement of the setting angles of 4551 reflections from the data collection. The space group was determined to be *Cc* (No. 9). Data were corrected for absorption through use of the *SADABS* procedure. See Table 2 for a summary of crystal data and X-ray data collection information.

The structure of **36** was solved using the Patterson search and structure expansion routines as implemented in the *DIRDIF-99*⁵⁸ program system. Refinement was completed using the program *SHELXL-93*.⁵⁹ Hydrogen atoms were assigned positions based on the geometries of their attached carbon atoms, and were given thermal parameters 20% greater than those of the attached carbons. The metal atom sites were found to be disordered; the atom labeled Ir in Figure 1 was refined as a combination of 60% Ir and 40% Ru, while the Ru atom was refined at 60% Ru and 40% Ir. The iridium-bound methyl group and the carbonyl group attached to ruthenium trans to iridium (C(6)O(6) in Figure 3.1) were likewise disordered, with O(6) and the hydrogens attached to C(3) refined with an occupancy factor of 60% (the oxygen attached to C(3) and the hydrogens on the minor-occupancy species, attached to C(6), were refined at 40% occupancy). One of the triflate counterions was also disordered, resulting in the splitting of its fluorine, oxygen, and carbon atoms into two sets of equally abundant positions sharing the same sulfur atom. The final model for **36** was refined to values of $R_1(F) = 0.0413$ (for 11689 data with $F_o^2 \geq 2\sigma(F_o^2)$) and $wR_2(F^2) = 0.0913$ (for all 13742 independent data).

(b) Colorless crystals of $[\text{IrRu}(\text{CO})_4(\mu\text{-C}(\text{CH}_3)\text{O})(\text{dppm})_2][\text{BF}_4]_2 \cdot 3\text{CH}_2\text{Cl}_2$ (**39-BF₄**) were obtained *via* slow evaporation of a dichloromethane solution of the compound. Data were collected and corrected for absorption as for **36** above (see Table 2). Unit cell parameters were obtained from a least-squares refinement of the setting angles of 5570 reflections from the data collection, and the space group was determined to be *C2/c* (No. 15). The structure of **39-BF₄** was solved using the direct-methods program *SHELXS-86*,⁶⁰ and refinement was completed using the program *SHELXL-93*, during which the hydrogen atoms were treated as for

Table 3.2. Crystallographic Data for Compounds **36**, **39**, **40** and **42**.

	[IrRu(CH ₃)(CO) ₅ (dppm) ₂][CF ₃ SO ₃] ₂	[IrRu(CO) ₄ (μ-C(CH ₃)O)- (dppm) ₂][BF ₄] ₂ (39)•3CH ₂ Cl ₂	[IrRu(CO) ₃ (μ-C(CH ₃)O)- (dppm) ₂][BF ₄] ₂ (40)•3CH ₂ Cl ₂	[IrRu(CF ₃ SO ₃)(CO) ₂ (μ-C(CH ₃)O)(dppm) ₂][CF ₃ SO ₃] (42)•2CH ₂ Cl ₂
formula	C ₆₁ H ₅₃ Cl ₆ F ₆ IrO ₁₁ P ₄ RuS ₂	C ₅₉ H ₅₃ B ₂ Cl ₆ F ₈ IrO ₃ P ₄ Ru	C ₅₈ H ₅₃ B ₂ Cl ₆ F ₈ O ₄ P ₄ Ru	C ₅₈ H ₅₁ Cl ₄ F ₆ IrO ₉ P ₄ RuS ₂
fw	1770.00	1645.48	1617.47	1629.06
cryst dimens, mm	0.57×0.11×0.04	0.23×0.10×0.08	0.24×0.24×0.06	0.26×0.16×0.04
cryst syst	monoclinic	monoclinic	monoclinic	orthorhombic
space group	<i>Cc</i> (No. 9)	<i>C2/c</i> (No. 15)	<i>P2₁/c</i> (No. 14)	<i>P2₁2₁2₁</i> (No. 19)
<i>a</i> , Å	11.3730(8) ^a	37.384(3) ^b	18.899(3) ^c	14.609(1) ^d
<i>b</i> , Å	35.712(2)	14.505(1)	14.728(3)	17.007(1)
<i>c</i> , Å	16.776(1)	23.947(2)	24.634(4)	24.688(2)
β, deg	95.644(1)	99.127(2)	112.097(3)	90
<i>V</i> , Å ³	6780.7(8)	12821(2)	6353(2)	6133.9(9)
<i>Z</i>	4	8	4	4
<i>d</i> _{calc} , g cm ⁻³	1.734	1.705	1.691	1.764
μ, mm ⁻¹	2.649	2.730	2.752	2.834

continued next page...

Table 3.2. (continued) Crystallographic Data for Compounds **36**, **39**, **40** and **42**

<i>radiation</i> (λ , Å)		graphite-monochromated Mo K α (0.71073)	
<i>T</i> , °C	-80	-80	-80
<i>scan type</i>	ω scans (0.2°)	ω scans (0.2°)	ϕ rotations (0.3°)/ ω scans
	(15 s exposures)	(25 s exposures)	(0.3°) (30 s exposures)
<i>2θ(max)</i> , deg	52.78	52.78	52.90
<i>no. of unique rflns</i>	13742 ($R_{\text{int}}=0.0460$)	13011 ($R_{\text{int}}=0.0742$)	13001 ($R_{\text{int}}=0.0695$)
<i>no. of observns</i>	11689 ($F_o^2 \geq 2\sigma(F_o^2)$)	8788 ($F_o^2 \geq 2\sigma(F_o^2)$)	7896 ($F_o^2 \geq 2\sigma(F_o^2)$)
<i>range of transmn</i>	0.9014-0.3135	0.8112-0.5725	0.8310-0.5203
<i>factors</i>			
<i>no. of</i>	13742 ($F_o^2 \geq -$	13011 ($F_o^2 \geq -$	13001 ($F_o^2 \geq -$
<i>data/restraints/params</i>	3 $\sigma(F_o^2)$ /18/838	3 $\sigma(F_o^2)$ /4/763	3 $\sigma(F_o^2)$ /0/758
<i>residual density</i> , e/Å ³	1.037 and -0.817	2.191 and -0.858	3.71 and -3.108
R_1 ($F_o^2 \geq 2\sigma(F_o^2)$)	0.0413	0.0516	0.0560
wR ₂ ($F_o^2 \geq 3\sigma(F_o^2)$)	0.0913	0.1159	0.1499
<i>GOF</i> (s)	1.010	1.003	0.968

^a Cell parameters obtained from least-squares refinement of 4551 centered reflections. ^b Cell parameters from 5570 reflections. ^c Cell parameters from 5177 reflections. ^d Cell parameters from 4777 reflections. ^e $R_1 = \Sigma||F_o| - |F_c||/\Sigma|F_o|$; wR₂ = $[\Sigma w(F_o^2 - F_c^2)^2/\Sigma w(F_o^4)]^{1/2}$. ^f $S = [\Sigma w(F_o^2 - F_c^2)^2/(n-p)]^{1/2}$ (n = number of data; p = number of parameters varied; w = $[\sigma^2(F_o^2) + (a_0P)^2 + a_1P]^{-1}$, where $P = [\max(F_o^2, 0) = 2F_c^2]/3$). For **36** $a_0 = 0.0260$ and $a_1 = 5.3436$; for **39** $a_0 = 0.0496$ and $a_1 = 2.2684$; for **7** $a_0 = 0.0778$ and $a_1 = 0.0$; for **42** $a_0 = 0.0433$ and $a_1 = 0.040$

36. For **39-BF₄** the Cl–C distances within one of the solvent dichloromethane molecules (containing a carbon atom that was disordered over two positions) were given a fixed idealized value (1.80Å). The final model was refined to values of $R_1(F) = 0.0516$ (for 8788 data with $F_o^2 \geq 2\sigma(F_o^2)$) and $wR_2(F^2) = 0.1159$ (for all 13011 independent data).

(c) Red-orange crystals of $[\text{IrRu}(\text{CO})_3(\mu\text{-C}(\text{CH}_3)\text{O})(\text{dppm})_2][\text{BF}_4]_2 \cdot 3\text{CH}_2\text{Cl}_2$ (**40**) were obtained *via* slow evaporation of a dichloromethane solution of the compound. Data were collected on a Bruker P4/RA/SMART 1000 CCD diffractometer using Mo K α radiation at –80 °C and corrected for absorption as for **36** above (see Table 2.2). Unit cell parameters were obtained from a least-squares refinement of the setting angles of 5177 reflections from the data collection, and the space group was determined to be $P2_1/c$ (No. 14). The structure of **40** was solved as for **36** (*DIRDIF-99*), and refinement was completed using the program *SHELXL-93*, during which the hydrogen atoms were treated as for **36**. The final model was refined to values of $R_1(F) = 0.0560$ (for 7896 data with $F_o^2 \geq 2\sigma(F_o^2)$) and $wR_2(F^2) = 0.1499$ (for all 13001 independent data).

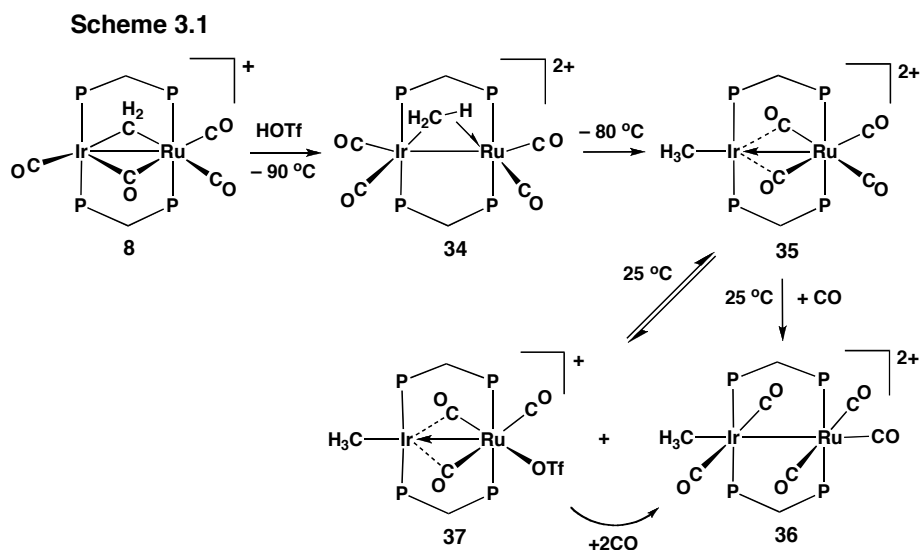
(d) Crystals of $[\text{IrRu}(\text{O}_3\text{SCF}_3)(\text{CO})_2(\mu\text{-C}(\text{CH}_3)\text{O})(\text{dppm})_2][\text{CF}_3\text{SO}_3] \cdot 2\text{CH}_2\text{Cl}_2$ (**42**) were obtained as orange plates from a dichloromethane solution of the compound. Data were collected and corrected for absorption as for **36**. Unit cell parameters were obtained from a least-squares refinement of the setting angles of 4777 reflections from the data collection, and the space group determined to be $P2_12_12_1$ (No. 19). The structure of **42** was solved as for **36** (*DIRDIF-99*), and refinement was completed using the program *SHELXL-93*, during which the hydrogen atoms were treated as for **36**. The final model was refined to values of $R_1(F) = 0.0418$ (for 10244 data with $F_o^2 \geq 2\sigma(F_o^2)$) and $wR_2(F^2) = 0.0943$ (for all 12557 independent data).

3.3 Results and Discussion

3.3.1 Methyl Complexes

In our previous studies on the Rh/Os³¹ and Rh/Ru³⁰ systems, protonation of the methylene-bridged complexes $[\text{RhM}(\text{CO})_4(\mu\text{-CH}_2)(\text{dppm})_2]^+$ (M=Ru, Os) at temperatures below $-40\text{ }^\circ\text{C}$ yielded methyl-bridged products $[\text{RhM}(\text{CO})_4(\mu\text{-CH}_3)(\text{dppm})_2]^{2+}$, in which the methyl group in each case was carbon-bound to the group 8 metal while being involved in an agostic interaction with Rh. Even at temperatures down to $-90\text{ }^\circ\text{C}$ no metal hydride species was observed in these protonation reactions, suggesting direct protonation of the methylene group. We undertook the present study, in part, to determine whether a metal-hydride species could be observed. The greater Ir-C and Ir-H bond strengths⁶¹ suggested that the methylene/hydride species may be favored in this system over the bridged, agostic methyl product.

Protonation of the methylene-bridged compound $[\text{IrRu}(\text{CO})_3(\mu\text{-CH}_2)(\mu\text{-CO})(\text{dppm})_2][\text{CF}_3\text{SO}_3]$ (**8**) at $-90\text{ }^\circ\text{C}$ using triflic acid yields the dicationic methyl-bridged product, $[\text{IrRu}(\text{CO})_4(\mu\text{-CH}_3)(\text{dppm})_2][\text{CF}_3\text{SO}_3]_2$ (**34**) as outlined in Scheme 3.1. The $^{31}\text{P}\{^1\text{H}\}$ NMR spectrum of **34** displays a pattern that is



typical of this IrRu dpmm system, in which the Ru-bound ^{31}P nuclei appear as a multiplet downfield (δ 25.8) than those bound to Ir (δ -13.7). The ^1H resonances for the methyl group at -90 °C appear as two broad unresolved signals; the resonance at δ -10.88, integrates as one proton, while that at δ 3.79 integrates as two. Although the chemical shifts of these resonances are suggestive of a metal-bound hydride and a methylene group, respectively, a bridged agostic methyl interaction has been established on the basis of the $^1\text{J}_{\text{CH}}$ values observed in the sample prepared using $^{13}\text{CH}_2$ -enriched compound **8**. In this experiment the upfield proton signal shows a coupling of 65 Hz to carbon while the resonance for the other pair of protons displays a coupling of 146 Hz. The former coupling is far too large to correspond to coupling between separate hydride and methylene groups, while the latter coupling is somewhat larger than the normal range observed for terminal methyls (120 – 135 Hz). This latter coupling is in line with what has been observed for the terminal C-H moieties in agostic alkyl groups,^{46,47} and has been attributed to the increase in *s*-character in these non-bridging bonds.⁴⁶ It should also be noted that values of $^1\text{J}_{\text{CH}}$, close to what we observe for the downfield methyl protons in **34**, have also been reported for some terminally-bound methyl groups.^{8,54}

The observation of separate signals for the hydrogen involved in the agostic interaction and the two terminal hydrogens, and therefore the direct observation of both C-H coupling constants, is highly unusual. In general, exchange of the three methyl hydrogens is facile on the NMR time scale, even at low temperature, giving rise to only a single ^1H resonance which display a splitting pattern that corresponds to the weighted average of the two coupling constants.^{30-32,46,47} We are aware of only one previous example, in which both the agostic and terminal C-H resonances for a bridging methyl group have been resolved,⁵⁵ for which the agostic interaction displays a C-H coupling constant of 88 Hz. The very low value of $^1\text{J}_{\text{CH}}$ observed in **34** suggests a very strong agostic interaction in this case and a concomitant substantially weakened C-H bond. In addition, this value lies in the range of 50 to 100 Hz that has been reported for agostic interactions involving bridging, substituted alkyl groups.^{46,47} No spin-spin

coupling between the chemically inequivalent protons could be resolved, owing to the breadth of both signals (35 Hz and 25 Hz peak widths at half height, respectively), even upon broad-band ^{31}P decoupling. The bridging methyl group in **34** is proposed, on the basis of selective ^{31}P -decoupling experiments, to have the connectivity shown in Scheme 2.1, in which it is carbon-bound to Ir with the agostic interaction with Ru. Although both methyl signals in the ^1H -NMR spectrum are broad and unresolved, decoupling the phosphorus resonances corresponding to the Ru-bound ends of the dpmm ligands results in a slight sharpening of the upfield methyl resonance ($\delta -10.88$) while decoupling of the Ir-bound ends of the diphosphine has no effect on this signal. Conversely, the ^1H methyl signal at $\delta 3.79$ sharpens slightly on decoupling the Ir-bound phosphine signal but is unaffected by decoupling of the Ru-bound phosphine signal. In a $^{13}\text{CH}_3$ -enriched sample of **34** the broad signal in the $^{13}\text{C}\{^1\text{H}\}$ NMR spectrum at $\delta 18.7$ for this methyl group sharpens on ^{31}P decoupling of the Ir-bound phosphorus nuclei, but remains unaffected when the Ru-bound phosphorus resonances are decoupled. This again supports the structure shown in Scheme 3.1.

Unfortunately, the connectivity involving the carbonyl ligands could not be unambiguously established through selective ^{31}P -decoupling experiments owing to the breadth of the carbonyl signals in the $^{13}\text{C}\{^1\text{H}\}$ NMR spectra, which remained unaffected during all ^{31}P -decoupling experiments. Nevertheless, the connectivity could be established with some confidence on the basis of the chemical shifts of these carbonyls. Two carbonyl resonances appear relatively upfield ($\delta 161.2, 170.0$) and are assumed to be bound to Ir, while the two downfield resonances ($\delta 186.0, 195.6$) are assumed to be Ru-bound; such upfield and downfield signals for carbonyls bound to 3^{rd} - and 2^{nd} -row metals, respectively, have previously been observed in IrRu complexes⁵⁶ and in related mixed-metal complexes involving other combinations of 2^{nd} - and 3^{rd} -row transition metals.^{31,32,62} Although all chemical shifts appear to be consistent with terminally bound carbonyls, the furthest downfield resonance may correspond to a carbonyl having some weak semi-bridging interaction with the adjacent metal.

Warming a solution of **34** only slightly to $-80\text{ }^{\circ}\text{C}$ for 30 min results in complete conversion to a new product, $[\text{IrRu}(\text{CH}_3)(\text{CO})_4(\text{dppm})_2][\text{CF}_3\text{SO}_3]_2$ (**4**), in which the bridging methyl group of **34** has migrated to a terminal site on Ir. Although, as noted above, in previous work,⁵⁶ and in some of what follows, the Ir-bound ^{31}P nuclei usually appear at significantly higher-field in the $^{31}\text{P}\{^1\text{H}\}$ NMR spectra than those bound to Ru, aiding significantly in the spectroscopic characterization of the compounds, this is not the case for **35** (and for some other compounds in this chapter), for which the pair of ^{31}P resonances appear at very similar chemical shifts (δ 20.8 and 18.3). The close proximity of these two resonances leads to some equivocation in structural assignment since the Ir- and Ru-bound ^{31}P resonances cannot be unambiguously distinguished. However, if it is assumed that the ^{31}P signal slightly upfield corresponds to the Ir-bound ends of the diphosphines, the resulting structural assignment for this species is more consistent with those of the subsequent products and with the geometries established for the analogous Rh/Os³¹ and Rh/Ru³⁰ compounds. In the ^1H NMR spectrum of **35** a resonance corresponding to a methyl group appears as a triplet at δ 2.10 and selective ^{31}P decoupling confirms that its multiplicity results from coupling to the ^{31}P nuclei appearing upfield. On the basis of our assumption above, this suggests that the methyl group is also Ir-bound. This assignment is consistent with that of the subsequent product **36**, for which the methyl group is clearly bound to Ir (*vide infra*). In a $^{13}\text{CH}_3$ -enriched sample of **35** the value of $^1J_{\text{CH}} = 135\text{ Hz}$ is to be as expected for a terminally bound methyl group. Also in the ^1H NMR spectrum all four dppm methylene protons appear as a single resonance at δ 3.79, suggesting front-back symmetry of the complex on either side of the IrRuP_4 plane. Two carbonyl resonances appear in the $^{13}\text{C}\{^1\text{H}\}$ NMR spectrum; one at δ 187.0 corresponds to the pair that are terminally bound to Ru while the downfield signal at δ 215.8 represents a pair of semi-bridging carbonyls. These assignments are based on a series of $^{13}\text{C}\{^1\text{H}, \text{selective } ^{31}\text{P}\}$ decoupling experiments in which the downfield carbonyl signal shows coupling to all ^{31}P nuclei while the upfield signal couples only to the ^{31}P nucleus resonating downfield. These ^{13}CO resonances also closely resemble those of the RhRu

analogue.³⁰ The methyl group of compound **35** appears as a broad signal at δ 39.8 in the $^{13}\text{C}\{^1\text{H}\}$ NMR spectrum and ^{31}P decoupling experiments result in sharpening of this signal only on decoupling the Ir-bound phosphorous nuclei.

The proposed connectivity for **35** is similar to those reported for the Rh/Os³¹ and Rh/Ru³⁰ analogues, the spectral characterization of which was unambiguous owing to the presence of spin-spin coupling involving the ^{103}Rh nuclei in these cases. Although we describe the connectivity with some confidence on the basis of the spectral data, the oxidation states of the metals and the resulting nature of the Ir-Ru bond remains unclear; such a situation is common in binuclear complexes. In our structural assignment for **35**, shown in Scheme 3.1, we assume Ir(I)/Ru(II) oxidation states, necessitating a dative Ru \rightarrow Ir bond.

The bonding of the bridging methyl group in **34** is subtly different from that observed in the Rh/Os and Rh/Ru analogues. Whereas the methyl group in **34** is carbon-bound to Ir and binds to Ru *via* an agostic interaction, the reverse is true in the Rh systems³⁰⁻³² in which the methyl group is bound to the group 8 metal while having an agostic interaction with Rh. We assume that this difference reflects the stronger Ir-CH₃ vs. Ru-CH₃ bond⁶¹ in **34**. Our proposal that the primary metal-carbon interaction in **34** is to Ir is also consistent with the significantly more facile bridging methyl-to-terminal methyl transformation (**34** \rightarrow **35**) which occurs upon warming only slightly to -80 °C; the analogous transformation for both the Rh/Os and Rh/Ru systems required warming to -40 °C. The higher barrier for the latter two cases is consistent with the necessity of the methyl group to migrate from metal-to-metal, breaking both the agostic interaction and the Os-CH₃ or Ru-CH₃ sigma bonds, before the partial “merry-go-round” motion takes it to its favored terminal site on the group 9 metal. By contrast, migration of the methyl group in the conversion of **34** to **35** requires only breaking of the weaker agostic interaction while maintaining the strong Ir-CH₃ bond.

Warming a solution of **35** (as the triflate salt) to -60 °C results in the gradual appearance of two new species (**36** and **37**) in equal proportions, and warming to -20 °C for 30 min gives rise to an equilibrium mixture of compounds

35, **36** and **37** in an approximate 1:1:1 ratio. However, species **37** is unstable and begins decomposing into unidentified products within hours, ultimately leaving only $[\text{IrRu}(\text{CH}_3)(\text{CO})_5(\text{dppm})_2][\text{CF}_3\text{SO}_3]_2$ (**36**) and unidentified decomposition products. This latter species can be obtained as the sole product upon reaction of either **35** or a mixture of **35**, **36** and **37** with carbon monoxide, and is the only product obtained upon ambient temperature protonation of **8** under a carbon monoxide rich atmosphere. The $^{31}\text{P}\{^1\text{H}\}$ NMR spectrum of **36** displays the conventional AA'BB' pattern in which the Ir-bound ^{31}P nuclei appear upfield ($\delta -19.5$) while those bound to Ru are at characteristically downfield ($\delta 20.9$). In the ^1H NMR spectrum a methyl signal appears at $\delta 1.11$, and its coupling to the upfield ^{31}P nuclei was confirmed by ^{31}P -decoupling experiments. In the $^{13}\text{CH}_3$ -enriched sample a value for $^1J_{\text{CH}} = 140$ Hz was observed. Three carbonyl resonances, in a 2:2:1 ratio, appear in the $^{13}\text{C}\{^1\text{H}\}$ NMR spectrum and their connectivity was also established by decoupling experiments; a triplet at $\delta 181.6$ corresponds to two equivalent Ir-bound carbonyls, a triplet at $\delta 202.0$ represents two equivalent Ru-bound carbonyls, and a triplet at $\delta 185.7$ corresponds to a single unique carbonyl on Ru. In addition, the methyl resonance in the $^{13}\text{CH}_3$ -enriched sample appears as a partially resolved triplet ($^2J_{\text{PC}} = 3.2$ Hz) at $\delta -18.5$ and selective ^{31}P decoupling establishes that this group is bound to Ir.

The structure proposed for **36** is analogous to that proposed for the isoelectronic diruthenium species $[\text{Ru}_2(\text{CH}_3)(\text{CO})_5(\text{dmpm})_2][\text{CF}_3\text{SO}_3]$ ($\text{dmpm} = \text{Me}_2\text{PCH}_2\text{PMe}_2$)⁶³ and has been confirmed by an X-ray structure determination. A representation of the complex cation is shown in Figure 3.1 with relevant bond lengths and angles given in Table 3.3. Although the structure has a disordered “ $\text{H}_3\text{C}-\text{Ir}-\text{Ru}-\text{CO}$ ” fragment as explained in the Experimental section, the location of the methyl group on Ir and the unique carbonyl on Ru was established on the basis of the different occupancy factors for the disordered atoms. Both metals have a relatively undistorted octahedral geometry, in which one coordination site on each is occupied by the bond to the adjacent metal. The resulting Ir–Ru separation (2.9143(5) Å) is long for a single bond, reflecting the repulsions between the two pairs of carbonyls on the adjacent metals that lie *cis* to the Ir–Ru

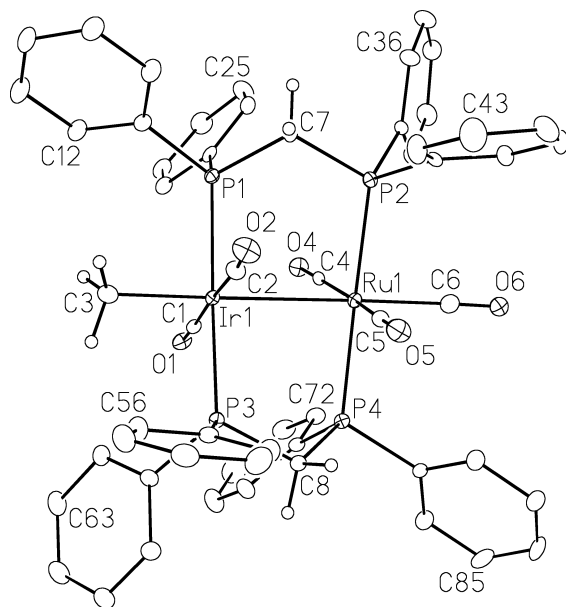


Figure 3.1. Perspective view of the complex cation of $[\text{IrRu}(\text{CH}_3)(\text{CO})_5(\text{dppm})_2]^{2+}$ (**36**) showing the atom numbering scheme. Non-hydrogen atoms are represented by Gaussian ellipsoids at the 20% probability level. Hydrogen atoms are shown with arbitrarily small thermal parameters except for phenyl hydrogens which are omitted. Ir–Ru = 2.9143(5) Å.

bond, and is certainly longer than those observed for compounds **39**, **40** and **42** (*vide infra*). Nevertheless, this metal–metal separation is less than the intra-ligand P···P separations (3.092(2), 3.097(3) Å) consistent with a mutual attraction of the metals and the presence of a metal–metal bond. The repulsions between adjacent ligands on both metals are further manifest in a staggering of the two adjoining octahedra by approximately 26.8° as can be seen in Figure 3.1. All bond lengths and angles within the complex cation appear to be normal, although the disorder, noted above, means that the precise location of the methyl group and the axial carbonyl on Ru can not be determined, so the metrical parameters involving these groups must be viewed with caution.

The $^{31}\text{P}\{^1\text{H}\}$ NMR spectrum of the other product in the transformation of **35**, namely $[\text{IrRu}(\text{CH}_3)(\text{OSO}_2\text{CF}_3)(\text{CO})_3(\text{dppm})_2][\text{CF}_3\text{SO}_3]$ (**37**), shows that, like **35**, it is atypical, having two closely spaced resonances at δ 19.8 and 18.0. In this case it also appears that the slightly higher-field chemical shift corresponds to the phosphorus nuclei bound to Ru. The similarity in the chemical shifts of these

Table 3.3: Selected Distances and Angles for Compound **36**.

<i>Distances (Å)</i>					
Atom 1	Atom 2	Distance	Atom 1	Atom 2	Distance
Ir(1)	Ru(1)	2.9143(5)	P(1)	C(7)	1.835(7)
Ir(1)	P(1)	2.3902(17)	P(2)	C(7)	1.838(7)
Ir(1)	P(3)	2.3778(17)	P(3)	P(4)	3.097(3) [†]
Ir(1)	C(1)	1.949(7)	P(3)	C(8)	1.825(7)
Ir(1)	C(2)	1.905(8)	P(4)	C(8)	1.835(7)
Ir(1)	C(3)	2.056(8)	C(1)	O(1)	1.129(8)
Ru(1)	P(2)	2.3699(18)	C(2)	O(2)	1.136(8)
Ru(1)	P(4)	2.3879(18)	C(3)	O(3)	1.046(16)
Ru(1)	C(4)	1.963(8)	C(4)	O(4)	1.128(8)
Ru(1)	C(5)	1.899(7)	C(5)	O(5)	1.151(8)
Ru(1)	C(6)	2.015(8)	C(6)	O(6)	1.049(10)
P(1)	P(2)	3.092(2) [†]			

[†] Non-bonded distance

<i>Angles (deg)</i>							
Atom 1	Atom 2	Atom 3	Angle	Atom 1	Atom 2	Atom 3	Angle
P(1)	Ir(1)	P(3)	175.37(6)	P(2)	Ru(1)	C(6)	88.8(2)
P(1)	Ir(1)	C(1)	94.3(2)	P(4)	Ru(1)	C(4)	93.4(2)
P(1)	Ir(1)	C(2)	87.4(2)	P(4)	Ru(1)	C(5)	88.9(2)
P(1)	Ir(1)	C(3)	91.0(2)	P(4)	Ru(1)	C(6)	91.3(2)
P(3)	Ir(1)	C(1)	90.2(2)	C(4)	Ru(1)	C(5)	171.9(3)
P(3)	Ir(1)	C(2)	88.0(2)	C(4)	Ru(1)	C(6)	93.7(3)
P(3)	Ir(1)	C(3)	89.5(2)	C(5)	Ru(1)	C(6)	94.0(3)
C(1)	Ir(1)	C(2)	177.5(3)	Ir(1)	P(1)	C(7)	108.6(2)
C(1)	Ir(1)	C(3)	92.9(3)	Ru(1)	P(2)	C(7)	113.8(2)
C(2)	Ir(1)	C(3)	88.8(3)	Ir(1)	P(3)	C(8)	113.6(2)
P(2)	Ru(1)	P(4)	176.21(6)	Ru(1)	P(4)	C(8)	108.6(2)
P(2)	Ru(1)	C(4)	90.4(2)				
P(2)	Ru(1)	C(5)	87.3(2)				

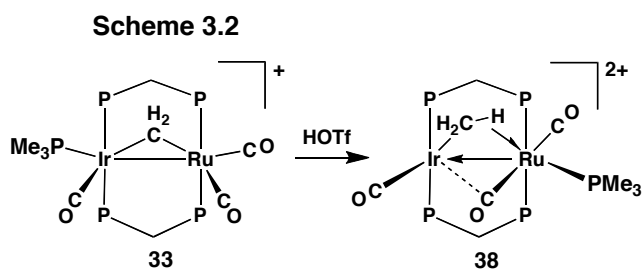
resonances to those of **35** suggests that the two may have similar structures. Compound **37** is shown, by its $^{13}\text{C}\{^1\text{H}\}$ NMR spectrum, to be a tricarbonyl species with three equal intensity carbonyl resonances at δ 188.4, 212.4 and 222.6, corresponding to a terminal and two semi-bridging carbonyls, respectively.

Selective ^{31}P -decoupling experiments show that the three carbonyl resonances sharpen upon decoupling the upfield phosphorus resonance, but show

little effect upon decoupling of the downfield resonance, suggesting that all three carbonyls are primarily bound to the same metal. Furthermore, the greater propensity of Ru to retain carbonyls and to adopt an 18-electron configuration,⁶⁴ as demonstrated for subsequent compounds in this report, leads us to make the structural assignment shown for **37** in Scheme 3.1. This, of course, leads to the assignment of the upfield ³¹P resonance as due to the Ru-bound ³¹P nuclei. In a sample of **37** that is ¹³CO enriched, the upfield ¹³C resonance and the one at δ 212.4 show mutual coupling of 21 Hz, suggesting that these carbonyls are mutually trans, and in the ¹³CH₃-enriched sample the methyl signal appears as a triplet (²J_{PC} = 8 Hz), with coupling to the Ir-bound phosphine. The ¹⁹F NMR spectrum of **37** displays two resonances: one for the free triflate anion at δ -78.9 and one for a coordinated triflate anion at δ -77.5, indicating that a triflate anion has replaced one of the carbonyl groups originally bound to Ru, maintaining the 18-electron configuration at this metal. The methyl resonance appears as a triplet at δ 1.58 showing coupling to only the Ir-bound ³¹P nuclei. In Scheme 3.1 we show an Ir(I)/Ru(II) formulation, similar to that described for complex **35**.

The transformations involving the BF₄⁻ salt of **34**, as the temperature was warmed above -90 °C, were not followed in the absence of CO. In the presence of CO, warming generated the BF₄⁻ salt of **36**.

In attempts to learn more about the methyl-bridged species, **34**, we also investigated the protonation of the PMe₃ analogue of **8**, namely, [IrRu(PMe₃)(CO)₃(μ -CH₂)(dppm)₂][CF₃SO₃] (**33**),⁵⁶ as shown in Scheme 3.2. By



substituting a carbonyl in **34** with a bulkier phosphine ligand we hoped to inhibit methyl migration to Ir and its accompanying partial “merry-go-round” motion of

the other ligands in the Ir–Ru–CH₃ plane. This approach had been successful in the analogous Rh/Os system in which the methyl-bridged tetracarbonyl species was only stable below –40 °C³¹ whereas the phosphine-substituted products [RhOs(PR₃)(CO)₃(μ-CH₃)(dppm)₂][CF₃SO₃]₂ were isolable at ambient temperature.³² We also reasoned that the greater basicity of the metals, resulting from substitution of CO by PMe₃, could lead to protonation directly at the metals and might favor a methylene/hydride product.

Protonation of **33** at ambient temperature generates [IrRu(PMe₃)(CO)₃(μ-CH₃)(dppm)₂][CF₃SO₃]₂ (**38**), in which an unsymmetrically bridged methyl group again results, apparently *via* direct protonation at the methylene group. At temperatures below –60 °C two separate signals, in a 2:1 ratio, are observed in the ¹H NMR spectrum as broad singlets at δ 2.93 and –9.09, respectively, much as was observed for **34** at –90 °C. Compound **38** can also be obtained by protonation at –90 °C with no other species being observed again supporting direct protonation at the methylene carbon rather than formation of a methylene hydride. With broadband phosphorus decoupling, these signals resolve into a broad doublet and a triplet, having mutual coupling of 13 Hz. A bridging agostic methyl group is again proposed for **38**, on the basis of the mutual 13 Hz coupling between the hydrogens, as noted above, which is too large for a methylene/hydride structure, and also on the basis of the individual C–H coupling constants for the agostic and terminal hydrogens, as described in what follows. In a sample of **38**, prepared from the ¹³CH₂-enriched **33**, the downfield proton signal displays additional 140 Hz coupling to carbon while the upfield signal displays 72 Hz coupling. As noted for **34**, the former coupling is typical for the terminal protons of a CH₃ moiety^{8,54} while the latter represents an agostic interaction.^{46,47} Although the C–H coupling constant for the agostic interaction is greater than that for **34**, it is nevertheless still very small. As noted earlier, the observation of two resonances for the methyl protons is unusual. Exchange of these agostic and terminal C–H groups is usually too rapid, even at low temperatures, giving rise to only one average signal for the CH₃ group; certainly this was the case for the

analogous Rh/Os^{31,32} and Rh/Ru³⁰ species for which only a single ¹H resonance for the methyl group was observed in each case.

A spin-saturation-transfer experiment at -60 °C indicates that exchange of the methyl protons is occurring at this temperature and a ΔG^\ddagger of 51.5 kJ mol⁻¹ has been calculated for this exchange based on an EXSY experiment (the spectra is shown in Figure AI.1 of Appendix I).⁶⁵ This rotation barrier is slightly higher than that of 41.0 kJ mol⁻¹ (acquired at -40 °C and at 90 MHz), reported by Grubbs and coworkers,⁵⁵ for proton exchange in a mixed Ti/Rh complex containing an unsymmetrically bridged methyl group.

Selective ³¹P-decoupling of the ¹H signals of **38** at temperatures below -60 °C indicates that the pair of downfield methyl protons are coupled to the Ir-bound ³¹P nuclei appearing upfield while, the upfield methyl proton, assigned to that involved in the agostic interaction, is coupled to the Ru-bound ³¹P nuclei. This defines the methyl group as being carbon-bound to Ir while bridging to Ru through the agostic interaction. The ¹³C{¹H} NMR spectra, with selective ³¹P decoupling indicate that the carbonyl resonances at δ 203.5 and 184.6 are Ru-bound while the third at δ 177.4 is Ir-bound, and in the isotopomer that is enriched in both ¹³CH₃ and ¹³CO, the methyl group and the Ir-bound carbonyl show a mutual coupling of 20 Hz, suggesting a mutually *trans* arrangement of these groups. In the ³¹P{¹H} NMR spectrum at -80 °C, the PMe₃ resonance appears as a broad, partially resolved quintet, displaying coupling to all dppm phosphorus nuclei, whereas the Ir- and Ru-bound ³¹P resonances of the dppm groups display 8 and 6 Hz coupling, respectively, to the PMe₃ group. On this basis, the location of the PMe₃ group is not clearly defined. This is not the first time that we have observed approximately equal coupling of a terminally bound ligand to both the adjacent and remote dppm phosphorus nuclei,^{56,66-68} and in fact this was also observed for the precursor, **33**, the structure of which was unambiguously established by X-ray crystallography.⁵⁶ However, it can be established with some confidence that the PMe₃ group is bound to Ru on the basis that this phosphine displays 6 and 18 Hz coupling to the Ru-bound carbonyls, suggesting an arrangement in which it is *cis* to both carbonyls with the smaller coupling constant

being to the one that is adjacent the Ir metal center; no coupling to the Ir-bound carbonyl is observed.

As shown in Scheme 3.2, protonation has resulted in PMe_3 migration from Ir to Ru. As such, the structure of **38** resembles the Rh/Ru³⁰ and Rh/Os³¹ analogues more than it does compound **34**, having a more coordinatively saturated environment at the group 8 metal instead of the more symmetric arrangement of **34**. Nevertheless, the bridging methyl group is C-bonded to Ir in both **34** and **38**.

Warming **38** to ambient temperature results in no significant change in most of the $^{31}\text{P}\{^1\text{H}\}$, $^{13}\text{C}\{^1\text{H}\}$ and ^1H NMR spectral parameters, suggesting no significant structural changes occur over this temperature range. However, a somewhat different picture emerges upon monitoring the spectral parameters for the methyl group. Warming **38** above $-60\text{ }^\circ\text{C}$ results in a broadening of both methyl signals in the ^1H NMR spectrum and by $-40\text{ }^\circ\text{C}$ both have disappeared into the baseline. Surprisingly, no coalesced signal appears until near ambient temperature, at which point a signal at $\delta\ 0.2$ appears. This chemical shift is more in line with a terminal methyl group than the value expected for the weighted average of the two low-temperature signals (ca. $\delta\ -1.1$). Furthermore, in the $^{13}\text{CH}_3$ isotopomer the C-H coupling constant at ambient temperatures is 133 Hz, again corresponding to a terminally bound methyl group.

Our failure to observe a coalesced signal at lower temperature and the discrepancies between the ambient and low-temperature spectra suggest a more complicated fluxional process than merely exchange of agostic and terminal methyl protons. Fortunately, the ^{13}C NMR spectrum gives additional spectral information about the transformation of the methyl ligand. At $-80\text{ }^\circ\text{C}$ the ^{13}C NMR spectrum appears as a triplet of doublets having the appropriate coupling to the inequivalent protons ($^1J_{\text{CH}} = 140, 72\text{ Hz}$). Warming results in broadening and coalescence of the signal and by $-20\text{ }^\circ\text{C}$ it appears as a quartet having the 117 Hz coupling to the three methyl protons. This coupling is exactly the weighted average of the two values obtained at lower temperature, consistent with rapid exchange of the agostic and terminal protons at $-20\text{ }^\circ\text{C}$. Further warming again results in broadening of this signal, but by ambient temperature this resonance has

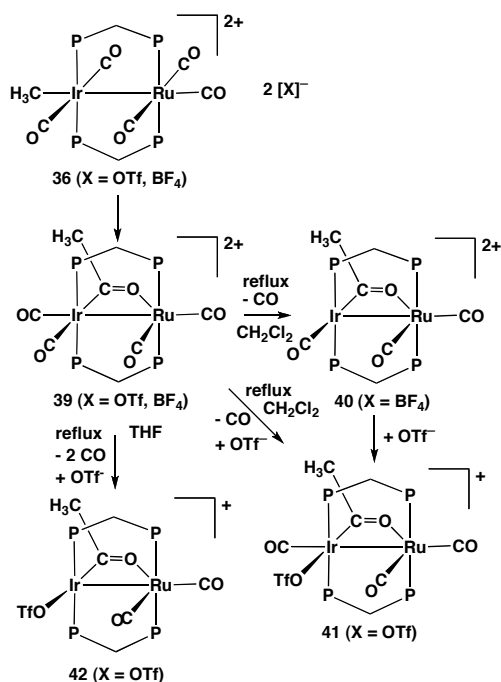
sharpened into a quartet with 133 Hz C–H coupling. This significantly larger coupling is characteristic of a terminal methyl group indicating that at this temperature the agostic interaction with Ru no longer persists. On the basis that all other spectral parameters are close to those at $-80\text{ }^{\circ}\text{C}$, we propose that at ambient temperature the structure of **38** is much as it appears in Scheme 3.2, except without the agostic interaction.

Surprisingly, the chemical shift of the methyl carbon varies very little shifting from δ 12.8 to 13.0 between $-80\text{ }^{\circ}\text{C}$ and ambient temperature, respectively. It is significant to note that as observed in the Rh/Os and Rh/Ru analogues, substitution of a carbonyl by a monophosphine ligand inhibits the “merry-go-round” motion of the equatorial ligands, so that monophosphine analogues of **35** are not observed.

3.3.2 Acetyl-bridged Complexes

As was the case for the PR_3 adducts of the methyl-bridged Rh/Os compounds,³² compound **38** does not undergo subsequent migratory insertion, even at ambient temperature, although this species does begin to decompose to a complex mixture of uncharacterized products after several hours at this temperature. In contrast, the pentacarbonyl methyl complex **36** slowly transforms in solution over several days into a single acetyl-bridged product $[\text{IrRu}(\text{CO})_4(\mu\text{-C}(\text{CH}_3)\text{O})(\text{dppm})_2][\text{CF}_3\text{SO}_3]_2$ (**39**) as shown in Scheme 3.3. Unlike the three methyl complexes (**35** – **37**) for which the methyl resonances in the ^1H NMR spectrum appear as triplets, displaying coupling to two adjacent, metal-bound ^{31}P nuclei, the methyl resonance of **39** shows no ^{31}P coupling, appearing instead as a singlet at δ 2.43, suggesting that it is not directly bound to either metal. Five carbonyl resonances are observed in the $^{13}\text{C}\{^1\text{H}\}$ NMR spectrum; two at δ 204.6 and 187.5 are Ru-bound while two at δ 172.4 and 157.7 are Ir-bound as established by ^{31}P -decoupling experiments. The fifth downfield resonance at δ 251.2 is typical of an acyl group.^{63,69-71} We were unable to obtain suitable

Scheme 3.3



crystals of **39** as the triflate salt; however, crystals of the BF₄⁻ salt (**39-BF₄**) were obtained.

Spectroscopically, the parameters for the complex cations of both salts are indistinguishable. The structure of **39-BF₄**, shown in Figure 3.2 (selected bond distances and angles for **30-BF₄** are given in Table 3.4) confirms the acetyl-group formulation and establishes that it is carbon-bound to Ir and oxygen-bound to Ru. A similar bridging arrangement of acetyl groups was observed in the related Rh/Os³¹ and Rh/Ru³⁰ chemistry, and again the acyl carbon was bound to the group 9 metal with the oxygen bound to the group 8 metal. Bridging acetyl groups were also observed in closely related Rh₂⁷¹ and Ru₂^{63,70} complexes. Each metal in **39** displays a distorted octahedral environment in which one site on each is occupied by the metal-metal bond. In each case the distortion results from the constraints arising from the bridging acetyl group, in which the acute Ru-*Ir*-C(5) and *Ir*-Ru-O(5) angles of 65.7(2)° and 69.0(1)°, respectively, differ substantially from the idealized value of 90°. The short *Ir*-C(5) distance (2.060(6) Å) and the long C(5)-O(5) distance (1.250(8) Å) suggest some degree of oxycarbene

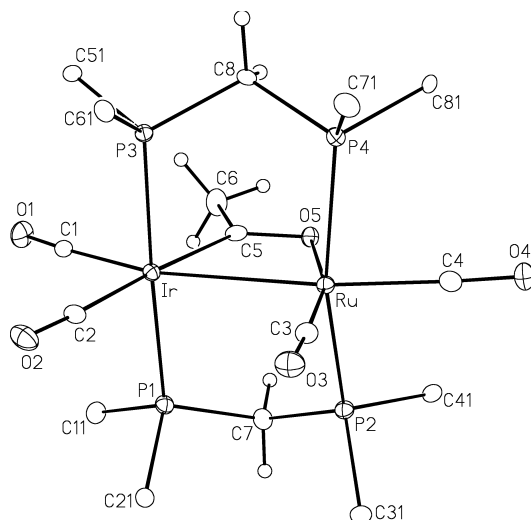


Figure 3.2. Perspective view of the complex cation of $[\text{IrRu}(\text{CO})_4(\mu\text{-C}(\text{CH}_3)\text{O})(\text{dppm})_2][\text{BF}_4]_2$ (**39-BF₄**) showing the atom-labeling scheme. Thermal parameters as described for Figure 3.1. Only the ipso carbons of the dppm phenyl groups are shown.

character, but this appears to be much less pronounced than was observed for the related metal-metal bonded Rh/Os³¹ and Rh/Ru³⁰ systems in which Rh–C distances were near 1.91 Å and C–O distances were near 1.27 Å. The lower degree of carbene character in the present case is consistent with a more upfield ¹³C signal for the acyl group of **39** than those previously reported.

Refluxing a solution of the BF₄[−] salt of **39** in dichloromethane results in the loss of an iridium-bound carbonyl yielding $[\text{IrRu}(\text{CO})_3(\mu\text{-C}(\text{CH}_3)\text{O})(\text{dppm})_2][\text{BF}_4]_2$ (**40**). The methyl group appears in the ¹H NMR spectrum as a singlet at δ 2.02, suggesting that the acetyl group has remained intact upon carbonyl loss, and this is supported by the very downfield resonance (δ 287.0) for the acyl carbonyl in the ¹³C{¹H} NMR spectrum. Three other carbonyl resonances are observed at δ 179.8, 189.0 and 206.0, with the upfield and downfield signals corresponding to the pair of Ru-bound carbonyls while the intermediate signal corresponds to the Ir-bound carbonyl, as determined by selective ³¹P-decoupling experiments. As we have previously noted, the lower-field carbonyl resonance on a given metal usually corresponds to the group that is in the immediate vicinity of an adjacent metal.⁶² It appears that for terminal

Table 3.4: Selected Distances and Angles for Compound **39-BF₄**.

<i>Distances (Å)</i>							
Atom 1	Atom 2	Distance	Atom 1	Atom 2	Distance		
Ir	Ru	2.8599(6)	Ru	C(4)	1.928(7)		
Ir	P(1)	2.3707(17)	P(1)	C(7)	1.827(7)		
Ir	P(3)	2.3628(16)	P(3)	C(8)	1.822(6)		
Ir	C(1)	1.978(7)	P(4)	C(8)	1.827(6)		
Ir	C(2)	1.954(6)	C(1)	O(1)	1.138(8)		
Ir	C(5)	2.060(6)	C(2)	O(2)	1.132(7)		
Ru	P(2)	2.4005(18)	C(3)	O(3)	1.143(7)		
Ru	P(4)	2.3973(18)	C(4)	O(4)	1.126(8)		
Ru	O(5)	2.137(4)	C(5)	O(5)	1.250(8)		
Ru	C(3)	1.860(7)	C(5)	C(6)	1.509(9)		

† Non-bonded distance

<i>Angles (deg)</i>							
Atom 1	Atom 2	Atom 3	Angle	Atom 1	Atom 2	Atom 3	Angle
Ru	Ir	C(5)	65.68(19)	Ir	Ru	C(3)	95.6(2)
P(1)	Ir	P(3)	177.14(6)	P(2)	Ru	C(3)	98.7(2)
P(1)	Ir	C(1)	91.48(19)	P(2)	Ru	C(4)	86.6(2)
P(1)	Ir	C(2)	90.39(19)	P(4)	Ru	O(5)	86.26(12)
P(1)	Ir	C(5)	90.53(18)	P(4)	Ru	C(3)	95.1(2)
P(3)	Ir	C(1)	91.36(19)	P(4)	Ru	C(4)	83.3(2)
P(3)	Ir	C(2)	89.66(19)	O(5)	Ru	C(3)	164.5(2)
P(3)	Ir	C(5)	89.05(18)	O(5)	Ru	C(4)	100.6(2)
C(1)	Ir	C(2)	96.1(3)	O(5)	C(5)	C(6)	114.4(6)
C(1)	Ir	C(5)	91.1(3)	C(3)	Ru	C(4)	94.9(3)
C(2)	Ir	C(5)	172.6(3)	Ru	O(5)	C(5)	105.6(4)
Ir	Ru	O(5)	68.97(11)	Ir	C(5)	O(5)	119.7(5)
Ir	Ru	C(4)	169.4(2)	Ir	C(5)	C(6)	125.9(5)
P(2)	Ru	P(4)	163.50(6)	P(1)	C(7)	P(2)	108.4(3)
P(2)	Ru	O(5)	82.88(12)	P(3)	C(8)	P(4)	110.6(3)

carbonyls bound in a site near to the adjacent metal, weak interactions with this metal (even though not structurally obvious) can lead to a downfield shift of this resonance. The IR spectrum displays three bands corresponding to the terminal carbonyls, but no stretch is seen for the bridging acetyl group. We have been unable to unambiguously identify the carbonyl stretch for the bridging acyl group in any of the compounds in this chapter, or in our previous reports.^{30,31} The X-ray

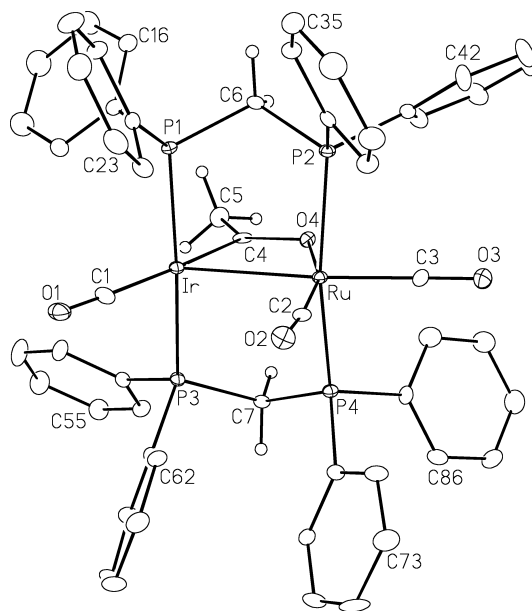


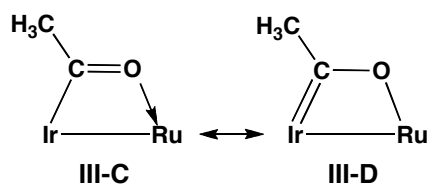
Figure 3.3. *Perspective view of the complex cation of [IrRu(CO)₃(μ-C(CH₃)O)(dppm)₂]-[BF₄]₂ (**40**) showing the atom-labeling scheme. Thermal parameters are as described for Figure 3.1.*

structure determination of **40** confirms the proposed structure, as shown in Figure 3.3 with relevant bond angles and distances given in Table 3.5. Apart from a few minor differences, the structure of **40** appears very similar to that of **39** in which the Ir-bound carbonyl opposite the metal–metal bond has been removed. Removal of the carbonyl has resulted in a significant shortening of the Ir–acyl bond (from 2.060(6) to 2.028(8) Å) and a corresponding lengthening of the acyl C–O bond (from 1.250(8) to 1.285(8) Å), indicating a shift from the conventional acyl extreme towards the oxycarbene formulation (structures **III-C** and **III-D**, respectively, in Chart 3.2 below). This proposed transformation is also consistent with the significant downfield shift of the ¹³C resonance of this group, as noted earlier.

Table 3.5: Selected Distances and Angles for Compound **40**.

<i>Distances (Å)</i>					
Atom 1	Atom 2	Distance	Atom 1	Atom 2	Distance
Ir	Ru	2.7949(7)	Ru	C(2)	1.874(8)
Ir	P(1)	2.3318(18)	Ru	C(3)	1.884(7)
Ir	P(3)	2.3356(18)	O(1)	C(1)	1.128(9)
Ir	C(1)	1.943(8)	O(2)	C(2)	1.135(9)
Ir	C(4)	2.028(8)	O(3)	C(3)	1.148(8)
Ru	P(2)	2.4125(19)	O(4)	C(4)	1.285(8)
Ru	P(4)	2.4175(19)	C(4)	C(5)	1.486(9)
Ru	O(4)	2.132(5)			

<i>Angles (deg)</i>							
Atom 1	Atom 2	Atom 3	Angle	Atom 1	Atom 2	Atom 3	Angle
P(1)	Ir	P(3)	173.74(7)	P(2)	Ru	C(3)	85.3(2)
P(1)	Ir	C(1)	90.6(2)	P(4)	Ru	O(4)	85.17(13)
P(1)	Ir	C(4)	88.35(18)	P(4)	Ru	C(2)	95.4(2)
P(3)	Ir	C(1)	91.6(2)	P(4)	Ru	C(3)	87.6(2)
P(3)	Ir	C(4)	89.22(18)	O(4)	Ru	C(2)	163.6(3)
C(1)	Ir	C(4)	177.4(3)	O(4)	Ru	C(3)	102.5(2)
Ir	Ru	O(4)	70.43(13)	C(2)	Ru	C(3)	93.9(3)
P(2)	Ru	P(4)	167.74(7)	Ir	C(4)	O(4)	119.9(4)
P(2)	Ru	O(4)	86.60(13)	Ir	C(4)	C(5)	123.0(6)
P(2)	Ru	C(2)	95.1(2)	O(4)	C(4)	C(5)	117.1(7)

Chart 3.2

If the triflate salt of **39** (instead of the BF_4^- salt) is refluxed in CH_2Cl_2 , the carbonyl loss noted above is accompanied by triflate coordination at Ir yielding $[\text{IrRu}(\text{OSO}_2\text{CF}_3)(\text{CO})_3(\mu\text{-C}(\text{CH}_3)\text{O})(\text{dppm})_2][\text{CF}_3\text{SO}_3]$ (**41**), as demonstrated by two resonances in the ^{19}F NMR spectrum corresponding to free ($\delta -78.9$) and coordinated ($\delta -77.8$) triflate ion. The formulation shown for **41** in Scheme 3.3 is based upon selective ^{31}P -decoupling experiments through which it was established that the upfield carbonyl resonance in the $^{13}\text{C}\{^1\text{H}\}$ NMR spectrum corresponds to the one bound to Ir, while the other two carbonyls are Ru-bound. Furthermore,

the upfield chemical shift for the Ir-bound carbonyl (δ 168.6), suggests that it is in a position remote from the adjacent metal.⁶² Similarly, the downfield Ru-bound carbonyl (δ 205.6) is assigned to the one that occupies the site adjacent to Ir, while the intermediate signal corresponds to the Ru-bound CO opposite the metal–metal bond. Upon triflate ion coordination, the acyl-carbonyl resonance has moved to significantly upfield (from 287.0 to δ 231.4), suggesting that this group is a normal bridging acyl group having little carbene character.

Refluxing the triflate salt of compound **39** in THF results in the loss of *two* carbonyls yielding the acetyl-bridged dicarbonyl product, $[\text{IrRu}(\text{OSO}_2\text{CF}_3)(\text{CO})_2(\mu\text{-C}(\text{CH}_3)\text{O})(\text{dppm})_2][\text{CF}_3\text{SO}_3]$ (**42**). In the ^1H NMR spectrum the acetyl methyl group appears as a singlet at δ 1.57. The acyl carbonyl appears at δ 231.4 in the $^{13}\text{C}\{^1\text{H}\}$ NMR spectrum, displaying coupling to the Ir-bound phosphorus nuclei, while the carbonyl ligands appear at δ 186.7 and δ 205.6 and both show coupling to the pair of Ru-bound phosphorus nuclei. The downfield carbonyl signal corresponds to the one that approaches the bridging site between the metals. ^{19}F NMR spectroscopy displays two signals of equal intensity and these are assigned to a coordinated and free triflate ion (δ -78.1 and -78.9 , respectively). It is assumed that the coordinated triflate ion is bound to Ir, completing its coordination geometry.

An X-ray structural determination of **42**, shown in Figure 3.4 (see Table 3.6 for relevant bond distances and angles), confirms the above structural assignment. This structure closely resembles that of **40**, in which the Ir-bound carbonyl has been replaced by a triflate anion. Although most differences between the two compounds are minor, the Ir–Ru bond (2.7037(6) Å) in **42** is the shortest in this series of acetyl-bridged species. In addition, the Ir–C(3) bond (1.919(7) Å) involving the acyl group is extremely short and is comparable to the Rh–acyl distances in a series of related Rh/Os and Rh/Ru compounds, and the C(3)–O(3) bond (1.292(8) Å) is longer than those previously noted. Both parameters suggest a tendency towards the oxycarbene formulation **III-D**, although the ^{13}C resonance for this group, as noted above, is not unusual for an acyl group and does not by itself suggest the carbene formulation.

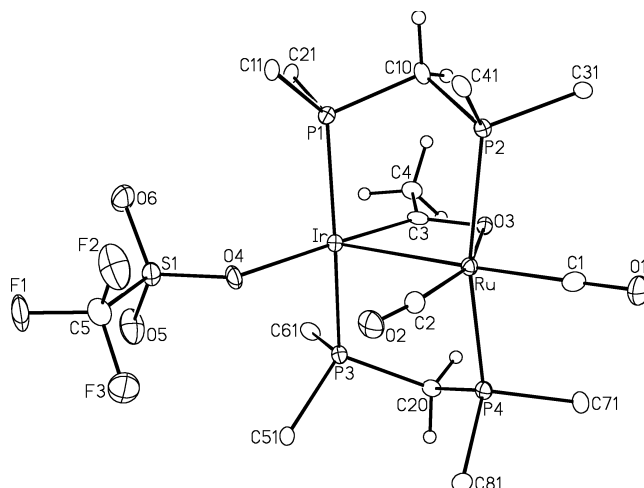


Figure 3.4. Perspective view of the complex cation of $[\text{IrRu}(\text{OSO}_2\text{CF}_3)(\text{CO})_2(\mu\text{-C}(\text{CH}_3)\text{O})\text{-(dppm)}_2][\text{CF}_3\text{SO}_3]$ (**42**) showing the atom-labeling scheme. Thermal parameters as described for Figure 3.1. Only the ipso carbons of the dppm phenyl rings are shown.

Table 3.6: Selected Distances and Angles for Compound **42**.

<i>Distances (Å)</i>							
Atom 1	Atom 2	Distance	Atom 1	Atom 2	Distance		
Ir	Ru	2.7037(6)	Ru	C(1)	1.887(7)		
Ir	P(1)	2.3196(19)	Ru	C(2)	1.858(7)		
Ir	P(3)	2.3185(17)	P(1)	P(2)	2.985(3) [†]		
Ir	O(4)	2.224(4)	P(3)	P(4)	2.989(3) [†]		
Ir	C(3)	1.919(7)	C(1)	O(1)	1.139(8)		
Ru	P(2)	2.4073(19)	C(2)	O(2)	1.156(8)		
Ru	P(4)	2.411(2)	C(3)	O(3)	1.292(8)		
Ru	O(3)	2.123(4)	C(3)	C(4)	1.507(9)		

[†] Non-bonded distance

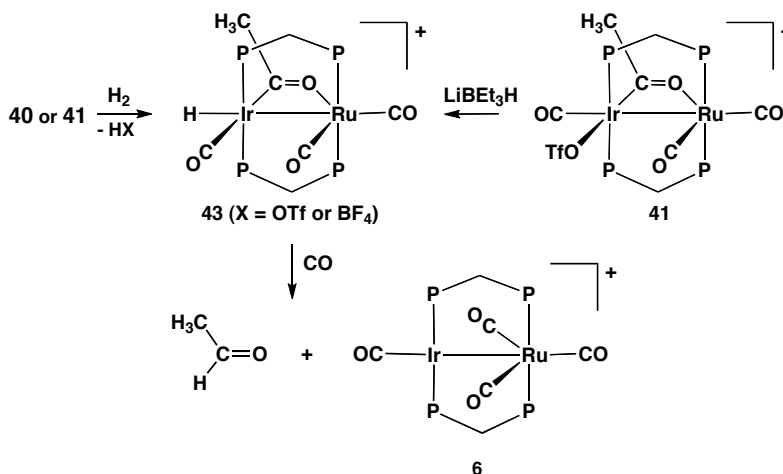
<i>Angles (deg)</i>							
Atom 1	Atom 2	Atom 3	Angle	Atom 1	Atom 2	Atom 3	Angle
Ru	Ir	O(4)	109.32(12)	P(2)	Ru	C(2)	97.1(3)
Ru	Ir	C(3)	68.7(2)	P(4)	Ru	O(3)	85.43(14)
P(1)	Ir	P(3)	167.64(6)	P(4)	Ru	C(1)	86.9(2)
P(1)	Ir	O(4)	93.68(14)	P(4)	Ru	C(2)	96.1(3)
P(1)	Ir	C(3)	87.3(2)	O(3)	Ru	C(1)	106.7(2)
P(3)	Ir	O(4)	92.75(14)	O(3)	Ru	C(2)	159.2(2)
P(3)	Ir	C(3)	86.6(2)	C(1)	Ru	C(2)	94.1(3)
O(4)	Ir	C(3)	177.9(2)	C(4)	C(3)	O(3)	114.6(6)
P(2)	Ru	P(4)	165.58(7)	Ir	C(3)	C(4)	125.0(5)
P(2)	Ru	O(3)	84.20(14)	Ir	C(3)	O(3)	120.4(5)
P(2)	Ru	C(1)	86.5(2)				

3.3.4 Reactions with H₂

In our previous studies on the Rh/Ru³⁰ and Rh/Os³¹ systems we had attempted the reactions of the acetyl-bridged complexes with H₂. Although we anticipated acetaldehyde as the probable product, we had wondered whether the oxycarbene-like nature of these groups (at least in their structural and spectroscopic characteristics) might give rise to unexpected reactivity, generating, for example, a hydroxycarbene group by hydrogen transfer to oxygen instead of to the acyl carbon. Unfortunately, the Rh-containing systems showed no reactivity with H₂ over the short term. After several days small amounts of methane were detected – presumably by slow reversion to a methyl species, which then reacted with H₂. One reason for investigating the Ir/Ru system was the anticipation that oxidative addition of H₂ at Ir would be more favorable, and this has proven to be the case for at least three of the acetyl-bridged products.

Reaction of either [IrRu(CO)₃(μ-C(CH₃)O)(dppm)₂][BF₄]₂ (**40**) or [IrRu(OSO₂CF₃)(CO)₃(μ-C(CH₃)O)(dppm)₂][CF₃SO₃] (**41**) with H₂ at ambient temperature yields the monohydride products [IrRuH(CO)₃(μ-C(CH₃)O)(dppm)₂][X] (**43**; X = CF₃SO₃, BF₄) as outlined in Scheme 3.4. The ¹H

Scheme 3.4



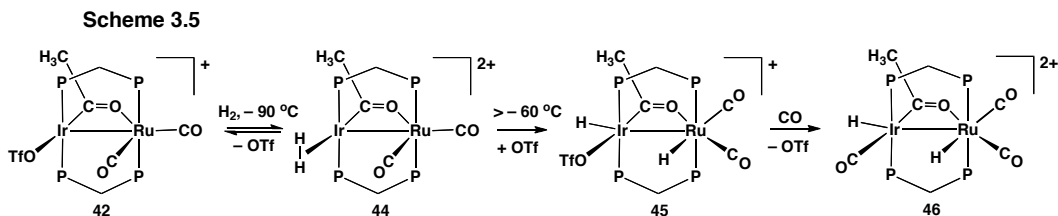
NMR spectrum of **43** (reported as the triflate salt) displays a hydride signal at δ – 10.35 with coupling to only the iridium-bound phosphorus nuclei, suggesting that it is terminally bound to this metal. The acetyl protons appear as a singlet at δ 1.22, while the dppm methylene protons appear at δ 3.95 (all with the appropriate integrations). When a ^{13}C -enriched sample of **43** is prepared, starting from **40**(^{13}CO) or **41**(^{13}CO) the ^{13}C NMR spectrum shows the acyl carbonyl at typically downfield (δ 260.2). Through a series of $^{13}\text{C}\{^{31}\text{P}\}$ NMR experiments, two carbonyls at δ 212.0 and 188.0 are assigned as being terminally bound to Ru while the third, at δ 183.4, is terminally bound to Ir. A mutual coupling of 30 Hz between the acyl carbonyl and the most upfield carbonyl suggests that they are mutually *trans*.

By performing the reaction of **41** with dihydrogen at lower temperatures we hoped to observe intermediates in the formation of **43**. However, this was not the case. Compound **43** was the only species observed at -40°C ; below this temperature, no reaction was observed with either **40** or **41**. This mono-hydride product can also be formed more directly through addition of one equiv of superhydride (LiBEt_3H) to **41** at ambient temperature, further supporting its formulation.

The formation of the monohydride (**43**) from either **40** or **41** appears to result from heterolytic cleavage of H_2 in which a hydride is delivered to the complex. Presumably, facile deprotonation of an unobserved dihydrogen complex by the counter ion (triflate or fluoroborate) occurs, although no evidence of the corresponding acids were observed in the ^1H NMR spectra down to -80°C . The acidity of dihydrogen complexes is well documented.⁷²

Although reactions of **40** or **41** with H_2 did not yield acetaldehyde, the subsequent reaction of **43** with CO does generate this product together with the previously characterized $[\text{IrRu}(\text{CO})_4(\text{dppm})_2][\text{OTf}]$ ⁵⁶ and small amounts of uncharacterized dppm-containing products. The 0.2 equiv of acetaldehyde observed is significantly lower than anticipated, presumably through its loss due to displacement under the stream of CO gas.

The dicarbonyl species **42** also reacts with hydrogen gas, even at $-90\text{ }^{\circ}\text{C}$ yielding what we propose to be the dihydrogen adduct $[\text{IrRu}(\text{H}_2)(\text{CO})_2(\mu\text{-C}(\text{CH}_3)\text{O})(\text{dppm})_2][\text{CF}_3\text{SO}_3]_2$ (**44**) as shown in Scheme 3.5. We assume that in



this product, the dihydrogen ligand replaces the triflate ion of the precursor since no coordinated triflate is observed in the ^{19}F NMR spectra. In the $^{31}\text{P}\{^1\text{H}\}$ NMR spectra compound **44** appears as one broad signal centred at δ 16.0, furthermore the $^{31}\text{P}\{^1\text{H}\}$ NMR spectroscopy shows that compound **42** is in equilibrium with **44**, with the ^{31}P integrals showing a 1:1 ratio of these compounds at a H_2 pressure of approximately 1 atm. The resonance for the H_2 ligand is observed in the ^1H NMR as a broad signal at δ -0.03 . This H_2 ligand is extremely labile, so warming a mixture of **42** and **44** above $-90\text{ }^{\circ}\text{C}$ results in a decrease in the concentration of **44** and by $-80\text{ }^{\circ}\text{C}$ none of **44** remains.

In attempts to obtain the H–D coupling constant for the HD isotopomer of **44**, the H_2 ligand was displaced by passing HD through a sample at $-90\text{ }^{\circ}\text{C}$. Although the substitution appeared to succeed, as witnessed by the 50% reduction in the intensity of the peak attributed to the H_2 ligand while the ratio of **42** and **44** did not change appreciably in the ^{31}P NMR spectrum, we were unable to observe the expected coupling (*ca.* 30 Hz)⁷² owing to the breadth of this signal (*ca.* 120 Hz at half-height). Unfortunately, T_1 measurements, although supportive of a dihydrogen complex, are also inconclusive owing to the instability of **44** at temperatures above $-90\text{ }^{\circ}\text{C}$. One indication of an H_2 complex is a short $(T_1)_{\text{min}}$ – generally below 100ms (at 200 MHz).⁷² For compound **44** the relaxation time (at 200 MHz) is found to be 112 ms at $-90\text{ }^{\circ}\text{C}$ (the spectral array to calculate T_1 is shown in Figure AI.2 of Appendix I). However, we suggest that the true $(T_1)_{\text{min}}$ is probably significantly less than this. In general, T_1 and T_2 are comparable and

both decrease with decreasing temperature in what is referred to as the “extreme narrowing” region.⁷³ However, T_1 reaches a minimum ($(T_1)_{\min}$) after which it begins to increase with decreasing temperature while T_2 continues to decrease. The large discrepancy in T_1 and T_2 values for compound **44**, for which $T_2 = 2.7$ ms, suggests that we are at too low a temperature, so increasing the temperature (which is not possible for **44**) would be required to obtain $(T_1)_{\min}$.

Upon warming above -60 °C homolytic cleavage of H_2 occurs yielding the dihydride species, $[IrRu(OSO_2CF_3)(H)_2(CO)_2(\mu-C(CH_3)O)(dppm)_2][CF_3SO_3]$ (**45**). The 1H NMR spectrum of **45** shows two hydride signals: one at $\delta -12.28$, which shows coupling to the Ir-bound phosphorus nuclei, and the other at $\delta -9.95$, which shows coupling to the Ru-bound phosphorus nuclei suggesting that both hydrides are terminally bound to different metals. In addition, both hydrides display mutual coupling of 5 Hz, which is presumably transmitted via the metal-metal bond. The hydride at $\delta -9.95$ shows additional coupling of 15 Hz to the Ru-bound carbonyl *trans* to it when a ^{13}CO -enriched sample is used; furthermore, in this isotopomer, the Ir-bound hydride at $\delta -12.28$ displays no coupling to the acyl carbon suggesting that they are mutually *cis*. The acetyl methyl signal appears at $\delta 0.94$ in the 1H NMR spectrum. The $^{13}C\{^1H\}$ NMR spectrum displays a triplet at $\delta 235.6$ with 5 Hz coupling to the Ir-bound phosphorus nuclei. The relatively upfield shift of this acyl group is very similar to that of the starting dicarbonyl compound, **42**, suggesting an acyl structure closer to representation **III-C** shown earlier in Chart 3.2. The two carbonyl ligands are shown to be terminally bound to ruthenium and appear at $\delta 192.8$ and 191.8 ; the lack of coupling between them suggests that they are mutually *cis*. ^{19}F NMR spectroscopy shows two signals; one at $\delta -78.9$ is assigned to the free triflate counter-ion and another at $\delta -79.5$ is attributed to the bound triflate anion. It is assumed that this anion is coordinated to Ir since Ru is coordinatively saturated.

The instability of compound **44** above -90 °C casts some doubt on whether this species is the immediate precursor to the dihydride **45** (Scheme 3.5) or whether another, unobserved H_2 complex is involved.

Surprisingly, compound **45** does not give rise to detectable amounts of acetaldehyde, either when left in solution or when reacted with CO. Under an atmosphere of CO, triflate-ion displacement by CO occurs yielding $[\text{IrRu}(\text{H})_2(\text{CO})_3(\mu\text{-C}(\text{CH}_3)\text{O})(\text{dppm})_2][\text{CF}_3\text{SO}_3]_2$ (**46**), which is stable for extended periods of time and does not yield detectable quantities of acetaldehyde. NMR spectroscopy (with appropriate heteronuclear decoupling experiments) supports the structure for **46** in which the coordinated triflate ion in **45** has been replaced by CO.

3.4 Conclusions

The present study was initiated to determine how an Ir/Ru-based system might differ from analogous Rh/Ru³⁰ and Rh/Os³¹ systems, with a view to establishing the roles of the different metals in substrate activation and subsequent transformations.

As is outlined in this chapter, some reactivity differences between the Ir and Rh-based systems were predictable on the basis of well-established differences in these metals, although others were unexpected. In the overall conversion of a bridging methylene group to a bridging acetyl group, through protonation followed by ligand migration and migratory insertion, the three systems behaved quite similarly. In all cases (Rh/Ru,³⁰ Rh/Os³¹ and Ir/Ru) protonation of the $\mu\text{-CH}_2$ moiety gave an unsymmetrically bridged methyl group at low temperature, which migrated to a terminal site on the group 9 metal, followed by migratory insertion at that metal to give the bridging acetyl group. The low-temperature NMR studies on the three metal combinations, in which only the methyl-bridged products are observed, suggest direct protonation at the methylene group, rather than prior protonation at the metals followed by migration to the methylene carbon. Although we cannot rule out that the latter process is extremely facile and not observed, the failure to observe the methyl/hydride intermediate at $-90\text{ }^\circ\text{C}$ for all of the three metal combinations (Rh/Ru, Rh/Os and Ir/Ru) suggests to us that a metal hydride is not involved.

Notably, there are some subtle, although significant differences between the Rh- and Ir-based systems. First, the unsymmetrically bridged methyl group is σ -bound to Ir while involved in an agostic interaction with Ru in the current study, whereas for the Rh-based systems, the reverse is true, with the σ -bond being to the group 8 metal. Certainly, in this study the greater strength of the Ir-C bond compared to Ru-C or Rh-C⁶¹ must be a dominant factor in this observation. In addition, the two compounds containing bridging methyl groups in this study were highly unusual in having very slow exchange (on the NMR time-scale) between the “terminal” and “agostic” methyl hydrogens at low temperature, allowing the two different C-H coupling constants to be measured. As a consequence, these coupling constants for the agostic interactions in both species (65 and 72 Hz) are believed to be the lowest yet observed for unsymmetrically bridged methyl groups. Stronger interactions (lower $^1J_{CH}$ values) have been observed in mononuclear, electron-poor systems and in substituted bridging alkyl fragments.⁴⁷

A further (predictable) difference between the Ir- and Rh-based systems is the rate of migratory insertion, which is orders of magnitude slower at Ir than at Rh, again in keeping with the stronger bonds involving the former. It may seem unusual that migratory insertion did not occur at the (presumed) more labile Ru center in the current study. However, in this system the methyl group is primarily bound to Ir and is involved with Ru only through a labile agostic interaction at very low temperature.

Although acetyl-bridged complexes are well precedented, an aspect of note is the irreversibility of their formation. In mononuclear chemistry, conversion of an alkyl/carbonyl species to the corresponding acyl product upon addition of CO or another Lewis base is generally reversed upon removal of a ligand. This did not occur in the chemistry described herein, or in our previous studies.^{30,31} Removal of up to two carbonyl ligands in this Ir/Ru system left the bridging acetyl group intact. One major difference between terminal and bridging acetyl groups is that in the former, this group functions as a 1-electron donor. Removal of a carbonyl (or other ligand) from the complex leads to deinsertion in

order to satisfy the electronic requirements of the metal regenerating a methyl and a carbonyl ligand which together supply 3 electrons to the metal, thereby compensating for the lost ligand. In the bridging mode, the acetyl group functions as a 3-electron donor, so from the perspective of electron counting, nothing is gained upon deinsertion. In the binuclear system stabilization of an unsaturated species cannot be achieved through deinsertion and must be accommodated for in other ways by interactions with the adjacent metal or its ligands. Of course, anion coordination can also serve this function.

In investigating the Ir/Ru system we had hoped to exploit one major difference between Rh and Ir, namely the greater tendency of the latter to undergo oxidative addition. This was certainly observed in the reaction with H₂; whereas both Rh systems were unreactive to H₂, the three Ir/Ru compounds investigated reacted readily with H₂. Both heterolytic and homolytic cleavage of H₂ were observed. In reactions with the cationic tricarbonyl precursors [IrRu(OSO₂CF₃)(CO)₃(μ-C(CH₃)O)(dppm)₂][CF₃SO₃] (**41**) and [IrRu(CO)₃(μ-C(CH₃)O)(dppm)₂][BF₄]₂ (**40**), the only products observed were the monohydrides, [IrRu(H)(CO)₃(μ-C(CH₃)O)(dppm)₂][X] (X = BF₄, CF₃SO₃), whereas reaction of the dicarbonyl analogue, [IrRu(OSO₂CF₃)(CO)₂(μ-C(CH₃)O)(dppm)₂][CF₃SO₃] (**42**) at -90 °C yielded a dihydrogen complex, which underwent homolytic H₂ cleavage to yield a dihydride at somewhat higher temperatures. The tendency of the first two species to undergo heterolytic cleavage is consistent with these species being more electron poor (one additional π-acceptor CO ligand) than **42**, therefore more Lewis acidic.⁷²

3.5 References

1. Collman, J. P.; Hegedus, L. S.; Norton, J. R.; Finke, R. G. *Principles and Applications of Organotransition Metal Chemistry*. University Science Books: Mill Valley, CA, 1987, Chapter 12.
2. Niu, S.; Hall, M. B. *Chem. Rev.* **2000**, *100*, 353.
3. Pruett, R. L. *Adv. Organomet. Chem.* **1979**, *17*, 1.

4. Pruett, R. L. *Chem. Educ.* **1986**, *63*, 196.
5. Trzeciak, A. M.; Ziolkowski, J. J. *Coord. Chem. Rev.* **1999**, *190-192*, 883.
6. Howard, M. J.; Jones, M. D.; Roberts, M. S.; Taylor, S. A. *Catal. Today* **1993**, *18*, 325.
7. Yoneda, N.; Kusano, S.; Yasui, M.; Pujado, P.; Wilcher, S. *Appl. Catal.* **2001**, *221*, 253.
8. Haynes, A.; Mann, B. E.; Morris, G. E.; Maitlis, P. M. *J. Am. Chem. Soc.* **1993**, *115*, (10), 4093.
9. Haynes, A.; Maitlis, P. M.; Morris, G. E.; Sunley, G. J.; Adams, H.; Badger, P. W.; Bowers, C. M.; Cook, D. B.; Elliott, P. I. P.; Ghaffar, T.; Green, H.; Griffin, T. R.; Payne, M.; Pearson, J. M.; Taylor, M. J.; Vickers, P. W.; Watt, R. J. *J. Am. Chem. Soc.* **2004**, *126*, (9), 2847.
10. Selected Reviews: (a) Sen, A. *Acc. Chem. Res.* **1993**, *26*, 303. (b) Drent, E.; Budzelaar, P.H.M. *Chem. Rev.* **1996**, *96*, 663. (c) Robertson, R.A.M.; Cole-Hamilton, D.J.C. *Coord. Chem. Rev.* **2002**, *225*, 67. (d) Bianchini, C.; Meli, A.; Oberhauser, W. *Dalton Trans.* **2003**, 2627.
11. Recent papers: (a) Cavinato, G.; Vavasori, A.; Anadio, E.; Toniolo, L. *J. Molec. Catal. A* **2007**, *278*, 251. (b) Rampersad, M.V., Zuidema, E.; Ernsting, J.M.; van Leeuwen, P.W.N.M.; Darensbourg, M.Y. *Organometallics*, **2007**, *26*, 783. (c) Muñoz-Moreno, B.K.; Claver, C.; Ruiz, A.; Bianchini, C.; Meli, A.; Oberhauser, W. *Dalton Trans*, **2008**, 2741.
12. Watson, P. R.; Somorjai, G. A. *J. Catal.* **1981**, *72*, 347.
13. Fukushima, T.; Arakawa, H.; Ichikawa, M. *J. Phys. Chem.* **1985**, *89*, 4440.
14. Fukushima, T.; Arakawa, H.; Ichikawa, M. *J. Chem. Soc. Chem. Commun.* **1985**, 729.
15. Ichikawa, M. *Polyhedron* **1988**, *7*, 2351.
16. Shulz, H. *Appl. Catal. A.: Gen.* **1999**, *186*, 3.
17. Overett, M. J.; Hill, R. O.; Moss, J. R. *Coord. Chem. Rev.* **2000**, *206-207*, 581.
18. Wang, X.; Weitz, E. *J. Organomet. Chem.* **2004**, *689*, 2354.

19. George, R.; Andersen, J. M.; Moss, J. R. *J. Organomet. Chem.* **1995**, *505*, 131.
20. Matthews, R. C.; Howell, D. K.; Peng, W.-J.; Train, S. G.; Treheaver, W. D.; Stanley, G. G. *Angew. Chem, Int. Ed. Engl.* **1996**, *35*, 2253.
21. Broussard, M. E.; Juma, B.; Train, S. G.; Peng, W.-J.; Laneman, S. A.; Stanley, G. G. *Science* **1993**, *260*, 1784.
22. Hidai, M.; Fukuska, A.; Koyasu, Y.; Uchida, Y. *J. Mol. Catal.* **1986**, *35*, 29.
23. Hidai, M.; Orisaku, M.; Ue, M.; Koyasu, Y.; Komada, T.; Uchida, Y. *Organometallics* **1983**, *2*, 292.
24. Fukuska, A.; Fukugawa, S.; Hirano, M.; Komiya, S. *Chem. Lett.* **1997**, 377.
25. Ishii, Y.; Hidai, M., *Catal. Today* **2001**, *66*, 53.
26. Van den Beuken, E. K.; Feringa, B. L. *Tetrahedron* **1998**, *54*, 12985.
27. Komiya, S.; Yasuda, T.; Hirano, A.; Fukuoka, M. *J. Mol. Catal. A.: Chem.* **2000**, *159*, 63.
28. Ishii, Y.; Miyashita, K.; Kamita, K.; Hidai, M. *J. Am. Chem. Soc.* **1997**, *119*, 6448.
29. Fukuoka, A.; Fukugawa, S.; Hirano, M.; Koga, N.; Komiya, S. *Organometallics*, **2001**, *20*, 2065.
30. Rowsell, B. D.; McDonald, R.; Cowie, M. *Organometallics* **2004**, *23*, 3873.
31. Trepanier, S. J.; McDonald, R.; Cowie, M. *Organometallics* **2003**, *22*, 2638.
32. Wigginton, J. R.; Trepanier, S. J.; McDonald, R.; Ferguson, M. J.; Cowie, M. *Organometallics* **2005**, *24*, 6194.
33. Byram, S. K.; Fawcett, J. K.; Nyburg, S. C.; O'Brien, R. J. *J. Chem. Soc. D* **1970**, 16.
34. Evans, W. J.; Anwender, R.; Ziller, J. W. *Organometallics* **1995**, *14*, 1107.
35. Holton, J.; Lappert, M. F.; Scollary, G. R.; Ballard, D. G. H.; Pearce, R.; Atwood, J. L.; Hunter, W. E. *J. Chem. Soc., Chem. Commun.* **1976**, 425.

36. Holton, J.; Lappert, M. F.; Ballard, D. G. H.; Pearce, R.; Atwood, J. L.; Hunter, W. E. *J. Chem. Soc., Dalton Trans.* **1979**, 54.
37. Huffman, J. C.; Streib, W. E. *J. Chem. Soc. D* **1971**, 911.
38. Klooster, W. T.; Lu, R. S.; Anwender, R.; Evans, W. J.; Koetzle, T. F.; Bau, R. *Angew. Chem., Int. Ed. Engl.* **1998**, *37*, 1268.
39. Waezsada, S. D.; Liu, F.-Q.; Murphy, E. F.; Roesky, H. W.; Teichert, M.; Usón, I.; Schmidt, H.-G.; Albers, T.; Parisini, E.; Noltemeyer, M. *Organometallics* **1997**, *16*, 1260.
40. Yu, Z.; Wittbrodt, J. M.; Heeg, M. J.; Schlegel, H. B.; Winter, C. H. *J. Am. Chem. Soc.* **2000**, *122*, 9338.
41. Beringhelli, T.; D'Alfonso, G.; Panigati, M.; Porta, F.; Mercandelli, P.; Moret, M.; Sironi, A. *J. Am. Chem. Soc.* **1999**, *121*, 2307.
42. Kruger, C.; Sekutowski, J. C.; Berke, H.; Hoffmann, R. *Z. Naturforsch.* **1978**, *33 B*, 1110.
43. Kulzick, M. A.; Price, R. T.; Andersen, R. A.; Muetterties, E. L. *J. Organomet. Chem.* **1987**, *333*, 105.
44. Reinking, M. K.; Fanwick, P. E.; Kubiak, C. P. *Angew. Chem., Int. Ed. Engl.* **1989**, *28*, 1377.
45. Schmidt, G. F.; Muetterties, E. L.; Beno, M. A.; Williams, J. M. *Proc. Natl. Acad. Sci. U.S.A.* **1981**, *78*, 1318.
46. Brookhart, M.; Green, M. L. H. *J. Organomet. Chem.* **1983**, 395.
47. (a) Brookhart, M.; Green, M. L. H.; Wong, L.-L. *Prog. Inorg. Chem.* **1988**, *36*, 1. (b) Brookhart, M.; Green, M. L. H.; Parkin, G. *Proc. Nat. Acad. Sci. USA* **2007**, *104*, 6908.
48. Calvert, R. B.; Shapley, J. R. *J. Am. Chem. Soc.* **1978**, *100*, 7726.
49. Casey, C. P.; Fagan, P. J.; Miles, W. H. *J. Am. Chem. Soc.* **1982**, *104*, 1134.
50. Dawkins, G. M.; Green, M.; Orpen, A. G.; Stone, F. G. A. *J. Chem. Soc., Chem. Commun.* **1982**, 41.
51. Hursthouse, M. B.; Jones, R. A.; Abdul Malik, K. M.; Wilkinson, G. J. *Am. Chem. Soc.* **1979**, *101*, 4128.

52. Jones, R. A.; Wilkinson, G.; Galas, A. M. R.; Hursthouse, M. B.; Malik, K. M. A. *J. Chem. Soc., Dalton Trans.* **1980**, 1771.
53. (a) [Anon] *Chem. Britain* **1996**, 32(10), 7. (b) Howard, M. J.; Sunley, G. J.; Poole, A. D.; Watt, R. J.; Sharma, B. K. *Stud. Surf. Sci. Catal.* **1999**, 121, 61. (c) Sunley, G. J.; Watson, D. J. *Catal. Today* **2000**, 58, 293. (d) Jones, J. H. *Platinum Metals Rev.*, **2000**, 44, 94. (e) Haynes, A. *Educ. Chem.* **2001**, 38, 99.
54. Siedle, A. R.; Newmark, R. A.; Pignolet, L. H. *Organometallics* **1984**, 3, 855.
55. Park, J. W.; Mackenzie, P. B.; Schaefer, W. P.; Grubbs, R. H. *J. Am. Chem. Soc.* **1986**, 108, 6402.
56. Dell'Anna, M. M.; Trepanier, S. J.; McDonald, R.; Cowie, M. *Organometallics* **2001**, 20, 88.
57. Programs for diffractometer operation, data collection, data reduction and absorption correction were those supplied by Bruker.
58. Beurskens, P. T.; Beurskens, G.; de Gelder, R.; Garcia-Granda, S.; Isreal, R.; Gould, R. O.; Smits, J. M. M. (1999). The *DIRDIF-99* program system. Crystallography Laboratory, University of Nijmegen, the Netherlands.
59. Sheldrick, G. M. *SHELXL-93*. Program for crystal structure determination. University of Göttingen, Germany, 1993.
60. Sheldrick, G. M. *Acta Crystallogr.* **1990**, A46, 467.
61. (a) Ziegler, T.; Tschinke, V. In *Bonding Energetics in Organometallic Compounds*; Marks, T.J., Ed. ACS, Washington, DC, 1990; Chapter 19. (b) Ziegler, T.; Tschinke, V., Ursenbach, B. *J. Am. Chem. Soc.* **1987**, 109, 4825; (c) Armentrout, P.B. In *Bonding Energetics in Organometallic Compound*; Marks, T.J., Ed. ACS, Washington, DC, 1990; Chapter 2.
62. George, D. S. A.; McDonald, R.; Cowie, M. *Organometallics* **1998**, 17, 2553.
63. Johnson, K. A.; Gladfelter, W. L. *Organometallics* **1990**, 9, 2101.

64. Parkin, G. *Comprehensive Organometallic Chemistry III*. Elsevier Ltd., Oxford, **2007**. Eds. R.H. Crabtree, D.M. P. Mingos. Vol 1.
65. Perrin, C.L.; Dwyer, T.J. *Chem. Rev.*, **1990**, *90*, 935.
66. Anderson, D. J. PhD Thesis, University of Alberta, 2007.
67. Rowsell, B. D.; Trepanier, S. J.; Lam, R.; McDonald, R.; Cowie, M. *Organometallics* **2002**, *21*, 3228.
68. Oke, O.; McDonald, R.; Cowie, M. *Organometallics* **1999**, *18*, 1629.
69. Jeffrey, J. C.; Orpen, A. G.; Stone, F. G. A.; Went, M. J. *J. Chem. Soc., Dalton Trans.* **1986**, 173.
70. Gao, Y.; Jennings, M. C.; Puddephatt, R. J. *Organometallics* **2001**, *20*, 1882.
71. Shafiq, F.; Kramarz, K. W.; Eisenberg, R. *Inorg. Chim. Acta* **1993**, *213*, 111.
72. (a) Kubas, G.J. *Comprehensive Organometallic Chemistry III*. Elsevier Ltd., Oxford, **2007**. Eds. R.H. Crabtree, D.M. P. Mingos. Vol 1., Chpt 1.24. (b) Kubas, G. J. *Proc. Nat. Acad. Sci. U.S.A.* **2007**, *104*, 6901. (c) Heinekey, D.M.; Oldham, W.J. *Chem. Rev.* **1993**, *93*, 913. (d) Jessop, P.G.; Morris, R.H. *Coord. Chem. Rev.* **1992**, *121*, 155.
74. Harris, R.K. *Nuclear Magnetic Resonance Spectroscopy - A Physicochemical View*, Longman Scientific and Technical, Harlow, Essex, UK, **1994**.
75. (a) Trepanier, S.J.; Dennett, D.N.L.; Sterenberg, B.T.; McDonald, R.; Cowie, M. *J. Am. Chem. Soc.* **2004**, *126*, 8046. (b) Cowie, M. *Can. J. Chem.* **2005**, *83*, 1043.

Chapter 4: Geminal C-H Activation of α -Olefins Promoted by IrRu Systems: Mechanistic Insights

4.1 Introduction

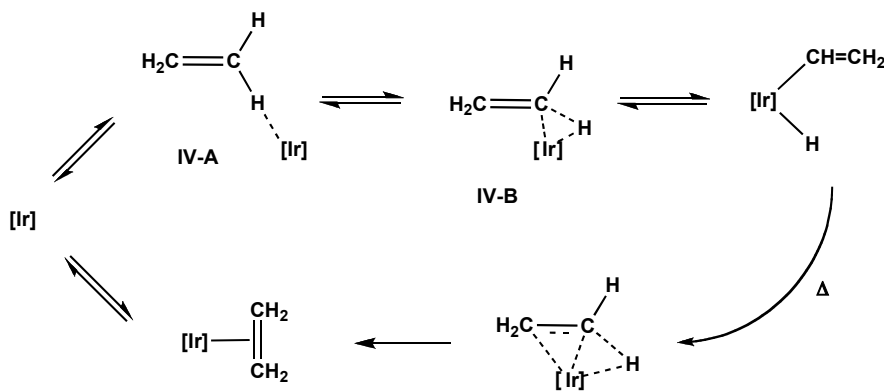
The late transition metal-mediated activation of C-H bonds is an active area of research in organometallic chemistry,¹⁻⁴ due primarily to the importance of this transformation in the selective conversion of inexpensive and generally unreactive hydrocarbon feedstocks into more complex and value-added targets. For the most part, these efforts have focused on monometallic systems, many of which have proven adept at the cleavage of a single C-H bond.

There have been a few reports of geminal C-H bond activation (in which *two* geminal C-H bonds are activated), the majority of which involve alkyl C-H bonds of non-innocent ancillary ligands or substrates that coordinate through a heteroatom prior to C-H bond cleavage.⁵⁻¹⁷ In these cases, the C-H bonds are pre-oriented to facilitate facile geminal C-H bond cleavage. The cleavage of two geminal C-H bonds of substrates without heteroatoms, such as α -olefins, is more challenging, and to our knowledge only five systems have been reported that are capable of olefin geminal C-H activation.¹⁸⁻²¹ The first two examples reported by Deeming *et al.* showed that a refluxing octane solution of the trinuclear complexes $M_3(CO)_{12}$ ($M = Ru, Os$) in an ethylene-rich atmosphere yields the vinylidene-bridged dihydrides $M_3H_2(CO)_9(\mu-C=CH_2)$.^{18a-d} A decade later Green and associates demonstrated the ability of the mononuclear iron tris(dimethylphosphinomethyl)methylsilane complex, $[Fe((Me_2PCH_2)_3(SiMe))(\eta^4-C_6H_6)]$, to react with ethylene under elevated temperature (50 °C) and pressure (7 atm) to generate the diiron vinylidene-bridged dihydrido species $[Fe_2(\mu-H)_2((Me_2PCH_2)_3(SiMe))_2(\mu-CCH_2)]$.^{18e,f} Shortly after, Perutz and coworkers reported a mononuclear Ir piano stool complex which, under photochemical conditions, facilitates geminal C-H activation of an ethylene ligand.²⁰ Finally, in the most recent report, our group has reported that the

diiridium complex $[\text{Ir}_2(\text{CH}_3)(\text{CO})_2(\text{dppm})_2][\text{OTf}]$ ($\text{dppm} = \mu\text{-Ph}_2\text{PCH}_2\text{PPh}_2$; $\text{OTf} = \text{CF}_3\text{SO}_3$) reacts slowly with 1,3-butadiene at ambient temperature to give the vinyl vinylidene-bridged dihydride, $[\text{Ir}_2(\text{H})_2(\text{CH}_3)(\text{CO})_2(\mu\text{-C}=\text{C}(\text{H})\text{C}(\text{H})=\text{CH}_2)(\text{dppm})_2][\text{OTf}]$,¹⁹ *via* geminal C-H activation at one end of the butadiene molecule. It is important to note that of these four cases only one, the diiridium system, exhibits geminal C-H activation under ambient conditions, without the need for prior ligand loss from the activating complex. A report by Suzuki and associates should also be noted in which the authors reported an overall, step-wise, geminal C-H activation by reaction of the diruthenium complex $[(\eta^5\text{-C}_5\text{Me}_5)\text{Ru}(\mu\text{-H})_4\text{Ru}(\eta^5\text{-C}_5\text{Me}_5)]$ with ethylene to give the ethylene divinyl product $[(\eta^5\text{-C}_5\text{Me}_5)\text{Ru}(\text{C}_2\text{H}_4)(\text{CH}=\text{CH}_2)_2\text{Ru}(\eta^5\text{-C}_5\text{Me}_5)]$.²¹ Substitution of the ethylene ligand by methyl vinyl ketone and heating the resulting adduct in toluene yielded a vinylidene-bridged species.

The cleavage of olefinic C-H bonds by monometallic late transition metal systems is well understood.²²⁻²⁹ Although it was initially believed that precoordination of the olefin to the metal centre was a prerequisite for C-H activation, Bergman *et al.* demonstrated that this is not necessarily the case.²⁷⁻²⁹ These researchers established two competing pathways – one yielding a vinyl hydride (the product of C-H oxidative addition) and another leading to the η^2 -olefin adduct (Scheme 4.1 below).²⁸ The authors proposed, and later supported by

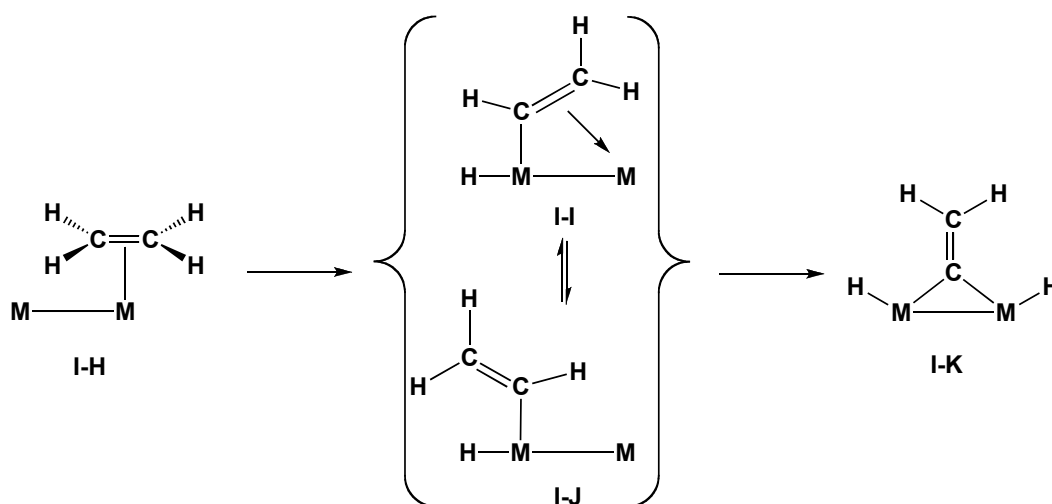
Scheme 4.1



computational methods,²⁹ that the vinyl hydride and η^2 -olefin do not lie on the same reaction pathway. The pathway leading to the vinyl hydride begins by approach of the ethylene molecule along the C-H bond axis (**IV-A** in Scheme 4.1). As the ethylene draws closer to the Ir centre, the transition state **IV-B**, not unlike a C-H agostic interaction, leads to the vinyl hydrido species, the product of C-H oxidative addition at Ir.

However, in the multimetallic systems noted above the roles of the adjacent metals remain unclear. One can envision cooperative involvement of the adjacent metals during C-H activation in which the substrate binds to one metal centre, and in so doing, orients the olefinic C-H bond with respect to the adjacent metal. For example, in **I-H** (see Chart 4.1 below) the olefin is π -bound to one metal and as a result one of the C-H bonds is oriented in an arrangement with respect to the other, adjacent, metal not unlike **IV-A**, thereby facilitating the facile C-H bond cleavage by this adjacent metal centre. Once the first C-H activation has occurred, orientation of the geminal C-H bond in a position adjacent to the second metal can be envisioned to lead to the second activation as shown in Chart 4.1. It is this availability of a second metal, capable of subsequent C-H activation, which is the subject of this Chapter.

Chart 4.1



In the study presented in this chapter our objectives are: (1) to determine whether an IrRu system, somewhat analogous to our original Ir₂ system, is also capable of facile geminal C-H activation, and if so; (2) to attempt to determine the roles of the adjacent metal centres and thereby rationalize the enhanced reactivity of multinuclear complexes in such transformations.

4.2 Experimental Section

4.2.1 General Comments:

All solvents were dried (using appropriate drying agents), distilled before use and stored under nitrogen. Reactions were performed under an argon atmosphere using standard Schlenk techniques unless otherwise noted. Triruthenium dodecacarbonyl and Ammonium hexachloroiridate(IV) were purchased from Strem Chemicals. Allene, propene, propyne and butadiene were purchased from Praxair, whereas methylallene was purchased from Organic Technologies, 1,1-dimethylallene from Aldrich, and ethylene, acetylene, 2-methylpropene and *cis*-butene from Matheson. Both ¹³C₂-ethylene and 1,1-d₂ ethylene were purchased from Cambridge Isotopes. The fluoroolefins 1,1-difluoroethylene and *cis*-difluoroethylene were purchased from Aldrich and SynQuest Labs, respectively. [IrRu(CO)₄(dppm)₂][OTf]³⁰ (**6**), [IrRu(CO)₄(μ-CH₂)(dppm)₂][OTf]³⁰ (**8**) and diethyl diazomalonate³¹ were prepared by their respective literature procedures.

All ¹H NMR, and ³¹P{¹H} NMR spectra were recorded on a Varian Inova spectrometer operating at 399.9 MHz and 161.9 MHz, respectively, or a Varian DirectDrive spectrometer operating at 499.8 MHz and 202.3 MHz, respectively. ¹³C{¹H} NMR and all variable-temperature NMR spectra were recorded on a Varian Inova spectrometer operating at 100.6 Hz for ¹³C, 161.9 MHz for ³¹P and 400.4 MHz for ¹H. Infrared spectra were recorded in CH₂Cl₂ solution on a Nicolet Avatar 370 DTGS spectrometer. Elemental analyses were performed by the microanalytical services within the department. Mass

Spectrometry measurements were performed by the electro-spray ionization technique on a Micromass ZabSpec TOF spectrometer by the Mass Spectrometry facility of the department. Spectroscopic data for all compounds prepared are given in Table 4.1.

Table 4.1. Spectroscopic Data for Compounds

Compound	IR (cm ⁻¹) ^a	$\delta(^3\text{P}\{\text{H}\})^d$	$\delta(\text{H})^e$	$\delta(^{13}\text{C}\{\text{H}\})^f$
[IrRu(CO) ₄ (μ-C=CH ₂)(dppm) ₂]-[OTf] (47)	2048 (s), 1999 (s), 1947 (s), 1805 (s)	31.3 (m, 2P), 4.3 (m, 2P)	dppm: 3.99 (m, 2H, ² J _{HH} = 14 Hz), 2.93 (m, 2H, ² J _{HH} = 4 Hz) C ₂ H ₂ : 6.69 (br, 1H); 5.03 (br, 1H)	Ir-CO: 179.3 (t, ² J _{CP} = 10.9 Hz) Ru-CO: 193.2 (t, ² J _{CP} = 12.4 Hz), 196.1 (t, ² J _{CP} = 10.0 Hz) μ-CO: 203.5 (m)
[IrRu(CO) ₄ (μ-C=C(H)-CH ₃)(dppm) ₂][OTf] (48)	1799 (m), 1984 (s), 1996 (s), 2048 (s)	29.8 (m, 2P), -0.4 (m, 2P)	C ₃ H ₄ : CH ₃ 0.78 (dtt, 3H, ³ J _{HH} = 6.4 Hz, ⁵ J _{HP(tr)} = 1.8 Hz, ⁵ J _{HP(Ru)} = 1.8 Hz); CH: 6.91 (qtt, 1H, ³ J _{HH} = 6.4 Hz, ⁴ J _{HP(tr)} = 1.5 Hz, ⁴ J _{HP(Ru)} = 1.0 Hz) dppm: CH ₂ : 3.04 (m, 2H); 4.01 (m, 2H)	Ru-CO: 195.0 (t, ² J _{CP(Ru)} = 11 Hz), 192.8 (t, ² J _{CP(Ru)} = 12 Hz) Ir-CO: 182.2 (t, ² J _{CP(tr)} = 12 Hz) μ-CO: 209.0 (tt, ² J _{CP(Ru)} = 9 Hz, ² J _{CP(tr)} = 6 Hz) C ₃ H ₄ : μ-CCHCH ₃ (200.9 (tt, ² J _{CP(Ru)} = 7 Hz, ² J _{CP(tr)} = 11 Hz), μ-CCHCH ₃ 139.2 (s), μ-CCHCH ₃ 24.7 (s)
[IrRu(CO) ₄ (μ-C=C(H)-CH ₂ CH ₃)(dppm) ₂][OTf] (49)	2047 (s), 2030 (s), 1995 (s), 1780 (s)	29.8 (m, 2P), -0.1 (m, 2P)	C ₄ H ₆ : CH ₃ 0.42 (t, 3H, ³ J _{HH} = 7.7 Hz); CH ₂ 1.11 (m, 2H, ³ J _{HH} = 7.7 Hz, ³ J _{HH} = 6.5 Hz); CH 6.75 (dtt, ³ J _{HH} = 6.5 Hz, ⁵ J _{HP(Ru)} = 1.0 Hz, ⁵ J _{HP(tr)} = 1.2 Hz) dppm: CH ₂ 4.12 (m, 2H); 3.09 (m, 2H)	Ru-CO: 192.5 (m, 1C, ² J _{CC} = 24 Hz, ² J _{CP(Ru)} = 12 Hz), 194.8 (t, 1C, ² J _{CP} = 11.0 Hz), 208.9 (m, 1C, ² J _{CC} = 24 Hz, ² J _{CP(Ru)} = 9 Hz, ² J _{CP(tr)} = 5 Hz) Ir-CO: 182.1 (t, 1C, ² J _{CP(tr)} = 12 Hz)
[IrRu(CO) ₄ (μ-C=C(H)-C(CH ₃)=CH ₂)(dppm) ₂]-[OTf] (50)	2051 (s), 2000 (s), 1978 (s), 1792 (m)	27.1 (m, 2P), -4.2 (m, 2P)	C ₄ H ₆ : CH ₂ 4.72 (dm, 1H, ¹ J _{HH} = 2.4 Hz,); 4.41 (dm, 1H, ¹ J _{HH} = 2.4 Hz); CH 7.89 (br, s, 1H), CH ₃ 0.41 (m, 3H) dppm: CH ₂ 3.92 (m, 2H); 3.03 (m, 2H)	Ru-CO: 191.6 (dtd, 1C, ² J _{CC} = 25 Hz, ² J _{CP(Ru)} = 3 Hz); 193.5 (dt, 1C, ² J _{CP(Ru)} = 10 Hz, ² J _{CC} = 3 Hz) Ir-CO: 182.2 (t, 1C, ² J _{CP(tr)} = 12 Hz) μ-CO: 211.5 (m, 1C, ² J _{CC} = 25 Hz, ² J _{CP(Ru)} = 13 Hz, ² J _{CC} = 3 Hz)

Table 4.1. (continued) Spectroscopic Data for Compounds

NMR ^{c,d}				
Compound	IR (cm ⁻¹) ^a	$\delta(^3\text{P}\{\text{H}\})^d$	$\delta(^1\text{H})^e$	
			$\delta(^{13}\text{C}\{\text{H}\})^f$	
[IrRu(H)(CO) ₃ -(C(H)=CH ₂)(dppm) ₂]-[OTf] (51) ^g	n/a	23.6 (m, 2P), 6.1 (m, 2P)	H: -9.32 (m, 1H, ² J _{HP(Ir)}} = 7.9 Hz, ⁴ J _{HH} = 3.5 Hz, ⁴J_{HH} = 6.2 Hz) C₂H₃: 6.84 (m, 1H, ³J_{HH(trans)}} = 12.4 Hz, ³J_{HH(cis)}} = 4.0 Hz), 4.74 (m, 2H, ³J_{HH(trans)}} = 12.4 Hz, ³J_{HH(cis)}} = 4.0 Hz) dppm: 4.18 (m, ²J_{HH} = 13.5 Hz, ⁴J_{HH} = 3.5 Hz), 5.08 (m, ²J_{HH} = 13.5 Hz, ⁴J_{HH} = 6.2 Hz)}}}}}}	Ir-CO: 169.1 (t, 1C, ² J _{CP(Ir)}} = 11.1 Hz) Ru-CO: 189.9 (m, 1C, ² J _{CC} = 26.7 Hz, ²J_{CP(Ru)}} = 11.8 Hz), 214.3 (m, 1C, ²J_{CC} = 26.7 Hz, ²J_{CP(Ru)}} = 10.3 Hz) C(H)=CH₂: CH: 130.6; CH₂: 60.8}}
[IrRu(CO) ₃ (μ-C=CH ₂)-(dppm) ₂][OTf] (52)	n/a	29.0 (m, 2P), -10.8 (m, 2P)	dppm: 4.94 (m, 2H); 4.31 (m, 2H) C ₂ H ₂ : 6.21 (m), 7.13 (m)	Ir-CO: 176.7 (t, ² J _{CP(Ir)}} = 6.6 Hz) Ru-CO: 197.8 (t, ² J _{CP(Ru)}} = 7.4 Hz), 199.7 (t, ² J _{CP(Ru)}} = 8.9 Hz)
[IrRu(H)(CO) ₃ (C(H)=C(H)CH ₃)(dppm) ₂][OTf] (53)	n/a	23.6 (m, 2P), 6.1 (m, 2P)	H: -9.32 (m, 1H, ² J _{HP(Ir)}} = 12 Hz, ⁴ J _{HH} = 6.1 Hz, ⁴J_{HH} = 3.3 Hz) dppm: 4.17 (m, 2H, ²J_{HH} = 13.5 Hz, ⁴J_{HH} = 3.3 Hz), 5.08 (m, 2H, ²J_{HH} = 13.5 Hz, ⁴J_{HH} = 6.1 Hz) C(H)=C(H)CH₃: C(H)CH₃ 6.19 (dq, 0.75 H, ³J_{HH(trans)}} = 16.8 Hz, ³J_{HH} = 3.2 Hz)}}}}}}}	n/a
[IrRu(CO) ₃ (μ-C=C(H)-CH ₃)(dppm) ₂][OTf] (54)	n/a	29.2 (m, 2P), -3.13 (m, 2P)	C ₃ H ₄ : CH: 5.73 (qtt, 1H, ⁴ J _{HH} = 6.5 Hz, ⁴J_{HP(Ru)}} = 1.7 Hz, ⁴J_{HP(Ir)}} = 1.6 Hz); CH₃: 1.95 (dt, 3H, ⁴J_{HH} = 6.5 Hz, ⁴J_{HP(Ir)}} = 2.4 Hz) dppm: 3.90 (dm, 2H, ²J_{HH} = 14.0 Hz); 3.01 (dm, 2H, ²J_{HH} = 14.0 Hz)}}}}	Ir-CO: 176.4 (t, 1C, ² J _{CP(Ir)}} = 12.7 Hz) Ru-CO: 194.6 (t, 1C, ² J _{CP(Ru)}} = 11.5 Hz); 197.6 (t, 1C, ² J _{CP(Ru)}} = 11.3 Hz)

Table 4.1. (continued) Spectroscopic Data for Compounds

		NMR ^{c,d}		
Compound	IR (cm ⁻¹) ^a	$\delta(^3\text{P}\{\text{H}\})^d$	$\delta(\text{H})^e$	$\delta(^{13}\text{C}\{\text{H}\})^f$
[IrRu(CO) ₃ (η^2 -H ₂ C=C=CH ₂)(CO)(dppm) ₂][OTf] (55) ^h	n/a	29.8 (m, 2P), ^g -5.9 (m, 2P)	C ₃ H ₆ : agostic C-H: -2.5 (br,t)	Ru-CO: 192.4 (tm, 1C, ² J _{CP(Ru)}} = 12 Hz) Ir-CO: 175.0 (t, 1C, ² J _{CP(Ir)}} = 10 Hz) μ -CO: 208.9 (m, 1C) n/a
[IrRu(CO) ₃ (H)(μ - η^1 : η^2 -C(H)=C=CH ₂)(CO)-(dppm) ₂][OTf] (56) ^h	n/a	P _A : 48.4 (ddd, 1P, ² J _{PAPB} = 253 Hz, ³ J _{PAPC} = 33 Hz, ³ J _{PAPD} = 9.5 Hz), ^g P _B : 24.4 (ddd, 1P, ² J _{PAPB} = 253 Hz, ³ J _{PBPD} = 62 Hz, ³ J _{PBPC} = 20 Hz), ^g P _C : 5.3 (ddd, 1P, ² J _{PCPD} = 331 Hz, ³ J _{PAPC} = 33 Hz, ³ J _{PBPC} = 20 Hz), ^g P _D : -11.1 (ddd, 1P, ² J _{PCPD} = 331 Hz, ³ J _{PBPD} = 62 Hz, ³ J _{PAPD} = 9.5 Hz) ^g	H: -10.0 (ddm, 1H, ² J _{PH} = 17.0 Hz, ² J _{PH} = 5.1 Hz) ^g	

^a IR abbreviations: s = strong, m = medium, br = broad. Dichloromethane solution; in units of cm⁻¹. ^b IR obtained by IR microscope. ^c NMR abbreviations: s = singlet, d = doublet, t = triplet, m = multiplet, br = broad. NMR data at 27 °C in CD₂Cl₂ unless otherwise indicated. ^d ³¹P chemical shifts referenced to external 85% H₃PO₄. ^e ¹H and ¹³C chemical shifts referenced to TMS. ^f Chemical shifts for the phenyl carbons not given. ^g data acquired at -20 °C. ^h data acquired at -60 °C.

4.2.2 Preparation of Compounds

(a) [IrRu(CO)₄(μ-η¹-C=CH₂)(dppm)₂][OTf] (47). *Method (i):* In an NMR tube, fitted with a J. Young valve, a solution of compound **6** (45 mg, 0.034 mmol) in 0.7 mL of CD₂Cl₂ was cooled to -78 °C and the tube evacuated. Ethylene gas (2.5 mL, ca. 2 atm) was introduced to the evacuated NMR tube by gas-tight syringe and the sample was warmed to ambient temperature. After 16 h complete conversion to the product, compound **47**, was confirmed by ³¹P and ¹H NMR spectroscopy. *Method (ii):* Acetylene gas (5 mL) was passed through a solution of compound **6** (100 mg, 0.080 mmol) in 5 mL of CH₂Cl₂. After 4 h of stirring the bright yellow solution had turned deep orange and ³¹P{¹H} NMR spectroscopy revealed compound **47** as the only phosphorus-containing compound. An orange powder was obtained by the addition of 20 mL of Et₂O followed by 40 mL of pentane. After removal of the clear supernatant the product was rinsed with three portions of 10 mL of Et₂O and the residual solvent was removed under an Ar stream before being placed under vacuum for 16 h. (Yield: 90%) Anal. Calcd for C_{57.5}H₅₁ClF₃IrO₇P₄RuS: C 49.48; H 3.68. Found: C 49.55; H 3.43 (incorporation of 0.5 equiv of CH₂Cl₂ was confirmed by the X-ray crystal structure analysis)

(b) [IrRu(CO)₄(μ-η¹-C=C(H)CH₃)(dppm)₂][OTf] (48). *Method (i):* In an NMR tube fitted with a J. Young valve, compound **6** (45 mg, 0.034 mmol) was dissolved in 0.7 mL of CD₂Cl₂. The solution was cooled to -78 °C and the tube evacuated. The evacuated tube was charged with propene gas (2.5 mL, ca. 2 atm) and warmed to ambient temperature. After 16 h ³¹P{¹H} NMR spectroscopy revealed complete conversion to the product, compound **48**. *Method (ii):* A solution of compound **6** (125 mg, 0.1 mmol) in 5 mL of CH₂Cl₂ was saturated with propyne gas. The mixture was left to stir for 16 h at which time ³¹P{¹H} NMR spectroscopy revealed compound **48** as the sole phosphorus-containing product. Addition of 20 mL of Et₂O followed by 50 mL of pentane afforded a yellow powder. After removal of the clear supernatant the crude yellow product was rinsed 2 times with 10 mL portions of Et₂O before complete solvent removal

under vacuum. *Method (iii)*: A solution of compound **6** (100 mg, 0.07 mmol) in 5 mL of CH₂Cl₂ was saturated with allene gas. No colour change was noted, but after 16 h ³¹P NMR spectroscopy revealed compound **48** as the sole phosphorus-containing product. After reduction of the solvent volume by 50% addition of 20 mL of Et₂O followed by 20 mL of pentane afforded a crude yellow product. The crude product was rinsed 3 times with 10 mL portions of Et₂O before complete solvent removal *in vacuo*. (Yield: 85%) Anal Calcd for C_{62.5}H₅₉F₃P₄O₈ClIrRu: C, 50.73; H, 4.02. Found C, 50.31; H, 3.73 (the inclusion of one equiv of Et₂O and 0.5 equiv of CH₂Cl₂ was confirmed by X-ray crystal structure analysis (see part (n) for details). HRMS *m/z* Calcd for C₅₇H₄₈ P₄O₃IrRu (M⁺ – CF₃SO₃, CO) 1186.16056. Found: 1186.122689.

(c) [IrRu(CO)₄(μ-η¹-C=C(H)CH₂CH₃)(dppm)₂][OTf] (49). 1,2-butadiene (methylallene) was passed through a stirring yellow solution of **6** (92 mg, 0.069 mmol) in CH₂Cl₂ (8 mL) for 1 min at a rate of 0.1 mL/s. After 4 h the solution had turned light orange and after 24 h the solution was deep orange in colour at which time complete conversion to the product, compound **49**, was confirmed by ³¹P NMR spectroscopy. Slow addition of 80 mL of pentane afforded a crude orange product, which, after removal of the clear supernatant, was rinsed 3 times with 10 mL portions of Et₂O. After removal of the clear supernatant the product was dried under an Ar stream before being placed under vacuum for 16 h. (Yield 80 %) Anal. Calcd for C₅₉H₅₀F₃O₇PSIrRu: C, 51.38; H, 3.63. Found: C, 51.03; H, 3.98. HRMS *m/z* Calcd for C₅₈H₅₀O₄P₄RuIr (M⁺ – CF₃SO₃): 1229.13271. Found: 1229.13306 (M⁺ – CF₃SO₃).

(d) [IrRu(CO)₄(μ-η¹-C=C(H)C(CH₃)=CH₂)(dppm)₂][OTf] (50). All glassware was dried at 120 °C for 16 h and assembled while hot. Compound **6** (73 mg 0.055 mmol) was dissolved in 4 mL of a 1:1 CH₂Cl₂/THF mixture to give a yellow solution. To this yellow solution 100 μL of methylallene (0.1 mmol) was added. The solution was left to stir under a slight pressure of Ar for 48 h at which time complete conversion to the product, compound **50**, was confirmed by ³¹P NMR spectroscopy. Addition of 20 mL of Et₂O followed by 40 mL of pentane yielded

a yellow powder. The crude yellow powder was rinsed with three 10 mL portions of Et₂O. The clear supernatant was decanted and the remaining solvent was removed by placing the product under vacuum for 16 h. HRMS Calcd for C₅₉H₅₀O₄P₄RuIr (M⁺ – CF₃O₃): 1241.13271. Found: 1241.13270 (M⁺ – CF₃SO₃). The instability of compound **50** has prevented us from obtaining suitable elemental analysis data as well as growing crystals for X-ray structural determination. Structural characterization for compound **50** is based on multinuclear NMR spectroscopy.

(e) [IrRu(CO)₃(H)(C(H)=CH₂)(dppm)₂][OTf] (51**).** A yellow solution of compound **6** in 0.7 mL of CD₂Cl₂ in an NMR tube fitted with a J. Young valve was cooled to –78 °C before being evacuated. The NMR tube was filled with ethylene gas (7 mL, ca. 7 atm), and inserted into an NMR probe which had been precooled to –80 °C. The sample was warmed in 10 °C intervals indicating that no new species was observed below 0 °C. At 0 °C compound **51** formed in a 1:2 ratio with compound **6** (based on integration of the ³¹P{¹H} NMR spectrum) and over time at this temperature compound **47** begins to form at the expense of compound **6** and **51**. The conversion of **51** to **47** occurs at temperatures above –20 °C and so **51** could not be isolated and purified; its characterization is based on multinuclear NMR spectroscopy at –20 °C.

(f) [IrRu(CO)₃(μ-η¹-C=CH₂)(dppm)₂][OTf] (52**).** *Method (i):* In an NMR tube, a solution of compound **6** (15 mg, 0.01 mmol) in 0.7 mL of CD₂Cl₂ was cooled to –78 °C. Acetylene gas was passed through the solution for 2 min at a rate of 0.05 mL/sec. The sample was inserted into an NMR probe that had been precooled to –80 °C and warming to –40 °C resulted in the formation of compound **52** in a 1:1 ratio with **47** (no other species was observed in the temperature range of –80 °C to –40 °C). Over the course of several minutes all of **52** converted to **47** even at temperatures as low as –80 °C. Compound **53** proved to be unstable, even in the solid state, rapidly decomposing into numerous unidentified decomposition products. *Method (ii):* Trimethylamine-*N*-oxide (TMNO) (0.83 mL of a 10 mg/mL CH₂Cl₂ solution) was slowly added to a stirring orange solution of compound **47** (150 mg, 0.1 mmol) in CH₂Cl₂ (5 mL). The solution turned light

brown and $^{31}\text{P}\{^1\text{H}\}$ NMR spectroscopy showed compound **52** as the major phosphorus-containing product, accompanied by numerous unknown decomposition products (ca. 20% by integration of the $^{31}\text{P}\{^1\text{H}\}$ NMR spectrum) that could not be separated from **52**. Addition of 20 mL of Et₂O followed by 50 mL of pentane afforded a rust-coloured product, which was rinsed 5 times with 20 mL portions of Et₂O before complete solvent removal under vacuum. Compound **52** decomposed over the course of 30 min in solution and 24 h in the solid state, as a result its characterization is based on multinuclear NMR spectroscopy.

(g) [IrRu(H)(CO)₃(C(H)=C(H)CH₃)(dppm)₂][OTf] (53). A solution of compound **6** (15 mg, 0.01 mmol; 0.7 mL CD₂Cl₂) in an NMR tube fitted with a J. Young valve was cooled to -78 °C and evacuated. The NMR tube was then charged with 7 mL of propylene gas (ca. 7 atm). The mixture was placed in an NMR probe that had been precooled to -80 °C. Warming in 10 °C increments yielded no new species until 0 °C at which temperature compound **53** formed in a 1:5 ratio with compound **6**. Compound **53** reacted further to form **48** at temperatures above -20 °C so its characterization is based on NMR spectroscopy at -20 °C.

(h) [IrRu(CO)₃(μ-η¹:η¹-C(H)C(CH₃))(dppm)₂][OTf] (54). A solution of compound **6** (15 mg, 0.01 mmol) in 0.7 mL of CD₂Cl₂ was cooled to 0 °C and saturated with propyne gas. The mixture was allowed to sit at 0 °C for 16 h before being placed in an NMR probe that had been precooled to 0 °C and $^{31}\text{P}\{^1\text{H}\}$ NMR spectroscopy revealed the formation of both compounds **54** and **48** in a 1:1 ratio. At temperatures above -20 °C, compound **54** continued to convert to compound **48** and, over the course of several hours **48** was the only species observed. As a result, compound **52** has been characterized by multinuclear NMR spectroscopy at -20 °C.

(i) [IrRu(CO)₃(μ-η¹:η¹-H₂C=C=CH₂)(dppm)₂][OTf] (55). A yellow solution of compound **6** (20 mg, 0.015 mmol) dissolved in 0.7 mL of CD₂Cl₂ in an NMR tube was cooled to -78 °C. Allene gas (5 mL) was passed through the sample *via* a gas-tight syringe. The mixture was placed in an NMR probe which had been precooled to -80 °C. The sample was warmed in 10 °C increments and held at

each temperature for 1 h while being monitored by $^{31}\text{P}\{^1\text{H}\}$ NMR spectroscopy. No new species was observed until warming to $-10\text{ }^\circ\text{C}$, at which temperature compound **55** formed. After 40 min at $-10\text{ }^\circ\text{C}$, **55** was present in a 1:2:1 ratio with compounds **6** and **56**, respectively. Beyond 40 min the concentration of **55** began to diminish as **49** formed in conjunction with other unidentified decomposition products (ca. 20% of all phosphorus-containing products).

(j) $[\text{IrRu}(\text{CO})_3(\text{H})(\mu\text{-}\eta^1\text{:}\eta^2\text{-C}(\text{H})=\text{C}=\text{CH}_2)(\text{dppm})_2][\text{OTf}]$ (56**).** In an NMR tube, allene gas (5 mL) was passed through a solution of **6** (20 mg, 0.015 mmol) in 0.7 mL of CD_2Cl_2 at $-78\text{ }^\circ\text{C}$. The sample was inserted into an NMR probe which had been pre-cooled to $-80\text{ }^\circ\text{C}$. The sample was warmed to $-10\text{ }^\circ\text{C}$ (see part (h) for details) and after 40 min $^{31}\text{P}\{^1\text{H}\}$ NMR spectroscopy revealed compound **56** in a 1:2:1 ratio with compounds **6** and **54**. Beyond 40 min the relative concentration of both compounds **54** and **55** diminished as compound **49** and other unknown products begin to form at their expense.

(k) Attempted reactions of compound 47 with diazoalkanes. In an NMR tube, 15 mg of compound **47** (0.01 mmol) was dissolved in 0.7 mL of CD_2Cl_2 . A 10-fold excess of diazoalkane was added either as a gas in the case of N_2CH_2 (generated from Diazald) or neat in the case of diethyldiazomalonate (DEDM). In all cases no new products were observed in the $^{31}\text{P}\{^1\text{H}\}$ NMR over the period of 5 days.

(l) Reaction of compound 52 with diazomethane. Compound **52** was prepared *in situ* in an NMR tube by the slow addition of a TMNO solution (164 μL , 5 mg/mL) to a solution of **47** in 0.7 mL of CD_2Cl_2 . The formation of **52** was confirmed by $^{31}\text{P}\{^1\text{H}\}$ NMR spectroscopy. The solution was then transferred to an NMR tube fitted with a J. Young valve and the tube evacuated. The tube was filled with diazomethane gas (ca. 1 atm, prepared from 200 mg of Diazald[®]). The $^{31}\text{P}\{^1\text{H}\}$ NMR spectrum of the mixture revealed numerous uncharacterized decomposition products, whereas ^1H NMR spectroscopy showed the presence of allene (δ 4.21 (s)).

(m) Reaction of compound 52 with diethyl diazomalonate (DEDM).

Compound **52** was prepared *in situ* in an NMR tube by the slow addition of a TMNO solution (164 μL , 5 mg/mL) to a solution of **47** (15 mg, 0.011 mmol) in 0.7 mL of CD_2Cl_2 . ^{31}P NMR spectroscopy revealed complete conversion to compound **52**. To the solution of compound **52** was added an excess of DEDM (ca. 5 eq). The $^{31}\text{P}\{^1\text{H}\}$ NMR spectrum of the mixture revealed numerous uncharacterized decomposition products, whereas ^1H NMR spectroscopy showed the presence of diethyl 2-vinylidene malonate (δ 5.12 (s, 2H); 4.23 (q, 4H); 1.62 (t, 6H)).

(n) X-ray Data Collection.

All X-ray crystallographic data were collected and analyzed by Dr. R. McDonald and Dr. M. J. Ferguson of the Departmental X-ray Services laboratory. Weighted R -factors wR_2 and all goodnesses of fit S ($S = [\sum w(F_o^2 - F_c^2)^2 / (n - p)]^{1/2}$ (n = number of data; p = number of parameters varied; $w = [\sigma^2(F_o^2) + (0.0645P)^2]^{-1}$ where $P = [\text{Max}(F_o^2, 0) + 2F_c^2] / 3$) are based on F_o^2 ; conventional R -factors R_1 are based on F_o , with F_o set to zero for negative F_o^2 . The observed criterion of $F_o^2 > 2\sigma(F_o^2)$ is used only for calculating R_1 ($R_1 = \sum ||F_o| - |F_c|| / \sum |F_o|$; $wR_2 = [\sum w(F_o^2 - F_c^2)^2 / \sum w(F_o^4)]^{1/2}$), and is not relevant to the choice of reflections for refinement. R -factors based on F_o^2 are statistically about twice as large as those based on F_o , and R -factors based on ALL data will be even larger.

(a) Bright orange crystals of compound **47** were grown by slow diffusion of Et_2O into a saturated solution of compound **47** in CH_2Cl_2 . Data were collected on a Bruker P4/RA/SMART 1000 CCD diffractometer using Mo $K\alpha$ radiation at -80°C and corrected for absorption through use of the *SADABS* procedure within the software provided by Bruker (programs for diffractometer operation, data collection, data reduction and absorption correction were those supplied by Bruker).³² See Table 4.2 for a summary of crystal data and X-ray data collection information. Unit cell parameters were obtained from a least-squares refinement of the setting angles of 7473 reflections, with $4.36^\circ < 2\theta < 54.86^\circ$ and the space

group was determined to be $I2/a$ (an alternate setting of $C2/c$ [No. 15]).

The structure of **47** was solved using the Patterson search and structure expansion routines as implemented in the *DIRDIF-99* program system. Refinement was completed using the program *SHELXL-93*. Hydrogen atoms were assigned positions based on the geometries of their attached carbon atoms, and were given thermal parameters 20% greater than those of the attached carbons. The triflate ion was determined to be disordered over two different sites. At one of these (at approximate crystal coordinates [0.38, 0.46, 0.52]) the triflate ion occupied two sets of equally-abundant (25% occupancy) positions ($\{S(2A), F(94A), F(95A), F(96A), O(94A), O(95A), O(96A),$

Table 4.2. Crystallographic Experimental Details for Compound **47**

A. Crystal Data	
formula	C _{57.5} H ₄₇ ClF ₃ IrO ₇ P ₄ RuS
formula weight	1391.61
crystal dimensions (mm)	0.38 × 0.38 × 0.11
crystal system	monoclinic
space group	<i>I</i> 2/ <i>a</i> (an alternate setting of <i>C</i> 2/ <i>c</i> [No. 15])
unit cell parameters	
<i>a</i> (Å)	17.5797 (11)
<i>b</i> (Å)	23.6325 (15)
<i>c</i> (Å)	26.4280 (17)
β (deg)	95.2753 (9)
<i>V</i> (Å ³)	10933.1 (12)
<i>Z</i>	8
ρ _{calcd} (g cm ⁻³)	1.691
μ (mm ⁻¹)	2.975
B. Data Collection and Refinement Conditions	
diffractometer	Bruker PLATFORM/SMART 1000 CCD
radiation (λ [Å])	graphite-monochromated Mo Kα (0.71073)
temperature (°C)	-80
scan type	ω scans (0.3°) (20 s exposures)
data collection 2θ limit (deg)	54.90
total data collected	45746 (-22 ≤ <i>h</i> ≤ 22, -30 ≤ <i>k</i> ≤ 30, -34 ≤ <i>l</i> ≤ 34)
independent reflections	12470 (<i>R</i> _{int} = 0.0308)
number of observed reflections (<i>NO</i>)	10108 [<i>F</i> _o ² ≥ 2σ(<i>F</i> _o ²)]
structure solution method	direct methods (<i>SHELXS-97</i> ³¹)
refinement method	full-matrix least-squares on <i>F</i> ² (<i>SHELXL-97</i> ³¹)
absorption correction method	multi-scan (<i>SADABS</i>)
range of transmission factors	0.7355–0.3977
data/restraints/parameters	12470 [<i>F</i> _o ² ≥ -3σ(<i>F</i> _o ²)] / 29 / 737
goodness-of-fit (<i>S</i>)	1.122 [<i>F</i> _o ² ≥ -3σ(<i>F</i> _o ²)]
final <i>R</i> indices	
<i>R</i> ₁ [<i>F</i> _o ² ≥ 2σ(<i>F</i> _o ²)]	0.0303
<i>wR</i> ₂ [<i>F</i> _o ² ≥ -3σ(<i>F</i> _o ²)]	0.0911
largest difference peak and hole	1.478 and -0.864 e Å ⁻³

C(92A)} and {S(2B), F(94B), F(95B), F(96B), O(94B), O(95B), O(96B), C(92B)}). Distances within these sets of atoms were restrained during refinement: $d(\text{S-O}) = 1.45(1) \text{ \AA}$; $d(\text{S-C}) = 1.80(1) \text{ \AA}$; $d(\text{F-C}) = 1.35(1) \text{ \AA}$; $d(\text{F}\cdots\text{F}) = 2.20(1) \text{ \AA}$; $d(\text{O}\cdots\text{O}) = 2.37(1) \text{ \AA}$. Also located at this site is a solvent dichloromethane molecule, refined with an occupancy factor of 50% and the following restraints: $d(\text{Cl-C}) = 1.80(1) \text{ \AA}$; $d(\text{Cl}\cdots\text{Cl}) = 2.95(1) \text{ \AA}$. The atoms at the other triflate ion site [0.76, 0.42, 0.0], located near the crystallographic twofold rotational axis [$3/4, y, 0$], were refined with an occupancy factor of 50% and with no geometric restraints applied.

(b) Yellow crystals of compound **48** were obtained by slow diffusion of Et_2O into a dichloromethane solution. Data were collected and corrected for absorption as for **48** (see Table 4.3). Unit cell parameters were obtained from a least-squares refinement of the setting angles of 5502 reflections from the data collection, and the space group was determined to be $C2/c$ (No. 15).

The structure of **48** was solved and refined using the same procedure as for **47**. Hydrogen atoms were assigned positions based on the geometries of their attached carbon atoms, and were given thermal parameters 20% greater than those of the attached carbons. Attempts to refine peaks of residual electron density as partially occupied/disordered solvent dichloromethane and diethylether molecules were unsuccessful. The data were corrected for disordered electron density through use of the SQUEEZE procedure as implemented in PLATON.³² A total solvent accessible void volume of 1885.2 \AA^3 and electron count of 685.4 electrons were found, consistent with an additional 1 equivalent of diethylether and 0.5 equivalents of dichloromethane molecules per asymmetric unit. The minor orientation of the disordered triflate was restrained to have the same geometry as that of the major orientation during refinement by use of the SHELXL SAME instruction.³²

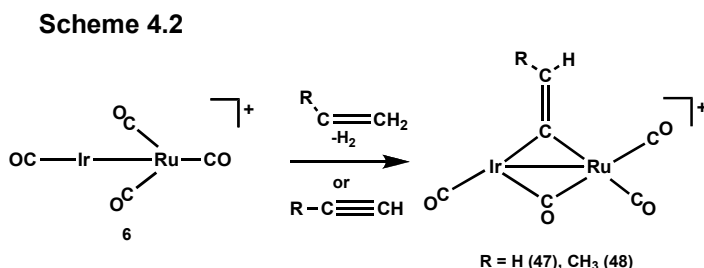
Table 4.3. Crystallographic Experimental Details for Compound **48**

A. Crystal Data	
formula	C ₆₂ H ₅₉ ClF ₃ IrO ₈ P ₄ RuS
formula weight	1461.23
crystal dimensions (mm)	0.32 × 0.24 × 0.15
crystal system	monoclinic
space group	C2/c (No. 15)
unit cell parameters	
<i>a</i> (Å)	34.714 (3)
<i>b</i> (Å)	17.3092 (14)
<i>c</i> (Å)	20.5712 (17)
β (deg)	96.598 (2)
<i>V</i> (Å ³)	12278.8 (18)
<i>Z</i>	8
ρ _{calcd} (g cm ⁻³)	1.601
μ (mm ⁻¹)	2.656
B. Data Collection and Refinement Conditions	
diffractometer	Bruker PLATFORM/SMART 1000 CCD
radiation (λ [Å])	graphite-monochromated Mo Kα (0.71073)
temperature (°C)	-80
scan type	ω scans (0.3°) (20 s exposures)
data collection 2θ limit (deg)	52.78
total data collected	46539 (-43 ≤ <i>h</i> ≤ 43, -21 ≤ <i>k</i> ≤ 21, -25 ≤ <i>l</i> ≤ 25)
independent reflections	12566 (<i>R</i> _{int} = 0.0531)
number of observed reflections (<i>NO</i>)	8816 [<i>F</i> _o ² ≥ 2σ(<i>F</i> _o ²)]
structure solution method	direct methods (<i>SHELXS-86</i> ^{32a})
refinement method	full-matrix least-squares on <i>F</i> ² (<i>SHELXL-93</i> ³²)
absorption correction method	multi-scan (<i>SADABS</i>)
range of transmission factors	0.6915–0.4837
data/restraints/parameters	12566 [<i>F</i> _o ² ≥ -3σ(<i>F</i> _o ²)] / 19 / 704
goodness-of-fit (<i>S</i>)	1.003 [<i>F</i> _o ² ≥ -3σ(<i>F</i> _o ²)]
final <i>R</i> indices	
<i>R</i> ₁ [<i>F</i> _o ² ≥ 2σ(<i>F</i> _o ²)]	0.0416
<i>wR</i> ₂ [<i>F</i> _o ² ≥ -3σ(<i>F</i> _o ²)]	0.1103
largest difference peak and hole	1.849 and -1.137 e Å ⁻³

4.3 Results and Discussion

4.3.1 Olefin Activation

Treatment of compound **6** with ethylene results in the unusual activation of two geminal C-H bonds to give H₂ and the vinylidene-bridged product, [IrRu(CO)₄(μ-C=CH₂)(dppm)₂][OTf] (**2**), over the course of 16 h (see Scheme 4.2). A more conventional route, reaction of **6** with acetylene, also gives the



* dppm ligands have been omitted for clarity

vinylidene-bridged compound **47** via a 1,2-hydride shift over the course of 4 h. Although not previously observed for the IrRu systems reported in this study, the metal-promoted transformation of a terminal alkyne to a vinylidene ligand is well precedented.³⁴⁻³⁸ The ³¹P{¹H} NMR spectrum of compound **47** shows two multiplets at δ 31.3 and 4.3. As noted in Chapter 3, it is generally observed for dppm-bridged IrRu complexes that the upfield ³¹P signal arises from the phosphorus nuclei bound to Ir whereas the downfield signal is due to the Ru-bound phosphorus nuclei;³⁰ we have assigned the ³¹P shifts for compound **47** accordingly.

In the ¹H NMR spectrum of **47** the methylene protons of the new vinylidene ligand appear as two broad singlets at δ 6.69 and 5.03, while the methylene protons of the dppm bridge appear as two separate multiplets at δ 3.99 and 2.93; the inequivalence of the dppm methylene protons is diagnostic of different chemical environments on either side of the approximate IrRuP₄ plane, as might result if the vinylidene ligand were bridging. Finally, the ¹³C{¹H} NMR spectrum of the ¹³CO-labeled isotopomer of compound **47** shows four signals for

the carbonyl ligands at δ 179.3 (triplet), 193.2 (triplet), 196.1 (triplet) and 203.5 (multiplet). Based on $^{13}\text{C}\{^1\text{H}\}$ NMR spectroscopy with selective ^{31}P decoupling we have assigned the upfield resonance to an Ir-bound carbonyl, the downfield resonance to that of a bridging-carbonyl and the two remaining signals to two carbonyls bound terminally to Ru. This arrangement of carbonyls, three terminal and one bridging, is supported by the IR spectrum of compound **47** with three bands characteristic of terminal carbonyls (2048, 1999, 1947 cm^{-1}) and one in the bridging carbonyl region (1805 cm^{-1}).

An X-ray crystal structure determination of compound **47** confirms the structure proposed above (see Figure 4.1 for the atom labeling scheme and Table 4.4 for selected bond distances and angles). The new vinylidene ligand bridges

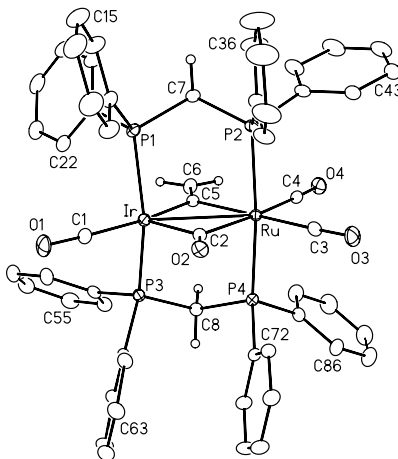


Figure 4.1. Perspective view of the $[\text{IrRu}(\text{CO})_3(\mu\text{-CO})(\mu\text{-C}=\text{CH}_2)(\text{dppm})_2]^+$ complex cation of compound **47**, showing the atom labeling scheme. Non-hydrogen atoms are represented by Gaussian ellipsoids at the 20% probability level. Hydrogen atoms attached to C(6), C(7), and C(8) are shown with arbitrarily small thermal parameters; dppm phenyl hydrogens are not shown.

the two metal centres unsymmetrically (Ir-C(5) = 2.050(3) Å, Ru-C(5) = 2.151(3) Å). The longer Ru-C(5) distance is most likely a result of the increased steric crowding about the Ru centre due to its greater coordination number. In accordance with the $^{13}\text{C}\{^1\text{H}\}$ NMR spectrum one carbonyl is terminally bound to Ir (Ir-C(1) = 1.881(4) Å), two are terminally bound to Ru (Ru-C(3) = 1.939(4) Å, Ru-C(4) = 1.913(4) Å) and one is bridging both metals (Ir-C(2) = 2.001(3) Å, Ru-

Table 4.4. Selected Distances and Angles for Compound **47**

Distances (Å)							
Atom1	Atom2	Distance	Atom1	Atom2	Distance		
Ir	Ru	2.9278(3)	Ru	P(4)	2.3906(9)		
Ir	P1	2.3372(10)	Ru	C(2)	2.194(3)		
Ir	P3	2.3314(10)	Ru	C(3)	1.939(4)		
Ir	C(1)	1.881(4)	Ru	C(4)	1.913(4)		
Ir	C(2)	2.001(3)	Ru	C(5)	2.151(3)		
Ir	C(5)	2.050(3)	C5	C(6)	1.309(5)		
Ru	P(2)	2.3815(10)	P(1)	P(2)	3.0664(13) [†]		
			P(3)	P(4)	3.0445(12) [†]		

Angles (deg)							
Atom1	Atom2	Atom3	Angle	Atom1	Atom2	Atom3	Angle
P(1)	Ir	P(3)	152.65(3)	P(2)	Ru	C(4)	88.94(11)
P(1)	Ir	C(1)	94.52(12)	P(2)	Ru	C(5)	86.63(10)
P(1)	Ir	C(2)	102.54(10)	C(2)	Ru	C(3)	90.25(14)
P(1)	Ir	C(5)	83.11(10)	C(2)	Ru	C(4)	175.18(14)
P(3)	Ir	C(1)	92.35(12)	C(2)	Ru	C(5)	87.52(13)
P(3)	Ir	C(2)	102.79(10)	C(3)	Ru	C(4)	94.48(15)
P(3)	Ir	C(5)	84.25(10)	C(3)	Ru	C(5)	177.66(14)
C(1)	Ir	C(2)	97.31(15)	C(4)	Ru	C(5)	87.75(14)
C(1)	Ir	C(5)	166.92(15)	Ir	C(2)	O(2)	134.1(3)
C(2)	Ir	C(5)	95.75(13)	Ru	C(2)	O(2)	137.5(3)
P(2)	Ru	P(4)	173.78(3)	Ir	C(5)	Ru	88.32(13)
P(2)	Ru	C(2)	89.89(9)	Ir	C(5)	C(6)	138.6(3)
P(2)	Ru	C(3)	92.69(12)	Ru	C(5)	C(6)	133.1(3)

[†]Nonbonded distances

C(2) = 2.194(3) Å). The unsymmetrical binding of this bridging carbonyl is presumably a result of the same steric considerations noted above for the vinylidene bridge. Interestingly, despite the asymmetry in metal-C bond lengths involving both the bridging vinylidene and carbonyl groups, the angles at both α -carbons are reasonably symmetric (Ir-C(2)-O(2) = 134.1°; Ru-C(2)-O(2) = 137.5(3)°; Ir-C(5)-C(6) = 138.6(3)°; Ru-C(5)-C(6) = 133.1(3)°).

The intermetallic distance of 2.9278(3) Å is long for an Ir-Ru single bond, generally observed to be \leq ca. 2.8 Å (for example, compounds **39**, **40**, and **42** of Chapter 3). However, the strained Ir-C(5)-Ru bond angle of 88.32(13)° is much smaller than the ideal 120° angle for sp^2 hybridized carbon, suggesting a mutual attraction between the two metals. Moreover, the intraligand P \cdots P separations within the dpmm ligands (3.0445(12) Å and 3.0664(13) Å) are greater than the Ir-Ru separation suggesting an attractive interaction between the two metals. The inclusion of a metal-metal bond gives both the Ir and Ru centres 18-electron

configurations. If the Ir-Ru bond is omitted in describing the geometries at each metal the Ir geometry can be described as a distorted square-based pyramid – with a bridging CO at the apical site – while that of Ru appears as a pseudo-octahedral.

In a similar way, propylene and propyne also react with compound **6** to give the methylvinylidene-bridged product, $[\text{IrRu}(\text{CO})_4(\mu\text{-C}=\text{C}(\text{H})\text{CH}_3)\text{-}(\text{dppm})_2][\text{OTf}]$ (**48**), through either geminal C-H activation and H_2 elimination, or a 1,2 hydride shift, respectively (see Scheme 4.2); both reactions exhibit similar reaction time-scales as observed for the formation of **47** by analogous routes (*vide supra*). By and large, the spectral characteristics of **48** are similar to those of **47** and can be found in Table 4.1.

The X-ray structure determination of **48** again confirms the structure proposed (see Figure 4.2 for the atom labeling scheme, and Table 4.5 for relevant

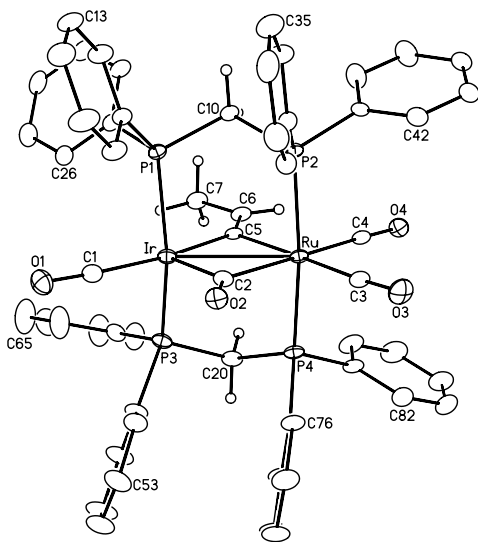


Figure 4.2 Perspective view of the $[\text{IrRu}(\text{CO})_3(\mu\text{-CO})(\mu\text{-C}=\text{CHCH}_3)(\text{dppm})_2]^+$ cation of compound **48**, showing the atom labeling scheme. Non-hydrogen atoms are represented by Gaussian ellipsoids at the 20% probability level. Hydrogen atoms attached to C(6), C(7), C(10) and C(20) are shown with arbitrarily small thermal parameters. Hydrogen atoms attached to the phenyl carbons of the dppm ligands are not shown.

bond distances and angles), showing that the propylene (or propyne) substrate has been transformed into a propenylidene fragment that bridges both metal centres.

Table 4.5. Selected Distances and Angles for Compound **48**

Distances (Å)							
Atom 1	Atom2	Distance	Atom1	Atom2	Distance		
Ir	Ru	2.9282(5)	Ru	P4	2.3973(13)		
Ir	P(1)	2.3259(12)	Ru	C(2)	2.178(5)		
Ir	P(3)	2.3237(13)	Ru	C(3)	1.947(5)		
Ir	C(1)	1.886(6)	Ru	C(4)	1.907(5)		
Ir	C(2)	1.998(5)	Ru	C(5)	2.141(5)		
Ir	C(5)	2.060(5)	C(5)	C(6)	1.337(6)		
Ru	P(2)	2.3943(12)	C(6)	C(7)	1.471(7)		
P(1)	P(2)	3.0437(19) [†]	P(3)	P(4)	3.050(2) [†]		
			C(6)	C(7)	1.471(7)		

Angles (deg)							
Atom1	Atom2	Atom3	Angle	Atom1	Atom2	Atom3	Angle
P(1)	Ir	P(3)	151.45(5)	P(2)	Ru	C(4)	89.53(14)
P(1)	Ir	C(1)	93.72(16)	P(2)	Ru	C(5)	85.26(12)
P(1)	Ir	C(2)	102.13(14)	C(2)	Ru	C(3)	89.5(2)
P(1)	Ir	C(5)	83.16(12)	C(2)	Ru	C(4)	179.7(2)
P(3)	Ir	C(1)	93.25(17)	C(2)	Ru	C(5)	87.70(19)
P(3)	Ir	C(2)	104.60(14)	C(3)	Ru	C(4)	90.8(2)
P(3)	Ir	C(5)	84.69(12)	C(3)	Ru	C(5)	177.2(2)
C(1)	Ir	C(2)	96.1(2)	C(4)	Ru	C(5)	92.07(19)
C(1)	Ir	C(5)	168.8(2)	Ir	C(2)	O(2)	134.4(4)
C(2)	Ir	C(5)	95.0(2)	Ru	C(2)	O(2)	136.6(4)
P(2)	Ru	P(4)	169.58(5)	Ir	C(5)	Ru	88.35(17)
P(2)	Ru	C(2)	90.26(13)	Ir	C(5)	C(6)	141.4(4)
P(2)	Ru	C(3)	94.63(15)	Ru	C(5)	C(6)	130.2(4)

[†]Nonbonded distances

Again, most structural parameters are in line with those of **47**. The C(5)-C(6) and C(6)-C(7) distances (1.309(5) Å and 1.471(7) Å, respectively) are typical of those observed for C-C double and single bonds, respectively,³⁸ the latter involving sp² and sp³ hybridized carbon. As observed for **47**, the new vinylidene ligand in **48** bridges the metal centres unsymmetrically, again having a shorter Ir-C(5) bond (2.060(5) Å) than Ru-C(5) bond (2.141(5) Å). In this case however, the Ir-C(5)-C(6) and Ru-C(5)-C(6) bond angles also differ significantly at 141.4(4)° and 130.2(4)° both slightly greater than the idealized value for an sp² carbon centre. This opening of the Ir-C(5)-C(6) and C(5)-C(6)-C(7) bond angles is most likely due to steric repulsions between the methyl substituent and the phenyl rings of the dppm ligands. Surprisingly, the two phosphorus atoms on Ir are bent *towards* the vinylidene group (P(1)-Ir-P(3) = 151.45(5)°). This distortion appears necessary in order to accommodate the phenyl groups on the side of the complex remote from

the vinylidene fragment, which are aimed into the void between the carbonyls C(1)O(1) and C(2)O(2).

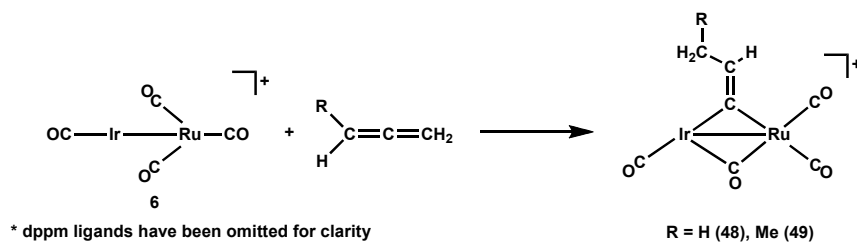
All carbonyls are normal, in which the metal-carbon distances involving the bridging group (C(2)O(2)) are longer than the terminally bound ones. The bonding arrangement of the bridging carbonyl is similar to what was observed for **47** in which Ir-C(2)-O(2) and Ru-C(2)-O(2) angles are comparable ($134.4(4)^\circ$ and $136.6(4)^\circ$, respectively) and this group is shifted significantly towards Ir (Ir-C(2) = $1.998(5)$ Å, Ru-C(2) = $2.178(5)$ Å). Finally, both the geometries about the two metal centres and the Ir-Ru distances for **48** ($2.9282(5)$ Å) are similar to those of **47**.

Attempts to generate a related vinylvinylidene-bridged species by reaction of compound **6** with 1,3-butadiene were unsuccessful; no reaction was detected after 24 h, and after several days only compound **6** and unidentified decomposition products were observed in a 5:1 ratio (**6**:unidentified decomposition products) as determined by integration of the resonances in the $^{31}\text{P}\{^1\text{H}\}$ NMR spectrum of the mixture. The lack of reactivity of **6** is in contrast to the geminal C-H activation of butadiene by the less crowded diiridium system, $[\text{Ir}_2(\text{CH}_3)(\text{CO})_2(\text{dppm})_2][\text{OTf}]$.¹⁹ In this latter system, precoordination of both π bonds of the butadiene substrate – one to each metal – was postulated. No such species is observed in the case of the IrRu system, even at temperatures as low as -80 °C. We speculate that the more crowded environment at Ru of compound **6** prevents a similar coordination of butadiene in this system.

4.3.2 Cumulene Activation

Compound **6** also facilitates geminal C-H activation of terminal cumulene substrates at ambient temperatures, giving vinylidene-bridged products like those observed in the activation of ethylene and propylene. For example, reaction of **6** with propadiene (allene) gives the methylvinylidene-bridged compound **48** over the course of 16 h, as illustrated in Scheme 4.3. As with propylene, the cleavage

Scheme 4.3

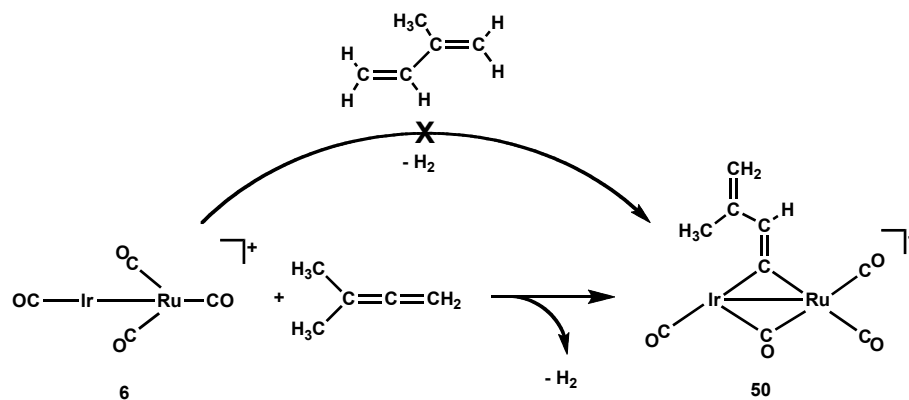


of two geminal C-H bonds has occurred. However, rather than H₂ elimination, as was observed with propylene, the hydrogen atoms generated in the double C-H activation steps in this case have been transferred to the central and terminal carbons of the former cumulene fragment, to give the propenylidene moiety.

Compound **6** also reacts with 1,2-butadiene (methylallene) to give the analogous butenylidene-bridged product, [IrRu(CO)₄(μ-C=C(H)CH₂CH₃)(dppm)₂][OTf] (**49**) as also shown in Scheme 4.3 above. Complete conversion to **49** occurs in ca. 24 h. The spectroscopic parameters for compound **49** are similar to those of compounds **47** and **48** and can be found in Table 4.1, so this product is assigned an analogous structure.

Reaction of **6** with the larger 3-methyl-1,2-butadiene (1,1-dimethylallene) again proceeds by apparent geminal C-H activation. However, in addition to both geminal C-H bonds being activated, a *third* C-H bond of a methyl group has also been cleaved to give the unexpected product [IrRu(CO)₄(μ-C=C(H)C(Me)=CH₂)(dppm)₂][OTf] (**50**), shown in Scheme 4.4. In the formation of compound **50** the cleavage of three C-H bonds is accompanied by the elimination of H₂ and the migration of one proton to the central carbon of the former cumulene fragment. This reaction involving 1,1-dimethylallene is slow compared to those of both allene and methylallene, taking several days for complete conversion. Furthermore, compound **50** decomposes readily in solution in the presence of air and moisture necessitating their rigorous exclusion.

Scheme 4.4



* dppm ligands have been omitted for clarity

³¹P{¹H} NMR spectroscopy of compound **50** reveals an AA'BB' splitting pattern similar to those of **47**, **48**, and **49** with the Ru-bound end of the diphosphines appearing as the downfield signal (δ 27.1) and the Ir-bound ones as the upfield signal (δ -4.1). In the ¹H NMR spectrum of **50** the dppm methylene protons appear as multiplets at δ 3.92 and δ 3.03 exhibiting coupling to both sets of phosphorus nuclei as well as each other. Four additional signals corresponding to the bridging vinylidene ligand, appear in the ¹H NMR spectrum (see Figure 4.3 for proton labeling scheme): two doublets of multiplets at δ 4.72 (H_a) and δ 4.41

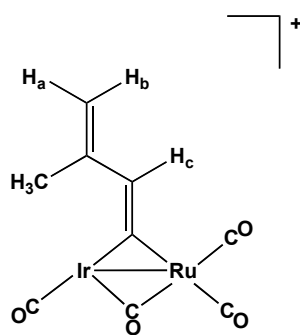


Figure 4.3. Proton labeling scheme for the 3-methyl-1,3-butadienylidene fragment of compound **50** (dppm ligands omitted).

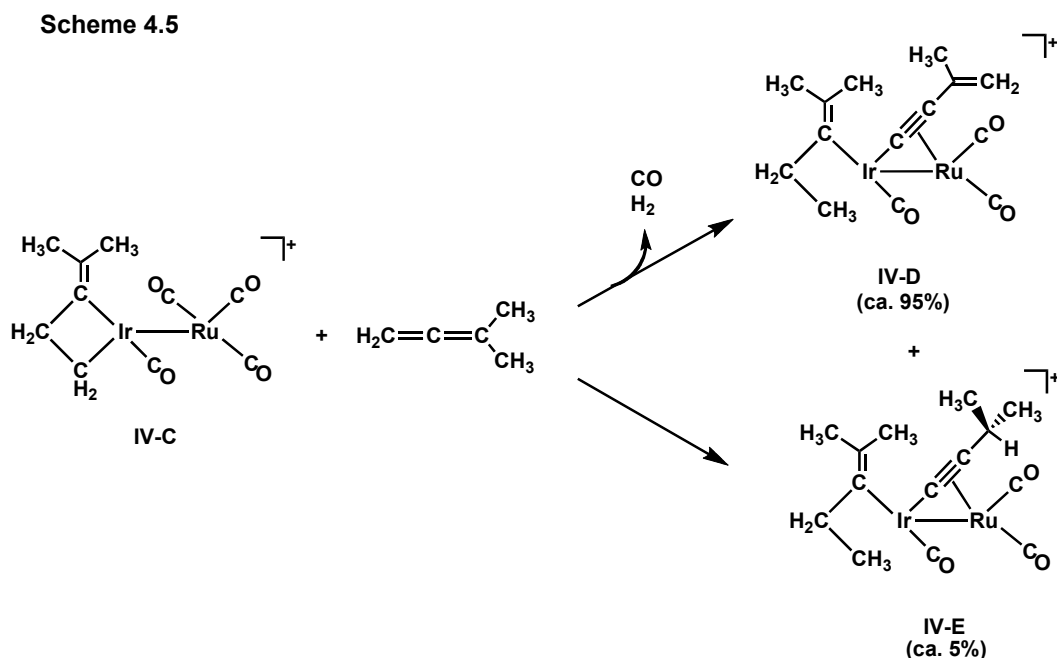
(H_b), a broad multiplet at δ 7.86 (H_c) and one multiplet at δ 0.41 (CH₃). A 2D ¹H correlation experiment clearly shows that H_c is spin-spin coupled to the methyl

group (unresolved), which in turn shows additional coupling to both H_a and H_b (unresolved). Protons H_a and H_b display a mutual coupling of 2.4 Hz. In addition, NOE experiments show strong NOEs between H_a and H_b, between H_a and the methyl protons and between H_b and H_c. Based on the chemical shifts, integration, spin-spin coupling and NOE experiments the signal at δ 0.41 has been assigned to the methyl group. The strong NOE and the weak 2.4 Hz coupling between H_a and H_b indicate that these two protons are geminal and have been assigned accordingly. Finally, on the basis of integration, NOE and spin-spin coupling to the methyl group the signal at δ 7.86 is assigned to H_c. These ¹H NMR data support the structure shown in Figure 4.3 for the 3-methyl-1,3-butadienyliidene fragment.

Four carbonyl resonances at δ 211.5, 193.5, 191.6 and 182.2 are evident in the ³¹C{¹H} NMR spectrum of compound **50**. The two at δ 193.5 and 191.6 have been assigned to the two carbonyls terminally bound to Ru, on the basis of their coupling to the Ru-bound phosphorus nuclei (10 Hz and 13 Hz, respectively) and mutual 3 Hz *cis* coupling. Moreover, the signal at δ 193.5 displays an additional 25 Hz *trans* coupling to the ¹³C nucleus resonating at δ 211.5 and 3 Hz *cis* coupling to the ¹³C nucleus that resonates at δ 191.6. This signal at δ 211.5 has been assigned to a bridging carbonyl on the basis of its coupling to both the Ru-bound phosphorus nuclei (13 Hz) and Ir-bound phosphorus nuclei (unresolved) as well as its additional spin-spin coupling to the two Ru-bound carbonyls at δ 191.6 and δ 193.5, as noted above. Finally, the upfield resonance at δ 182.2 is assigned to the carbonyl terminally bound to Ir with the appropriate 12 Hz coupling to the Ir-bound phosphorus nuclei; no coupling of this carbonyl is observed to the Ru-bound phosphorus nuclei or to the bridging carbonyl. In agreement with the ¹³C NMR data, the carbonyl region of the IR spectrum of compound **50** clearly shows three stretches for the terminally bound carbonyls (2051, 2000, 1978 cm⁻¹) and one for the bridging carbonyl (1792 cm⁻¹). Based on the spectroscopic evidence presented above, the structure shown in Scheme 4.3 is proposed for compound **50** in which the new vinylidene fragment bridges the two metal centres.

Clearly, activation of both geminal C-H bonds remote to the methyl substituent in 2-methyl-1,3-butadiene would also generate compound **50** (see Scheme 4.4). However, as was observed with butadiene, this methyl-substituted analogue also failed to react with compound **6**.

The instability of compound **50** in solution did not allow suitable crystals to be obtained, precluding an X-ray crystal structure determination. However, a very similar transformation has been observed in the reaction of 1,1-dimethylallene with $[\text{IrRu}(\text{CO})_4(\kappa^1:\kappa^1\text{-C}(\text{=C}(\text{CH}_3)_2)\text{CH}_2\text{CH}_2)(\text{dppm})_2][\text{OTf}]$ (**IV-C**), shown below in Scheme 4.5.³⁹ Treatment of compound **IV-C** with 1,1-dimethylallene



yields two species; the major species (95%) is the vinyl acetylide-bridged compound $[\text{IrRu}(\text{CO})_3(\text{C}(\text{=C}(\text{CH}_3)_2)\text{CH}_2\text{CH}_3)(\mu\text{-}\eta^1:\eta^2\text{-CCC}(\text{=CH}_2)\text{CH}_3)(\text{dppm})_2][\text{OTf}]$ (**IV-D**), and the minor species (5%) is the isopropyl acetylide-bridged species $[\text{IrRu}(\text{CO})_3(\text{C}(\text{=C}(\text{CH}_3)_2)\text{CH}_2\text{CH}_3)(\mu\text{-}\eta^1:\eta^2\text{-CCC}(\text{H})(\text{CH}_3)_2)(\text{dppm})_2][\text{OTf}]$ (**IV-E**). X-ray structural determination of **IV-D** confirms the structure of this product and suggests a process that involves the activation of the geminal C-H bonds of the 1,1-dimethylallene, additional activation of a methyl C-

H bond and the elimination of H₂.³⁹ It is particularly important to note that **IV-E** forms *without* either C-H activation of a methyl group or H₂ loss; both protons have been retained by the complex and transferred, one to each Ir-bound hydrocarbyl fragment. Moreover, **IV-E** does not transform into the major species **IV-D**.

4.3.3 Mechanistic Studies

In attempts to gain a more complete understanding of the roles of the adjacent metals in the above geminal C-H activation processes we initiated a number of low-temperature NMR studies. The goal of these studies was to observe key intermediates that might help determine how, and at what stage, the adjacent metals are involved during these transformations, and thus providing a better understanding of their synergy.

(a) Reactions of **6** with Ethylene and Acetylene

(i) Ethylene

Addition of ethylene (ca. 7 atm) to a solution of compound **6** at -78 °C and warming to 0 °C results in the formation of the tricarbonyl vinyl hydride complex, [IrRu(CO)₃(H)(C(H)=CH₂)(dppm)₂][OTf] (**51**), in a 1:2 ratio with **6** (Scheme 4.6;

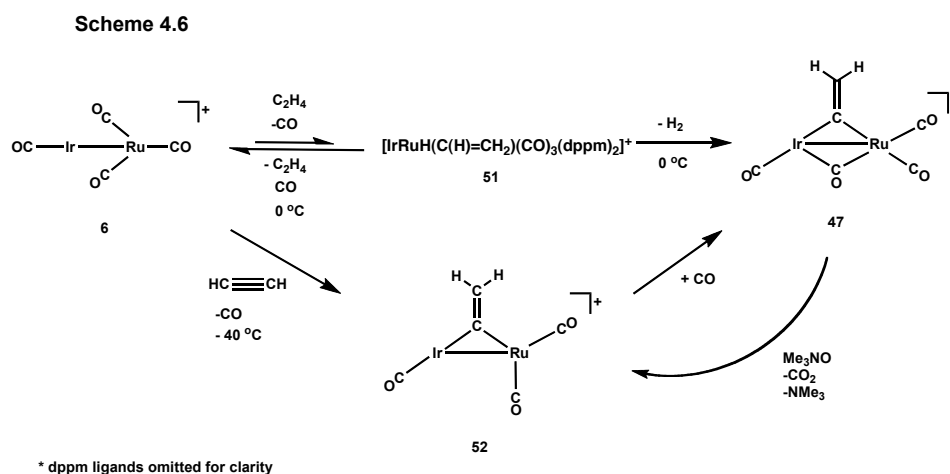


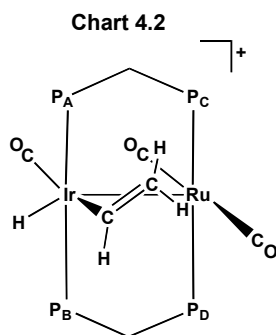
Figure AI.3 shows the ^{31}P NMR spectra). No reaction is observed at lower temperatures. Compound **51** has formed by the loss of one carbonyl ligand and oxidative addition of one ethylene molecule. Although the reaction of **6** with ethylene in a sealed tube to form **47** proceeds by overall retention of all carbonyls, it is apparent from this study that CO loss at an early stage is pivotal in the formation of the intermediate **51**. No other species was observed in this temperature range. The ratio of **6:51** is dependent on ethylene concentration; decreasing the ethylene pressure results in a decrease in the relative concentration of **51**. In addition, removal of both ethylene and carbon monoxide results in the decomposition of **51** over a 24 h period, leaving only unreacted compound **6** and decomposition products. Moreover, the presence of excess carbon monoxide inhibits the production of **51** and similarly if CO is added to a mixture of **51** and **6** compound **51** reverts back to **6**. The observations that the **51:6** ratio is dependent on the concentrations of both ethylene and CO suggest that compounds **51** and **6** are in equilibrium, as depicted above in Scheme 4.6, in which the formation of **6** requires the loss of one CO ligand and addition of one ethylene molecule; conversely, conversion of **51** to **6** requires the replacement of ethylene by CO. Unfortunately, spin-saturation transfer experiments were inconclusive in establishing exchange between the vinyl ligand and ethylene substrate; no exchange between free ethylene and the vinyl ligand was observed. At temperatures above $-20\text{ }^{\circ}\text{C}$ compound **51** slowly converts to compound **47** over a period of several hours (except in the absence of CO gas as noted above), so its characterization is based on NMR spectroscopy at this temperature.

Compound **51** gives rise to two signals in the $^{31}\text{P}\{^1\text{H}\}$ NMR spectrum at δ 23.6 for the Ru-bound end of the diphosphines and δ 6.1 for the Ir-bound ends. The methylene protons of the dpmm ligand appear as two multiplets at δ 4.18 and 5.08 in the ^1H NMR spectrum of **51**. Both of these resonances are spin-spin coupled to an upfield signal at δ -9.32 (3.5 Hz and 6.2 Hz, respectively) which in turn shows additional spin-spin coupling to the Ir-bound phosphorus nuclei (7.9

Hz), but not to those bound to Ru. This upfield signal has been assigned to a hydride that is terminally bound to Ir. Finally, three additional ^1H resonances are attributed to the vinyl ligand; the proton bound to C^α resonates at δ 6.87 and shows unresolved coupling to the phosphorus nuclei bound to Ir as well as *trans* and *cis* coupling ($^3J_{\text{HH}(\text{trans})} = 12.4$ Hz, $^3J_{\text{HH}(\text{cis})} = 4.0$ Hz) to the two protons bound to C^β , which are coincidentally overlapped at δ 4.74. The small $^3J_{\text{HH}(\text{trans})}$ noted above may be indicative of a vinyl ligand that is bridging two metal centres in a σ - π binding mode; it is generally observed that vinyl ligands coordinated in this binding mode exhibit $^3J_{\text{HH}(\text{trans})} \approx 9$ -12 Hz) whereas those bound terminally exhibit $^3J_{\text{HH}(\text{trans})} \approx 17$ Hz.⁴⁰⁻⁴³ Moreover, recently in our group a related IrOs σ - π vinyl species, $[\text{IrOs}(\text{CO})_4(\mu\text{-}\eta^1\text{:}\eta^2\text{-C(H)=CH}_2)(\text{dppm})_2][\text{OTf}]$, has been prepared, for which the σ - π vinyl binding mode has been established by an X-ray structure determination. This IrOs species exhibits a $^3J_{\text{HH}(\text{trans})}$ between the C^α - and C^β -bound protons of 11.8 Hz, comparable to what is observed for compound **51**.⁴⁴ However, some of the subsequent spectroscopy for **51** is inconsistent with a bridging vinyl structure.

The $^{13}\text{C}\{^1\text{H}\}$ NMR spectrum of **51**- ^{13}CO displays three signals of equal intensity; a triplet at δ 169.08, and two multiplets at δ 189.85 and 214.26. The presence of only three carbonyl ligands clearly shows that CO loss has occurred. Selective ^{31}P decoupling experiments clearly demonstrate that the signal at δ 189.85 is coupled to the Ru-bound phosphorus nuclei (11.8 Hz) but not the Ir-bound ones; an additional coupling (25 Hz) is also observed to the signal at δ 214.26. This large 25 Hz coupling suggests that these two carbonyls are mutually *trans*. The signal at δ 214.26 shows additional coupling to the Ru-bound ends of the diphosphines but not to the Ir-bound ends, suggesting that it is terminally bound to Ru. However, the relatively downfield chemical shift suggests that it may also be involved in a weak, possibly semi-bridging, interaction with Ir. This proposed interaction is sufficient to cause the downfield shift of its ^{13}C NMR resonance, but too weak to give rise to any observable coupling to the Ir-bound phosphines. Failure to observe ^{31}P - ^{13}C coupling in cases

such as this, where subtle interactions between the carbonyl and the adjacent metal exists has been previously observed in our group; see for example compound **36** (Chapter 3) for which an X-ray structure determination has led to an unambiguous structural assignment. Finally, the upfield resonance at δ 169.08 exhibits coupling to only the Ir-bound phosphorus nuclei (11.1 Hz), indicating it is terminally bound to this metal. Surprisingly, we have been unable to observe resonances for the vinyl ligand in the $^{13}\text{C}\{^1\text{H}\}$ spectrum of a $^{13}\text{C}_2\text{H}_3$ -enriched sample of **51**, even at temperatures as low as -20 °C. However, we have been able to locate these resonances by HSQC spectroscopy. The vinyl proton exhibits a correlation with a resonance at δ 130.6 (C^α), whereas the olefinic protons show a correlation to a resonance at δ 60.8 (C^β); these resonances are suggestive of a μ - σ - π bound vinyl group, in which the C^α and C^β resonances appear upfield and downfield of free ethylene, respectively,^{40c, 41, 43d} and, combined with the $^3J_{\text{HH}}$ coupling noted above, supports a μ - σ - π -binding mode. However, it should be noted that such an arrangement of the vinyl ligand would be expected to give rise to an ABCD spin system for the ^{31}P nuclei and therefore four resonances, one for each phosphorus nucleus, in the $^{31}\text{P}\{^1\text{H}\}$ NMR spectrum, yet only two resonances are observed for compound **51**. One possibility for the deceptively simple appearance of the $^{31}\text{P}\{^1\text{H}\}$ NMR spectrum of **51** is a fluxional process in which the vinyl ligand rotates about the Ir-C bond, rendering the two sets of phosphorus nuclei, $\text{P}_\text{A}/\text{P}_\text{B}$ and $\text{P}_\text{C}/\text{P}_\text{D}$ (see Chart 4.2 for the labeling of the inequivalent ^{31}P nuclei), chemically equivalent on the NMR timescale; similar fluxional processes



have been observed for μ - σ - π bound vinyl ligands.^{40c,43b,g} To our surprise, cooling **51** to -80 °C does not give rise to four separate resonances in the $^{31}\text{P}\{^1\text{H}\}$ NMR spectrum, suggesting that this proposed fluxionality is not occurring; it seems unlikely that such a fluxional process is occurring at this temperature. Chart 4.2 shows the proposed σ - π binding mode for the vinyl ligand. Although this arrangement results in top-bottom asymmetry, the ligand is only slightly biased toward one orientation and the differences between the two environments is small. It may be that this slight difference in chemical environments results in the AB and CD portions of the ABCD spin system, respectively, being coincidentally degenerate. As a result of the spectral inconsistencies the coordination mode for the vinyl ligand (terminal versus bridging) remains unclear. However, in more detailed discussion later it will be evident that the coordination mode of this vinyl group in intermediate **51** is irrelevant in subsequent steps.

(ii) *Acetylene*

Addition of acetylene to a solution of compound **6** at -78 °C and warming in 10 °C increments yields no new species until -40 °C at which temperature the tricarbonyl vinylidene-bridged complex, $[\text{IrRu}(\text{CO})_3(\mu\text{-}\eta^1\text{-C=CH}_2)(\text{dppm})_2][\text{OTf}]$ (**52**) (Scheme 4.6), is observed in a 1:1 ratio with compound **47**. In the presence of CO all of compound **52** transforms to **47** after several minutes, even at temperatures as low as -80 °C and conversely, compound **52** can be prepared from **47** by removal of one carbonyl ligand with TMNO (see Scheme 4.6). Unfortunately, compound **52** is unstable, even in the solid state, rapidly decomposing into unknown decomposition products within 30 min in solution and over the course of 24 h in the solid state; its characterization is based on NMR spectroscopy at -80 °C.

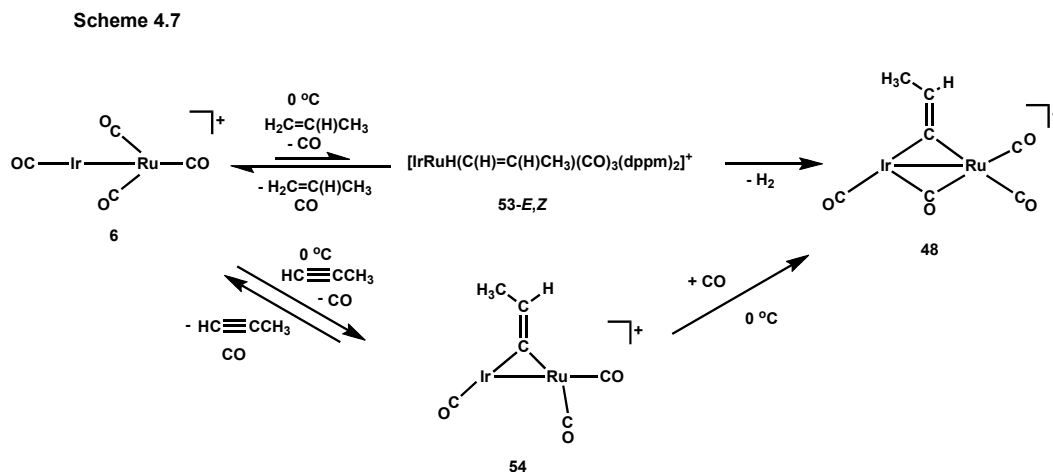
Compound **52** appears as two multiplets in the $^{31}\text{P}\{^1\text{H}\}$ NMR spectrum at δ 29.0 (Ru-*P*) and -10.8 (Ir-*P*). In the ^1H NMR spectrum, the methylene protons of the dppm ligands resonate at δ 4.94 and 4.31 while the vinylidene protons appear as a two broad singlets at δ 6.21 and 7.13 with unresolved coupling to both

sets of phosphorus nuclei. A sample of **52**- ^{13}C O gives rise to three carbonyl resonances of equal intensity in the $^{13}\text{C}\{^1\text{H}\}$ NMR spectrum (δ 176.7 (t), 197.8 (t) and 199.7(t)). On the basis of $^{13}\text{C}\{^1\text{H}, \text{selective } ^{31}\text{P}\}$ experiments the upfield resonance has been assigned to a terminal Ir-bound carbonyl, whereas the two downfield resonances have been assigned to two terminal Ru-bound carbonyls (see Table 4.1 for coupling constants). Based on these spectroscopic data we have proposed a structure for **52** (shown in Scheme 4.6) that is similar to **47**.

(b) *Reactions of 6 with Propylene and Propyne*

(i) *Propylene*

Initial reaction of compound **6** with propylene (7 atm and 0 °C) leads to the propenyl hydride complex $[\text{IrRu}(\text{H})(\text{CO})_3(\text{C}(\text{H})=\text{CHMe})(\text{dppm})_2][\text{OTf}]$ (**53**) shown in Scheme 4.7, in a 1:5 ratio with **6** over the course of several hours.



Compound **53** converts to **48** at temperatures above 0 °C, analogous to the conversion of **51** into **47**. The spectral parameters for **53** mirror those of **51** and are given in Table 4.1. Unfortunately, we have been unable to unambiguously assign ^1H resonances for the propenyl ligand; the low concentration of compound **53** combined with the presence of propylene gas, compound **6**, residual solvents and unknown decomposition products in the ^1H NMR spectrum do not allow the

resonances associated with the propenyl ligand to be identified. As a result we are unable to assign the stereochemistry of this ligand as either *E* or *Z*; most likely both are present. In a previous report of propylene activation at Ir, Carmona and associates noted that both isomers were present with the *E* isomer being the major species.⁴⁵ The presence of both isomers of **53** would serve to diminish the intensities of the peaks associated with this ligand, making meaningful assignments even more challenging. However, we believe that a multiplet in the ¹H NMR spectrum at δ 6.18 corresponds to the proton bound to C^β of the *E* isomer. A tentative match of this resonance to a simulated one is achieved if it is described as a doublet of quartets with 16.8 Hz coupling to the proton at C^α and 3.2 Hz coupling to the methyl group (see Figure 4.4 below). This resonance

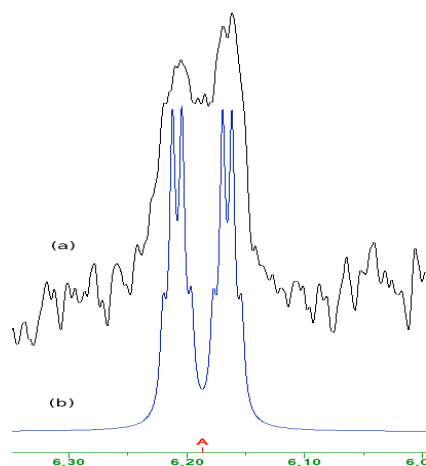


Figure 4.4 Selected region of the ¹H NMR spectrum showing (a) the experimental and (b) the simulated resonance for the olefinic proton of the propenyl ligand of compound **53**. The simulated spectrum was generated using $^3J_{HH(trans)} = 16.8$ Hz and $^3J_{HH} = 3.2$ Hz.

integrates to 0.75 H with respect to the methylene protons of the dppm ligand suggesting that the *E* isomer is in ca. 75 % abundance; the preference for the *E* isomer would be in agreement with Carmona's observations.

As with compound **51**, the coordination mode of the methyl vinyl ligand is ambiguous in the case of **53**; the large 16.8 Hz *trans* coupling between the vinylic and olefinic protons is too large for a bridging vinyl ligand and is more in line with a terminally bound vinyl group (*vide supra*). Unfortunately, we have been

unable to collect sufficient $^{13}\text{C}\{^1\text{H}\}$ NMR data to assign resonances for the carbonyls of **53**. However, based on the similar ^{13}P and ^1H NMR parameters for **51** and **53**, we assume that the two have related structures in which there are only three carbonyl ligands.

(ii) *Propyne*

If a solution of compound **6** at 0 °C is saturated with propyne the tricarbonyl methylvinylidene adduct, $[\text{IrRu}(\text{CO})_3(\text{CC}(\text{H})\text{Me})(\text{dppm})_2][\text{OTf}]$ (**54**), is observed in a 1:1 ratio with compound **48** (shown in Scheme 4.7) and, over the course of 24 h at this temperature, only compound **48** remains. Addition of CO to **54** regenerates both compounds **6** and **48**. Compound **54** gives rise to two resonances in the $^{31}\text{P}\{^1\text{H}\}$ NMR spectrum at δ 29.2 and -3.13 for the Ru- and Ir-bound ends of the diphosphines, respectively (see Figure AI.4). The methylene protons of the dppm ligands appear as two separate resonances in the ^1H NMR spectrum (δ 3.90, 3.00) reflecting the asymmetry about the $\text{MM}'\text{P}_4$ plane (*vide supra*), whereas the methylvinylidene bridge appears as two signals at δ 5.73 (*CH*) and 1.95 (*CH*₃) in a 1:3 intensity ratio. The signal of the *CH* proton at δ 5.73 exhibits coupling to the Ru-bound phosphorus nuclei ($^4J_{\text{P}(\text{Ru})\text{H}} = 1.6$ Hz) as well as the Ir-bound phosphines ($^4J_{\text{P}(\text{Ir})\text{H}} = 1.7$ Hz) in addition to 6.5 Hz coupling to the methyl protons at δ 1.95, which display 2.4 Hz coupling to the Ir-bound phosphines and unresolved coupling to the Ru-bound phosphines (see Figure AI.5 for the $^1\text{H}\{\text{selective } ^{31}\text{P}\}$ NMR spectra). Compound **54** gives rise to three carbonyl resonances at δ 176.4, 194.6 and 197.6, very similar to the analogous vinylidene-bridged compound **51**. The upfield signal is assigned to a terminally bound carbonyl on Ir while the two downfield signals are assigned to two terminally bound carbonyls on Ru, based on their respective $^2J_{\text{CP}}$ couplings and chemical shifts. The structure in Scheme 4.7 has been proposed on the basis of the above data in which the methylvinylidene ligand bridges the two metals in an arrangement that places the methyl group adjacent to the Ir centre. The formation

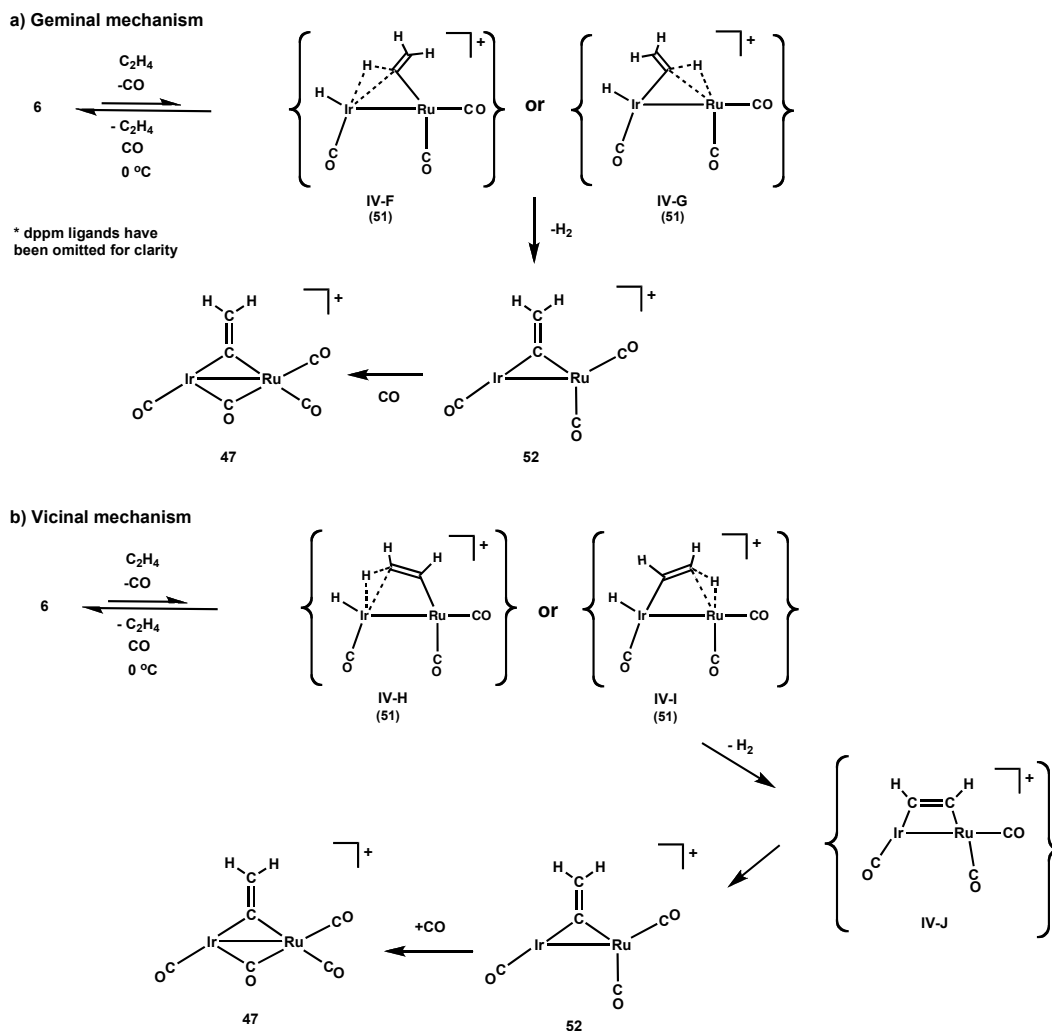
of an Ir-Ru bond provides the Ir and Ru metal centres with 16- and 18-electron configurations, respectively.

(c) *Geminal or Vicinal Activation?*

The low temperature NMR studies discussed above suggest the conversion of an alkenyl fragment to a bridging-alkylidene ligand; similar transformations have been noted previously by Deeming,¹⁸ Green^{43b} and Casey,^{43c} although the example by Casey involved base-assisted hydrogen abstraction. In addition Casey *et al.* have also observed the related transformation of a bridging-vinylidene to a bridging-alkylidene.^{43c} There are two mechanistic possibilities for the second C-H activation necessary for the transformation of the alkenyl fragment to a bridging-alkylidene ligand; both are outlined in Scheme 4.8 below, using ethylene as the prototypical example. Scheme 4.8a illustrates the ‘geminal’ mechanism in which rotation of the vinyl group in **51** can lead to an agostic-like interaction, much like **IV-B** proposed by Bergman,²⁷ as shown for the proposed transition states **IV-F** and **IV-G**. In the case of **IV-F** the vinyl group is bound to Ru whereas for **IV-G** it is bound to Ir; most likely these two isomers can interconvert by facile vinyl migration from metal to metal. The interaction of the α -hydrogen with either Ir (structure **IV-F**) or Ru (structure **IV-G**) could lead to C-H bond activation, and followed by H₂ elimination would give compound **52**. Subsequent CO coordination would lead to compound **47**. The intermediate **IV-F** may be the preferred transition state in this process as activation of the geminal C-H bond will lead to both hydrides being bound to Ir, making H₂ elimination more facile than if the hydrides were bound to separate metal centres.

In the ‘vicinal’ mechanism outlined in Scheme 4.8b the vinyl ligand is oriented such that the agostic-like interaction now involves the C ^{β} -H bond yielding the transient species **IV-H** and **IV-I** for the Ru- and Ir-bound vinyl group, respectively. C-H activation of this bond followed by H₂ elimination gives the alkyne-bridged species **IV-J** and isomerization of the terminal alkyne to a

Scheme 4.8

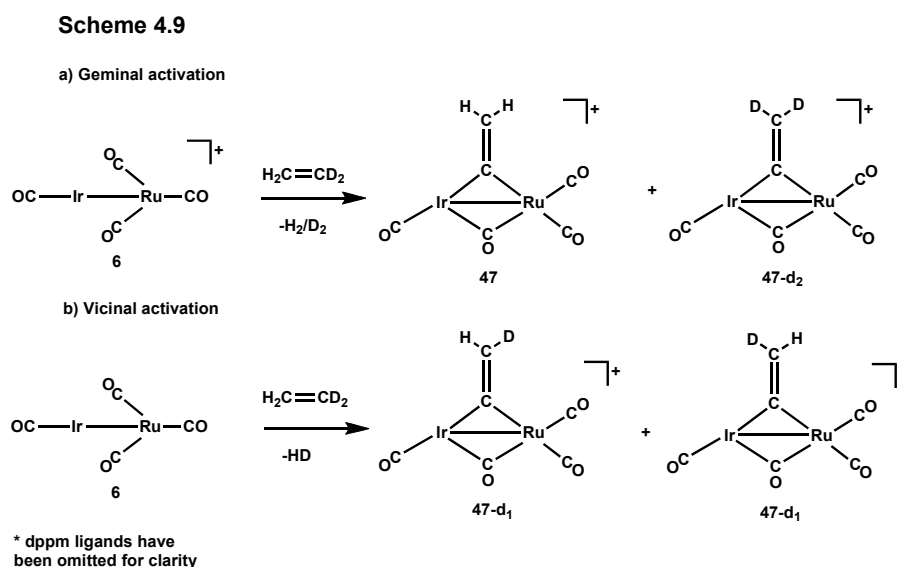


bridging-vinylidene group would yield compound **52**. We have not observed an alkyne-bridged species analogous to **IV-J**, however, we have observed the facile conversion of alkynes into vinylidene fragments in this IrRu system (*vide supra*), and this transformation is commonly observed.³⁴⁻³⁸

Attempts to observe the presumed dihydride intermediates prior to H₂ elimination have been unsuccessful. Reaction of ethylene with compound **6** in an H₂-rich environment or addition of H₂ to a mixture of **6** and **51** gives the known dihydrido species [IrRu(CO)₃(μ-H)₂(dppm)₂][OTf] in both cases,^{36a} whereas addition of H₂ gas to a solution of **52** generated *in situ* or addition of TMNO to **51** in an H₂-rich atmosphere yields only numerous unknown decomposition products.

We anticipated that the reactions of 1,1-disubstituted and 1,2-disubstituted olefins could shed light on the mechanism of action (geminal versus vicinal) for this transformation; if the transformation in question occurred *via* a geminal activation, the 1,2-disubstituted substrate should be unreactive beyond the first C-H activation process, whereas if the mechanism involves vicinal activation the 1,1-disubstituted substrate should be unreactive to the second C-H activation. Unfortunately neither isobutene nor *cis*-butene react with compound **6**; presumably the additional bulk introduced by the second methyl substituent prevents sufficient access to the metal centres. Likewise, both 1,1-difluoroethylene and *cis*-difluoroethylene are unreactive towards compound **6**. However, in this latter regard, it is generally accepted that difluoroethylenes are poor ligands, having low binding affinities to transition metals.^{47f,g} In addition, fluorination of hydrocarbyl substrates only serves to strengthen the remaining bonds at C^α.^{47a-e} For these reasons, fluorocarbons are substantially more difficult to activate than hydrocarbon substrates.^{40e,f,47}

Reaction of **6** with 1,1-d₂ ethylene should also distinguish between the geminal and vicinal mechanisms, as each will lead to different isotopomer products (Scheme 4.9 below). In the case of the geminal mechanism (Scheme



4.9a) both compound **47** and the dideutero isotopomer **47-d₂** should be observed, whereas the vicinal mechanism (Scheme 4.9b) can be expected to give only the isotopically scrambled product **47-d₁** in which only one deuterium atom is incorporated in the vinylidene fragment.

In the ¹H NMR spectrum of a sample containing the products of the reaction between **6** and 1,1-d₂-ethylene the resonances associated with the vinylidene group appear as two broad resonances at δ 6.69 and 5.03. The ²H NMR spectrum of this sample displays two broad resonances at δ 6.69 and 5.03, paralleling the ¹H NMR spectrum. In the absence of resolvable coupling between the geminal protons, the ¹H and ²H NMR data cannot distinguish between the isotopomer products generated. Although, reaction of the ¹³C₂H₂D₂ could provide some valuable ¹³C{¹H} data, this isotopomer is rare and expensive. Alternatively detection of H₂ gas liberation by MS may allow for determination of the presence H₂, D₂, HD or a combination of the three isotopomers. However, such an experiment requires specialized equipment that is not readily available to us. However, an examination of the observed MS isotopic pattern provides some valuable insight. Shown in Figure 4.5 is the observed isotope pattern together with the calculated patterns for three isotopomer ratios. Figure 4.5a shows the observed pattern; Figure 4.5b shows the isotope pattern for a 1:1 mixture of **47** and **47-d₂**, the expected pattern for the geminal mechanism; Figure 4.5c shows the calculated pattern for 100% **47-d₁**, the isotopomer product of the vicinal mechanism; finally, Figure 4.5d shows the pattern associated with a mixture of the isotopomers. Clearly, the calculated patterns associated with the products of the exclusively geminal (Figure 4.4b) and vicinal pathways (Figure 4.4c) are poor matches to the observed pattern. A satisfactory pattern match can be achieved with an isotopomer distribution of 35% **47**, 30% **47-d₁**, and 35% **47-d₂** (Figure 4d) suggesting that all three isotopomers are present, leading to the conclusion that *both* mechanistic pathways are active, with the geminal pathway being dominant, giving rise to 70% of the observed product. It is noteworthy that in the

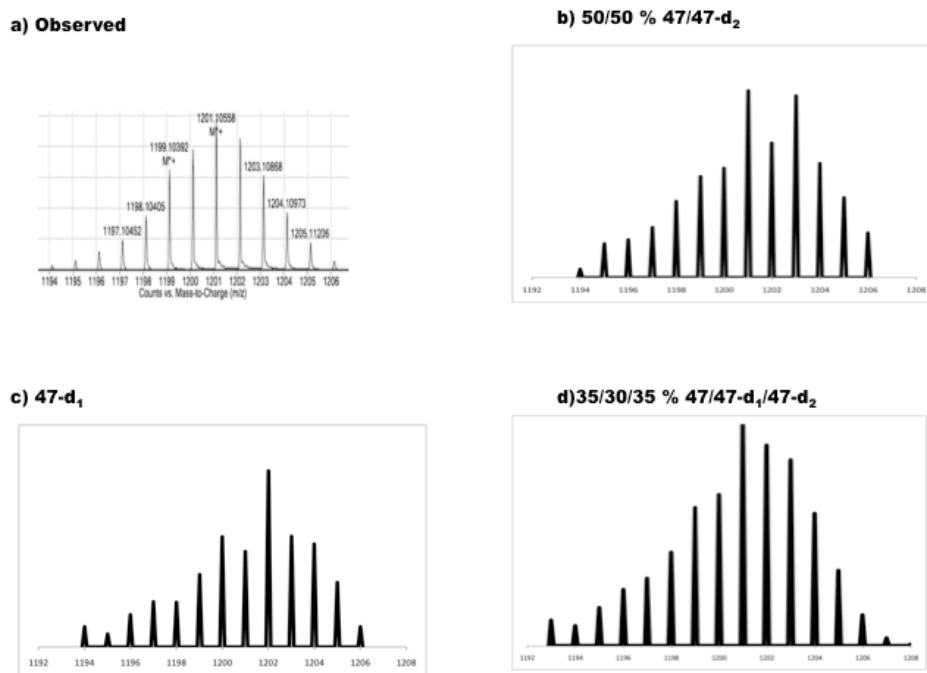


Figure 4.5 Isotope distribution patterns ($m/z=1201$) for a) the observed product mixture in the reaction of compound **6** with 1,1- d_2 ethylene, as well as simulated isotopic splitting patterns for b) 50/50% 47/47- d_2 , c) 100% 47- d_1 and d) 35%/30%/35% 47/47- d_1 /47- d_2 .

examples of unassisted vinyl-to-bridging-vinylidene transformations reported by Green *et al.* activation occurred *only* by the geminal pathway, as determined by deuterium labeling studies.^{43b} In the reports by Deeming and Underhill no distinction between the two mechanisms was provided.¹⁸

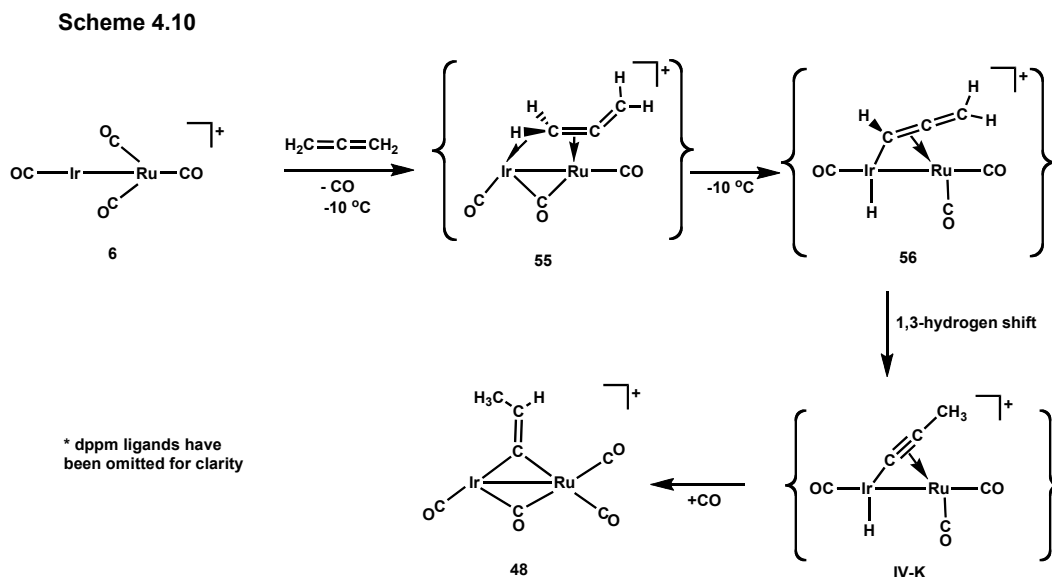
The observation that the geminal pathway is preferred over the vicinal in the IrRu system under investigation in this report can be rationalized by the relative acidities of the C^α and C^β protons of bridging vinylidene fragments. It is generally observed that the proton bound to C^α is more acidic than the ones bound to C^β , based on the 1H NMR chemical shifts (δ 6.84 and 4.74 for compound **51**, respectively).⁴⁰ In the case of ethylene, the increased acidity of the C^α proton leads to more facile activation of this C-H bond over C^β -H, hence the geminal pathway is kinetically preferred. Moreover, the increased lability of the C^α -H

bond is supported by the work of Green discussed above, in which only this bond was activated.^{43b}

(c) *Reactions of compound 6 with cumulenes*

In hopes of uncovering clues about the activation of cumylene substrates, we have attempted to detect intermediates by NMR spectroscopy at low temperatures, much as outlined above. Unfortunately, we have been unable to acquire sufficient data to confidently propose a mechanism for this transformation. What follows is a proposal based on, admittedly, a very limited data set.

A sample containing a mixture of compound **6** and an approximate 50-fold excess of allene at $-80\text{ }^{\circ}\text{C}$ was slowly warmed in $10\text{ }^{\circ}\text{C}$ increments. No new species was observed between $-80\text{ }^{\circ}\text{C}$ and $-10\text{ }^{\circ}\text{C}$, at which temperature a new complex, $[\text{IrRu}(\text{CO})_3(\eta^2:\eta^2\text{-H}_2\text{C}=\text{C}=\text{CH}_2)(\text{dppm})_2][\text{OTf}]$ (**55**), begins to form (see Scheme 4.10). Compound **55** converts directly to compound **48** upon warming



above $-10\text{ }^{\circ}\text{C}$, and reverts back to **6** in the absence of allene, even at $-80\text{ }^{\circ}\text{C}$, precluding its isolation. Its characterization is based on NMR spectroscopy at -80

°C. The $^{31}\text{P}\{^1\text{H}\}$ NMR spectrum of **55** displays two multiplets at δ 29.6 and -5.9 , assigned to the Ru-bound and the Ir-bound phosphorus nuclei, respectively. The ^1H NMR spectrum of **55** shows an upfield signal at δ -2.4 as a broad triplet coupled to the Ir-bound phosphines and has been assigned to a proton engaging in an agostic interaction with Ir, on the basis of its upfield chemical shift (recall from Chapter 3 that agostic protons generally exhibit upfield chemical shifts) and unresolved H-P coupling to only the Ir-bound ends of the diphosphines (established by $^1\text{H}\{\text{selective } ^{31}\text{P}\}$ NMR studies). Unfortunately, obstruction of the olefinic region of the ^1H NMR spectrum by the large excess of free allene present - required to stabilize compound **55** - precludes the unambiguous assignment of additional resonances in the ^1H NMR spectrum. The $^{13}\text{C}\{^1\text{H}\}$ NMR spectrum of compound **55** (^{13}CO enriched) shows three carbonyl resonances, again illustrating that carbonyl loss occurs at an early stage; one broad triplet at δ 192.4 with 12 Hz coupling to the Ru-bound phosphorus nuclei has been assigned to a carbonyl terminally bound to Ru, a triplet at δ 175.0 with 10 Hz coupling to the Ir-bound ^{31}P nuclei has been assigned to a carbonyl bound terminally to Ir and finally a downfield signal at δ 208.9 with unresolved coupling to both sets of phosphorus nuclei has been assigned to a bridging carbonyl. Based on the spectral parameters presented above we have tentatively proposed a structure for **55**, shown in Scheme 4.10, in which the allene ligand is η^2 -bound to Ru while engaged in an α -agostic interaction with Ir. Three carbonyls, one terminally bound to each metal and a third bridging both metals, complete the coordination of each metal, and along with the diphosphines and the inclusion of a metal-metal bond, give both metals 18-electron configurations.

After 20 min at -10 °C a new species, tentatively formulated as $[\text{IrRu}(\text{H})(\text{CO})_3(\mu\text{-}\eta^1\text{:}\eta^2\text{-HC=C=CH}_2)(\text{dppm})_2][\text{OTf}]$ (**56**), begins to emerge (see Scheme 4.10) and after 40 min it is observed with compounds **6** and **55** in a 1:2:1 ratio (compounds **56**:**6**:**55**). The $^{31}\text{P}\{^1\text{H}\}$ NMR spectrum of compound **56** appears as an ABCD pattern displaying four separate resonances, one for each phosphorus nucleus: a doublet of multiplets at δ 45.6, and three doublets of doublets of

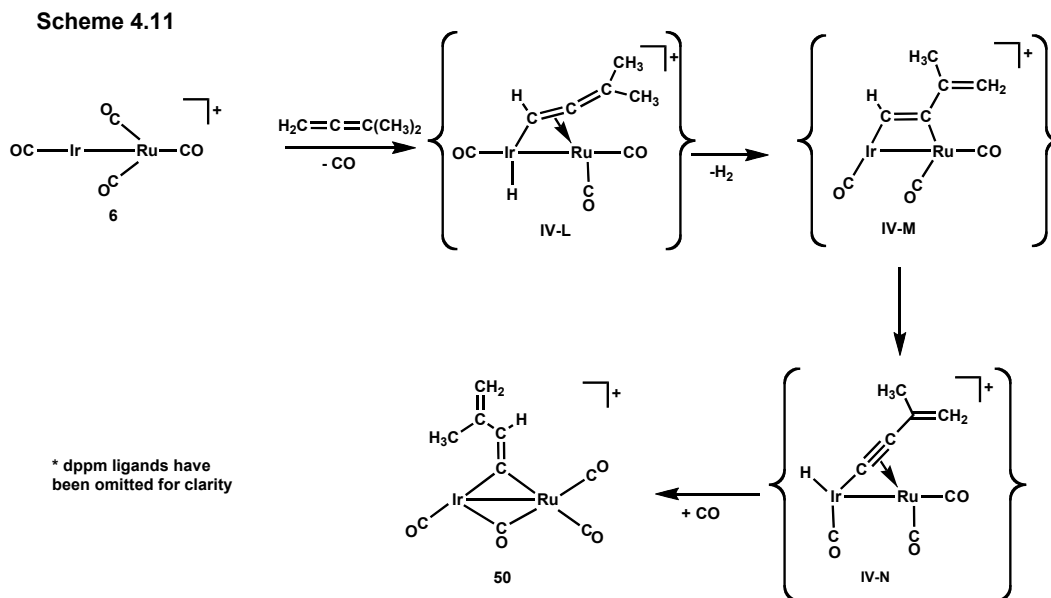
doublets at δ 24.4, 5.4 and -11.1 . The two upfield resonances have been assigned to the Ir-bound end of the diphosphines and show a strong mutual *trans* coupling of 331 Hz, whereas the two downfield resonances have been assigned to the Ru-bound ends of the diphosphines and show a mutual *trans* coupling of 253 Hz.

Of particular interest is an upfield resonance in the ^1H NMR spectrum at $\delta -10.0$ appearing as a doublet of doublet of multiplets exhibiting strong coupling to both the Ir-bound ^{31}P nuclei ($^2J_{\text{PH}} = 17$ Hz, 5.1 Hz) and weak unresolved coupling to the Ru-bound ^{31}P nuclei. This upfield chemical shift and strong coupling to the Ir-bound phosphorus nuclei suggest a terminal Ir-bound hydride, presumably generated by the cleavage of the formerly agostic C–H bond of the precursor, compound **55**. Compound **56** converts to **48** over the period of a few hours, even at -80 °C. As a result of this instability, we have been unable to acquire $^{13}\text{C}\{^1\text{H}\}$ NMR data for compound **56**, even in the case of the ^{13}CO isotopomer. However, in line with an earlier discussion the ABCD ^{31}P spin system suggests an arrangement not unlike a bridging vinyl group in which the allenyl fragment is bound to both metal centres in a σ - π fashion as shown in Scheme 4.10. Such a binding arrangement for allenyl fragments has been observed previously by Doherty and coworkers in a Fe_2 systems as well as by the group of Chiang on Ag surfaces.⁴⁸ We assume that like its precursor (**55**) compound **56** is a tricarbonyl. As noted above, compound **56** continues to react to produce compound **48**, although we have unfortunately not been able to observe any further species in this transformation.

We propose that the next step involves transfer of the proton bound to the α -carbon to the γ -carbon by a 1,3-hydrogen shift, giving the bridging propynyl species **IV-K**; such transformations have been previously reported.⁴⁸ For example, in the most recent report, Chiang *et al.* showed that an allenyl fragment can undergo a 1,3-sigmatropic shift on Ag surfaces to give a propynyl fragment analogous to **IV-K** proposed above.^{48a} Subsequent hydride migration to the β -carbon of the 1-propynyl fragment of **IV-K** followed by CO coordination gives compound **48**. Analogous hydride migrations have been observed for alkynyl

hydrido complexes both in our group^{49a} as well as in the group of Oro.⁴⁹ We propose that the transformation of methylallene to an ethyl vinylidene fragment occurs by the same mechanism.

The activation of 1,1-dimethylallene clearly differs from that of allene and methylallene. In this case the activation of *three* C–H bonds occurs together with H₂ elimination to give the vinylvinylidene-bridged species **50**. We propose that in this case initial activation occurs much as proposed for allene and methylallene; cleavage of a C–H bond at the terminal end of the cumulene substrate gives the cumulenylyl species **IV-L** shown in Scheme 4.11 below. We rule out the possibility



of a 1,3 hydrogen shift being involved at this stage to give an isopropyl-substituted alkenyl species on the basis of the earlier observation in the reaction of 1,1-dimethylallene with **IV-C** (see Scheme 4.5). The product of 1,3-hydrogen shift in **IV-L** would be analogous to **IV-E** discussed earlier, in which it was noted that this minor species did not transform with time to the major species **IV-D** and is probably produced by an independent pathway. Therefore it is unlikely that a similar bridging alkyne fragment in our series of reactions would lead to the vinyl vinylidene group in **50**. Activation of a methyl group of the cumulenylyl fragment

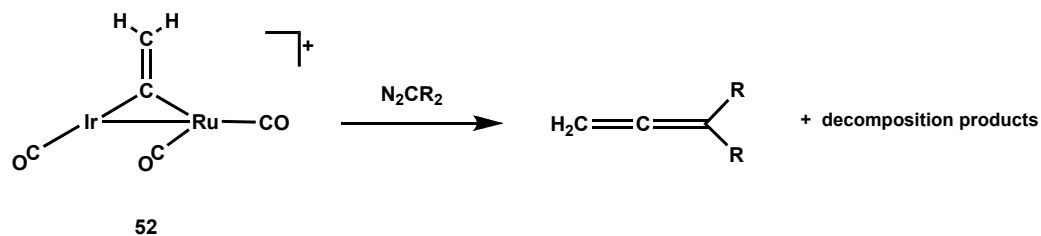
followed by H₂ elimination gives the alkyne-bridged species **IV-M** that may undergo cleavage of the geminal C-H bond to yield the $\mu\text{-}\eta^1\text{:}\eta^2$ alkynyl-bridged species **IV-N**, which is reminiscent of **IV-D**, the major product of triple C-H activation of 1,1-dimethylallene by the related IrRu complex **IV-C**. Hydride migration to the central carbon of the alkyne moiety and coordination of a CO ligand could lead to compound **50**.

4.3.4 Reactions of the Vinylidene Bridge

Metal-vinylidene species have been shown to be synthetically useful for the formation of carbon-carbon bonds.^{35,50-60} The functionalization of vinylidene fragments generated from the geminal activation of olefins could provide another useful strategy for the conversion of inexpensive olefins into value-added products. Unfortunately, no further reactivity was reported in the previous examples of vinylidene formation *via* olefin geminal C-H activation. We were interested in determining if the previously successful strategy for carbon-carbon bond formation, involving coupling of bridging vinylidenes with diazoalkane-generated alkylidenes,⁵⁷⁻⁶³ could be employed to generate functionalized cumulenes from the vinylidene-bridged systems in this study.

The vinylidene-bridged, tetracarbonyl compounds **47-50** are found to be inert towards additional reactions with diazomethane (N₂CH₂) or diethyl diazo malonate (N₂C(C(O)OCH₂CH₃)₂, DEDM). However, as observed in the related methylene-bridged RhOs and RhRu systems,⁶¹⁻⁶⁴ the tricarbonyl species displays a marked enhancement of reactivity over the tetracarbonyl analogues. In line with these previous observations, compound **52** reacts readily with diazomethane (N₂CH₂) or diethyl diazo malonate to generate allene (¹H NMR: δ 4.21 (s)) or diethyl 2-vinylidene malonate (¹H NMR: δ 5.12 (s, 2H), 4.23 (q, 4H), 1.62 (t, 6H)), respectively (see Scheme 4.12).

Scheme 4.12



R = H, CO₂Et

* dppm ligands have been omitted for clarity

In Chapter 2 it was shown that treatment of the methylene-bridged species [RhM(CO)₃(μ-CH₂)(dppm)₂][OTf] (M = Ru, Os) with diazoalkanes gave the corresponding olefin by coupling of the methylene group with the diazoalkane-generated alkylidene fragment.⁶² In that study we proposed that olefin formation occurred by coupling of a diazoalkane-generated alkylidene fragment and the methylene unit to give a putative C₂-bridged intermediate which rapidly decomposed to liberate the observed olefin. We propose a similar process for the transformation illustrated in Scheme 4.12 in which insertion of a diazoalkane-generated alkylidene unit into the Ir-C bond results in the elimination of the observed cumulene. However, it should be mentioned that in an earlier study by Hoel *et al* it was reported that treatment of the vinylidene-bridged diiron complex, [Cp₂Fe₂(CO)₂(μ-C=CH₂)], with diazomethane gave allene;⁵⁰ analogous to our observations. The authors proposed that alkylidene and vinylidene coupling occurred across the C=C bond of the vinylidene unit to give a cyclopropanyl moiety, which rearranged to give the allene molecule. A similar mechanism may be at work in this reaction.

It is interesting to note that this transformation requires unsaturation of the bimetallic core; compounds **47-50** failed to react while the tricarbonyl species **52** reacts readily. In a similar manner in Chapter 2 it was also observed that the saturated methylene-bridged tetracarbonyl species were unreactive towards diazoalkanes whereas their tricarbonyl analogues reacted. In that study the requirement for unsaturation was rationalized by a mechanism which involved N-

bound coordination of the diazoalkane substrate prior to alkylidene insertion (see Scheme 2.4).⁶³ We rationalize the requirement for unsaturation in this study in the same way.

4.4 Conclusion

The vast majority of research in olefinic C-H bond cleavage has focused on the development of monometallic systems capable of facilitating this process efficiently and selectively, yet little attention has been given to systems with adjacent metals. This is surprising, considering that of the five systems reported capable of geminal C-H bond cleavage of olefinic substrate, three systems were multimetallic including the only system to exhibit this reactivity under ambient conditions.

In a previous report by our group in which the Ir₂ system promoted geminal C-H activation of butadiene, the resulting product was a stable vinylidene-bridged, dihydride complex. Initially we were interested in determining if substitution of Ir for Ru would give a system capable of geminal C-H activation. This is indeed the case for ethylene and propene as well as three cumulenes. In fact, geminal activation of unhindered olefins occurs more readily with the present IrRu system than with the earlier Ir₂ system; only 1,3-butadiene gave geminal activation in the Ir₂ system whereas IrRu resulted in activation of a number of olefins. The failure of the IrRu system to activate butadiene is probably associated with the more crowded environment at Ru. Moreover, the current IrRu system also differs from Ir₂ (and other previous reports) in its tendency to eliminate H₂.

Generation of vinylidene-bridged species from the reaction of **6** with allene and methylallene differs from that of monoolefins in that H₂ elimination does not occur upon geminal C-H bond activation. Rather, migration of both hydrogens to the β and γ carbons occurred. The disubstituted 1,1-dimethylallene reacts somewhat differently with compound **6** giving the 3-methyl-1,3-

butadienyldiene-bridged species, compound **50**, through the activation of *three* C-H bonds of one cumulene molecule. In this case the reaction is accompanied by H₂ elimination and transfer of the third hydrogen to the β -carbon.

The reactivity of multimetallic systems can be much more complex than monometallic ones, due in part to cooperative interaction between adjacent metals. Often, the manner in which the adjacent metals interact to generate such unusual reactions is poorly understood and this was certainly the case in the activation of geminal C-H bonds of olefinic substrates. On the basis of our study we suggested a proposal for adjacent metal interaction that involves substrate precoordination to one metal and subsequent C-H bond cleavage by the adjacent metal to yield a vinyl hydride intermediate. It is unclear whether the vinyl hydride species is generated through the cooperativity of both metals by initial olefin coordination at Ru followed by bond cleavage at the adjacent Ir (as we optimistically suggest), or in the same way as C-H oxidative addition can occur at monometallic Ir centres, which has been well documented.^{30,31} However, it is the facile second activation step that is undoubtedly facilitated by the presence of the adjacent metal. Two possible mechanisms, the (more direct) geminal and the (less direct) vicinal mechanisms, were proposed. To our surprise, deuterium labeling studies on ethylene activation suggest that vinylidene formation occurs by *both* pathways. The observation that both the geminal and vicinal C-H bonds are cleaved illustrates the importance of interactions between substrate fragments bound to one metal whilst engaging with the adjacent metal like **I-I** and **I-J** of Chart 4.2. Most importantly, this study establishes the role of the adjacent metal in the transformation of α -olefins into bridging vinylidenes promoted by adjacent metal centres and further illustrates the utility of such multimetallic systems for unique substrate transformations. However, more work is still required to acquire a complete understanding of the mechanistic details. In particular, the complete spectral characterization of labile intermediates observed needs to be completed.

4.6 References

1. Lewis, J. C.; Bergman, R. G.; Ellman, J. A. *Acc. Chem. Res.* **2008**, *41*, 1013.
2. Dyker, G. *Handbook of C-H Transformations*; Wiley-VCH: Weinheim, 2005.
3. Labinger, J. A.; Bercaw, J. E. *Nature* **2002**, *417*, 507.
4. Slugovc, C.; Padilla-Martinez, I.; Sirol, S.; Carmona, E. *Coord. Chem. Rev.* **2001**, *213*, 129.
5. Kee, T. P.; Gibson, V. C.; Clegg, W. *J. Organomet. Chem.* **1987**, *325*, C14.
6. Gutierrez-Puebla, E.; Monge, A.; Nicasio, M. C.; Perez, P. J.; Poveda, M. L.; Carmona, E. *Chem. Eur. J.* **1998**, *4*, 2225.
7. Slugovc, C.; Mereiter, K.; Trofimenko, S.; Carmona, E. *Angew. Chem. Int. Ed.* **2000**, *39*, 2158.
8. Slugovc, C.; Mereiter, K.; Trofimenko, S.; Carmona, E. *Helv. Chim. Acta.* **2001**, *84*, 2868.
9. Lee, D.-G.; Chen, J.; Fuller, J. W.; Crabtree, R. H. *Chem. Commun.* **2001**, 213.
10. Gusev, D. G.; Lough, A. J. *Organometallics* **2002**, *21*, 2601.
11. Kakiuchi, F.; Chatani, N. *Adv Synth. Catal.* **2003**, *345*, 1077.
12. Crabtree, R. H. *J. Organomet. Chem.* **2004**, *689*, 4083.
13. Clot, E.; Chen, J.; Lee, D.-G.; Sung, S. Y.; Appelhans, L. N.; Faller, J. W.; Crabtree, R. H.; Eisenstien, O. *J. Am. Chem. Soc.* **2004**, *126*, 8795.
14. Grotjahn, D. B.; Hoerter, J. M.; Hubbard, J. L. *J. Am. Chem. Soc.* **2004**, *126*, 8866.
15. Rankin, M. A.; McDonald, R.; Ferguson, M. J.; Stradiotto, M. *Angew. Chem. Int. Ed.* **2005**, *44*, 3603.
16. Hong, S. H.; Chlenov, A.; Day, M. W.; Grubbs, R. H. *Angew. Chem. Int. Ed.* **2007**, *46*, 5148.

17. Rankin, M. A.; MacLean, D. F.; Schatte, G.; McDonald, R.; Stradiotto, M. *J. Am. Chem. Soc.* **2007**, *129*, 15855.
18. (a) Deeming, A. J.; Underhill, M. *J. Organomet. Chem.* **1972**, *42*, C60. (b) Deeming, A. J.; Hasso, S.; Underhill, M. *J. Chem. Soc., Chem. Commun.* **1974**, 807. (c) Deeming, A. J.; Underhill, M. *J. Chem. Soc., Chem. Commun.* **1973**, 277. (d) Deeming, A. J.; Underhill, M. *J. Chem. Soc., Dalton Trans.* **1974**, 1415. (e) Boncella J. M.; Green, M. L. H.; O'Hare, D. *J. Chem. Soc., Chem. Commun.* **1986**, 618. (f) Boncella, J. M.; Green, M. L. H. *J. Organomet. Chem.* **1987**, *325*, 217.
19. Ristic-Petrovic, D.; Torkelson, J. R.; Hilts, R. W.; McDonald, R.; Cowie, M. *Organometallics* **2000**, *19*, 4432.
20. (a) Bell, T. W.; Haddleton, D. M.; McCamley, A.; Partridge, M. G.; Perutz, R. N.; Willner, H. *J. Am. Chem. Soc.* **1990**, *112*, 9212.
21. Suzuki, H.; Omori, H.; Lee, D. H.; Yoshida, Y.; Fukushima, M.; Tanaka, M.; Moro-oka, Y. *Organometallics* **1994**, *13*, 1129.
22. Weiller, B. H.; Wasserman, E. P.; Bergman, R. G.; Moore, C. B.; Pimentel, G. C. *J. Am. Chem. Soc.* **1989**, *111*, 8288.
23. Crabtree, R. H.; Mellea, M. F.; Mihelcic, J. M.; Quirk, J. M. *J. Am. Chem. Soc.* **1982**, *104*, 107.
24. Hoyano, J. K.; Graham, W. A. G. *J. Am. Chem. Soc.* **1982**, *104*, 3723.
25. Janowicz, A. H.; Bergman, R. G. *J. Am. Chem. Soc.* **1982**, *104*, 352.
26. Hoyano, J. K.; McMaster, A. D.; Graham, W. A. G. *J. Am. Chem. Soc.* **1983**, *105*, 7190.
27. Janowicz, A. H.; Bergman, R. G. *J. Am. Chem. Soc.* **1983**, *105*, 3929.
28. Stoutland, P. O.; Bergman, R. G. *J. Am. Chem. Soc.* **1985**, *107*, 4581.
29. Silvestre, J.; Calhorda, M. J.; Hoffman, R.; Stoutland, P. O.; Bergman, R. G. *Organometallics* **1986**, *5*, 1841.
30. Dell'Anna, M. M.; Trepanier, S. J.; McDonald, R.; Cowie, M. *Organometallics* **2001**, *20*, 88.
31. Searle, N. E. *Org. Synth* **1956**, *36*, 25.

32. (a) Sheldrick, G. M. *Acta Crystallogr.* **2008**, *A64*, 112–122. (b) Sheldrick, G. M. *Acta Crystallogr.* **1990**, *A46*, 467–473.
33. Sheldrick, G. M. *SHELXL-93*. Program for crystal structure determination. University of Göttingen, Germany, 1993.
34. Werner, H. *Angew. Chem. Int. Ed.* **1990**, *29*, 1077.
35. Bruce, M. I. *Chem. Rev.* **1991**, *91*, 197.
36. (a) Wang, L.-S.; Cowie, M. *Organometallics* **1995**, *14*, 2374. (b) Wang, L.-S.; Cowie, M. *Organometallics* **1995**, *14*, 3040.
37. Xiao, J.; Cowie, M. *Organometallics* **1993**, *12*, 463.
38. Allen, F. H.; Kennard, O.; Watson, D. G.; Brammer, L.; Orpen, A. G.; Taylor, R. J. *J. Chem. Soc. Perkin Trans. II* **1987**, S1.
39. Dutton, J.; Trepanier S. J.; Cowie, M. *Unpublished results* **2005** University of Alberta; Edmonton AB, Canada
40. a) Knox, S. A. R.; Marchetti, F. *J. Organomet. Chem.* **2007**, *692*, 4119. b) Takahashi, Y.; Murakami, N.; Fujita, K.; Yamaguchi, R. *Dalton Trans.* **2009**, 2029. c) Garcia Alonso, F. J.; Riera, V.; Ruiz, M. A.; Tiripichio, A.; Camellini, M. T. *Organometallics* **1992**, *11*, 370. d) Gao, Y.; Jennings, M. C.; Puddephatt, R. J. *Dalton Trans.* **2003**, 261. e) Anderson, D.J.; McDonald, R.; Cowie, M. *Angew. Chem. Int. Ed.* **2007**, *46*, 3741. f) Anderson, D. J. C-F Activation in Diphosphine-Bridged Binuclear Complexes of Rhodium & Iridium Ph.D. Thesis, University of Alberta, Edmonton, Alberta, Canada, 2007
41. Solari, E.; Maltese, C.; Latronico, M.; Floriani, C.; Chiesi-Villa, A. *J. Chem Soc. Dalton Trans.* **1998**, 2395.
42. (a) Casey, C. P.; Carino, R. S.; Sakaba, H. *Organometallics* **1997**, *16*, 419. (b) Casey, C. P.; Hallenbeck, S. L.; Widenhoefer, R. A. *J. Am. Chem. Soc.* **1995**, *117*, 4607.
43. (a) Werner, H.; Wolf, J.; Nessel, A.; Fries, A.; Stempfle, B.; Nurnberg, O. *Can. J. Chem.* **1995**, *73*, 1050. (b) Casey, C. P.; Marder, S. R.; Adams, B. R. *J. Am. Chem. Soc.* **1985**, *107*, 7700. (c) Green, M.; Orpen, A. G.;

- Shaverien, C. J. *J. Chem. Soc., Dalton Trans.* **1989**, 1333. (e) Nobel, P. O.; Brown, T. L. *J. Chem. Soc., Dalton Trans.* **1975**, 1614. (f) Nobel, P. O.; Brown, T. L. *J. Am. Chem. Soc.* **1984**, *106*, 644. (g) Dyke, A. F.; Knox, S. A. R.; Morris, M. J.; Naish, P. I. *J. Chem. Soc., Dalton Trans.* **1983**, 1417.
44. Ulmer, T. J.; Cowie, M. *Unpublished Results* **2009** University of Alberta; Edmonton AB, Canada.
45. Alvarado, Y.; Boutry, O.; Gutierrez, E.; Monge, A.; Carmen Nicasio, M.; Poveda, M. L.; Perez, P. D.; Bianchini, C.; Carmona, E. *Chem. Eur. J.* **1997**, *3*, 860.
46. Silverstein, R. M.; Webster, F. X. *Spectroscopic Identification of Organic Compounds*; John Wiley and Sons Inc.: New York, 1998.
47. a) Peters, D. *J. Chem. Phys.* **1963**, *3*, 561. b) Bent, H. A. *J. Chem. Phys.* **1960**, *32*, 304 c) Bent, H. A. *J. Chem. Phys.* **1960**, *32*, 1258. d) Bent, H. A. *J. Chem. Phys.* **1960**, *32*, 1259. e) Bent, H. A. *J. Chem. Phys.* **1960**, *32*, 1260. f) Kiplinger, J. L.; Richmond, T. G.; Oseterberg, C. E. *Chem. Rev.* **1994**, *94*, 373. g) Kulaweic, R. J.; Crabtree, R. H. *Coord. Chem. Rev.* **1990**, *99*, 89.
48. a) Doherty, S.; Elsegood, M. R. J.; Clegg, W.; Ward, M. F.; Waugh, M. *Organometallics* **1997**, *16*, 4251. b) Kung, H.; Wu, S-M., Wu, Y-J., Yang, Y-W., Chiang, C-M. *J. Am. Chem. Soc.* **2008**, *130*, 10263.
49. a) George, D. S. A.; McDonald, R.; Cowie, M. *Organometallics* **1998**, *17*, 2553. b) Jimenez, M. V.; Sola, E.; Martinez, A. P.; Lahoz, F. J.; Oro, L. *Organometallics* **1999**, *18*, 1125.
50. Bruce, M. I.; Swincer, A. G. *Adv. Organomet. Chem.* **1983**, *22*, 59.
51. Hoel, E. L.; Ansell, G. B.; Leta, S. *Organometallics* **1984**, *3*, 1633.
51. (a) Casey, C. P.; Miles, W. H.; Fagan, P. J.; Haller, K. J. *Organometallics* **1985**, *4*, 559. (b) Casey, C. P.; Austin, E. A. *Organometallics* **1986**, *5*, 584.
53. Alt, H. G.; Engelhardt, H. E.; Rausch, M. D.; Kool, L. B. *J. Organomet. Chem.* **1987**, *329*, 61.
54. Berry, D. H.; Eisenberg *Organometallics* **1987**, *6*, 1796.

55. Gamble, A. S.; Birdwhistell, K. R.; Templeton, J. L. *Organometallics* **1988**, *7*, 1046.
56. Etienne, M.; Guerchais, J. E. *J. Chem. Soc., Dalton Trans.* **1989**, 2187.
57. Antonova, A. B. *Russ. Chem. Rev.* **1989**, *58*, 693.
58. Davies, S. G.; McNally, J. P.; Smallridge, A. J. *Adv. Organomet. Chem.* **1990**, *30*, 1.
59. Gibson, V. C.; Parkin, G.; Bercaw, J. E. *Organometallics* **1991**, *10*, 220.
60. Bruce, M. I. *Chem. Rev.* **1998**, *98*, 2797.
61. Trepanier, S. J.; Sterenberg, B. T.; McDonald, R.; Cowie, M. *J. Am. Chem. Soc.* **1999**, *121*, 2613.
62. Trepanier, S. J.; Dennett, J. N. L.; Sterenberg, B. T.; McDonald, R.; Cowie, M. *J. Am. Chem. Soc.* **2004**, *126*, 8046.
63. Samant, R. G.; Graham, T. W.; Rowsell, B. D.; McDonald, R.; Cowie, M. *Organometallics* **2008**, *27*, 3070.
64. Rowsell, B. D.; Trepanier, S. J.; Lam, R.; McDonald, R.; Cowie, M. *Organometallics* **2002**, *21*, 3228.

Chapter 5: Conclusions

5.1 Concluding Remarks

In the work presented within this dissertation our goal was to investigate substrate transformations promoted by adjacent metal sites, focusing on two key areas: (1) understanding the roles of adjacent metals during substrate transformations of homogeneous bimetallic systems as well as substrate transformations occurring on metal surfaces; (2) determining the influence of different metal combinations in heterobimetallic complexes, concentrating in this thesis on the IrRu combination and comparing its reactivity to the previously studied RhOs, RhRu and Ir₂ systems.

The work of Chapter 2 was a continuation of previous work in which it was reported that the RhOs system promoted the selective coupling of methylene units, depending on reaction conditions.¹ In that report, a mechanistic proposal was put forth that involved the sequential coupling of methylene units to generate sequentially C₂-, C₃- and C₄-bridged species and we wished to gain further insight into this process. We had initially hoped to use substituted diazoalkanes as a synthetic route to both C₁- and C₂-bridged complexes. Even though our initial goal may not have been realized, we did observe some interesting reactivity.

Attempts to generate C₂-bridged species by alkylidene insertion into the Rh-CH₂ bond resulted instead in the generation of substituted olefins by coupling of a diazoalkane-generated alkylidene unit and the bridging methylene group. Although the majority of the olefin intermediates were unstable, we were able to characterize an interesting, ethyl acrylate complex at low temperatures; presumably our inability to observe the putative C₂-bridged intermediate was the result of destabilizing steric interactions of the bulky substituents of the resulting olefin. Furthermore, our unsuccessful attempts to generate alkylidene-bridged products from a series of diazoalkanes produced three interesting and rather different complexes that involve incorporation of the intact diazoalkane functionality. Interestingly, upon coordination of EDA the diazoalkane carbon

undergoes a condensation reaction with an adjacent CO ligand to generate a bridging $\kappa^1:\kappa^1$ -diazoenolate ligand. The diazoalkane, DEDM, binds in a similar $\kappa^1:\kappa^1$ -bridging/chelating mode; however in this case the DEDM ligand chelates through one of its carboxylate groups which displaces an adjacent carbonyl ligand. Interestingly, TMSDM, which lacks carbonyl functionalities, prefers to bind terminally. It would seem that in the systems investigated in Chapter 2 the bridged binding mode for the diazoalkane is only preferred when the formation of a 5- (EDA) or 6-membered (DEDM) ring by chelation is possible. Presumably, the stabilizing chelate effect within compounds **27-31** is sufficient enough to overcome the destabilizing steric interactions between the bulky diazoalkane ligand and the phenyl groups of the dppm framework, whereas in the case of TSMDM, these interactions force the ligand into the less encumbered terminal site on the group 8 metal.

Attempts to generate alkylidene fragments from these diazoalkane adducts by either thermolytic or photolytic bond cleavage were unsuccessful in the case of the diazoalkane adducts in this study. In the case of compounds **27-30** the compounds remained unchanged after being subjected to such conditions. Again, it seems that stabilization by chelation in these complexes is significant. In contrast, compound **32**, in which the TMSDM ligand is bound terminally, decomposes even under ambient conditions. Our inability to generate alkylidenes from N-bound diazoalkanes supports the proposal by Milstein that the η^1 -C bound binding mode (coordination mode type **V** of Chart 2.1) is a prerequisite for the generation of metal-bound alkylidene units,² *via* N₂ loss.

It would seem that our failure to generate the targeted C₁- and C₂-bridged species is also largely due to steric influences of the diazoalkane substituents. In the case of C₁-bridge generation, access to the diazoalkane carbon center to generate the prerequisite η^1 -C coordination is impeded by the size of these substituents. Similar steric arguments explain the instability of targeted C₂-bridged species; the bulk of these substituents renders the C₂-bridge unstable resulting in the dissociation of the corresponding olefin.

It is interesting to note that the diazoalkanes investigated in this study are commonly used to generate alkylidenes in monometallic systems, whereas with the 'RhM'dppm' systems studied in Chapter 2 the intact diazoalkane adducts were observed. Although steric interactions between the diazoalkane substituents and the phenyl groups of the dppm ligands are likely an important contributing factor, the presence of an adjacent metal introduces the bridged binding modes (IV and V in Chart 2.1) and surely this plays a significant role in the stability of the products observed, at least in the case of EDA and DEDM. Moreover, EDA and DEDM exhibited the ability to chelate, either by condensation with a carbonyl in the case of EDA, or through one of the carbonyl groups of the DEDM, adding further to the stability of these bridging diazoalkane ligands. Indeed, their resistance to thermolytic and photolytic reactions further illustrates the stability of this bridging/chelating binding mode.

The vast majority of the recent 'MM'(dppm)₂' chemistry explored in our group has focused on the RhOs and RhRu metal combinations, so little was known about the Ir-based systems. Starting with the IrRu combination we have begun to explore the influence of descending the group 9 triad (Rh to Ir).

Our group has been interested in migratory insertion reactions occurring at multi-metal sites for some time. This interest has stemmed from the possibility of metal-metal cooperativity in heterobimetallic systems in this process and its significance in the formation of oxygenates in FT chemistry. Previous work in our group has focused on the RhOs and RhRu combinations³ and we were interested in determining the effect on the chemistry of substituting Rh by Ir. Many of the differences observed were predictable based on well-established periodic trends with the group 9 triad, but others were unexpected.

Overall, the conversion of a bridging methylene group to a bridging acetyl group is similar in all three cases (Rh/Ru, Rh/Os and Ir/Ru); protonation is followed by methyl group migration from bridging to terminal, and migratory insertion gives the bridging acetyl fragment. Furthermore, low-temperature NMR studies of all three combinations suggest direct protonation at the methylene group, rather than protonation at the metal followed by hydride migration to the

methylene carbon as proposed to occur under **FT** conditions in the formation of surface-bound methyl groups from surface-bound hydrides and methylene groups.⁴

However, there have been some notable differences between the Ir- and Rh-based systems. In the first step of the reaction sequence (protonation of the μ -CH₂ moiety), the resulting unsymmetrically bridging methyl group is σ -bound to Ir while involved in an agostic interaction with Ru. For the Rh-based systems, the reverse was observed; the methyl group was σ -bound to the group 8 metal. Furthermore, the two IrRu compounds containing bridging methyl groups in this study display slow (on the NMR time-scale) exchange between the “terminal” and “agostic” methyl proton at low temperature, allowing both the C-H “agostic” and C-H “terminal” coupling constants to be measured. The coupling constants for the agostic interactions in both species (65 and 72 Hz) are believed to be the lowest yet observed for unsymmetrically bridged methyl groups. Stronger interactions (lower ¹J_{CH} values) have been observed in mononuclear, electron-poor systems and in substituted bridging alkyl fragments.⁵

Another significant, albeit predictable, difference between the Ir- and Rh-based systems is the rate of migratory insertion, which is orders of magnitude slower for the IrRu system than for the Rh-based ones, consistent with the stronger Ir-C bonds. Although it may seem unusual that migratory insertion did not occur at the more labile Ru center in the IrRu system, it must be considered that in this system the methyl group is primarily bound to Ir having only a labile agostic interaction with Ru at very low temperature. Recall that in Chapter 1 we discussed the work of Komiya and coworkers who had reported a PdCo system that promoted migratory insertion reactions.⁶ In that system, migratory insertion occurred at the more labile Co centre after alkyl migration from Pd. Evidently, in the IrRu system studied in our work a similar alkyl migration from Ir to Ru is unfavorable, perhaps a reflection of the increased M-C bond strength of third row TM metals (Ir) over second row ones (Ru, Pd).

Another anticipated difference between the Ir-based system and the Rh-based ones is the greater tendency for Ir to undergo oxidative addition reactions.

Both Rh-based systems were found to be unreactive to H₂, whereas the three Ir/Ru acyl compounds investigated in Chapter 3 react readily, either by heterolytic or homolytic cleavage of H₂. In reactions with the cationic tricarbonyl precursors **40** and **41** (BF₄⁻ and OTf⁻ salts, respectively), the only product observed was the monohydride **43**, resulting from *heterolytic* H₂ cleavage. In addition, treatment of this monohydride complex with CO leads to the formation of acetaldehyde, mimicking the formation of this oxygenate in the FT process. In contrast, reaction of the dicarbonyl analogue (**42**) at -90 °C yielded a dihydrogen complex **44**, which at slightly higher temperature underwent *homolytic* H₂ cleavage to yield a dihydride. To our surprise, compound **45** did not yield acetaldehyde upon treatment with CO, instead only CO substitution of the OTf⁻ ligand was observed. The reason for the lack of acetaldehyde formation in the latter case, whereas in the former it forms readily, is unclear. It may be that in the case of monocationic **43** the bridging acyl group can be readily displaced from the bridging site upon CO coordination at Ru and concomitant cleavage of the Ru-O bond. The resulting terminally Ir-bound acyl group can readily undergo reductive elimination with the adjacent hydride ligand to give **6** and acetaldehyde. In the case of **45**, two factors contribute to the lack of acetaldehyde elimination: (1) the Ru centre in this complex is more crowded and so CO coordination may not be possible at this metal centre and (2) the Ru-O bond is much stronger in this dicationic complex and therefore less readily broken. As a result of these two factors, the acyl group remains in the bridging position and thus reductive elimination of acetaldehyde does not occur.

A noteworthy difference between terminal and bridging acetyl groups is the latter's stability against deinsertion. In mononuclear chemistry, the formation of an acyl group by CO migratory insertion is generally reversed by ligand removal. This is not the case in the study presented in Chapter 3, or in our previous studies of other metal combinations. In fact, the Ir/Ru systems allows for the removal of up to two carbonyl ligands while the integrity of the acyl group is maintained. It was argued earlier that the number of electrons that the acyl ligand may provide to the metal centre is the major contributing factor in the

increased stability of the bridging-acyl group over terminal ones (3-electron and 1-electron donors, respectively) and nothing is gained from this viewpoint upon deinsertion of the bridging-acyl. This stability towards deinsertion may be a significant contributor to the formation of oxygenates in FT chemistry, and may also be exploited in other transformations requiring CO migratory insertion, for example in the copolymerization of CO and ethylene.

The activation of geminal C-H bonds of olefinic substrates under ambient conditions is a transformation that is well suited to multimetallic systems. Surprisingly this process has received very little attention and so the roles of the adjacent metals in such a process are poorly defined. In Chapter 1 we proposed a sequence of steps through which adjacent metals could sequentially activate a pair of geminal C-H bonds in α -olefins. In this study we had hoped to find support for this proposal.

A previous study in the group had demonstrated the ability of a diiridium dppm system to activate geminal C-H bonds in 1,3-butadiene.⁷ We sought to investigate the influence of substituting one “IrMe” fragment of the Ir₂ systems by a “Ru(CO)₂” fragment. At first glance this substitution does not seem promising. It has already been established that substitution of Ir with more labile Rh yields a system that is apparently incapable of geminal C-H bond activation.⁷ In addition, substitution of an “IrMe” fragment by a “Ru(CO)₂” fragment introduces saturation at one metal centre; it would be expected that such saturation would reduce the reactivity of the resulting IrRu system. Furthermore, the π -acidity of the CO ligands of the “Ru(CO)₂” fragment versus the basicity of the Me ligand of the “IrMe” fragment does not favour oxidative addition in the case of the former. Despite these considerations, the IrRu system is capable of double geminal C-H activation of small olefins such as ethylene, propene and allenes, and in this regard is more reactive than the Ir₂ system, which did not activate these substrates. However, the IrRu system failed to react with 1,3-butadiene. We assume that this lack of reactivity of the larger substrate results from the greater number of ligands present in the IrRu system, limiting substrate access to the metal centres. In this respect, substituting the bulky dppm groups for much less bulky depm ligands

would be worth pursuing. The reduced steric bulk of depm over the dpmm would provide greater substrate access to the metals. In addition, although the increased basicity of depm will result in less favourable CO loss, which seems necessary for substrate attack, it should favour oxidative addition.

Another difference between the Ir₂ and the IrRu systems is the greater tendency of the latter to lose H₂. While the isolated product in the Ir₂ system was a vinylidene-bridged dihydride complex,⁷ the reaction of monoolefins with the IrRu system yielded only the vinylidene-bridged tetracarbonyl species without hydride ligands; attempts to generate the presumed dihydride intermediates were unsuccessful. In the case of the diiridium system the strong Ir-H bonds favours retention of the hydride groups, whereas it would seem that the substitution of one Ir centre for a more labile Ru centre is sufficient to facilitate H₂ elimination.

Additionally, in the few previous reports of geminal C-H bond cleavage, no further reactivity was reported for the products. The vinylidene tetracarbonyl complex **47** is also inert towards further reactions with diazomethane and DEDM. However, the tricarbonyl analogue **52** reacts readily to generate substituted cumulenes. In principle, this illustrates the potential for bimetallic systems (in particular IrRu ones) in the conversion of inexpensive terminal olefins into more valuable products, although more work is required in order to develop a system capable of such a transformation in an efficient and atom economical manner.

In an effort to clarify the roles of the metals in the activation steps we conducted a series of low temperature NMR studies in hopes of characterizing the intermediate species involved. Based on these studies the possible roles of the metal centres were discussed. It is still unclear whether the initial C-H activation is promoted by a single metal site or if both metals are involved. The second activation however, undoubtedly invokes the involvement of the adjacent metal. We proposed two possibilities; either the 'geminal mechanism', which leads directly to the vinylidene moiety, or the 'vicinal mechanism' which yields an unstable bridging alkyne that immediately transforms to a bridging vinylidene. In order to establish the possible involvement of these mechanisms we reacted the IrRu tetracarbonyl precursor (**6**) with 1,1-d₂ ethylene and, based upon the isotopic

splitting pattern of the mass spectra, we believe that the transformation of a terminal olefin into a bridging vinylidene can occur by the *both* mechanisms, with the geminal mechanism in this study being the dominate pathway (at least in the case of ethylene). The observation that the geminal pathway is preferred was rationalized by the increased acidity of the proton bound to C^α over the protons bound to C^β, rendering the latter C-H bond easier to cleave. These low temperature and deuterium labeling studies have provided some support for our initial proposal of adjacent metal involvement in the cleavage of two geminal C-H bonds. These results support the notion that coordination of the vinyl ligand to one metal can orientate either the C^α-H or the C^β-H bonds for facile cleavage, depending on the orientation of the vinyl ligand.

In addition, we have observed the geminal C-H activation of cumulenes to generate vinylidene-bridged species. This process must proceed by a somewhat different mechanism than the activation of monoolefins discussed above, since in the case of allene and methylallene activation the protons are retained and transferred to the former cumulene molecule forming a vinylidene-bridge. Interestingly, in the case of 1,1-dimethyl allene three C-H bonds are cleaved and only one proton retained (the other two protons are eliminated as H₂) to form a vinylvinylidene-bridge. Unfortunately, we were unable to collect sufficient data to confidently submit a proposal for the transformation of cumulenes to bridging vinylidenes. However, based on our limited observations, and those of both Doherty^{8a} and Chiang,^{8b} we have formulated a proposal that involves C-H oxidative addition of the terminal end of the cumulene molecule. At this stage the allenyl and methylallenyl fragments undergo a 1,3-hydrogen shift to give a bridging alkenyl hydride species, whereas the 1,1-dimethylallenyl fragment undergoes additional C-H bond cleavage of a methyl substituent, H₂ elimination, and cleavage of the C^α-H bond to give an alkenyl fragment like that observed in **IV-D**. From the alkenyl hydride complexes hydrogen transfer to the alkenyl fragment yields the bridging vinylidene species.

It seems that the initial concern related to substituting a “saturated” “Ru(CO)₂” fragment for an “unsaturated” “IrMe” fragment has in fact led to

enhancement rather than inhibition of reactivity. It appears that the lability of the Ru fragment plays a pivotal role in loss of a CO ligand at an early stage, which generates an unfavourable 16-electron Ru centre. Although the Ir₂ system already has two unsaturated Ir centres, these configurations are not unfavourable. Hence, the presence of this putative, highly reactive, 16-electron Ru centre results in greater reactivity.

Throughout the work in this thesis we have observed new reactions that arise through the interactions of two *different* metals which, together with previous work from our group, demonstrates that exchange of one metal by a metal of the same triad (in this case replacing Rh with Ir) can result in both subtle and pronounced differences in reactivity. It appears that in heterobinuclear systems, well established reactivity differences within metals of the same triad can play as important a role in the chemistry as metal-metal cooperativity between the adjacent metals of the complex.

A particularly noteworthy observation not specifically discussed in the previous chapters is the reduced stability of the tetracarbonyl IrRu complex (**6**) compared to the RhRu (**5**) and RhOs (**2**) analogues. For example, the tetracarbonyl precursors of the Rh-based systems are stable for long periods, these compounds have been known persist for over a year and can even be stored in air for extended periods of time. In contrast, the IrRu tetracarbonyl species readily decomposes over the course of several months, even when stored under nitrogen at sub-zero temperatures. For this reason, IrRu complexes must be prepared with great care and in small batches. One important difference between the tetracarbonyl analogues of these systems is the greater CO lability of compound **6** versus both the RhOs and RhRu tetracarbonyl compounds (compounds **2** and **5**, respectively); the carbonyls of **6** exchange rapidly on the NMR timescale at temperatures above -60 °C, whereas in the Rh-based analogues, **2** and **5**, these carbonyls exchange slowly on the NMR timescale at ambient temperatures. This increase in carbonyl lability of the IrRu system is also manifested in our inability to prepare a tricarbonyl methylene-bridged IrRu complex, even though the Rh-based analogous (M = Os (**25**) and M = Ru (**26**)) are relatively stable. The reason

for this increased carbonyl lability in the IrRu systems is unclear, especially when compared to the RhRu system. One contributing factor to this inability of the IrRu complex to retain its carbonyl ligands may be the strength of the metal-metal interaction of this system versus those of the Rh-based ones. However, the nature of these interactions is still poorly understood. It would appear that the role of the group 8 metal in this regard, and how this influence affects the lability of the carbonyls as well as subsequent chemistry, in particular those that involve CO loss or substitution, is rather complex. It is hoped that the IrOs combination will aid in elucidating the origins of these subtle, yet influential, differences.

It is clearer than ever that reactivity involving adjacent metal centers is inherently more complicated than that of a single metal. Even for the simplest “multi-metal” system – those containing only two metals – the different elementary steps in chemical transformations can, in principle, occur at either or both metals, and the subtle interactions between these metals can greatly influence the resulting reactivity. Throughout the studies presented in this dissertation we have discussed a number of examples in which the synergistic interactions of adjacent metals give rise to reactivity not observed by their monometallic counterparts. For example, in Chapter 2 we observed the generation of remarkably stable bridging/chelating diazoalkane adducts; in Chapter 3, an important aspect of the chemistry presented was the stability of bridging acyl groups versus terminal ones with respect to deinsertion; finally, the activation of two geminal C-H bonds of unsaturated hydrocarbyl substrates under ambient conditions was presented in Chapter 4.

Overall, the work within this thesis adds to the rich chemistry of multinuclear systems and further demonstrates their capacity to promote unique and useful transformations of substrate molecules not often observed with monometallic complexes. Together with other work in this field, a more complete picture is beginning to emerge and we are gaining a better understanding of the subtle interactions between adjacent metals in both homo- and heteronuclear systems, yet much work still remains. It is hoped that as a greater comprehension of these interactions is attained we approach a more rational strategy to both

multinuclear homogenous and heterogeneous catalyst design. In addition, it is hoped that the greater understanding of metal substitution may lead to the development of mixed-metal nanoparticle catalysts with controlled surface architecture. Most importantly, however, we are truly beginning to see that for a number of selective substrate transformations, two metals are better than one.

5.2 References

1. (a) Trepanier, S. J.; Dennett, J. N. L.; Sterenberg, B. T.; McDonald, R.; Cowie, M. *J. Am. Chem. Soc.* **2004**, *126*, 8046. (b) Trepanier, S. J.; Sterenberg, B. T.; McDonald, R.; Cowie, M. *J. Am. Chem. Soc.* **1999**, *121*, 2613.
2. Cohen, R.; Rybtchinski, B.; Gandelman, M.; Rozenberg, H.; Martin, J. M. L.; Milstien D. *J. Am. Chem. Soc.* **2003**, *125*, 6532.
3. (a) Rowsell, B. D.; McDonald, R.; Cowie, M. *Organometallics* **2004**, *23*, 3873. (b) Trepanier, S. T.; McDonald, R.; Cowie, M. *Organometallics* **2003**, *22*, 2638.
4. (a) Dry, M. E. *J. Chem. Technol. Biotech.* **2002**, *77*, 43. (b) Dry, M.E. *ACS Symp. Ser.* **1987**, *328*, 18. (c) Maitlis, P. M. *J. Organomet. Chem.* **1995**, *500*, 239. (d) Fischer, F.; Tropsch, H. *Brennst. Chem.* **1923**, *4*, 276. (e) Brady, R. C.; Pettit, R. *J. Am. Chem. Soc.* **1980**, *102*, 6181. (f) Brady, R. C.; Pettit, R. *J. Am. Chem. Soc.* **1981**, *103*, 1287. (g) Maitlis, P. M. *J. Mol. Catal. A: Chem.* **2003**, *204*, 55.
5. (a) Brookhart, M.; Green, M. L. H. *J. Organomet. Chem.* **1983**, (250), 395. (b) Brookhart, M.; Green, M. L. H.; Wong, L.-L. *Prog. Inorg. Chem.* **1988**, *36*, 1. (c) Brookhart, M.; Green, M. L. H.; Parkin, G. *Proc. Nat. Acad. Sci. USA* **2007**, *104*, 6908.
6. Fukuska, A.; Fukugawa, S.; Hirano, M.; Koga, N.; Komiya, S. *Organometallics* **2001**, *20*, 2065. (b) Fukuska, A.; Fukugawa, S.; Hirano, M.; Komiya, S. *Chem. Lett.* **1997**, 377. (c) Komiya, S.; Yasuda, T.; Hirano, M.; Fukuoka, M. *J. Mol. Catal. A: Chem.* **2000**, *159*, 63.

7. Ristic-Petrovic, D.; Torkelson, J. R.; Hiltz, R. W.; McDonald, R.; Cowie, M. *Organometallics* **2000**, *19*, 4432.
8. Doherty, S.; Elsegood, M. R. J.; Clegg, W.; Ward, M. F.; Waugh, M. *Organometallics* **1997**, *16*, 4251. (b) Kung, H.; Wu, S-M., Wu, Y-J., Yang, Y-W., Chiang, C-M. *J. Am. Chem. Soc.* **2008**, *130*, 10263.
9. Rowsell, B. D.; Trepanier, S. T.; Lam, R.; McDonald, R.; Cowie, M. *Organometallics* **2002**, *21*, 3228.

Appendix I: Selected NMR Spectra

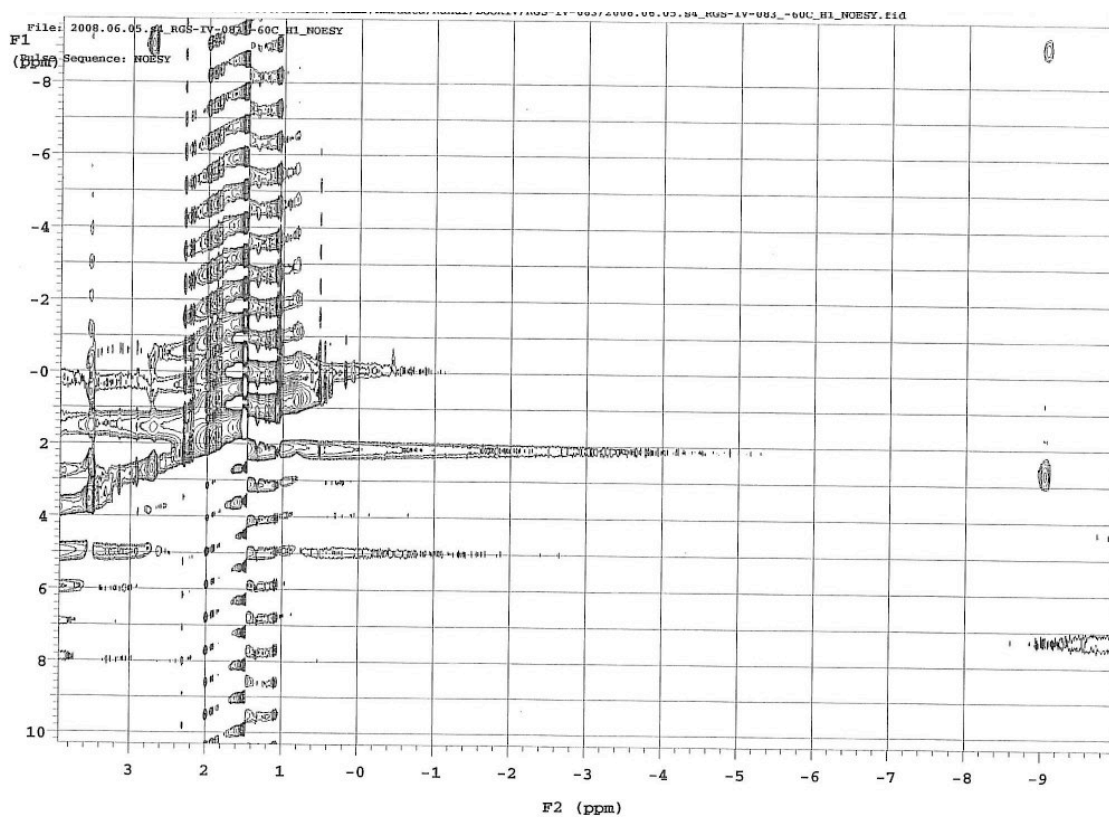


Figure AI.1: ^1H EXSY (400 MHz) spectroscopy spectrum of compound **38** at $-60\text{ }^\circ\text{C}$.

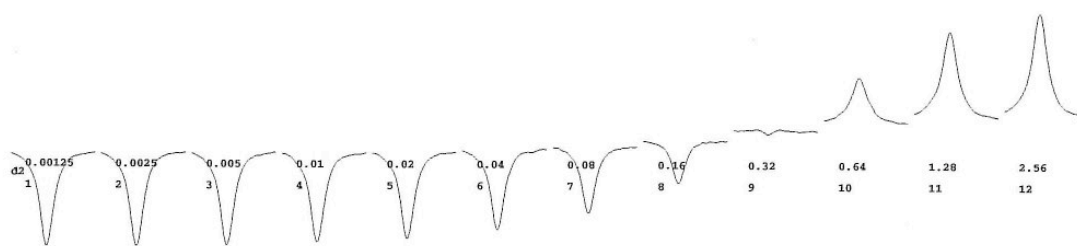


Figure AI.2: ^1H T1 measurement of compound 44 showing the resonance of the H_2 ligand (δ -0.03). Spectra taken at -90 °C on a 400 MHz spectrometer.

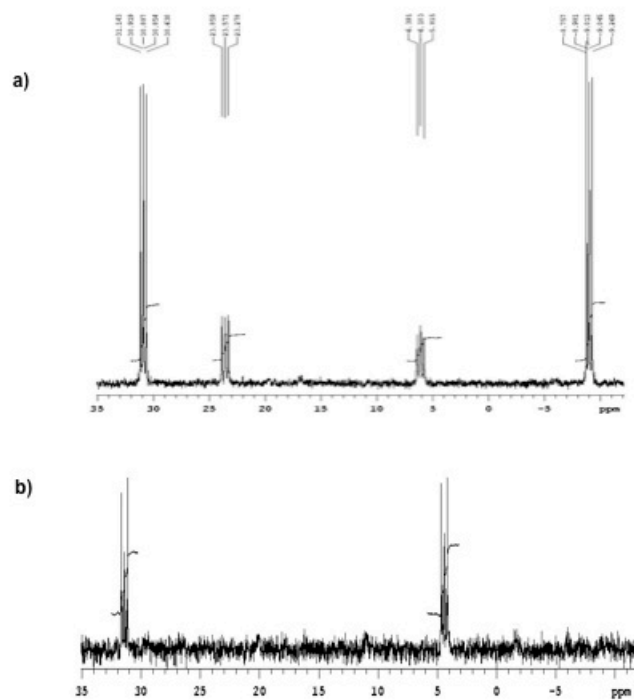


Figure AI.3: $^{31}\text{P}\{^1\text{H}\}$ (162 MHz for ^{31}P) spectra from the variable-temperature NMR studies of the reaction of **6** with ethylene showing a) a mixture of **6** and **51** after initial reaction of ethylene and **6** at $-20\text{ }^\circ\text{C}$ (spectra taken at $-20\text{ }^\circ\text{C}$) and b) the final product, **47**, after warming to ambient temperatures for 16 h.

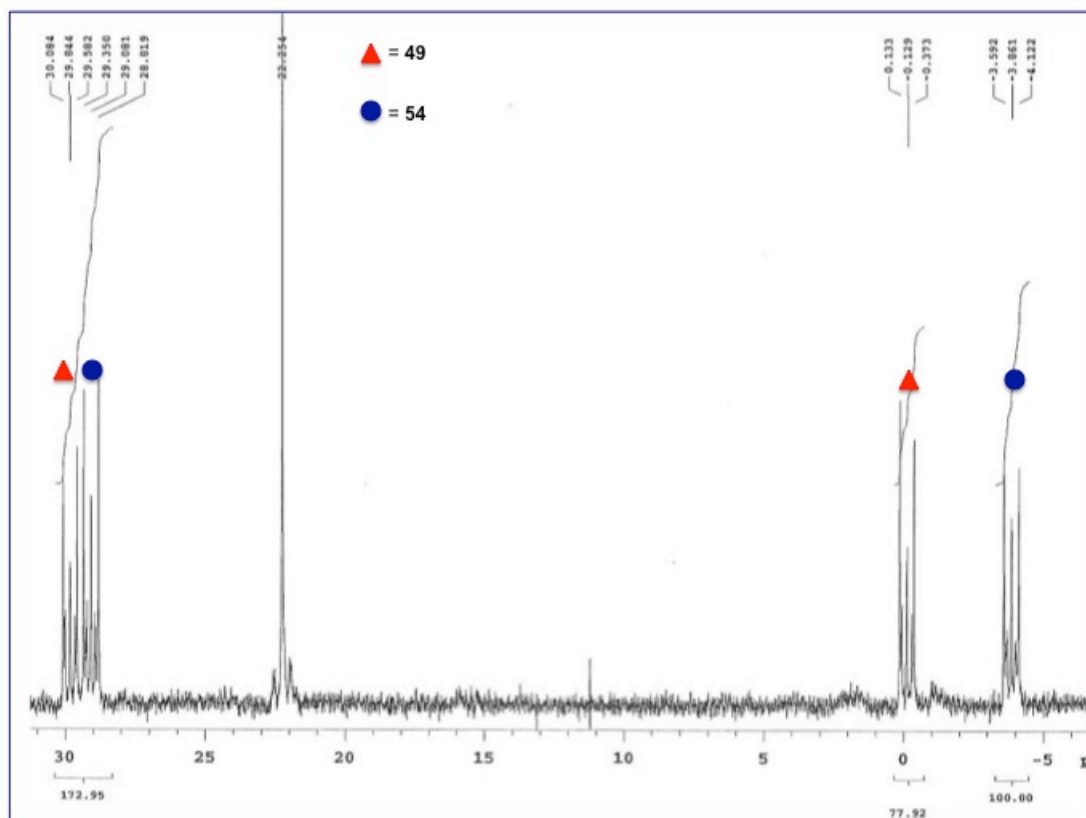


Figure A1.4: $^{31}\text{P}\{^1\text{H}\}$ NMR spectra, operating at 162 MHz for ^{31}P , the reaction mixture of **6** and acetylene after 16h at 0 °C showing a ca. 1:1 ratio of compounds **49** and **54**.

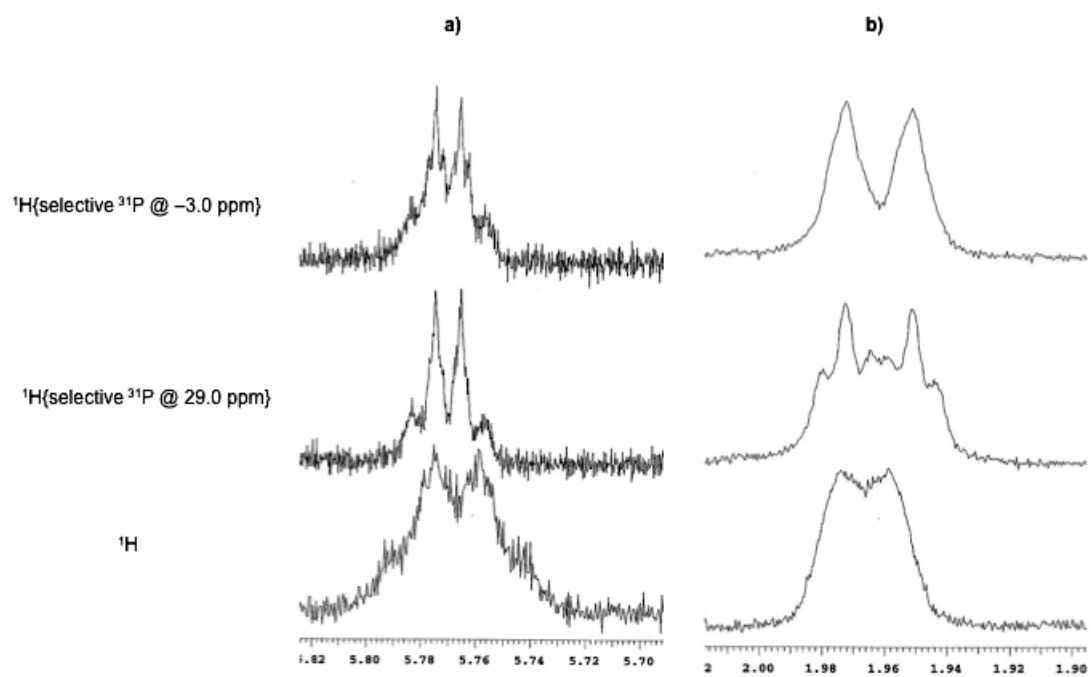


Figure A1.5: Selected regions of the $^1\text{H}\{\text{selective } ^{31}\text{P}\}$ NMR spectra (400 MHz) of compound **54** showing a) the $\text{C}=\underline{\text{C}}\text{H}(\text{CH}_3)$ resonance and b) the $\text{C}=\text{C}\underline{\text{H}}(\text{CH}_3)$ resonances.

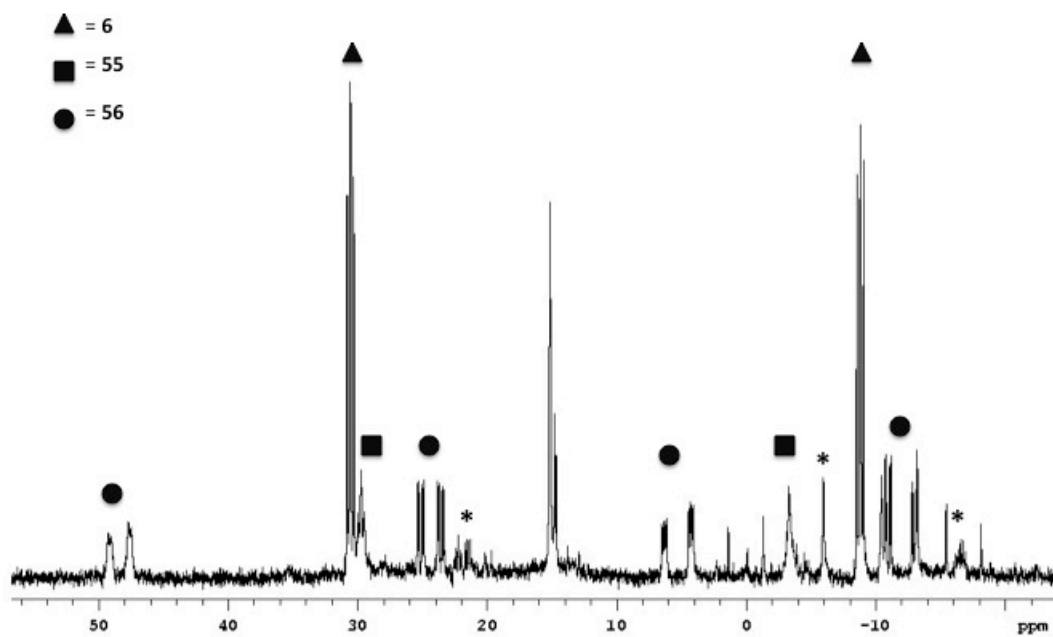


Figure A1.6: $^{31}\text{P}\{^1\text{H}\}$ NMR spectra of a mixture of compounds **6**, **55**, and **56** taken at $-80\text{ }^\circ\text{C}$. * unknown decomposition products and/or impurities.

^1H NMR spectra of a mixture of **55** and **56** at $-80\text{ }^\circ\text{C}$

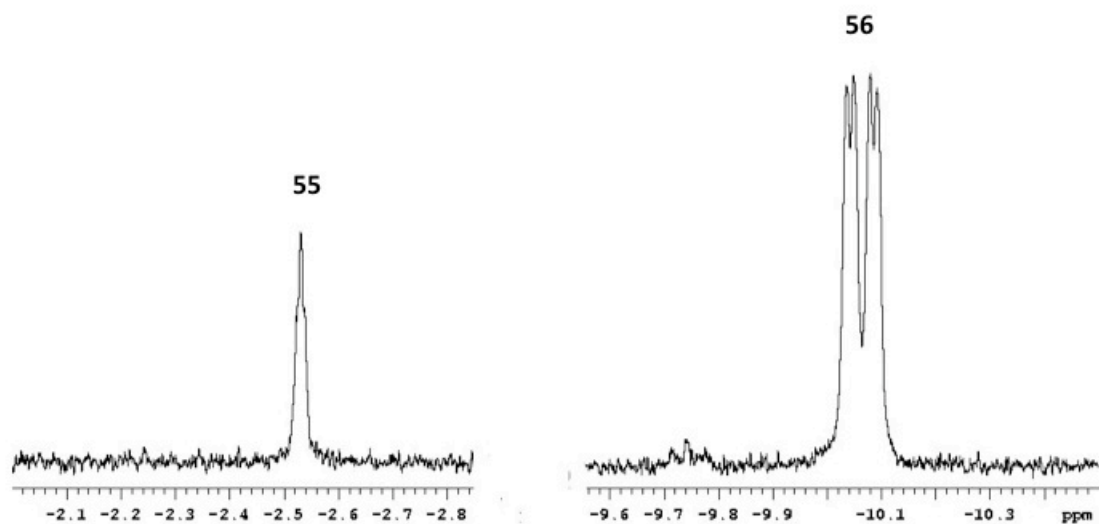


Figure AI.7: Selected regions of the ^1H NMR spectra of a mixture of **6**, **55** and **56** showing the agositic proton resonance of **55** (δ -2.5) and the hydride resonance of **56** (δ -10.0).

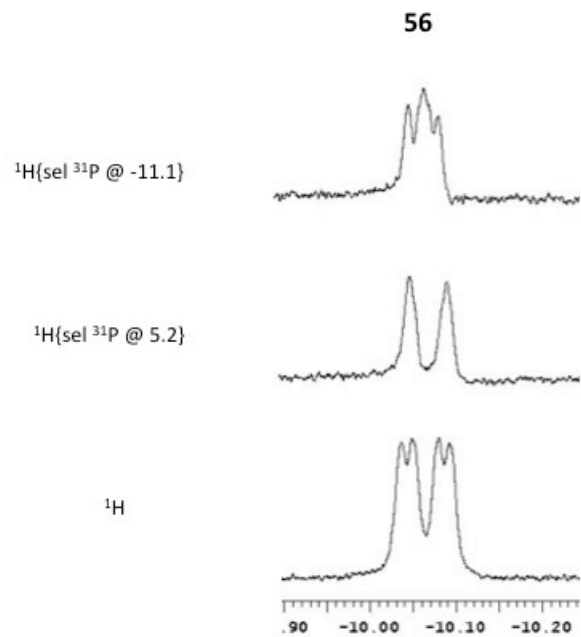


Figure AI.8: Spectra from the $^1\text{H}\{\text{sel } ^{31}\text{P}\}$ NMR experiments of **56** showing the hydride resonance with no ^{31}P decoupling (bottom), selective ^{31}P decoupling of the ^{31}P nucleus that resonates at 5.2 ppm (middle) and the ^{31}P nucleus that resonates at -11.1 ppm (top).

Appendix II: Drying Agents for Solvents

Solvent	Drying Agent
Nitromethane	CaH ₂
Acetonitrile	CaH ₂
THF	Na/benzophenone
Methylene Chloride	P ₂ O ₅
n-Pentane	Na/benzophenone
Diethylether	Na/benzophenone
Acetone	CaCl ₂
Methanol	MgSO ₄
Toluene	Na

Appendix III: Co-author Contributions

The following outlines the contributions of the author and coauthors in the studies presented in Chapters 2 and 3.

AIII.1 Chapter 2

Todd Graham was the first to prepare compound **27**. Todd obtained crystals of **27** as well as completed the majority of the spectroscopic characterization of this compound (with the exception of $^{13}\text{C}\{^1\text{H}\}$ NMR and elemental analysis). Bryan Rowsell prepared and spectroscopically characterized compound **28**. The author completed the remainder of the work discussed in Chapter 2.

AIII.2 Chapter 3

Steven Trepanier established much of the reaction sequence shown in Scheme 3.1 and contributed much of the characterization of compounds **34** – **37**. In addition, L. Xu worked with the BF_4 salts of compounds **34** – **37**. The author obtained the NMR spectroscopic data associated with the isotopomers **34**- $^{13}\text{CH}_3$, **35**- $^{13}\text{CH}_3$, **36**- $^{13}\text{CH}_3$. James Wigginton, prepared compound **38**, whereas the author established the structure and conducted the NMR spectroscopic studies of this system. In a similar way, James and the author collaborated in the study of compounds **43** – **45**. Steve and Xu established the chemistry of Scheme 3.3; L. Xu prepared the compounds **39-BF₄**, and **40**, whereas Steve prepared compounds **39-OTf**, **41**, and **42**. Steve, Xu, James, Mathias Berenstiel and the author contributed equally to the complete characterization of species **39-42**. The author established the remaining chemistry of Chapter 3.